

INSTITUTE ON LAKE SUPERIOR GEOLOGY

DULUTH, MINNESOTA MAY 4-8, 2016

HOSTED BY:

JAMES D. MILLER JR., UNIV. OF MINN. DULUTH
MEETING CHAIRPERSON

CHRISTIAN SCHARDT, UNIV. OF MINN. DULUTH

DEAN M. PETERSON, PETERSON GEOSCIENCE LLC

PROCEEDINGS
VOLUME 62

Part 2
Field Trip Guidebook

Compiled by Dean M. Peterson (Peterson Geoscience LLC)

TABLE OF CONTENTS

Proceedings Volume 62
Part 2 – Field Trips

PRE-MEETING FULL DAY FIELD TRIPS, WEDNESDAY, MAY 4

1) Glacial Geology of the Laurentian Uplands **1**
Trip Leaders: Phil Larsen (Vesterheim Geoscience PLC) and Howard Mooers (UMD)

2) Neoarchean Geology of the Western Vermilion District **14**
Trip Leaders: Mark Jirsa, Terry Boerboom, and Amy Radakovich (MGS)

3) Cu-Ni-PGE Deposits of the Duluth Complex **27**
Trip Leaders: Mark Severson (Teck American), Andrew Ware (PolyMet Mining), and Kevin Boerst (Twin Metals Minnesota), Steve Geerts (UMD-NRRI)

PRE-MEETING AFTERNOON FIELD TRIPS, WEDNESDAY, MAY 4

4) Duluth Stream Geomorphology and the June 2012 Flood – CANCELLED **79**
Trip Leader: Karen Gran (UMD)

5) Geology of the Endion Sill, Duluth **80**
Trip Leader: Jim Miller (UMD)

POST-MEETING EVENING FIELD TRIP, FRIDAY, MAY 6

6) Geology and Trout Fishing along Amity Creek, Duluth **102**
Trip Leaders: Dean Peterson (Peterson Geoscience) and George Hudak (UMD-NRRI)

POST-MEETING FULL-DAY TRIPS, SATURDAY, MAY 7 (and SUNDAY, MAY 8 for TRIP 7)

7) Archean and Proterozoic Geology of the Western Gunflint Trail (Two-Day Trip) **110**
Trip Leader: Mark Jirsa (MGS)

8) Keweenawan Geology of the Hovland Area **137**
Trip Leaders: Terry Boerboom (MGS) and John Green (UMD)

9) Duluth Harbor Geologic History Boat Cruise: Quaternary to Anthropocene **160**
Trip Leaders: Irv Mossberger, Mehgan Blair, Eric Dott (Barr Engineering), Andy Breckenridge (UW-Superior), Todd Kremmin (UMD)

FIELD TRIP 1

Wednesday, May 4, 2016

GLACIAL GEOLOGY OF THE LAURENTIAN UPLANDS

Phil Larson, Vesterheim Geoscience PLC

Howard Mooers, University of Minnesota Duluth

with contributions by
Margretta Meyer, University of Minnesota Duluth

INTRODUCTION

The glacial geology of NE Minnesota has been the subject of study for over 100 years and our knowledge of glacial history and chronology have steadily evolved. Within the area that is the focus of this field trip there has been relatively little study. Wright (1956) was first to describe in detail the glacial sediments and landforms. The only detailed investigations since then are the MS theses of Friedman (1981), Fenalon (1986), and Meyer (2009); the map compilation Hobbs et al. (1988); a study of the Rögen moraine by Kryzer (2013). However, the recent availability of high-resolution digital elevation LiDAR has changed the way we map and interpret glacial geology. This field trip will highlight heretofore unrecognized landforms that significantly change our understanding of glacial landform genesis, the history glacial recession, and the nature of subglacial erosional processes.

Widespread occurrence of ice-walled lake plains and other subtle ice-stagnation landforms reveal a complex history of ice recession punctuated by numerous ice-marginal stabilizations or minor readvances. These features suggest that the retreating ice must have been relatively debris poor and thin (2-3 meters) sheets of stagnant ice existed over large areas. Recognition of large tracts of Rögen moraine within the Toimi drumlin field the suggest an evolving subglacial erosional landscape that is interpreted as an indication that the subglacial system switched from depositional to erosional at or near the Last Glacial Maximum. The orientation of individual ridges within tracts of Rögen moraine and their association with eskers suggest that these features formed late during deglaciation in area of the glacier bed that were well drained.

Lastly, we will highlight aspects of the scoured bedrock surface that allow interpretation of the nature of the depth of glacial scour of bedrock. Saprolite of varying thickness is exposed sporadically throughout the region. These occurrences, often in fractures or other protected settings, indicate that in large part scour of the Precambrian shield was limited by the depth of preglacial weathering.

GLACIAL HISTORY

Northeastern Minnesota was continuously covered by ice from the earliest Late Wisconsin ice advance approximately 27-29ka (Clayton and Moran, 1982; Mooers and Lehr, 1997) until about 11ka by the Rainy and Superior lobes of the LIS (Fig. 1.). The earliest formal studies of glacial deposits in northeastern Minnesota were conducted by Upham (1894) who identified a series of moraines across Minnesota. He identified the Vermillion moraine, as the 12th moraine, although he did not define its entire length. Winchell (1900), as the first Minnesota state geologist, organized systematic mapping of the glacial geology of Minnesota. Along with Upham and others, Winchell (1899) was one of the first to map large portions of northeastern Minnesota and describe the surficial deposits. Todd (1898) postulated two lobes

of ice, the Lake Superior lobe, which flowed along the axis of Lake Superior, and the Red River lobe, which advanced from the west. Elftman (1898) suggested two lobes for the northeastern portion of Minnesota because of observed till differences and provenances; he named these the Superior and Rainy lobes; the Rainy lobe referring to the ice flowing from the Rainy River area.

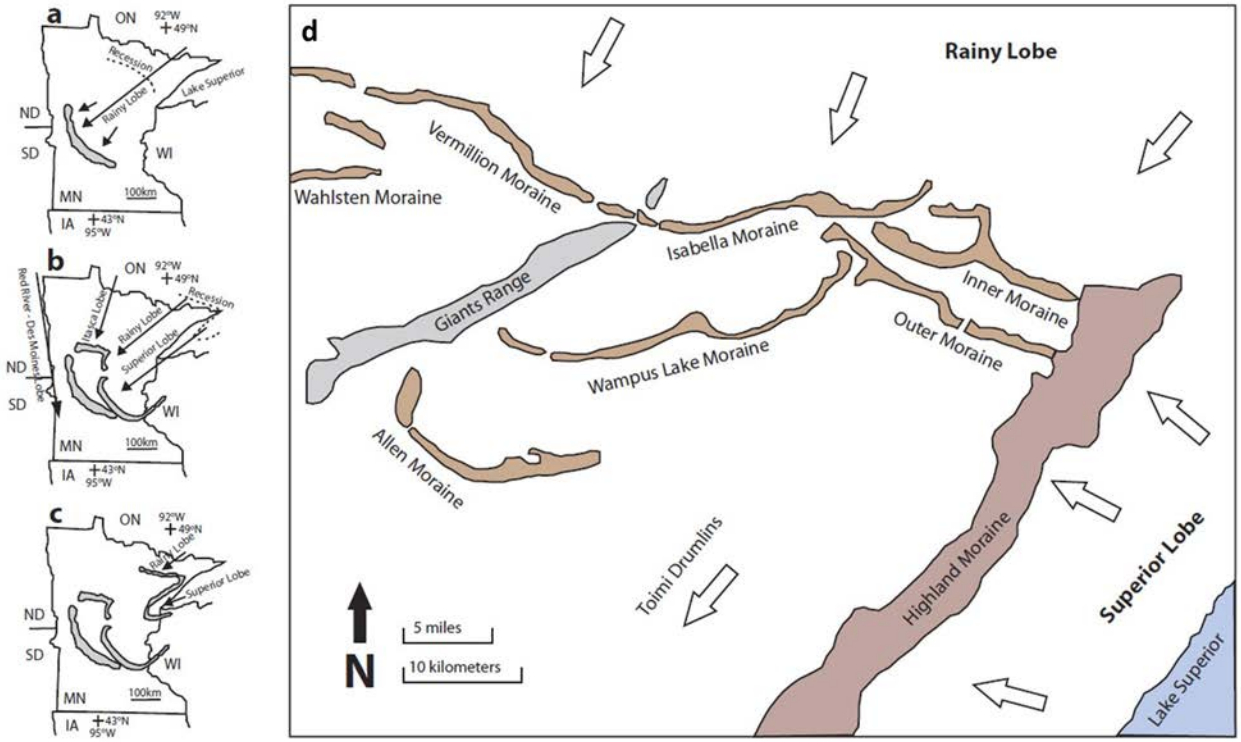


Figure 1. a-c, General sequence of glaciation modified from Mooers and Lehr (1996). d, landforms of NE Minnesota modified from Lehr and Hobbs (1992).

Leverett (1932), based mostly on the work of his predecessors, proposed that northeastern Minnesota was glaciated by three separate lobes of ice. He recognized that the earliest drift in the area was the result of ice flowing from the Patrician [Labradoran] ice center located in the Hudson Bay Lowlands between the Keewatin and Labradorean ice accumulation centers.
In terms of the overall glacial history of northeastern Minnesota, the modern understanding began with Wright (1956) who was the first to conduct systematic fieldwork in the area between the border lakes and Lake Superior. Wright (1964) recounted the glacial history of Minnesota as phases of the different ice lobes and was the first to identify and interpret tunnel valleys, drumlins, and eskers (Wright, 1972). In addition to laying out the general glacial geologic framework, Wright (1964, 1972) established the first regional chronology. The late Wisconsin maximum limit of the Rainy lobes was placed at the St. Croix moraine in central Minnesota (Wright 1964) ca. 20,500 BP. Wright (1972) then suggested that the Rainy lobe retreated and readvanced to the Vermilion moraine by about 18,000 BP, however, no evidence of ice recession between these two phases was presented.

Little additional work was done in this area until the MS theses of Friedman (1981) and Fenelon (1986) followed by the compilation of the surficial geologic map of the Isabella area by Hobbs et al. (1988). Lehr and Hobbs (1992) outline the glacial history and landforms of the area and

describe the stratigraphy of the Independence Till from three rotasonic cores in the Toimi drumlin field. Since the work of Lehr and Hobbs (1992) the only significant investigations of the glacial geology are those of Meyer (2009) and Kryzer et al. (2013), which focused on the distribution and genesis of Rögen moraine.

CHRONOLOGY

The chronology of Wright (1972) mentioned above has long been in question. The date of 20,500 for the St. Croix phase is based on the basal radiocarbon date at Wolf Creek, an inter-drumlin swale behind the St. Croix moraine (Wright, 1972; Birks, 1976). The Vermilion moraine was correlated with the Mille Lacs/Highland moraine system which was dated ca. 18,000 BP; a date inferred as intermediate between the 20,500 date at Wolf Creek (Wright, 1972; Birks, 1976) and a date of 16,150 BP at Kotiranta Lake associated with the Split Rock phase of the Superior lobe (Wright and Watts, 1969). There are, however, basal radiocarbon dates from lakes in the Toimi drumlin field. Florin and Wright (1969) and Banerjee et al. (1979) report basal dates on aquatic mosses of 14,690 BP at Weber Lake and 16,500 Kylen Lake, respectively. Lowell et al. (2009) got a similar date of 14,050 BP on aquatic moss from the base of a core of nearby Salo Lake. Despite the general agreement of radiocarbon ages from the Toimi drumlin field, the possibility of significant carbonate error exists as the Independence Till is calcareous at depth.

DESCRIPTION OF FIELD TRIP STOPS

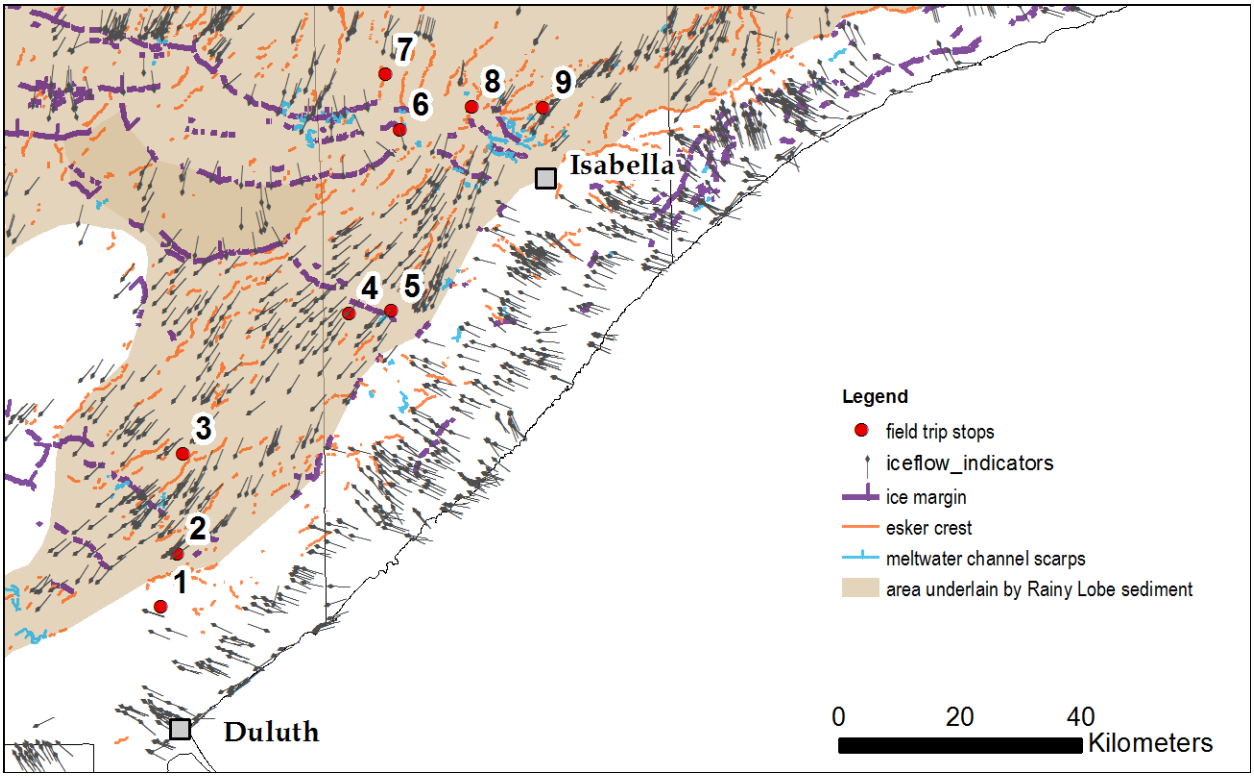
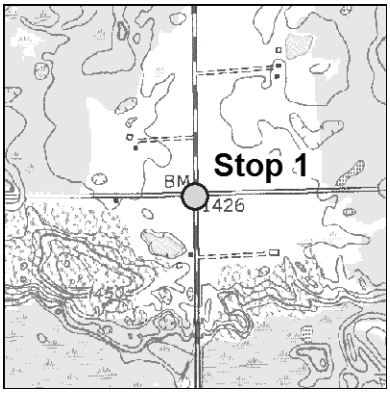


Figure 2. Location of field trip stops.

STOP 1 – Ice-walled Lake Plain in Highland Moraine

564355E/5201830N (UTM Zone 15, NAD83 datum)
Fredenberg 7.5' USGS Quadrangle



This site is located at a prominent ice-walled lake plain situated on the crest of the Highland Moraine (Fig. 3). Although composed predominantly of sand and gravel, this sediment is technically glaciolacustrine, deposited in an ice-dammed basin located in an ice-cored end moraine. The Highland Moraine is composed of hundreds of similar ice-walled lake plains, coalesced to form a belt over 100 km long and as much as 109 km wide; the massive volume of the moraine is a factor of the considerable length of time the Superior Lobe margin stood at this margin, the high sediment flux of the Superior Lobe, or both.

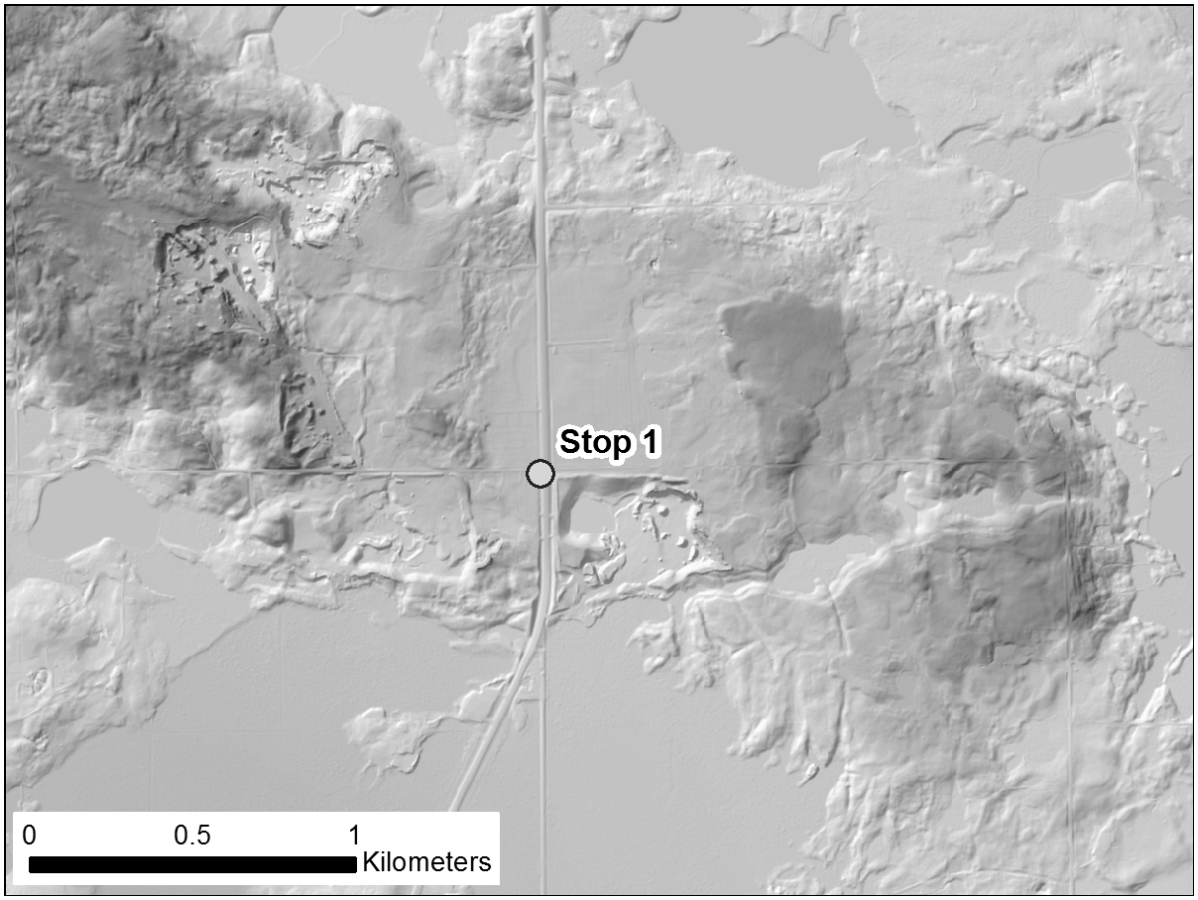
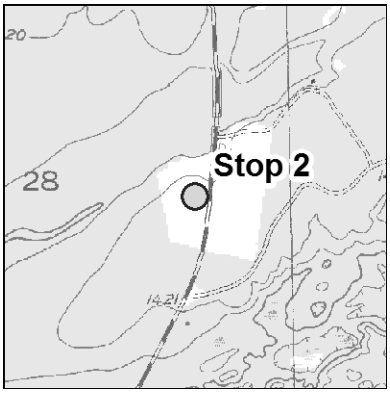


Figure 3. Ice-walled lake plain in Highland moraine north of Duluth.

STOP 2 - Superior Lobe Outwash Mantled Over Fluted Rainy Lobe Drift

567180E/5210690N (UTM Zone 15, NAD83 datum)
Thompson Lake 7.5' USGS Quadrangle



This site is located on an outwash plain extending westward from the junction of the Rainy and Superior Lobes (Fig. 4). The intersection of two ice lobes forms a trough on the ice surface that focuses both surface and subglacial meltwater and sediment discharge. Sediment-laden meltwater discharge deposited a relatively flat, westward sloping outwash surface. In the vicinity of Stop 2, the outwash plain is partially collapsed, revealing fluted subglacial topography associated with northeast- to southwest-flowing ice of an older Rainy Lobe phase. These relationships indicate that retreat of the active Rainy Lobe ice margin in this area was accompanied by stagnation of a large area of the marginal zone, rather than gradual retreat of the ice margin. Sediment-poor clear stagnant ice rapidly melted until incipient melting of the sediment-rich basal debris layer formed an insulating blanket of supraglacial sediment. The outwash plain was deposited over this relatively thin layer of stagnant ice, later collapsing as the last of the buried ice melted.

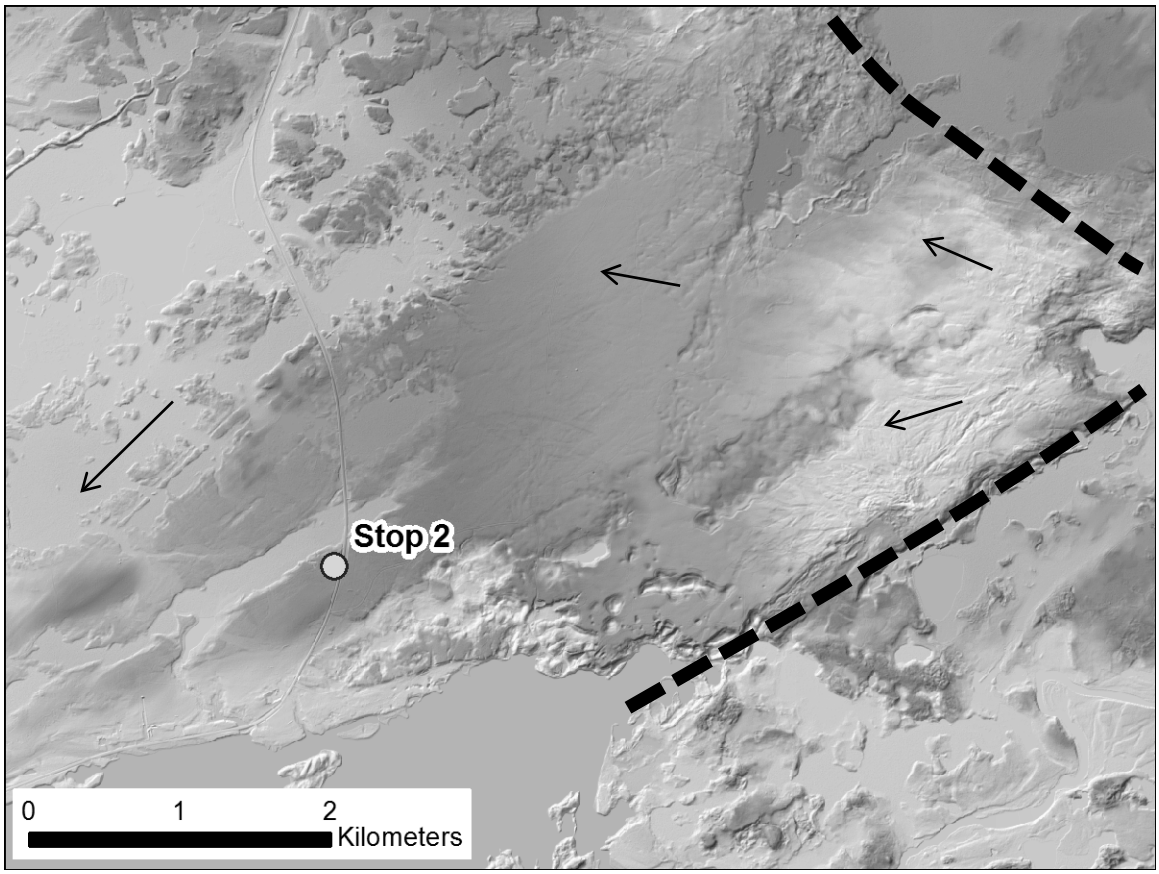
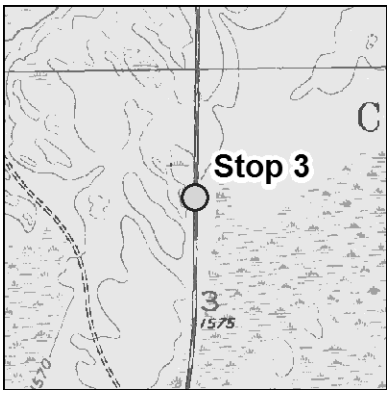


Figure 4. Collapsed outwash overlying Rainy Lobe stagnant ice topography. Ice margins indicated by dashed line, meltwater flow direction by blue arrows, and Rainy Lobe ice flow direction by black arrow.

The relative elevation difference between the intact surface of the outwash plain and the lowest parts of the collapsed area places an important constraint on the relative thickness of the basal debris layer of the Rainy Lobe ice. The apparent thickness – about 2 m – is consistent with basal debris layer thickness observed in the modern Greenland and Antarctic ice sheets.

STOP 3 - Rögen Moraine Superimposed on Drumlins

568050E/522170N (UTM Zone 15, NAD83 datum)
Boulder Lake Reservoir NE 7.5' USGS Quadrangle



Stop 3 is at a road cut through one of a series of ice flow-perpendicular sediment ridges known as Rögen moraine (Fig. 5). Rögen are a common occurrence in the Toimi Drumlin field and adjacent up-ice Rainy Lobe terrane. They appear to be the product of remobilization of older subglacial sediment by sliding glacial ice, in this case the underlying drumlins. The ridges themselves are characterized by about 5 m of relief, and are spaced at a characteristic 100 m along flow lines. Here and elsewhere in the Toimi Drumlin field, Rögen moraine shows a close spatial association with subglacial meltwater discharge (the esker). Ice flow-parallel elongate corridors of Rögen moraine commonly flank tunnel valleys and eskers. This suggests that Rögen formed under warmed-bedded conditions near the ice margin, a conclusion distinctly at odds with other models for their formation. It further suggests that periodic fluctuations in basal shear stress associated with annual variations in subglacial meltwater discharge may play a role in Rögen formation, in particular cyclic stick-slip coupling of basal ice to subglacial sediment.

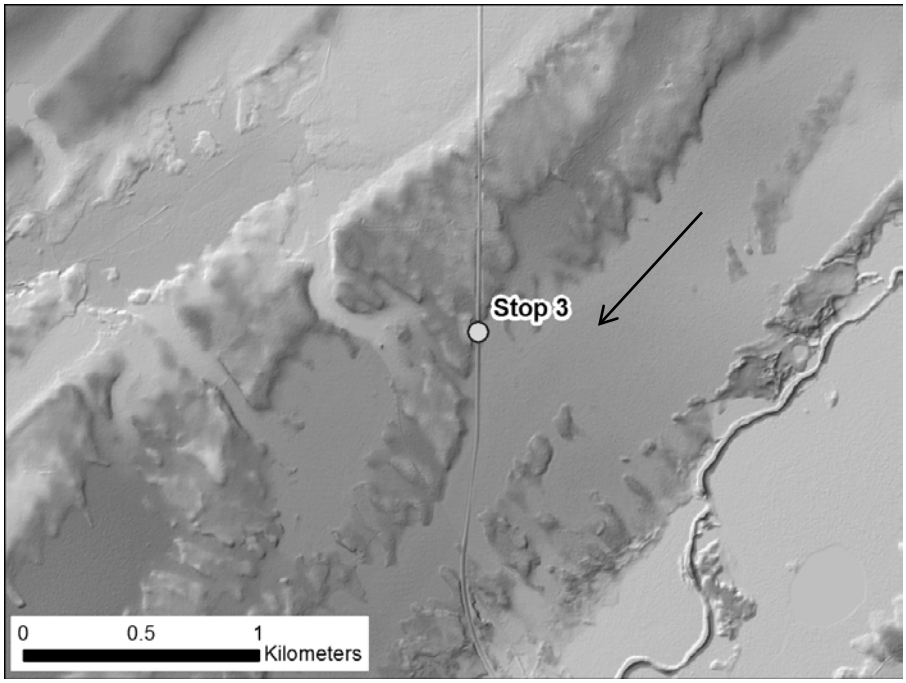
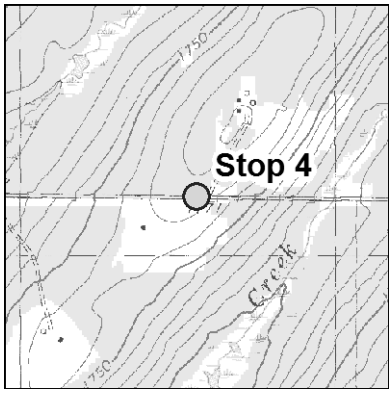


Figure 5. Ice-marginal Rögen moraine superimposed on drumlins. Esker is sinuous feature in southeast quadrant; ice flow direction indicated by arrow.

STOP 4 - Toimi Drumlin Field

595550E/5250390N (UTM Zone 15, NAD83 datum)
Mount Weber 7.5' USGS Quadrangle



Stop 4 is located at a road cut through one of the hundreds of drumlins that collectively form the Toimi Drumlin field (Fig. 6). This particular drumlin is located near the center of the field. Toward the east and northeast, in the up-ice flow direction, the drumlins show increasing frequency of bedrock cores and are perhaps better described as crag-and-tail features. Toward the southwest, in the down-ice flow direction, the drumlins display the characteristic streamlined form.

In the near vicinity, borehole records indicate drift thicknesses of 30 to 65 m, predominantly composed of till (Lehr and Hobbs, 1992). Relief on the drumlins is about 30 m, suggesting the drumlin field is composed of a somewhat discontinuous layer of drift. Significantly, deeper tills encounrtered in borehole are weakly to moderately calcareous.

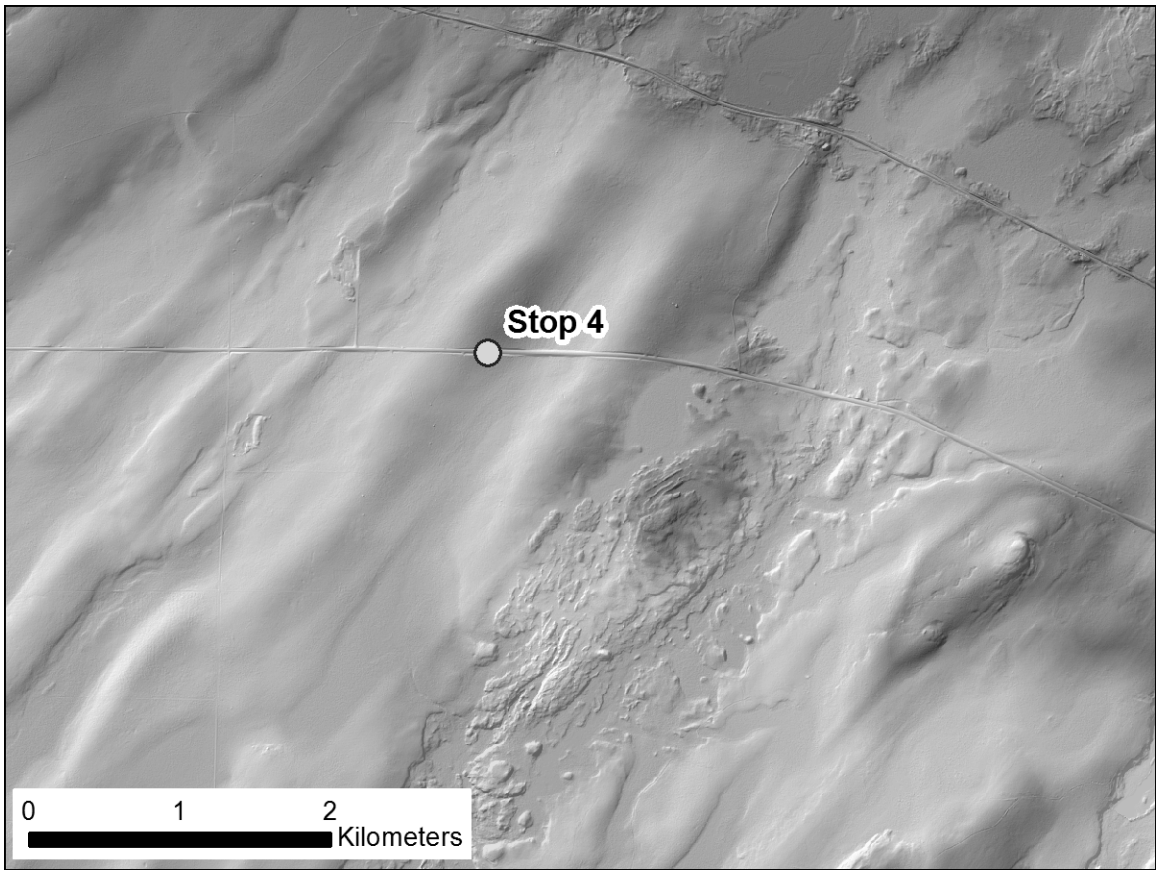
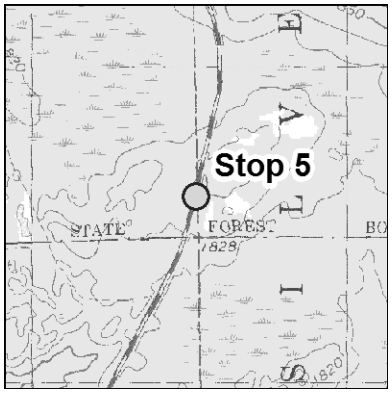


Figure 6. Typical Toimi drumlins, crag and tail features in the southeast quadrant.

STOP 5 - Thermokarst in Sediment-poor Stagnation Moraine

602510E/5250800N (UTM Zone 15, NAD83 datum)
Mount Weber 7.5' USGS Quadrangle



This stop is located in an ice flow-perpendicular belt characterized by thin ice-walled lake plains (*pannukaku*) (Fig. 7). *Pannukaku* typically show as little as 1 m of relief with their surroundings, and are commonly draped over subglacial topography.
Belts of *pannukaku* in the Toimi Drumlin field define minor surge-stagnation moraines deposited by the retreating Rainy Lobe. The relatively small volume of sediment contained in these moraines is a reflection of relatively low sediment flux on the part of the warmed-bedded Rainy Lobe.

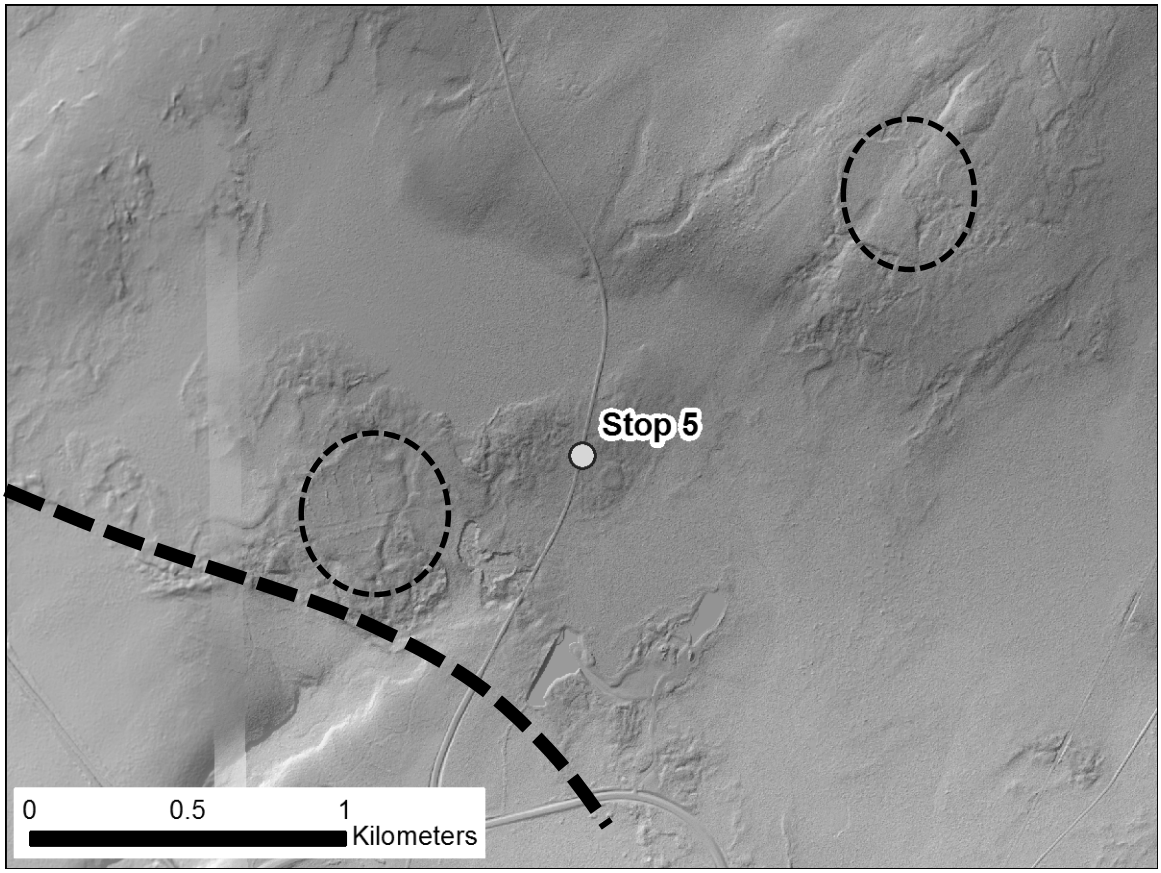
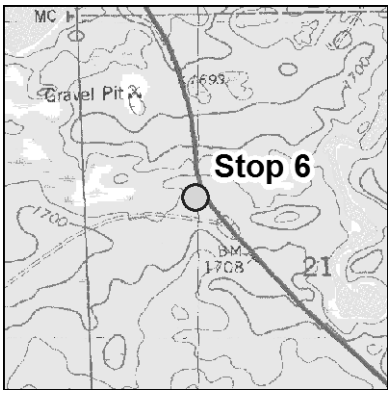


Figure 7. Rainy Lobe surge-stagnation moraine, defined by belt of *pannukaku*. Ice margin defined by dashed line, *pannukaku* by thin dashed outlines.

STOP 6 - Superior Lobe Outwash

603980E/5280650N (UTM Zone 15, NAD83 datum)
Slate Lake East 7.5' USGS Quadrangle



Stop 6 is located at a road cut through Superior Lobe sand and gravel, deposited by meltwater flowing from southeast to northwest (Fig. 8). Following retreat of the Rainy Lobe ice margin north of the Laurentian Upland, meltwater from the Superior Lobe was able to flow northwest into Glacial Lake Dunka and ultimately Glacial Lake Norwood. This meltwater deposited a distinct tongue of Superior Lobe-provenance sand and gravel cross-cutting continuous Rainy Lobe drift.

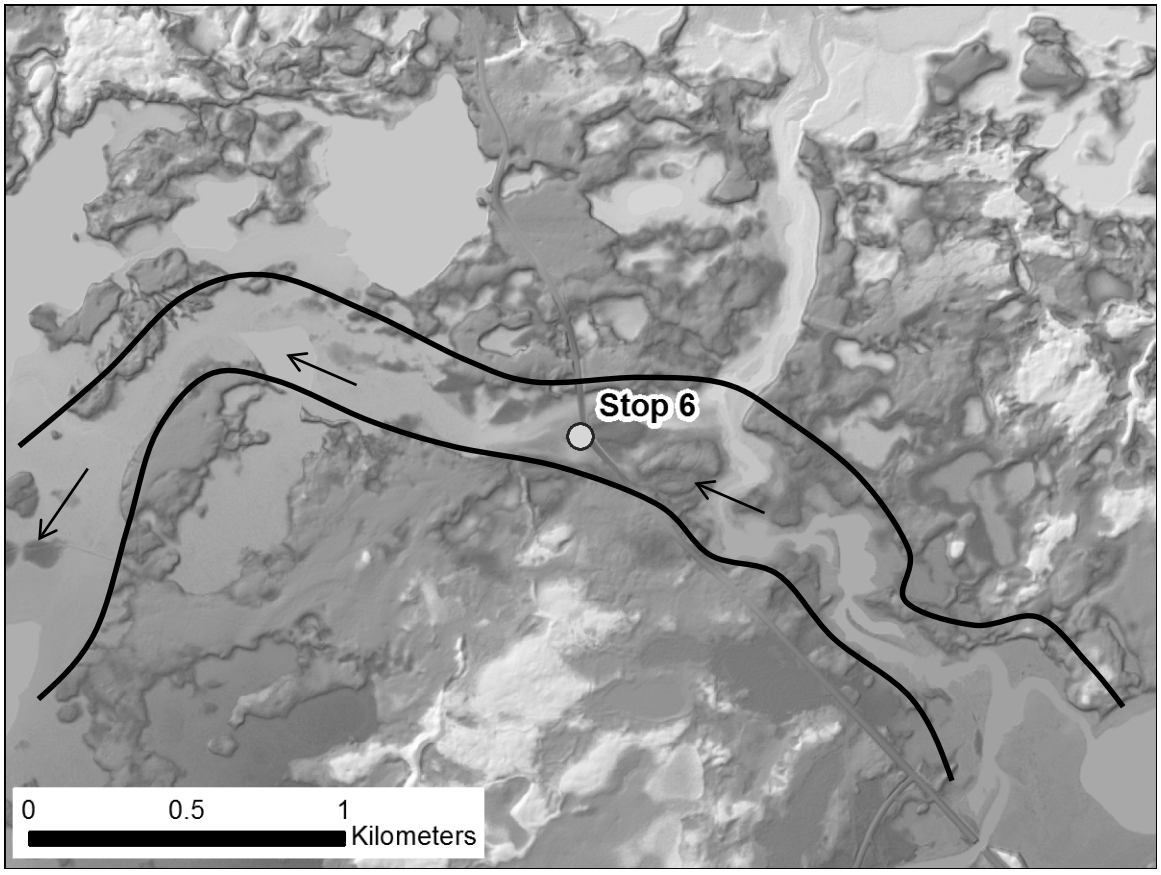
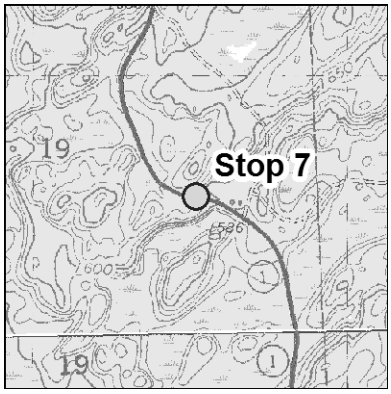


Figure 8. Superior Lobe meltwater channel cross-cutting older Rainy Lobe drift.

STOP 7 - Relict Pre-glacial Saprolite

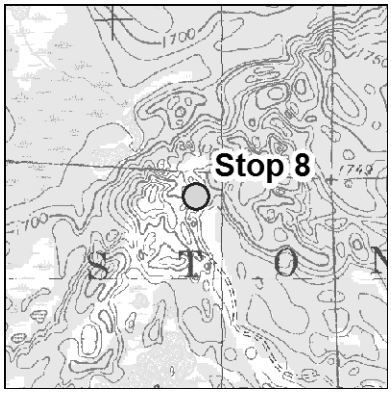
601510E/5289820N (UTM Zone 15, NAD83 datum)
Bogberry Lake 7.5' USGS Quadrangle



Much of what is commonly thought of as typical 'glacially sculpted' rugged shield topography is better explained as the morphology of the base of a pre-glacial saprolite (Feininger, 1971). This stop highlights relict pre-glacial saprolite exposed in a road cut during recent (2013) highway reconstruction.

STOP 8 - Ice-contact Outwash Fan

615910E/5284460N (UTM Zone 15, NAD83 datum)
Mitawan Lake 7.5' USGS Quadrangle



Stop 8 is located on an ice-contact outwash fan formed on a stagnant Rainy Lobe ice margin (Fig. 9). The fan itself is composed largely of sand and gravel, with some gravels at the proximal head of the fan approaching >1 m in mean grain size. Esker-like segments in the fan suggest deposition on stagnant ice. The volume and coarse-grained nature of the sediment suggest a highly energetic, high discharge meltwater system. A number of such fans are evident in the area, suggesting frequent reorganization of a broad zone of stagnant ice at the Rainy Lobe margin.

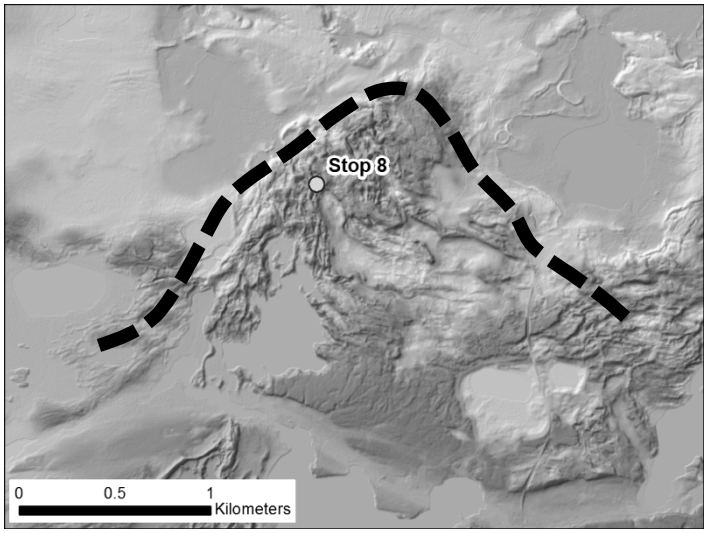
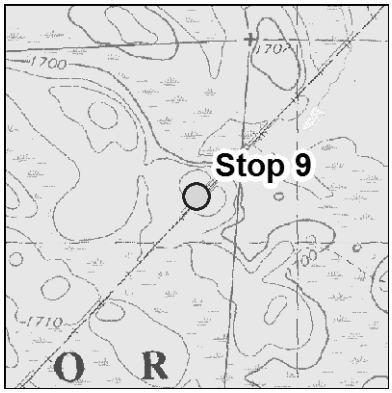


Figure 9. Ice-contact Rainy Lobe outwash fan.

STOP 9 - Rögen Moraine

627670E/5284350N (UTM Zone 15, NAD83 datum)
Sawbill Landing 7.5' USGS Quadrangle



Stop 9 is located in a road cut through a single Rögen moraine, described by Meyer (2009) (Fig. 10). The Rögen is composed of exceedingly dense till, and is part of a system of Rögen moraine characterized by 5-10 m of relief spaced 300-400 m apart along flow-lines. In this respect, these Rögen, situated at the very up-ice limit of the Toimi Drumlin field, are significantly different from the lower amplitude, shorter wavelength Rögen characteristic of the southwestern portion.

Ground-probing radar profiles through this and other Rögen ridges in the vicinity display structures evocative of northeast-dipping foresets, onlapping to the south (Fig. 11). These features suggest that Rögen may form by erosion of lee-side sediment and re-deposition on the stoss side of down-ice ridges, akin to migrating dune forms in fluvial systems. In this respect, Rögen may 'migrate' up-ice under flowing ice as the overall subglacial surface is lowered by net erosion.

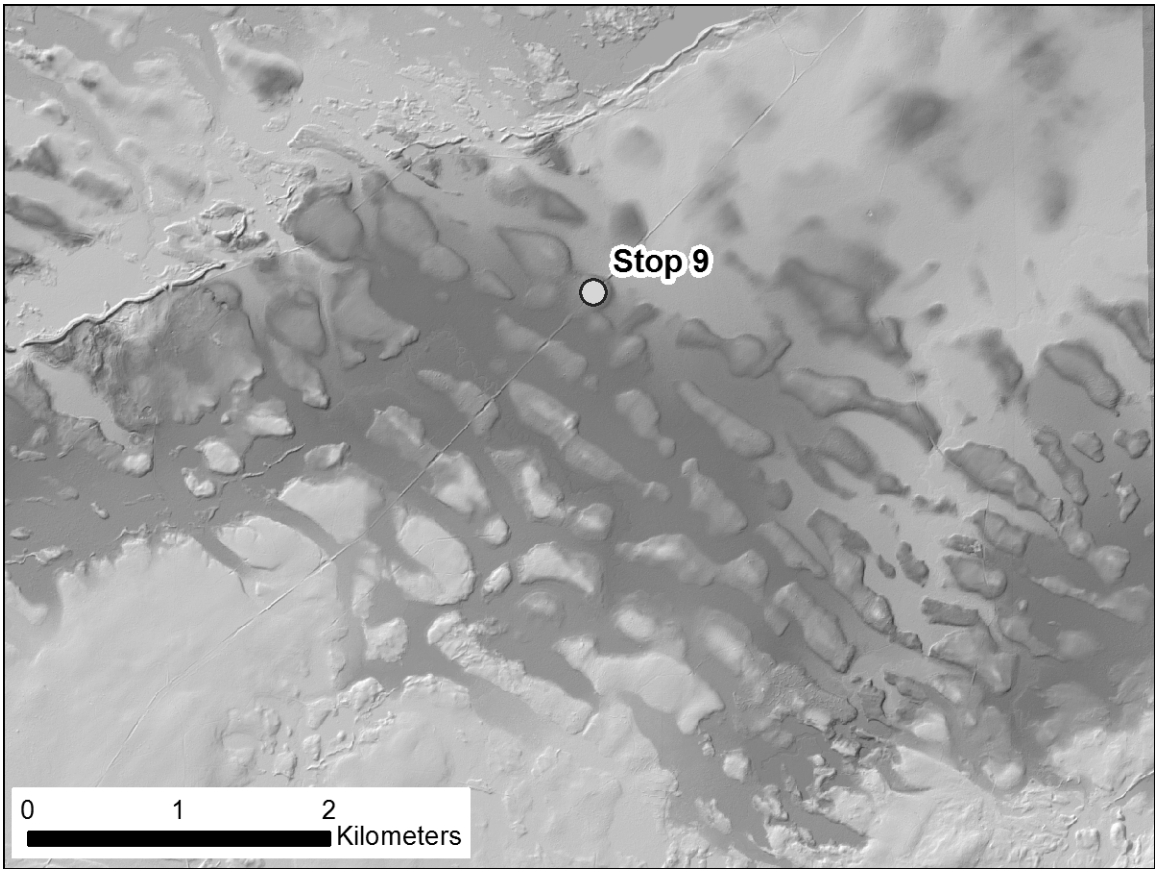


Figure 10. Rögen moraine near Sawbill Landing.

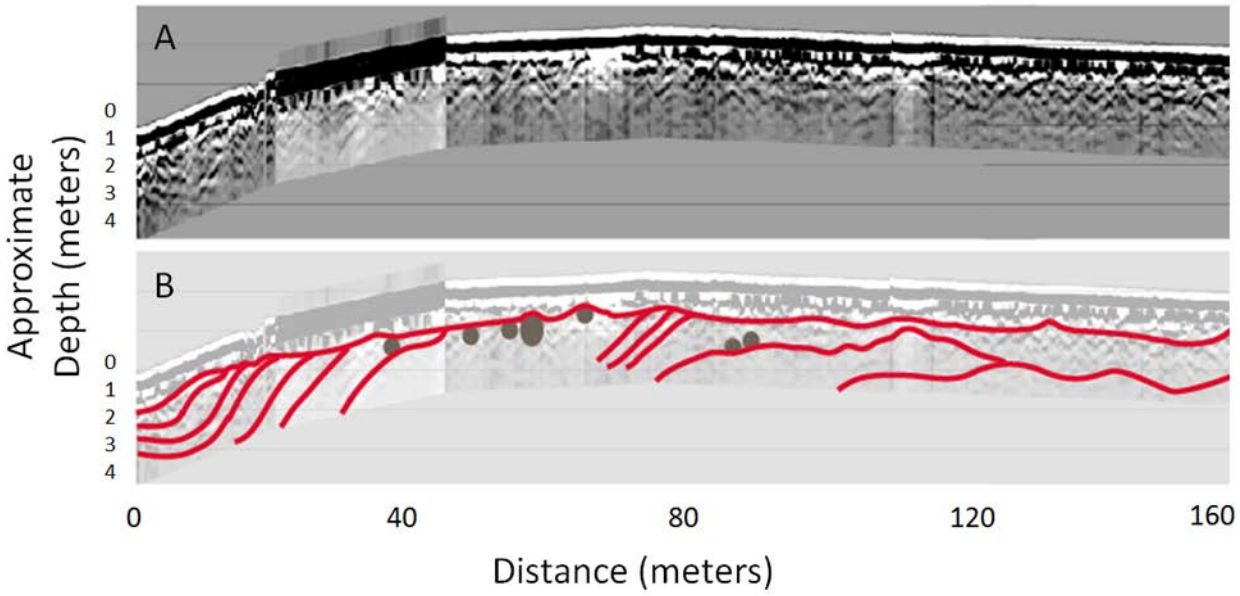


Figure 11. Ground penetrating radar (GPR) profile of a Rögen ridge near Sawbill Landing. Vertical scale is approximate based on radar two-way travel time. Ice flow direction is from left to right.

REFERENCES

Banerjee, S.K., and Lund, S.P., 1979, Geomagnetic record in Minnesota lake sediments - Absence of the Gothenburg and Erieau excursions: Geology, v. 7, p. 588–591.

Birks, H.J.B., 1976, Late Wisconsinan vegetational history at Wolf Creek, central Minnesota: Ecological Monographs v. 46, p. 395-429.

Birks, H.J.B., 1981, Late Wisconsin vegetational and climatic history at Kylen Lake, northeastern Minnesota: Quaternary Research, v. 16, p. 222–355.

Björck, S., 1990, Late Wisconsin History North of the Giants Range, Northern Minnesota, Inferred from Complex Stratigraphy: Quaternary Research, v. 33, p. 18–36.

Brown, T.R., 1988, Eskers and heavy mineral prospecting, northeastern Minnesota: M.S. Thesis, p. 103 p.

Buchheit, R.L., Malmquist, K.L., and Niebuhr, J.R., 1989, Glacial Drift Geochemistry for Strategic Minerals; Duluth Complex, Lake County, Minnesota: Minnesota Department of Natural Resource Division of Lands and Minerals Project, v. 262, no. part I, p. 95 p.

Clayton, L, and Moran, S.R., 1982, Chronology of late Wisconsin glaciation in middle North America. Quaternary Science Reviews, v.1, pp55-82.

Elftman, A.H., 1898, The geology of the Keweenawan Area in northeastern Minnesota, Part I.: The American Geologist, v. 21, p. 90–109.

Eyles, N., Putkinen, N., Sookhan, S., and Arbelaez-Moreno, L., 2016, Erosional origin of drumlins and megaridges: Sedimentary Geology, doi: 10.1016/j.sedgeo.2016.01.006.

Fenelon, J.M., 1986, Glacial geology of the Cramer quadrangle, northeastern Minnesota. [M.S. Thesis]: Milwaukee, University of Wisconsin, 76pp.

Florin, M.B. and Wright, H.E., 1969. Diatom evidence for the persistence of stagnant glacial ice in Minnesota, Geological Society of America Bulletin, 80(4), 695-704.

Friedman, A.L, 1981, Surficial geology of the Isabella quadrangle, northeastern Minnesota [M.S. thesis]: Minneapolis, University of Minnesota, 66pp.

Friedrich, H.G., 2011, Assessment of Sand and Gravel and Clay Deposits in Parts of Northern St. Louis and Lake Counties: Minnesota Department of Natural Resource Division of Lands and Minerals Project, v. 380, p. 1–47.Fries, M., 1962, Pollen Profiles of Late Pleistocene and Recent Sediments from Weber Lake, Northeastern Minnesota: Ecology, v. 43, no. 2, p. 295–308.

Hobbs, H.C., Friedman, A.L., Fenelon, J.M., and Stark, J.R., 1988, Surficial Geologic Map of the Greenwood Lake, Isabella, and Cramer Quadrangles, Minnesota: Minnesota Geological Survey Open-File Report, v. 88-02.

Johnson, M.D., Adams, R.S., Gowan, A.S., Harris, K.L., Hobbs, H.C., Jennings, C.E., Knaeble, A.R., Lusardi, B.A., and Meyer, G.N., 2016, Quaternary lithostratigraphic units of Minnesota: Minnesota Geological Survey Report of Investigations RI-68.

Kryzer, R., Mooers, H.D., and Larson, 2013, Rögen moraine as a transitional bedform in an erosional subglacial system: Geological Society of American Abstracts with Programs, v. 45, no. 7, p. 119.

Lehr, J.D., and Hobbs, H., 1992, Field Trip Guidebook for the Glacial Geology of the Laurentian Divide Area, St. Louis and Lake Counties, Minnesota: Minnesota Geological Survey Guidebook Series 18.

Leverett, F., 1932, Quaternary Geology of Minnesota and Parts of Adjacent States: USGS Professional Paper, v. 161, 149 pp.

Lowell, T. V., Fisher, T.G., Hajdas, I., Glover, K., Loope, H.M., and Henry, T., 2009, Radiocarbon deglaciation chronology of the Thunder Bay, Ontario area and implications for ice sheet retreat patterns: Quaternary Science Reviews, v. 28, no. 17-18, p. 1597–1607, doi: 10.1016/j.quascirev.2009.02.025.

Lund, S.P., and Banerjee, S.K., 1985, Late Quaternary paleomagnetic field secular variation from two Minnesota Lakes: Journal of Geophysical Research: Solid Earth, v. 90, no. B1, p. 803–825, doi: 10.1029/JB090iB01p00803.

Martin, D., and Eng, M., 1985, Esker Prospecting Over the Duluth Complex in Northeastern Minnesota: Minnesota Department of Natural Resource Division of Lands and Minerals Project, v. 246, p. 27.

Meyer, M.S., 2009, Paleoglaciological context of Rögen moraine, northeastern Minnesota: University of Minnesota Duluth, 71 p.

Mooers, H.D., and Lehr, J.D., 1997, Terrestrial record of Laurentide ice sheet reorganization during Heinrich events: Geology v. 25, p. 987-990.

Todd, J.E., 1898, A revision of the moraines of Minnesota: American Journal of Science (ser. 4), v. 6, p. 469-477.

Upham, W., 1894, Preliminary report of the field work during 1893 in northeastern Minnesota, chiefly relating to the glacial drift, in Winchell, N. H., Geological and Natural History Survey of Minnesota, 22nd Annual Report, for the year 1893, pp.18-86.

Winchell, N.H., 1899, The geology of the north part of St. Louis County, in Winchell, N.H., The geology of Minnesota, Volume IV of the final report: Geological and Natural History Survey of Minnesota, p. 222-265.

Winchell, N.H., 1900, Glacial Lakes of Minnesota. Geological Society of America Bulletin v. 12, p. 109-128.

Winter, T.C., 1971, Sequence of Glaciation in the Mesabi-Vermilion Iron Range Area, Northeastern Minnesota: USGS Professional Paper, v. 750-C, p. C82–C88.

Wright, H.E., and Watts, W.A., 1969, Glacial and Vegetational History of Northeastern Minnesota: Minnesota Geological Survey Special Publication, v. 11, 59 pp.

Wright, H. E. Jr., 1964, The classification of the Wisconsin Glacial Stage. Journal of Geology 72, 628-637.

Wright, H.E., 1972, Quaternary history of Minnesota, in Sims, P.K. and Morey, G.B. eds., Geology of Minnesota: A Centennial Volume, St. Paul, Minnesota, p. 515–547.

Wright, H.E., 1956, Sequence of glaciation in eastern Minnesota: Geological Society of America Guidebook for Field Trips, v. 3, p. 1–24.

FIELD TRIP 2

Wednesday, May 4, 2016

NEOARCHEAN GEOLOGY OF THE WESTERN VERMILION DISTRICT

Mark Jirsa, Terry Boerboom, and Amy Radakovich

Minnesota Geological Survey

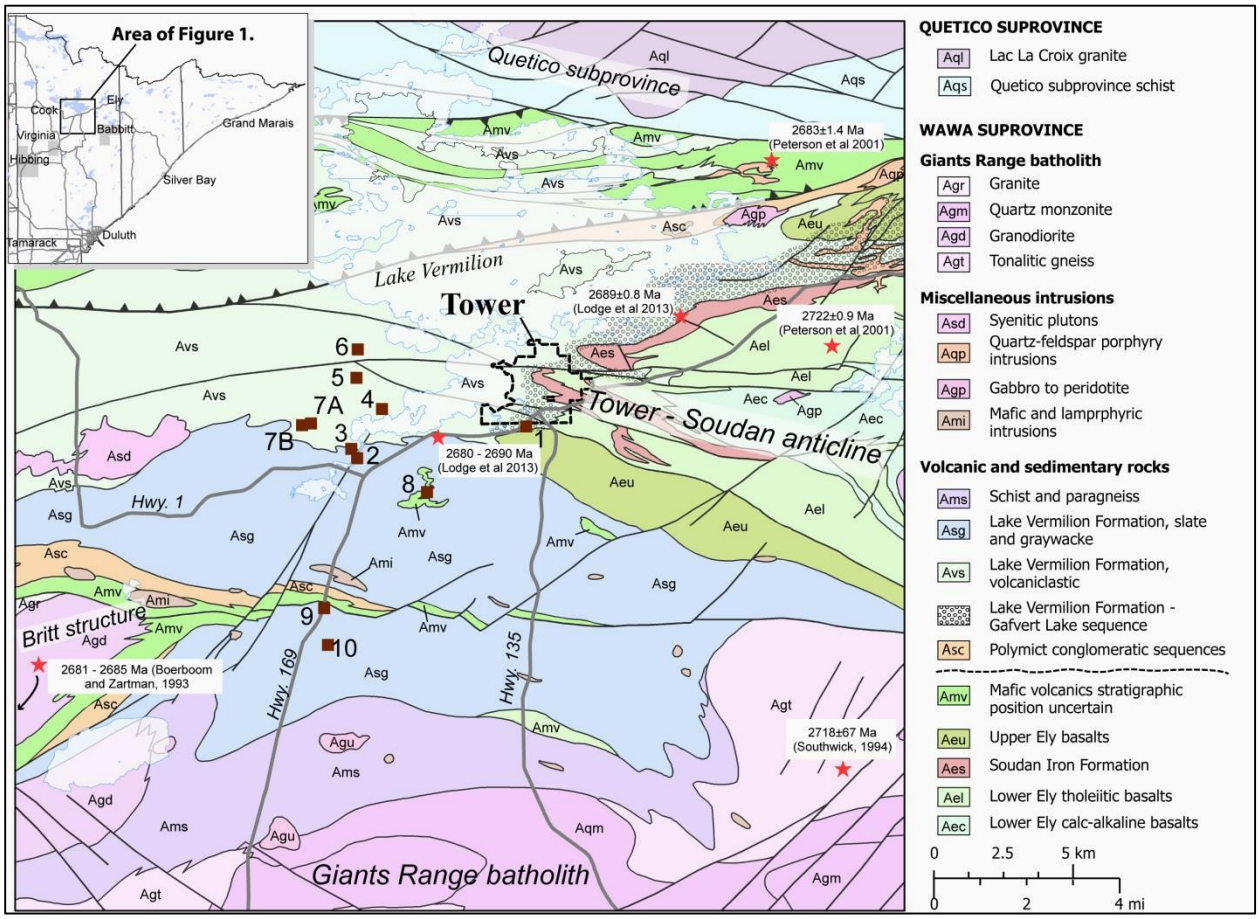


Figure 1. Regional bedrock geologic map showing locations of field trip stops (squares numbered 1-10), published geochronologic sample sites (stars), and pertinent geologic features. Modified from Jirsa and others, 2012.

INTRODUCTION

This field trip takes a preliminary look at stratigraphic relationships between older largely volcanic rocks inferred to be equivalent to the Ely Greenstone (~2720 Ma) and the apparently 30 Ma younger, volcanic, volcaniclastic, and epiclastic sedimentary strata of the Lake Vermilion Formation. New mapping supports recently acquired geochronologic data that indicates sediments of the Lake Vermilion Formation were deposited unconformably on the variably weathered, "deep-water" volcanic rocks. The significant hiatus, contrasting depositional environments, evidence for magmatism synchronous with sedimentation, and local unconformable contacts between the two units implies that the Lake Vermilion Formation formed in a late-tectonic extensional basin.

The field guide is brief, primarily for expediency, but also reflecting the tentative nature of newly acquired outcrop information on which it is based. The field work was the first phase of a multi-year effort by the Minnesota Geological Survey to create geologic atlases of St. Louis and Lake Counties—two of the largest counties in Minnesota. It was supported by a grant from the U.S. Geological Survey STATEMAP element of the National Geologic Mapping program, and by the Minnesota Environmental and Natural Resources Trust Fund. Although geochronologic analyses were conducted as part of this mapping, the new data are not yet ready for publication.

GEOLOGIC SETTING

The traditional definition of the Neoarchean Lake Vermilion Formation describes the unit as complexly interbedded strata that vary from felsic volcaniclastic rocks, to rocks having evidence of reworking, to mixed-source graywacke-siltstone. The informally named Gafvert Lake sequence (Fig. 1) consists of quartz- and plagioclase-phyric, dacitic to rhyodacitic breccia and tuff that yielded a $^{207}Pb/^{206}Pb$ age of 2689.7±0.8 Ma from magmatic zircons (Lodge and others, 2013). The sequence has been inferred to lie disconformably atop the Soudan Iron Formation member of the Ely Greenstone. Previous mapping (Jirsa and others, 2001) demonstrated that the iron-formation is transitional with metabasaltic rocks of the Lower Ely Greenstone, and a felsic unit within the greenstone yielded an age of 2722±0.9 Ma (Peterson and others, 2001). Thus, the Gafvert Lake sequence is approximately 30 Ma younger than the subjacent metabasalt- and iron-formation-bearing rocks. Quartzofeldspathic sediments apparently derived from the Gafvert Lake sequence make up a variable, but locally large proportion of the detritus in the Lake Vermilion Formation. Regionally, a series of outcrops from Gafvert Lake westward shows an irregular transition from proximal, perhaps subaerial deposition on the east, to distal submarine turbiditic fan deposition to the west. On this basis, the Gafvert is now considered part of the Lake Vermilion Formation, which by extension is also 30 Ma younger than greenstone. Recent field work was conducted in part to explore lithologic attributes of the Lake Vermilion Formation and ascertain the nature of contacts between these strata and the older greenstone. This field trip examines outcrop evidence that we believe documents the unconformable nature of these strata outboard of the Ely Greenstone. The evidence acquired to date is consistent with the inference that the Lake Vermilion Formation represents deposition in a Timiskaming-type successor basin, much like the equivalent Knife Lake Group to the northeast (Driese and others, 2011; Jirsa and others, in prep.) and the Midway sequence to the southwest (Jirsa, 2000).

The Ely Greenstone and Lake Vermilion Formation—as defined here—are part of the Wawa subprovince of the Superior Province. Temporal distinctions between various geologic components of this terrane are evolving with new geochronologic analyses. Nevertheless, they remain largely based on fabrics and structures that resulted from three major phases of deformation, denoted D_1, D_2, and D_3. The D_1 event involved generally pre-lithification deformation of graywacke sequences (in some localities forming large nappe structures), and tilting, broad folding, and thrust imbrication of the thick, more rigid volcanic strata. D_2 deformation accompanied regional metamorphism to greenschist to amphibolite facies, and produced pervasive metamorphic foliation and lineation, folding, and strike-slip faulting. U-Pb dates of intrusions bracket the D_2 event between about 2,674 and 2,685 Ma (Boerboom and Zartman, 1993). The Tower-Soudan anticline (Fig. 1) is considered a D_1 structure because both limbs of the complex fold are transected by D_2 cleavage that trends more northeasterly than bedding. Deposition of the Lake Vermilion Formation is bracketed to an approximately 10 million year period between volcanism of the Gafvert Lake sequence at ca. 2690 Ma, and its deformation during D_2 at ca. 2680 Ma. D_3 is assigned to partitioned deformation that produced crenulation and faults within rocks affected by D_2. All three deformation events can be attributed to variably north-northwest—south-southeast-directed transpression.

FIELD TRIP STOP DESCRIPTIONS

NOTE: all UTM coordinates are given in NAD 83, Zone 15



Figure 2. Poorly sorted fragmental rock containing clasts of quartz- and plagioclase-phyric dacite, rusty sulfides, and rare black mudstone. [Field station LS046]

STOP 1 – Felsic pyroclastic breccia and tuff—Gafvert Lake sequence; Lake Vermilion Formation

***Location*:** UTM: 0553467E/5294482N, Highways 1 and 169, west edge of village of Tower.

Description: The Gafvert Lake sequence consists of dacitic to rhyodacitic lava flows and pyroclastic rocks to the northeast that are more or less transitional with volcaniclastic strata to the west. This outcrop lies in the transition zone. It is poorly sorted and contains angular to subrounded clasts of dacitic composition (plagioclase and quartz-phyric) that range in size from several millimeters to 20 cm. Rare angular to ornate clasts of pyrrhotite and pyrite imply a pyroclastic origin. However, the presence of siltstone clasts locally, the subrounded nature of some dacitic fragments, and the rare appearance of bedding imply reworking has occurred.

DIRECTIONS: Continue west ~4 mi. along highways 1 and 169 to highway 77, turn north and proceed ~ 0.5 miles and cross Pike River to pull-off on west (left) side of highway.

STOP 2 – Feldspathic greywacke-mudstone of Lake Vermilion Formation—the "classic" outcrop

***Location*:** UTM: 0547272E/5293368N; west side of Hwy. 77, north side of Pike River near dam.

Description: This glacially scoured outcrop exposes a nearly perfect cross-section of tabular-bedded, variably graded, feldspathic graywacke and dark gray slate. The feldspar-rich, dacitic composition of the sandy textured beds is presumed to represent derivation from the Gafvert Lake sequence exposed to the east (Stop 1). The beds contain numerous "soft-sediment" deformation features including load structures, flames, intrafolial slump folds, and growth-faults. Bedding is nearly vertical, and graded beds indicate younging to the south. This topping direction is consistent with a position on the south limb of a large, south-overturned regional D_1 fold structure—inferred to be the western extension of the Tower-Soudan Anticline (Jirsa and Boerboom, 2003). Northeast-trending kink bands, fault zones, and quartz veins traversing the outcrop are assigned to the latest, D_3 deformation event.

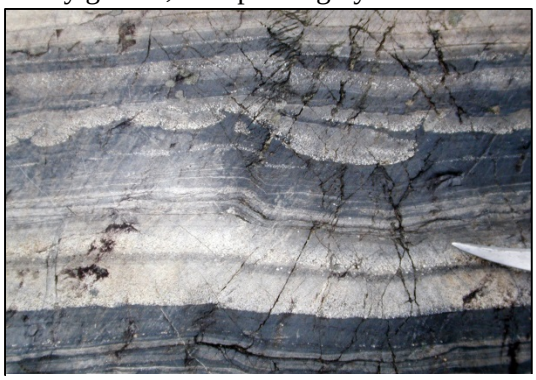


Figure 3. Road cut exposing white tonalite dike with large inclusions of adjacent black siltstone. Note 40 cm-long hammer in left-center of photo for scale. [Field station LS051]

DIRECTIONS: Walk/drive north ~700 feet to road cut on east (right) side of Highway 77

STOP 3 – Tonalitic dikes cutting sedimentary strata of the Lake Vermilion Formation

***Location*:** UTM: 0547193E/5293565N; road cut on east side of County Rd 77

Description: On first glance, this outcrop appears to represent chaotic dacitic (arkosic) sedimentary strata interbedded with gray sandstone and black siltstone, compositionally similar to that at Stops1 and 2.



Figure 4. Graded beds of white arkosic sandstone and feldspathic graywacke, black siltstone and mudstone. Stratigraphic facing is up in the photo (southward).

Graded sandstone-siltstone couplets indicate stratigraphic facing to the south, as at stop 2. Closer inspection reveals the "dacitic" rocks are tonalitic dikes emplaced more or less along bedding planes of the enclosing sandstone-siltstone. Discordance is only evident locally. Tonalitic dikes are fine- to medium-grained, equigranular, and contain abundant quartz. The intrusion suspended numerous angular to subangular xenolithic inclusions of mudstone and siltstone as large as 1m in diameter. Many of the inclusions have dark, presumably contact metamorphic rinds. A smaller tonalitic intrusion exposed in the northern part of the outcrop is cut by a 2-meter wide lamprophyric dike.

DIRECTIONS: Return to vehicle near Pike River; drive north on Hwy 77 approximately 1.3 mi. to County Road 104 (Bois Forte or Vermilion Reservation Rd.); drive east ~0.7 mi. to Waters if Vermilion Rd. on the south; drive south ~0.2 mi. to STOP 4.

STOP 4 – Arkosic sandstone and siltstone of Lake Vermilion Formation

***Location*:** UTM: 0548130E/5294880N; *PRIVATE PROPERTY!*

Description: This apparently blasted and cleaned outcrop consists of white, coarse to fine grained arkose, with rare gray-black siltstone layers. The arkose is inferred to have been sourced from the Gafvert Lake sequence. The exposure provides a 3-dimensional view of some inferred depositional, dewatering, and compaction features. Where it can be determined, stratigraphic facing is southward as at previous stops 2 and 3. The remarkable similarity between the arkose here and the tonalitic dikes at stop 3 invite correlation and a preliminary interpretation that magmatism was synchronous with sedimentation.

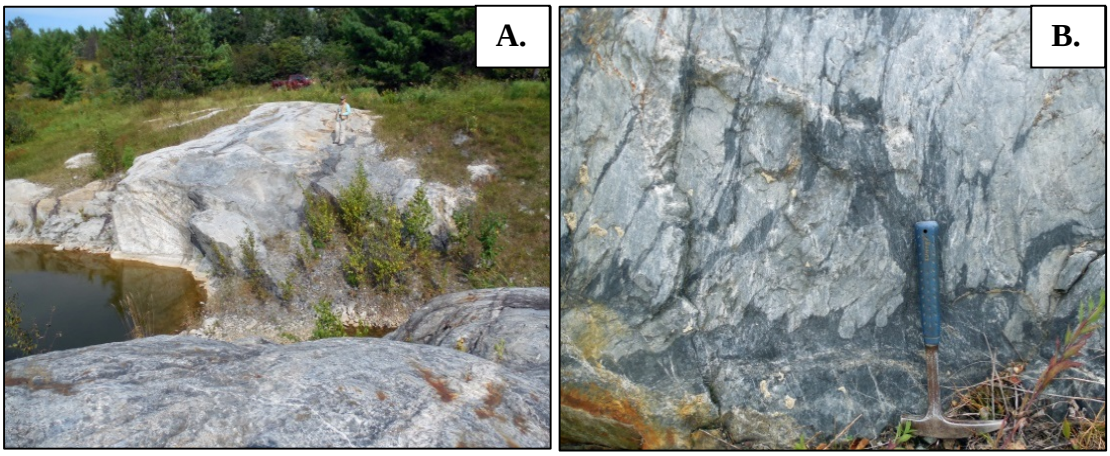


Figure 5. **A**. White arkose with rare lenses, layers, and fragments of black siltstone (Amy Radakovich for scale). **B.** Ball and pillow structures inferred to have formed during settling and dewatering of inferred mass flow deposit. [Field station LS056, "Majestic Rocks" development]

DIRECTIONS: Return to Highway 77, turn north (right) and proceed 0.6 miles to road cut on east side of highway.

STOP 5 – Mixed-source graywacke of Lake Vermilion Formation cut by quartz-plagioclase (tonalitic) dikes

***Location*:** UTM: 0547145E/5296230N; Long road cut on east side of Highway 77.

Description: Complex exposure of mixed-source graywacke cut by several fine- to medium-grained quartzofeldspathic (tonalitic) dikes. The southern third of the roadcut consists entirely of tonalite. Normal faulting is apparent locally. Stratigraphic facing is northward (Fig. 6A)—the inverse of that at prior stops 2-4—which reflects a geographic position north of an inferred D_1 antiformal nappe structure that may be the western extension of the Tower-Soudan anticline (see Jirsa and Boerboom, 2003).

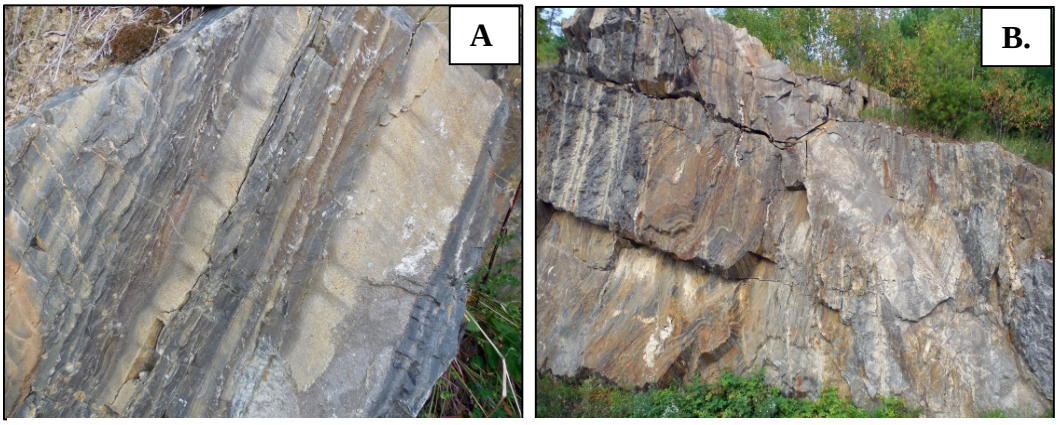


Figure 6. **A.** Graded bedding in mixed-source feldspathic graywacke-siltstone; stratigraphic facing is to the left in photo (north in outcrop). **B.** Mixed source graywacke-siltstone cut by one of several tonalitic dike dipping to right (south in outcrop). [Field station LS058]

DIRECTIONS: Continue north on Highway 77 for ~0.5 miles to road cut on east side of highway.

STOP 6 – Large D_2 folds and shear zones in mixed-source graywacke of Lake Vermilion Formation

***Location*:** UTM: 0546970E/5297030N; Road cut on east side of Highway 77.



Figure 7. D_2 folds (dashed white lines) of thinly bedded graywacke-siltstone [Field station LS059]

Description: Long road cut that exposes complex shearing and folding in mixed-source graywacke-siltstone beds. Shearing is manifest as ankerite-sericite-chlorite phyllite near the south end of the cut. Folds exposed farther north along the road cut are tight to isoclinal synforms and antiforms having D_2 fold axes that are steeply dipping. Considerable rodding lineation of more competent sandy beds indicates shallow plunge (~47°) to the east (away from the viewer).

DIRECTIONS: To STOP 7A—U-turn to head south on Highway 77 for ~1.4 mi. to Lost Lake Road; turn west (right) and proceed 0.8 miles to gated trail entry.
To STOP 7B—drive west on Lost Lake Road ~0.2 mi. and turn south (left) on Holter Road and proceed 0.2 mi. to shallow gravel pit on east side of road. NOTE: BOTH STOPS ON PRIVATE PROPERTY.

STOPS 7A, 7B –Conglomerate with abundant volcanic and sulfidic clasts similar to Stop 1

***Locations*: A.** UTM: 0545650E/5294580N; **B.** 0545365E/5294515N; both exposures on floors of shallow gravel pits—*PRIVATE PROPERTY!*

Description: These two stops (7A and B) expose slightly different versions of conglomerate in an area essentially surrounded by arkosic and mixed-source sedimentary strata similar to stops 2-6. Both stops are glacially polished outcrops of clast-supported conglomerate. The conglomerate contains abundant felsic to intermediate volcanic fragments, together with clasts of layered siliceous rock, dacitic porphyry, and sulfide-rich rock. Clasts vary from rounded to subangular. The overall composition of fragments and the presence of sulfide clasts indicates a potential correlation with volcanic strata of the Gafvert Lake sequence as seen at stop 1, which we interpret to lie stratigraphically beneath the exposures at stops 2-6. On this basis, we infer that the conglomerate represents a localized uplift of the basin floor on which other sediments of the Lake Vermilion Formation were deposited. This is consistent with a structural position near the axis of an antiformal D_1 nappe structure inferred to be the western extension of the Tower-Soudan anticline (as shown on Jirsa and Boerboom, 2003).



Figure 8. Lithologically diverse conglomerate (including abundant sulfide clasts on right side) at STOP 7A. [Field station LS141]

DIRECTIONS: Continue south on Holter road ~1 mi. to Highway 1; turn east on Hwy 1 and proceed 1.5 miles to junction with Highway 169; turn southwest (right) on 169 and travel 0.8 miles to Peyla Road; turn east and travel to STOP 8 described below. Access will depend on road conditions, and several scattered exposures off Peyla Road will be examined.

STOP 8 – Peyla sequence – basalt, conglomerate, and sandstone
***Location*:** UTM: 0549822E/5292233N and environs, Tower quadrangle, Peyla Road east of Highway 169.

Description: Near the end of Peyla Road is a series of outcrops of pillow basalt overlain by mafic conglomerate interbedded with sandstone (Figure 9). Published geologic maps (Ojakangas and others, 1978, Sims and Southwick, 1985, Southwick, 1993) show the basalts but do not distinguish the conglomerate and sandstone from the typical graywacke of the Lake Vermilion Formation.

The Peyla conglomerate and interbedded sandstone overlie variably variolitic pillow basalt (Figure 9). Clasts in the conglomerate range from less than 1 cm to as much as 40 cm in size and are very angular; in fact the term ‘sedimentary breccia’ might be more appropriate in most cases. Topping indicators in both the basalts and sediments are difficult to find.

The conglomerate (Figure 10A) is dominated by fine-grained basalt clasts that include weakly porphyritic, variolitic, and amygdaloidal phases. Medium-grained clasts of metagabbro/lamprophyre are common and in a few places predominant; other less common clast types include fine-grained possibly tuffaceous felsic rocks, and rare clasts of sulfides (pyrite) and hornblende-phyric andesitic hypabyssal intrusive rocks (Figure 10B). The matrix is similar to the adjacent sandstone. The varied types of basalt clasts (amygdaloidal, massive, variolitic, and porphyritic) imply reworking of the basalt substrate, and the polymictic nature of the conglomerate leads to the inference that this is a "Timiskaming-type" sedimentary package.

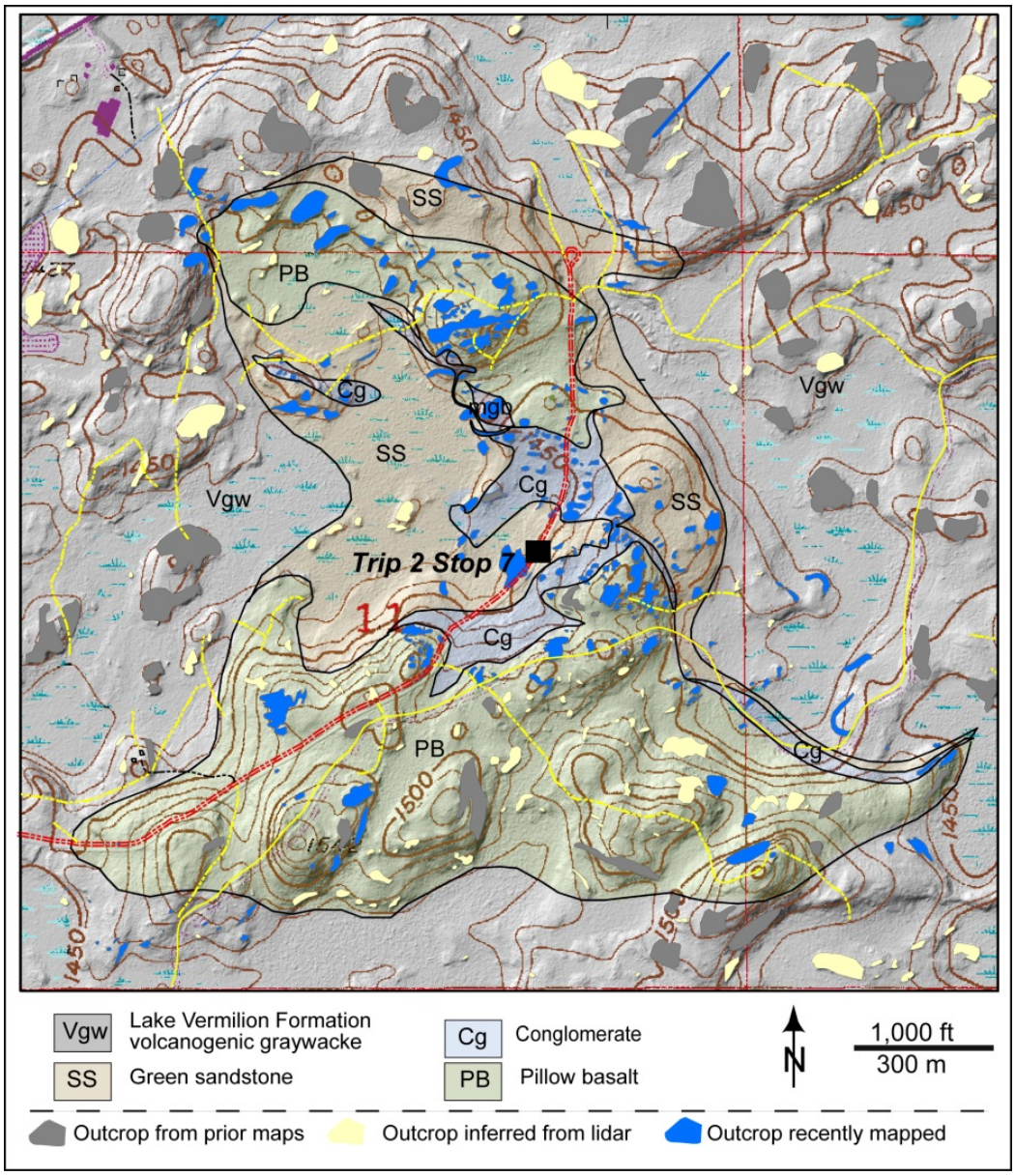


Figure 9. Preliminary geologic map of the Peyla sequence on a 1 m lidar base. Most of fringing area has not been re-examined as part of recent field work, and the full extent of Timiskaming-type sandstone and conglomerate has not been established. The units shown here as green sandstone and conglomerate had not been distinguished on prior published maps, thus the fringing area is subject to revision by future mapping endeavors.

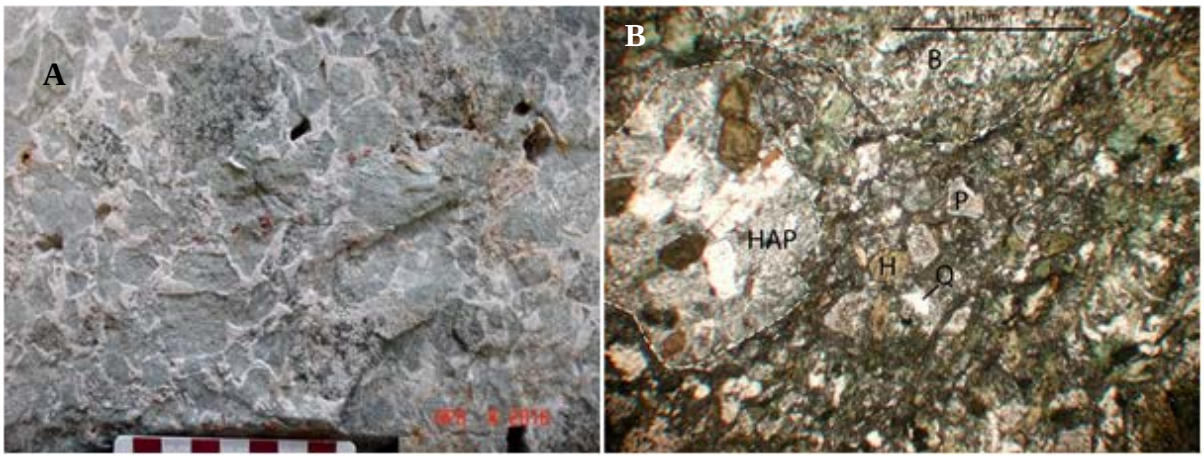


Figure 10. Photograph (A; scale in cm) and photomicrograph (B) of typical Peyla conglomerate. Photomicrograph shows the edge of a basalt clast (B), a clast of hornblende-plagioclase porphyry (HAP), and hornblende (H) and plagioclase crystals (P) in the sandy matrix, which also contains minor quartz (Q). Lithic clasts outlined by white dashed line. Scale bar= 1 mm. The photomicrograph is from a different sample than that shown in the left photo.

The 'green sandstone' (field term) interbedded with the conglomerate contains detrital plagioclase which commonly exhibits blocky and broken shapes, minor quartz derived from a volcanic source, blocky to euhedral detrital hornblende, small mafic to felsic volcanic rocks fragments, and rare detrital sphene and apatite along with metamorphic epidote, hornblende, biotite. The sandstone is typically quite massive and poorly bedded.

The Peyla basalts are commonly variolitic, with irregular pillow shapes that commonly don't yield reliable topping indicators. Locally the interiors of the pillows exhibit an incipient state of brecciation (Figure 11), outlining fragments similar in size and shape to those in the conglomerate. The reason for this brecciation is not known, but speculatively may be due to weathering and paleosol development prior to or during deposition of the overlying conglomerate and sandstone. Further development of this fracturing/brecciation process may have produced disaggregated fragments of angular basalt that were then shed into the adjacent sediments.



Figure 11. Incipient brecciation in basalt. The sizes and shapes of these fragments are similar to the angular basalt clasts in the overlying mafic conglomerate. The white veining between the fragments is composed of clinozoisite, quartz, and carbonate.

Mafic lamprophyric dikes, typically less than 2 meters wide and with sharp straight edges, intrude the sedimentary rocks, but none have been noted in the basalts so far. Multiple generations of lamprophyric dikes are visible on some outcrops, as well as rare instances of apparent lamprophyric peperite (Figure 12). The presence of mafic peperite and the clasts of hornblende-rich mafic intrusive rocks in the conglomerate imply that the lamprophyres may be related to subalkalic igneous activity contemporaneous with deposition of the sedimentary rocks. In contrast, very few if any mafic/lamprophyric dikes were noted in the Peyla basalts, based on the mapping completed thus far. The reason for this is not clear, but could be that the basalts were relatively impermeable to the dikes compared to the overlying sedimentary rocks.



Figure 12. Thin dark green lamprophyric intrusion; on one side is in sharp, straight contact with the conglomerate and on the other side is diffuse and peperitic.

DIRECTIONS: Return to Highway 169 and continue south. Drive ~2 miles from Peyla road to Flaim road, which is at the south end of a long road cut. Turn right (west) on Flaim road and park (STOP 9).

STOP 9 – Sandstone, pillowed basalt, and lamprophyric dikes.
***Location*:** UTM: 0546116E/5287910N (Intersection of Flaim Road and Hwy. 169; Park on Flaim Road).
Note: the road shown on the published Biwabik NW quadrangle is the old road which has been straightened and now cuts further west.

Description: This is a new road cut that runs north-south parallel to Highway 169, and along the north side of Flaim Road west of Highway 169. It exposes metasedimentary strata on the south, and metavolcanic strata on the north, and mafic dikes emplaced into both rock types. Start on the western-most outcrops along the north side of Flaim road and work east toward the highway. This glacially polished flat outcrop consists primarily of light tan-colored, fine-grained sandstone, having weakly graded beds that indicate southward stratigraphic facing. The sedimentary strata were intruded by 2 lamprophyric/dioritic dikes. Both the dikes and the bedding in the sedimentary strata dip steeply. One of the dikes contains xenoliths of varied rock types that range from 5 to 60 cm in size, and include layered

tonalitic gneiss, porphyritic dacitic volcanic rocks, granodioritic to tonalitic intrusive rocks, and mafic schist. Adjacent to (south of) the inclusion-rich lamprophyre is a >30 cm thick dike of hornblende- and plagioclase-phyric diorite. This dike contains abundant phenocrysts of equant hornblende and blocky plagioclase as large as 3mm (Figure 13A), and small apatite crystals visible only in thin section.

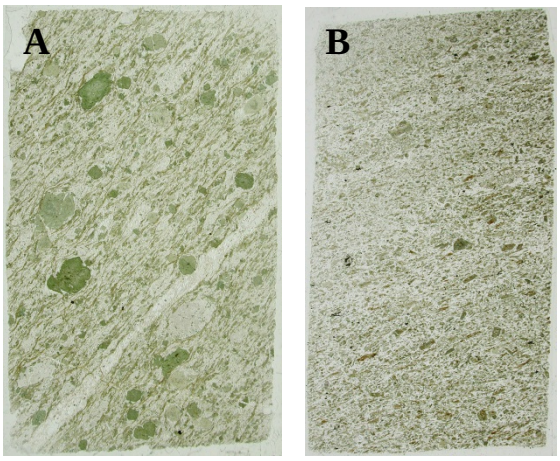


Figure 13. Plane light photographs of thin sections of samples from this stop (sections are approximately 2.5 cm wide).

A – Hornblende- and plagioclase-phyric lamprophyric dike that intruded sedimentary strata.

B – Lamprophyric dike that intruded pillow basalt showing trachytoid alignment of euhedral hornblende crystals.

Continue walking east to Highway 169 along the sandstone outcrop, then go north along the freshly blasted roadcut. It is difficult to distinguish between the sandstone and subjacent basalt on the fresh rock faces; however, the transition is marked by a rusty interval that is visible from a distance (look to the outcrops across the highway). Two cherty horizons occur within the basalt– a layer that is orange in color, and further north a black chert horizon that contains thin layers of pyrite. Numerous dark green 0.5 – 10 m thick lamprophyric/mafic dikes are present within the basalt.

Continue to north end of roadcut, climb up to top, and walk back south. Here on the glacially polished exposure one can see pillowed metabasalt and the mafic dikes emplaced into them. The dikes are weakly hornblende-phyric (Figure 13B), have chilled margins, and appear to be less deformed than the basaltic host. One highly unusual feature in the pillow basalt is the presence of two 7 cm rounded xenoliths of pink, medium-grained granite (Figure 14). The nearly vertical contact between the pillowed metabasalt to the north and adjacent metasedimentary strata to the south is fairly straight, abrupt, and lacks evidence for shearing that might indicate a fault origin. Although the contact zone is quite rusty (presumably pyritic), the contact is unremarkable. Nevertheless, the contrast in apparent depositional environments, and the abrupt termination of pillowed basalt (i.e., no gradation of pillows to flow-top breccia) implies that the contact is an unconformity.



Figure 14. Rounded xenolith of pink, medium-grained granite in pillow basalt, on upper flat outcrop surface. UTM coordinates notes as 546129, 5288055 (Nad83 zone 15).

STOP 10 – Conglomerate and metagraywacke, mafic dikes.
***Location*:** UTM: 0546327E/5286624N (Hwy. 26 0.6 mi east of Hwy. 169).

Description: Highly flattened/lineated multi-lithic conglomerate interbedded with tightly folded graywacke, which is cut by multiple north-dipping, weakly foliated mafic/lamprophyric dikes.

The conglomerate contains 1-10cm (longest dimension in end view) clasts that are also lineated (foliation N85°E, 70°N; lineation plunge 45° to N70°E). The clasts show weak size grading, and vary from felsic (light grayish-tan to pink and fine-grained) to mafic (dark green plagioclase-phyric, hornblende-rich; Figure 15). The matrix contains little if any quartz, and is generally dark green and amphibolitic; however it is commonly difficult to distinguish between matrix and pseudomatrix (i.e., flattened, less competent clasts). The surface of the conglomerate outcrops has a patchy pink staining, which is likely due to abundant microcline.

In thin section the fine-grained light-colored clasts are composed predominantly of finely granoblastic microcline, with some larger (but less than 1mm) grains of irregularly-shaped plagioclase that may have been phenocrysts, and little if any quartz. Other clasts cannot be distinguished from matrix/pseudomatrix. Some of the clasts are more coarse-grained and microcline-rich, and may in part be granoblastic-recrystallized syenite. The matrix is composed of granoblastic plagioclase and metamorphic amphibole, lesser K-feldspar, and minor carbonate, and has small blocky, saussuritized plagioclase crystals.

The metagraywacke in the western portion of this outcrop exhibits some weakly graded beds which mostly indicate south topping, thus are slightly overturned. Fine-grained amphibolitic lenses are present in the graywacke, and overall it has a slight orange stain due to finely disseminated pyrite.

The mafic dikes here are likely of the same timing as those which cut the pillow basalts at stop 9.

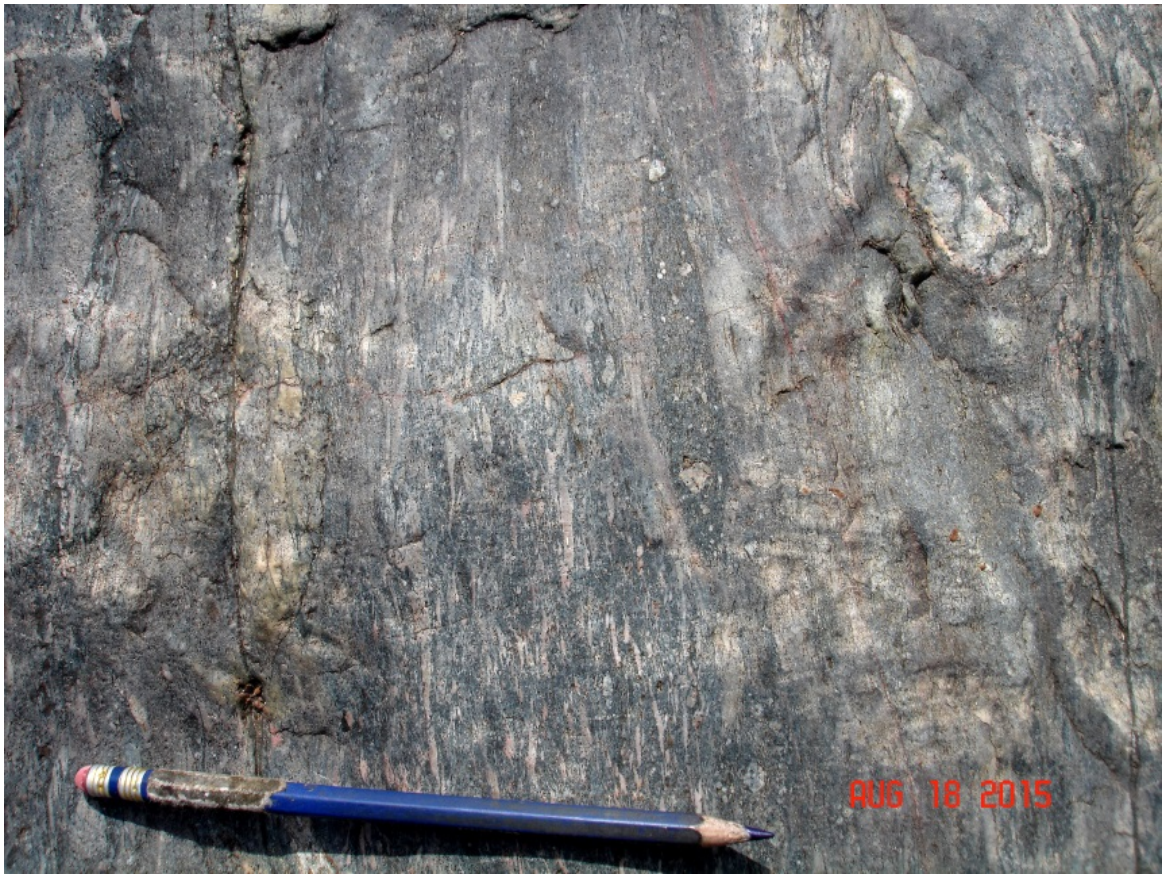


Figure 15. Strongly flattened and lineated dark green mafic-intermediate plagioclase-phyric clasts and smaller fine-grained, light-colored clasts in conglomerate.

REFERENCES

Boerboom, T.J., and Zartman, R.E., 1993, Geology, geochemistry, and geochronology of the central Giants Range batholith, northeastern Minnesota: Canadian Journal of Earth Science, v.30, p. 2510-2522.

Driese, S.G., Jirsa, M.A., Ren, M., Sheldon, N.D., Brantley, S.L., Parker, D., and Schmitz, M., 2011, Neoarchean paleoweathering of tonalite and metabasalt: Implications for reconstructions of 2.69 Ga early terrestrial ecosystems and paleoatmospheric chemistry: Precambrian Research, v. 189, p. 1-1.

Jirsa, M.A., 2000, The Midway sequence: a Timiskaming-type, pull-apart basin deposit in the western Wawa subprovince, Minnesota: Canadian Journal of Earth Sciences, 37:1-15.

Jirsa, M.A., and Boerboom, T.J., 2003, Bedrock geology of the Vermilion Lake 30' X 60' quadrangle, northeast Minnesota: Minnesota Geological Survey Miscellaneous Map M-141; scale 1:100,000.

Jirsa, M.A., Boerboom, T.J., and Chandler, V.W., 2012, Geologic map of Minnesota: Precambrian bedrock: Minnesota Geological Survey State Map Series S-22, scale 1:500,000.

Jirsa, M.A., and Boerboom, T.J., and Peterson, D.M., 2001, Bedrock geologic map of the Eagles Nest quadrangle, St Louis County, Minnesota: Minnesota Geological Survey Miscellaneous Map M-114; scale 1:24,000.

Jirsa, M.A., Starns, E., and Schmitz, M.D., *in prep*., Bedrock geologic map of the Cavity Lake fire area, northeastern Minnesota: Minnesota Geological Survey Miscellaneous Map M-193, scale 1:24,000 [*in preparation*—in the interim, refer to MGS Open-File Report OF-08-05, or contact lead author for details].

Lodge, R.W.D., Gibson, H.L., Stott, G.M., Hudak, G.J., and Jirsa, M.A., and Hamilton, M.A., 2013, New U-Pb geochronology from Timiskaming-type assemblages in the Shebandowan and Vermilion greenstone belts, Wawa subprovince, Superior Craton: Implications for the Neoarchean development of the southwestern Superior Province: Precambrian Research v. 235, p. 264-277.

Ojakangas, R.W., Sims, P.K., and Hooper, P.R., 1978, Geologic map of the Tower quadrangle, St. Louis County, Minnesota: U.S. Geological Survey geologic quadrangle map GQ-1457, scale 1:24,000.

Peterson, D.M., Gallup, C., Jirsa, M.A., and Davis, D.W., 2001, Correlation of Archean assemblages across the U.S.-Canadian border: Phase geochronology: Institute on Lake Superior Geology, 47th Annual Meeting, Madison, Wisc., Proceedings v. 47, Part 1., p.77-78.

Sims, P.K, and Southwick, D.L, 1985, Geologic maps of Archean rocks, western Vermilion District, northern Minnesota: U.S. Geological Survey Miscellaneous Investigation Series Map I-1527, scale 1:48,000.

Southwick, D.L., 1993, Geologic map of Archean bedrock, Soudan-Bigfork area, northern Minnesota: Minnesota Geological Survey Miscellaneous Map Series map M-79, scale 1:100,000.

Southwick, D.L., 1994, Assorted geochronologic studies of Precambrian terranes in Minnesota: A potpourri of timely information: *in* Southwick, D.L., (Ed.), Short contributions to the geology of Minnesota: Minnesota Geological Survey Report of Investigations 43, p. 1-19. [age reference in Figure 1]

CU-NI-PGE DEPOSITS OF THE DULUTH COMPLEX-GEOLOGY AND DEVELOPMENT

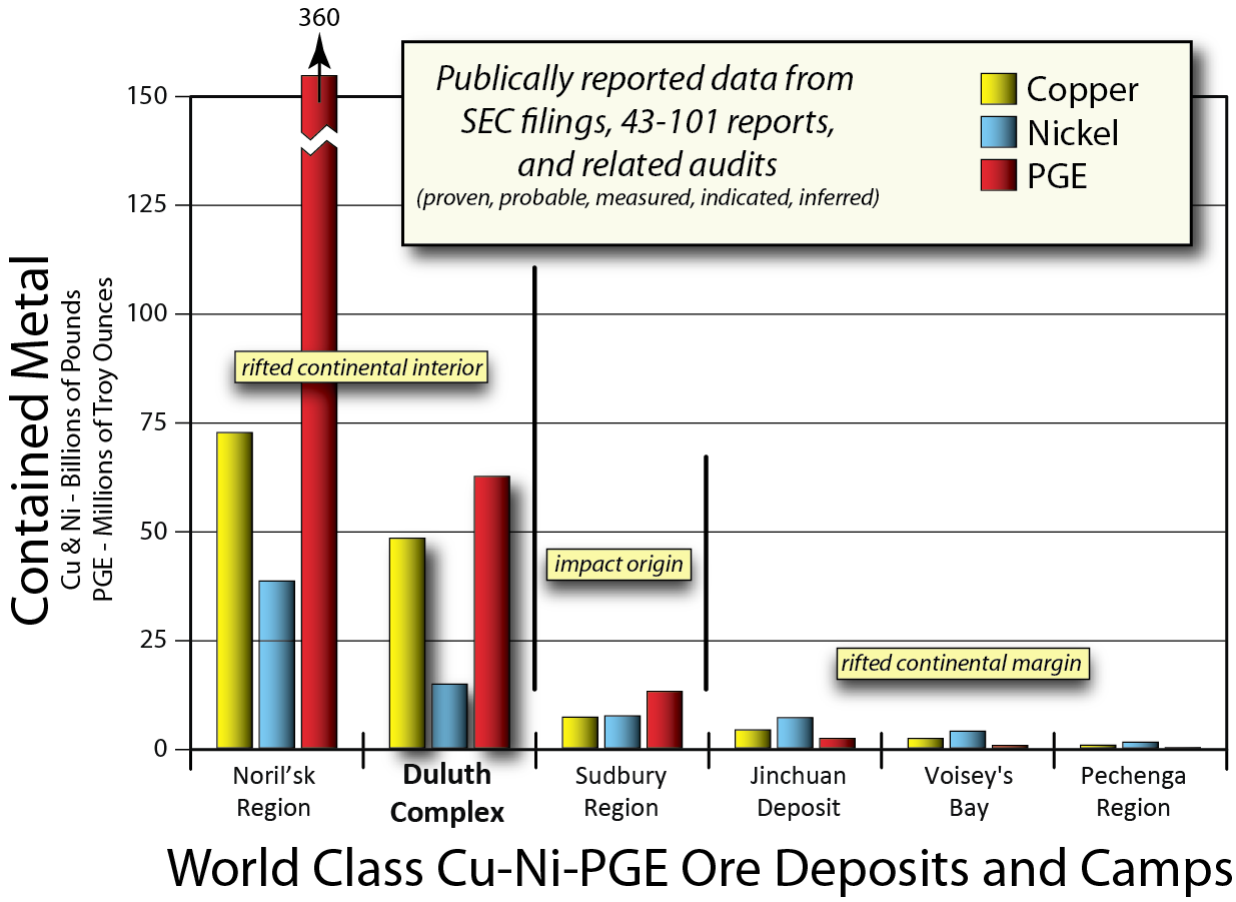


Figure from Dean Peterson.

(Note that resources are exclusive of reserves, and that various mineral resources were added to various mineral reserves just to allow comparisons in orders of magnitude. Note also that some of the categories only consider mineral in the ground and do not take into consideration the costs, recoveries, and other relevant factors associated with extraction and recovery of the metal or mineral)

Mark Severson (Teck American Incorporated)
Andrew Ware (PolyMet Mining)
Kevin Boerst (Twin Metals)
Stephen Monson Geerts (Natural Resources Research Institute)

Portions previously written by:
Richard L. Patelke (formerly with PolyMet Mining)
Tim Jefferson (formerly with Teck-Cominco Inc.)
Dean M. Peterson (formerly with Duluth Metals Limited)

EXPLORATION AND DEVELOPMENT BACKGROUND

By the late Richard Patelke (PolyMet Mining) with modifications by Mark Severson

Large resources of low-grade copper-nickel sulfide ore that locally contain PGE concentrations are well documented by drilling in the basal zones of the Partridge River, Bathtub, and South Kawishiwi intrusions. At least eleven occurrences of significant mineralization have been delineated in the basal 300 to 1000 feet of these intrusions. Of these eleven occurrences, two projects have undergone fairly recent definition drilling, including the Mesaba deposit (Teck American) and Maturi deposit (Twin Metals). Definition drilling at the Birch lake deposit (Twin Metals) took place up to four years ago. A fourth project, the NorthMet deposit (PolyMet Mining) is currently undergoing environmental review and mine permitting. Recent exploration drilling has taken place at the Serpentine deposit (Encampment Resources). Overall, the copper-nickel mineralization consists predominantly of disseminated sulfides that historically are estimated to contain over 4.4 billion tons of material averaging 0.66% Cu and 0.20% Ni at a 0.5% Cu cut-off, according to an earlier study (Listerud and Meineke, 1977): note that this estimate is historic and does not follow reporting guidelines as established by CIM Definition Standards).

As outlined in Miller et al. (2002a), serious exploration for Cu-Ni deposits at the base of the Duluth Complex began in 1948, about 8 miles to the southeast of Ely, MN, when strongly mineralized rocks were uncovered in an excavation used to source road material for Spruce Road. Local prospector Fred S. Childers of Ely noted copper stains in the material and he, along with Roger V. Whiteside of Duluth, began searching along the basal contact in the vicinity of the Kawishiwi River. In 1951, they diamond drilled a 188 foot deep hole and intersected mineralized gabbro that averaged 0.36% Cu and 0.13% Ni. In 1952, both Bear Creek Mining Company (BMC) and the International Nickel Company (INCO) began intensive exploration efforts along a 38 mile-long zone that coincided with the basal contact. INCO eventually picked up the Childers-Whiteside properties (Spruce Road and Maturi deposits); whereas, BMC concentrated most of their effort near the town of Babbitt which resulted in the discoveries of the Babbitt (formerly called Minnamax and now known as Mesaba) and Serpentine deposits. By 1960, these exploration efforts indicated that very large tonnages of disseminated Cu-Ni mineralization were present; however, the low-grade nature of the deposits and the unavailability of state-owned mineral lands at the time led to suspension of activities.

In 1966, state mineral leases were offered by the Minnesota Department of Natural Resources (DNR) and were awarded to successful bidders, resulting in renewed exploration activity (including the return of BMC and INCO). Since 1966, over 20 companies have been actively involved in exploration for Cu-Ni and Fe-Ti-V deposits along the basal contact of the Complex. Over 2,600 holes, totaling over 4.5 million feet of core, have been drilled. Exploration efforts during this period also defined several more deposits including: Dunka Road (now NorthMet) and Wyman Creek (United States Steel Corp.), Birch Lake (Duval Corporation and Newmont Mining), South Filson Creek (Hanna Mining), Dunka Pit (Erie Mining, BMC, and Exxon), and Wetlegs (BMC and Exxon). AMAX Exploration Inc. leased the Babbitt deposit from BMC and renamed it the Minnamax deposit in 1973. During mid to late 1970s, the Spruce Road and Minnamax deposits came closest to development. Mining plans were submitted, test shafts were sunk (one each at the Maturi and Minnamax/Mesaba deposits), surface bulk samples were collected from three sites, and various land-use and water-use permits were requested from State and Federal agencies. In 1974, the Minnesota Environmental Quality Board required that a regional Environmental Impact Statement (EIS) be conducted prior to acceptance of any site-specific EIS mining-related proposals. The DNR discontinued lease sales of State lands (1974-1982) until completion of the regional EIS. However, by the time the regional EIS was submitted in 1979, development of the Cu-Ni deposits was put on hold by the most of the mining companies involved due to weakened copper and nickel markets and the inability to make marketable (i.e., "smeltable") separate copper and nickel concentrates. Amax abandoned their plans to develop an underground high grade ore zone within the Minnamax/Mesaba deposit (known as the Local Boy ore body) in late 1982.

Then starts the "PGE" era. During the early period of drilling (prior to 1980), all of the exploration companies recognized that the Cu-Ni deposits had some potential for hosting PGEs. Based on very limited sampling, the companies assumed that the typical Cu-Ni ore contained no more than a few hundred parts per billion (ppb) combined platinum and palladium. In 1985, the DNR and Minerals Resource Research Center (MRRC of the U of M) conducted a geochemical evaluation of portions of a Duval drill hole (DU-15), from the Birch Lake area, and found significant values of up to 9 parts per million (ppm) combined Pt and Pd (Sabelin and Iwasaki, 1985, 1986). This was at a time when demand for these elements was increasing due to their use in automotive catalysts. A short time later, Morton and Hauck (1987) compiled all of the known PGE data for the Complex and reported the presence of anomalous PGE values, often associated with high Cu values, at several other Cu-Ni deposits. These discoveries sparked renewed interest in the Cu-Ni deposits as potential polymetallic deposits (Miller et al., 2002; and references therein). E.K. Lehman and Associates of Minnesota obtained mineral leases from the state of Minnesota and began drilling wedges off the discovery hole (DU-15W) in the Birch Lake area. These Lehmann leases were later incorporated into Franconia Minerals holdings. Additional drill holes were sampled and analyzed for PGEs by several other companies throughout the Duluth Complex, and as a result, significant PGEs were found at many deposits. The occurrences of PGE mineralization for each deposit will be more thoroughly discussed later in this guidebook.

Enter the "Hydromet" era. Early development of the deposits was hampered both by state leasing issues, complex metallurgy that resulted in an inability at the time to make marketable separate Cu and Ni concentrates, and by general environmental concerns regarding sulfide mining and conventional pyrometallurgical processes. In the mid to late 1990s, the potential of developing the Cu-Ni deposits using hydrometallurgical techniques once again sparked renewed activity in the Duluth Complex. PolyMet plans to use the PlatSol technique, developed and patented by SGS Lakefield on NorthMet ores, to recover Cu, Ni, Co, and PGE at the NorthMet deposit.

REGIONAL GEOLOGIC SETTING, DULUTH COMPLEX

The Duluth Complex and associated intrusions of Keweenawan age (~1.1 billion years) in northeastern Minnesota constitute one of the largest mafic intrusive complexes in the world, second only to the Bushveld Complex of South Africa (Miller et al., 2002). These rocks cover a 2,200 square mile (5,700 square km) arcuate area associated with the two strongest gravity anomalies (+50 and +70 milligals) in North America, that imply intrusive roots more than 8 miles (13 km) deep (Allen and others, 1997). The co-magmatic flood basalts and intrusive rocks underlying much of northeastern Minnesota were emplaced during development of the Mesoproterozoic Midcontinent rift, which can be traced geophysically from exposures in the Lake Superior region along a 1250 mile (2,000 km) long, segmented, arcuate path to Kansas and Lower Michigan. The Duluth Complex is defined as the more or less continuous mass of mafic to felsic plutonic rocks that extends for >170 miles (275 km) in an arcuate fashion from Duluth nearly to Grand Portage (Fig. 3-1). It is bounded by a footwall of Paleoproterozoic sedimentary rocks and Archean granite-greenstone terranes (Peterson and Severson, 2002), and a hanging wall largely of co-magmatic, rift related flood basalts and hypabyssal intrusions of the Beaver Bay Complex (Fig. 3-1). In genetic terms, the Duluth Complex is composed of multiple discrete intrusions of mafic to felsic tholeiitic magmas that were episodically emplaced into the base of a volcanic edifice between 1108 and 1098 Ma.

The geology of the Duluth Complex and adjacent areas has recently been described in two major publications by the Minnesota Geological Survey (MGS). These include a 1:200,000 scale regional bedrock geological map of northeastern Minnesota (Miller et al., 2001), and a comprehensive written description of the geology depicted on this map (Miller et al., 2002), commonly referred to as the "bible" by geologists working on Duluth Complex geology. Readers' interested in more detailed descriptions of

the geologic setting of the Duluth Complex should begin their quest for knowledge by downloading these publications from the MGS website (ftp://mgssun6.mngs.umn.edu/pub2/).

Within the nearly continuous mass of intrusive igneous rock forming the Duluth Complex, four general rock series are distinguished on the basis of age, dominant lithology, internal structure, and structural position within the complex.

Felsic series—Massive granophyric granite and smaller amounts of intermediate rock that occur as a semi-continuous mass of intrusions strung along the eastern and central roof zone of the complex, that were emplaced during an early stage magmatism (~1108 Ma).

Early gabbro series—Layered sequences of dominantly gabbroic cumulates that occur along the northeastern contact of the Duluth Complex, emplaced during early stage magmatism (~1108 Ma).

Anorthositic series—Structurally complex suite of foliated, but rarely layered, plagioclase-rich gabbroic cumulates emplaced throughout the complex during main stage magmatism (~1099 Ma).

Layered series—Suite of stratiform troctolitic intrusions that comprises at least 11 variably differentiated mafic layered intrusions that occur mostly along the base of the Duluth Complex. These intrusions were emplaced shortly after the Anorthositic series (~1099 Ma).

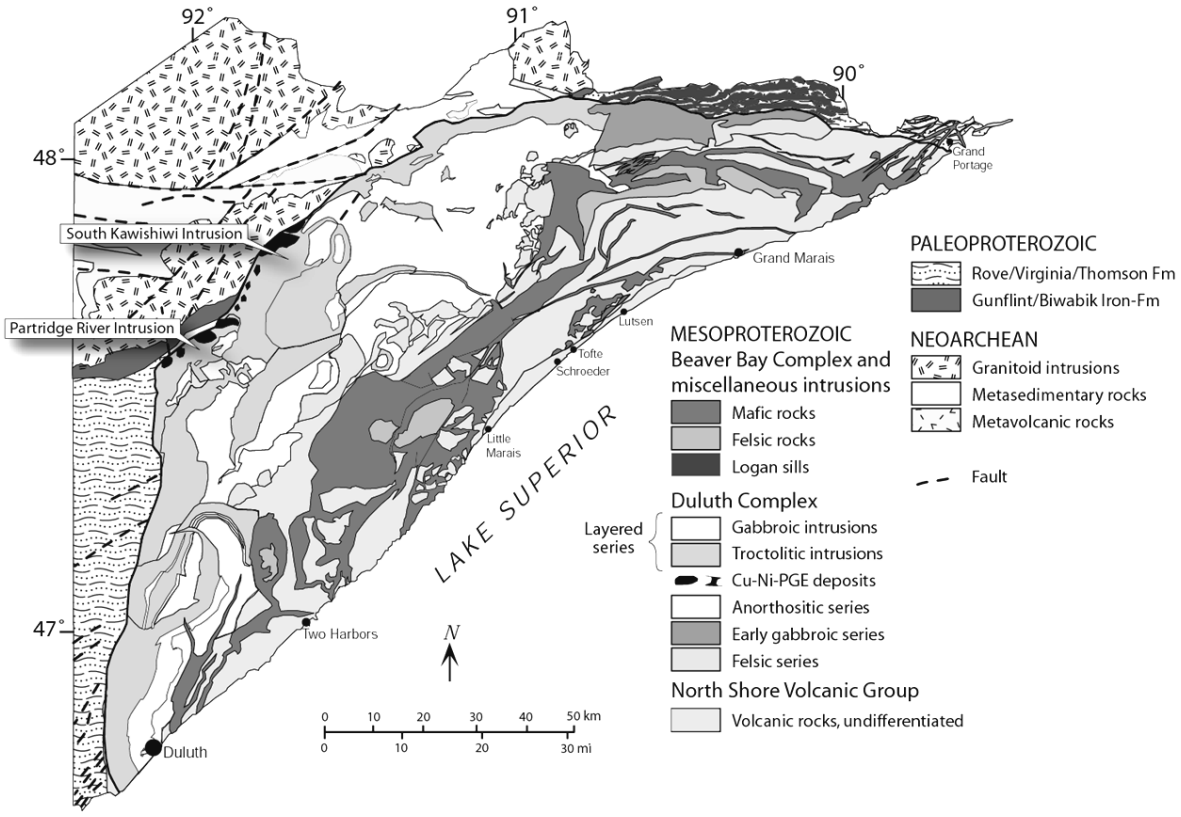


Figure 3-1. Generalized geologic map of northeastern Minnesota (modified from Miller et al., 2002).

Rock Type and Unit Classification

Igneous rock types in the Duluth Complex are classified at each of the deposits by visually estimating the modal percentages of plagioclase, olivine, and pyroxene, and using a rock classification scheme (Figure 3-2) modified from Phinney (1972). Using this classification, the majority of rocks at the various deposits consist of troctolite, augite troctolite, anorthositic troctolite, and norite (near the basal contact) with local

ultramafic layers consisting of melatroctolite to dunite. Due to subtle changes in the percentages of the estimated minerals, there can be subsequent variations in the defined rock types within a specific igneous stratigraphic rock unit on a hole by hole basis, on an interval by interval basis, and even on a geologist by geologist basis.

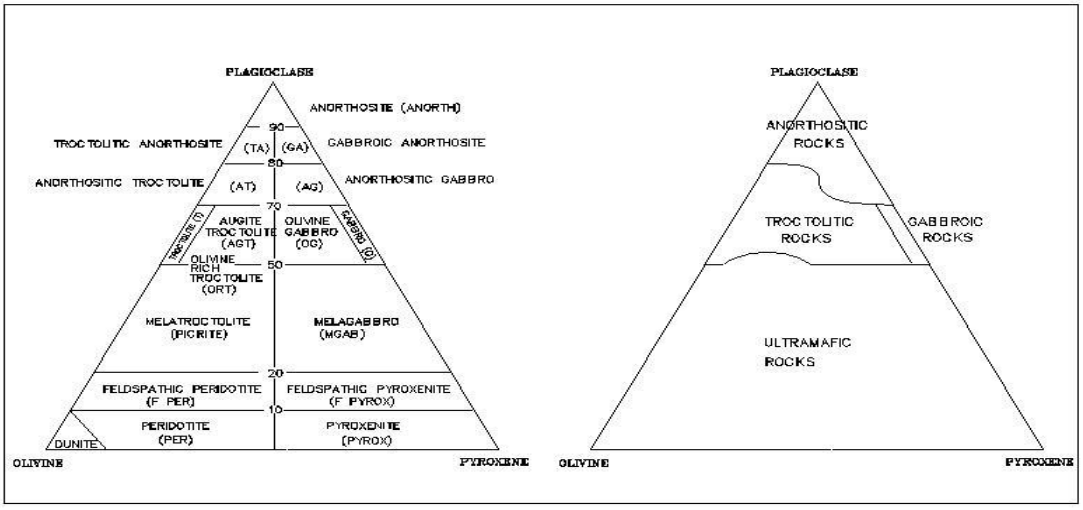


Figure 3-2. Modified Phinney (1972) diagram for rock type classification.

Overall, stratigraphic unit definitions are based on: dominant rock type; textural relationships; mineralogy; sulfide content; and context with respect to bounding surfaces (i.e., ultramafic horizons, oxide-rich horizons). Unit definitions are not always immediately clear in logging, but are usually clarified when drill holes are plotted on cross-sections. In other words, to correctly identify a particular stratigraphic unit, the context of the units directly above and below should also be considered.

LOCAL GEOLOGIC SETTING-PARTRIDGE RIVER, SOUTH KAWISHIWI, AND BATHTUB INTRUSIONS

By: Mark Severson

The three deposits under review for this trip are located in three of the oldest intrusions in the Duluth Complex. The NorthMet deposit and parts of the Mesaba deposit are in the Partridge River intrusion, the majority of the Mesaba deposit in the newly defined Bathtub intrusion, and Maturi deposit in the South Kawishiwi intrusion (Fig. 3-3).

Partridge River intrusion

The Partridge River intrusion (PRI) consists mainly of troctolitic cumulates, dips gently to the southeast, and is exposed in an arc-shaped area that extends from the Water Hen deposit, on the southwest, to the southern edge of the Mesaba/Babbitt deposit, on the northeast (Fig. 3-3). Footwall rocks include the Paleoproterozoic Virginia Formation and locally the Biwabik Iron Formation. The basal 3000 ft. (900 meters) are known in great detail from studies of abundant drill core (Severson and Hauck, 1990) and are subdivided into seven or more units that can be traced over a strike-length of 15 miles (24 kilometers).

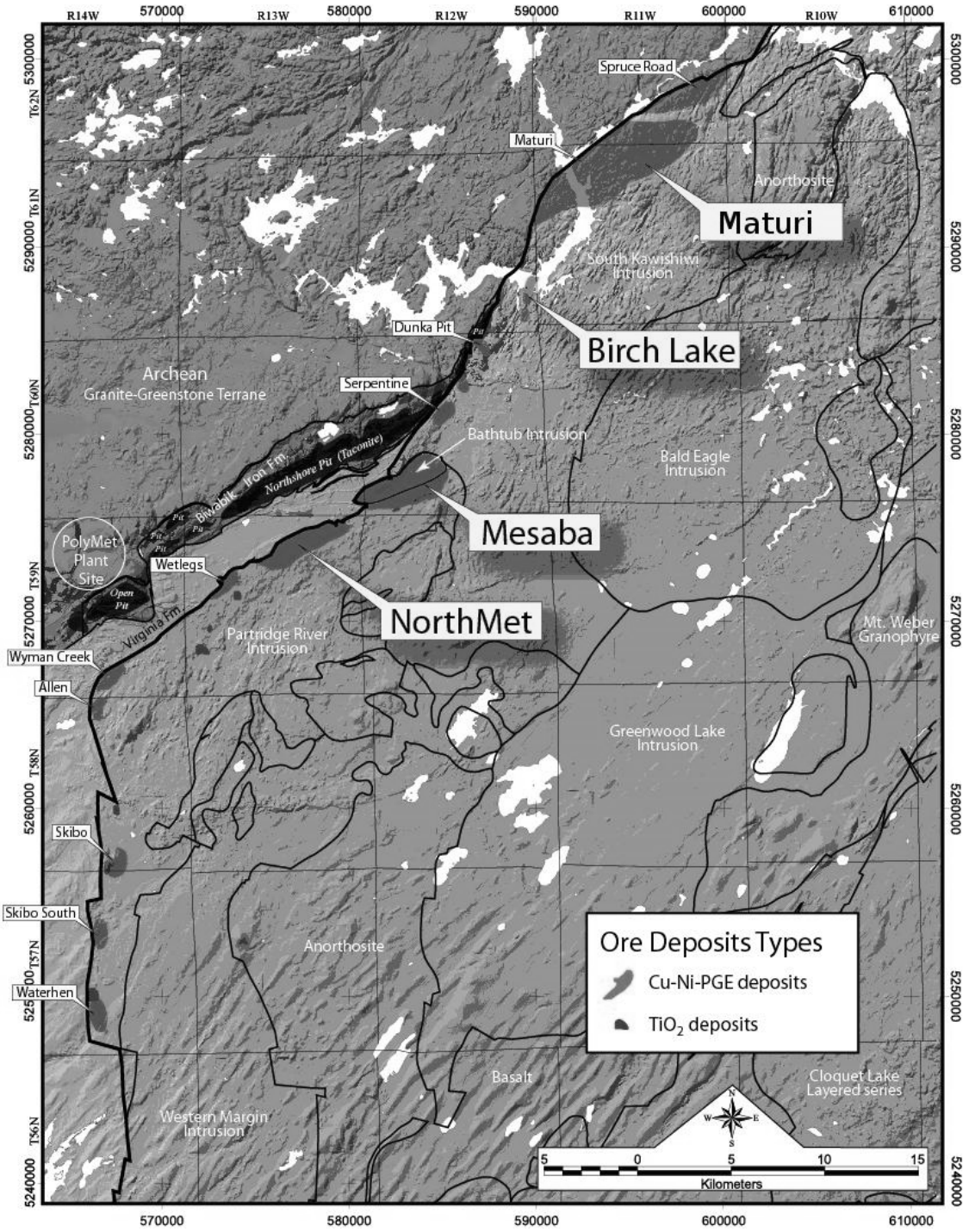


Figure 3-3. Location of Cu-Ni±PGE sulfide deposits, Fe-Ti±V oxide deposits (Oxide-bearing Ultramafic Intrusion - OUI), and other exploration areas along the western edge/base of the Duluth Complex. Note that the NorthMet deposit was referred to as the Dunka Road deposit and the Mesaba deposit was referred to as the Babbitt deposit; the most recent names for these two deposits are used in this guidebook. The Birch Lake deposit will not be discussed in this guidebook.

The units of the Partridge River intrusion (PRI) are recently described in Miller and Severson (2002) and are depicted in Figure 3-4. At the base of the PRI is Unit I which consists of a suite of heterogeneous-

textured troctolitic rocks that contain the vast majority of disseminated sulfide-mineralized zones. The top of Unit I is marked by a fairly persistent ultramafic horizon, which in actuality is at the base of Unit II. Within Unit I are several laterally-discontinuous ultramafic horizons and abundant footwall sedimentary inclusions of the Virginia Formation. Noritic rocks are common at the basal contact and adjacent to the inclusions due to silica contamination from assimilated footwall rocks. Unit II consists of more homogenous-textured troctolitic rocks with minor sulfide-bearing zones. However, at the Wetlegs deposit, both Units I and II contain abundant laterally-discontinuous ultramafic horizons, interbedded with troctolitic rocks that are collectively referred to as the Wetlegs Layered Interval (Fig. 3-4).

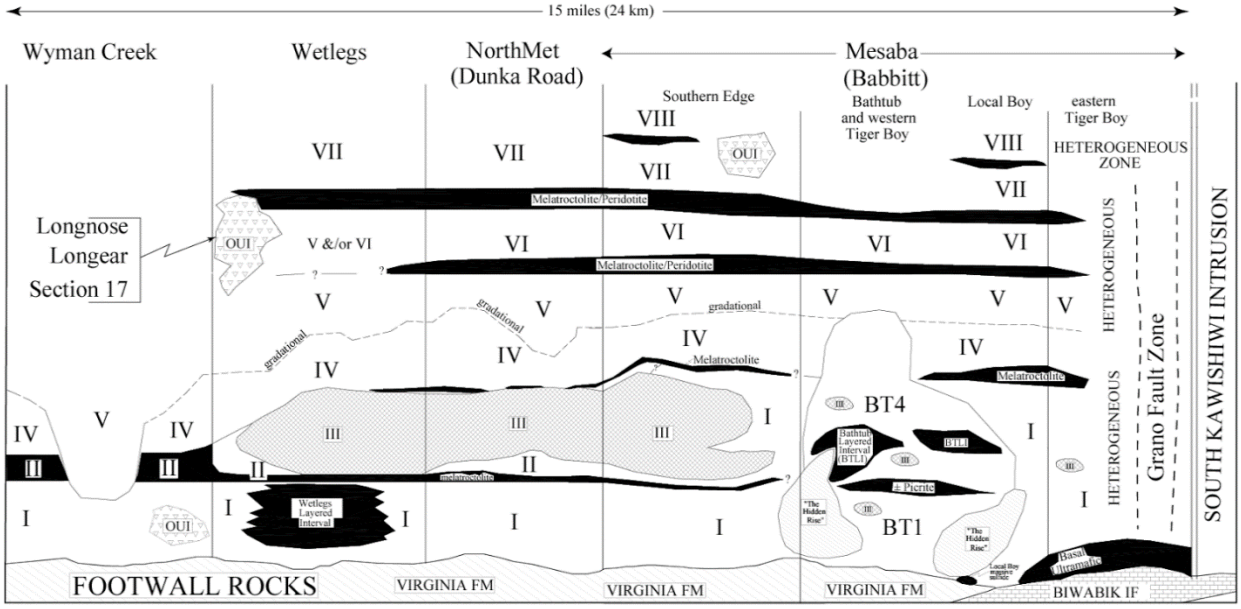


Figure 3-4. Generalized stratigraphy of the basal zone of the Partridge River intrusion (modified from Severson, 1994). Roman numerals (I through VIII) denote igneous units in the Partridge River intrusion; BT1 and BT4 denote igneous units in the Bathtub intrusion; and OUI denotes Oxide-bearing Ultramafic Intrusions.

Overlying Unit III in the PRI are units IV through VIII. Unit IV varies from a troctolite to augite troctolite, often contains an ultramafic base, and commonly grades upward into Unit V which is coarser-grained and varies from a troctolite to troctolitic anorthosite. Units VI and VII, and additional units above VII, are generally homogenous-textured troctolitic to anorthositic troctolitic rocks; each with a persistent ultramafic base that record magma injection events.

Unit III is a major marker bed throughout much of the PRI (Wetlegs to Mesaba deposits - Figs. 3-3 and 3-4) in that it is characterized by a poikilitic leucotroctolite with olivine oikocyrsts that are randomly dispersed throughout the rock giving it a mottled appearance. This mottled-appearance, and the relatively fine-grained nature of Unit III, give it a distinct appearance in drill core and it is easily identified. Unit III pinches out to the west of the Wetlegs deposit and is present on only the southern fringe of the Mesaba deposit. The rapid pinch-out of Unit III to the north within the Mesaba deposit appears to be related to emplacement of a distinctly different sub-intrusion herein referred to as the Bathtub intrusion (see discussion below).

Bathtub intrusion

The Bathtub intrusion (BTI) is wholly contained in the central portion of the Mesaba (Babbitt) deposit. It has recently been singled out as a separate intrusion to explain the abrupt change from typical Partridge

River intrusion stratigraphy in the extreme southern part of the deposit to a completely different stratigraphy, to the north in the remainder of the deposit (Severson and Hauck, 2008). There are three structural features that are pertinent to understanding the intrusive history of the BTI that include (Fig. 3-5): 1. an east-west trending paired syncline and anticline in the footwall rocks referred to as the Bathtub Syncline and Local Boy Anticline; 2. a zone that is closely associated with the Local Boy Anticline, referred to as the "Hidden Rise," that separates the PRI and BTI; and 3. a north-trending fault zone, referred to as the Grano Fault, that is situated on the extreme eastern portion of the Mesaba deposit – the fault has been postulated to have been the feeder zone for the BTI and footwall-injected massive sulfides of the Local Boy ore zone.

The "Hidden Rise" is a loosely-defined zone wherein scattered hornfels inclusions, and associated noritic rocks, are fairly common. When viewed collectively, the inclusions in "The Hidden Rise" define an east-west trending "ridge" that is coincident with the Local Boy Anticline and roughly positioned at the contact between the PRI and BTI. Thus, "the "Hidden Rise" is used to both define this hornfels-bearing "ridge" and to artistically, and conveniently, divide the BTI from the PRI (Fig. 3-5). The morphology of this feature suggests that it may have originally served as the southern edge of an earlier intruded BTI and later served as a wall along the floor and north edge of the PRI as its upper units were emplaced. The BTI has been subdivided into two main units, BT1 and BT4, each of which contain several internal subunits (Fig. 3-5). In the vicinity of the Bathtub Syncline, ultramafic layers and modally-bedded rocks are extremely common within the BT4 Unit and have been collectively referred to as the Bathtub Layered Interval (BTLI).

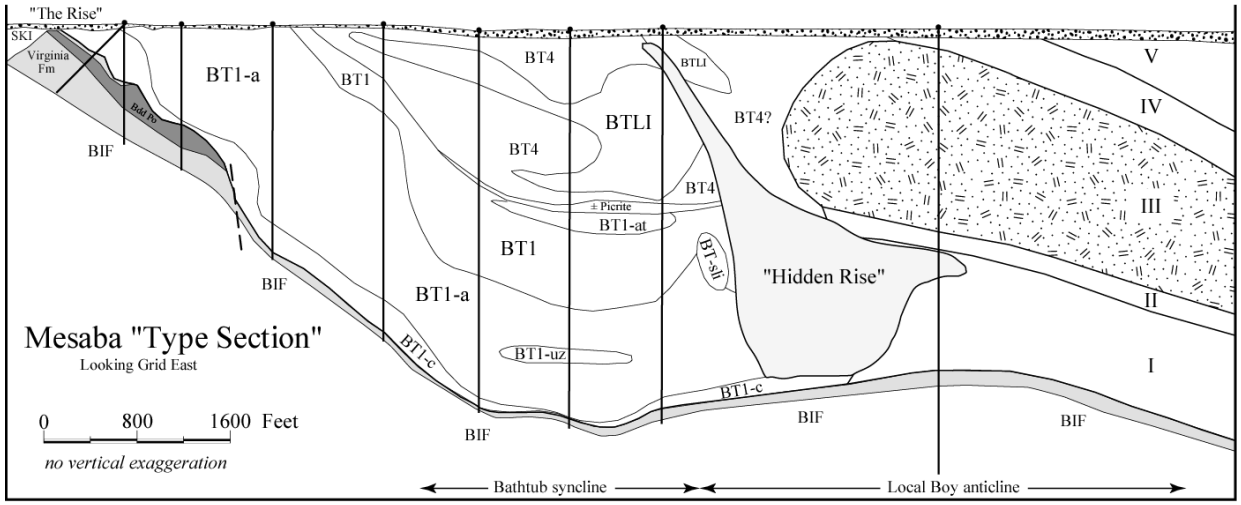


Figure 3-5. Schematic "type-section" looking east through the Mesaba deposit that crudely displays the spatial distribution of most of the igneous units in the Bathtub intrusion and pertinent structural features. Note that not all of the PRI units are shown on the right side of the figure.

Cu-rich massive sulfides are locally present at the Mesaba deposit in a small zone referred to as the Local Boy ore zone. Local Boy is positioned along the crest of the Local Boy Anticline, in close to proximity to the "Hidden Rise," and just west of the Grano Fault. Most of the massive sulfides are associated with either hornfelsed sedimentary inclusions above the basal contact or with footwall rocks below the contact while the interfingering intrusive rocks (mostly norite) are relatively barren of massive sulfides (Severson and Barnes, 1991). This suggests that the massive sulfide ores were not formed by the gravitational settling of sulfides, but rather, the ores formed by injection of an immiscible sulfide melt into structurally prepared areas within the footwall rocks along the Local Boy anticline in a vein-like setting. A possible

feeder vent for the sulfide injection event may have been the Grano Fault, which was repeatedly reactivated during emplacement of the Complex. West-directed increases in Cu and PGE, associated with the massive sulfides at Local Boy, suggest that the immiscible sulfide melt fractionally crystallized and became progressively enriched in Cu and PGE as it was deposited in an east-to-west direction.

Partridge River and Bathtub intrusion footwall rocks

Because the footwall at NorthMet and Mesaba is so similar, the following is a generic description appropriate to both deposits. The drilled footwall rock types at Mesaba and NorthMet consist mainly of the Virginia Formation and Biwabik Iron Formation. Both are Paleoproterozoic in age (approximately 1.9-1.8 Ga) and are the two upper units of the Animikie Group. Any discussion on these two formations must include a description of their type-section on the Mesabi Range, as well as, a description of them as related to the metamorphism and partial melting that was produced during emplacement of the Complex. Lying beneath the Biwabik Iron Formation, but encountered in only a few drill holes are the Paleoproterozoic Pokegama quartzite (also of the Animikie Group), along with granitic rocks of the Archean Giant's Range Batholith.

Biwabik Iron Formation

The Biwabik Iron Formation (BIF) exposed on the nearby Mesabi Range has typically been subdivided into four informal lithostratigraphic members (Wolff, 1917) that are, from the bottom up: Lower Cherty, Lower Slaty, Upper Cherty, and Upper Slaty. Diamond drill holes at Mesaba and NorthMet generally pierce the top submembers of the Upper Slaty, and end in submember C or D. Submember A is comprised of chert and marble, submember B is characterized by alternating bands of green diopside and chert with very coarse-grained hedenbergite, and submember C is a thin-bedded, green rock consisting of chert-fayalite-ferrohypersthene with black magnetite-rich bands.

Virginia Formation below the PRI and BTI

The Virginia Formation is a thick sequence of argillite, siltstone, and graywacke at the top of the Animikie Group. In close proximity to the Complex the effects of partial melting are profound and portions of the hornfelsed Virginia Formation no longer even remotely resemble a sedimentary rock. Severson et al. (1994a) subdivided the hornfelsed Virginia Formation, in both the footwall and in inclusions within the Duluth Complex, into at least five informal units based largely on metamorphic attributes, which are each related to varying degrees of partial melting. These members, and a pre-Duluth Complex sill, are described below and are schematically portrayed in Figure 3-6 - although in real occurrence, this idealized metamorphic progression is more erratic, often with rapid lateral and vertical changes between the four metamorphic units discussed below.

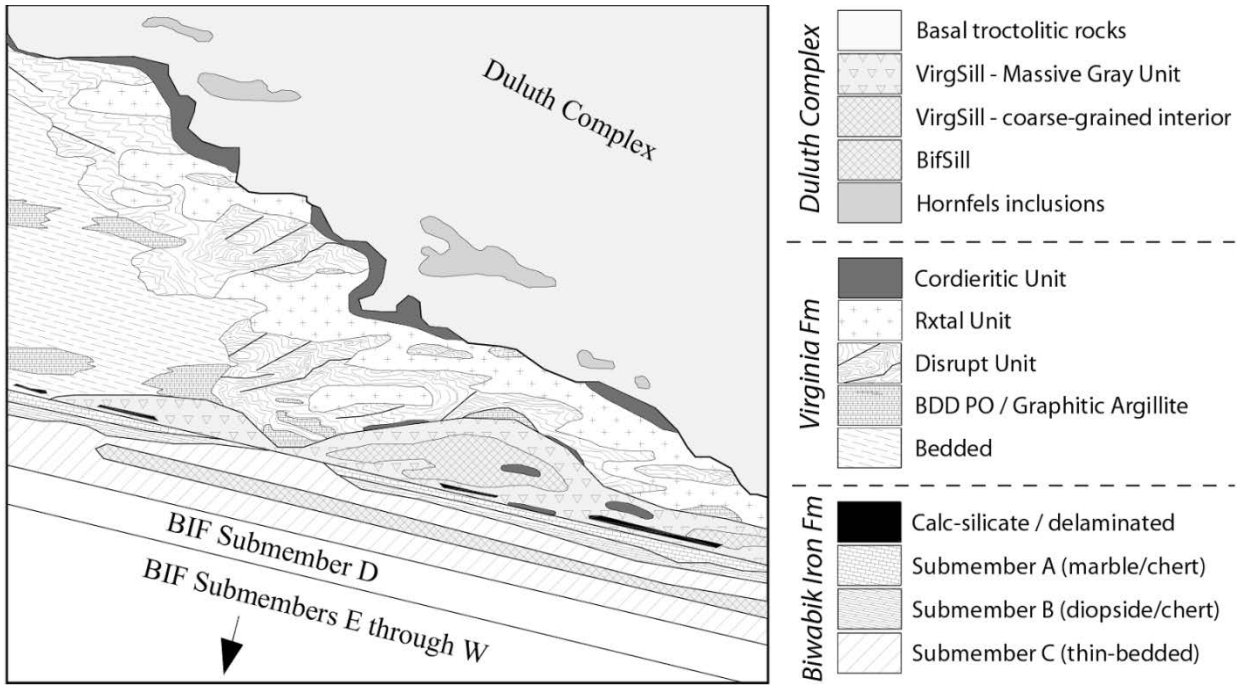


Figure 3-6. Schematic cross-section showing the general relationships of the metamorphosed footwall rocks beneath the Duluth Complex at the Mesaba, NorthMet, Wetlegs, and Serpentine deposits.

Cordieritic hornfels

Directly beneath the basal contact of the Duluth Complex, the adjacent Virginia Formation typically consists of massive/non-foliated, cordierite-rich hornfels that display a bluish-gray color in drill core. The rock is generally fine-grained, granoblastic, and biotite-poor (due to loss of water into the Complex) and locally may contain porphyroblastic and/or poikiloblastic cordierite. Original bedding planes are preserved in some localities, but mostly the bedding planes have been obliterated by contact metamorphism.

Recrystallized unit (RXTAL)

Beneath the cordieritic "capping" the next metamorphic variant of the Virginia Formation nearest to the Duluth Complex is a rock that is referred to as the RXTAL unit. The RXTAL unit is properly classed as a diatexite and is characterized by fine- to medium-grained cordierite, plagioclase, biotite, quartz, and K-spar with lesser amounts of Opx and opaques. Bedding planes of the original argillaceous rocks are obliterated and what remains is a massive recrystallized rock with decussate biotite that contains enclaves (blocks and folded boudins) of more structurally competent calc-silicate hornfels and thin-bedded siltstone

Disrupted unit (DISRUPT)

With increased distance from the Complex, the RXTAL unit progressively grades into the DISRUPT unit which is a thin-bedded rock that is visibly deformed and underwent less degrees of partial melting. Textures that characterize the DISRUPT unit are bedding planes that are extremely chaotic and random in orientation due to pervasive small-scale folding, faulting, and brecciation. Superimposed on this chaotic pattern are abundant zones of leucocratic partial melts that are also chaotic and folded. The rock consists of varying amounts of quartz, cordierite, K-spar, biotite, plagioclase, and muscovite with leucosome veins and patches containing quartz, K-spar (microperthite), plagioclase, and muscovite (Duchesne, 2004). The DISRUPT unit is properly classed as a metatexite.

Graphitic argillite and Bedded Pyrrhotite (BDD PO) units

Carbonaceous argillite of the lower portion of the Virginia Formation is commonly preserved as either the BDD PO unit, or graphitic argillite, in close proximity to the Duluth Complex. This rock commonly contains over 5% disseminated pyrrhotite and/or extremely thin-bedded pyrrhotite laminae (hairline-thick), and variable amounts of graphite, staurolite(?) and sillimanite. Wherever the unit contains conspicuous and regularly-spaced laminae of pyrrhotite (0.5-3.0 mm thick at 1-20 mm spacings) it is informally referred to as the bedded pyrrhotite unit (BDD PO unit). In some areas, the BDD PO served as a local sulfur source to both disseminated and massive sulfide occurrences at the base of the Duluth Complex.

VirgSill

The VirgSill is generally present in the bottom 0.5-130 feet of the Virginia Formation, and as local apophyses into the top of the Biwabik Iron Formation. The VirgSill was intruded along the contact between the Virginia Formation and Biwabik Iron Formation and exhibits a granoblastic texture indicating that it was metamorphosed by the Duluth Complex (and thus the VirgSill is pre-Duluth Complex in age). On this basis, the VirgSill is inferred to be equivalent to the Logan sills (circa 1,109 Ma); as is another sill, the BIFSill, in the C submember of the Biwabik Iron Formation (Hauck et al., 1997). However, the VirgSill and BIFSill are different chemical entities (the VirgSill is much more Cr-enriched), and thus, these two sills may be related to at least two different intrusive events. Identification of the VirgSill in drill core is hampered by the fine-grained granoblastic texture that makes it difficult to distinguish from the enclosing hornfelsed Virginia Formation rocks. The VirgSill is subdivided into two textural varieties (Severson et al., 1994a; Park et al., 1999) referred to as: 1. the Massive Gray unit (MG unit); and 2. a coarser-grained interior with obvious hornblende and/or olivine.

South Kawishiwi intrusion

The South Kawishiwi intrusion (SKI) consists mainly of troctolitic cumulates and dips gently to the southeast. The SKI is exposed in an arc-shaped area that extends from the Serpentine deposit, on the southwest, to the Spruce Road deposit, on the northeast (Fig. 3-3). Footwall rocks include the Paleoproterozoic Virginia Formation, Biwabik Iron Formation and Archean Giants Range Batholith, the latter is the dominant footwall rock type. The presence of Biwabik Iron Formation as inclusions, from the Birch Lake deposit to as far north as the Spruce Road deposit, indicates that the majority of Paleoproterozoic units were assimilated and removed from the footwall during emplacement of the South Kawishiwi intrusion (Severson et al., 2002). The basal stratigraphic section of the SKI is known in great detail from studies of abundant drill core and is subdivided into 17 different units (Fig. 3-7) that are present over a strike-length of 19 miles (31 kilometers). The lowermost units are unevenly distributed along the strike length of the intrusion in a "compartmentalized" fashion, suggesting a complicated intrusive history (Miller and Severson, 2002). A few salient features to keep in mind regarding the igneous stratigraphy of the SKI include:

- The vast majority of sulfide mineralization is confined to the BH (Basal Heterogeneous Unit), BAN (Basal Augite Troctolite and Norite Unit), UW (Updip Wedge Unit), and U3 (Ultramafic 3 Unit) – the latter three of these units are combined and referred to as the BMZ (Basal Mineralized Zone) by Twin Metals at their Maturi deposit;

- Major marker beds, at specific areas in the SKI, include three horizons that contain abundant cyclic ultramafic layers (U1, U2, and U3 Units) and a pegmatite-bearing unit (PEG Unit - originally recognized by Foose, 1984). The U1, U2 and U3 Units represent periods of rapid and

continuous magma replenishment that crystallized more primitive ultramafic layers before mixing with the resident magma (Severson et al., 2002);

- The U3 Unit is unique in that it contains several massive oxide pods (titanomagnetite-rich), as well as, recognizable inclusions of bedded Biwabik Iron Formation; especially at the Birch Lake deposit. The spatial correspondence between the U3 Unit and footwall iron-formation suggests that most of the massive oxide pods are iron-rich "restite" produced by assimilation and partial melting of the iron-formation (Muhich, 1993; Severson, 1994; Severson et al., 2002);

- The U3 Unit contains the vast majority of high PGE values, especially within the Birch Lake area and possibly at the Maturi deposit. However, high PGE values are also present in the PEG Unit (Birch Lake area and Maturi deposit), the top of the BH Unit (Maturi deposit), and very locally in troctolitic rocks situated well above the basal contact (South Filson Creek deposit); and

- A large inclusion/pillar of anorthosite is present at the Maturi deposit. This pillar, and possible proximity to a vent area and magma flow paths (see discussion for Maturi deposit) are some of the inferred reasons for high PGE values at the Maturi deposit.

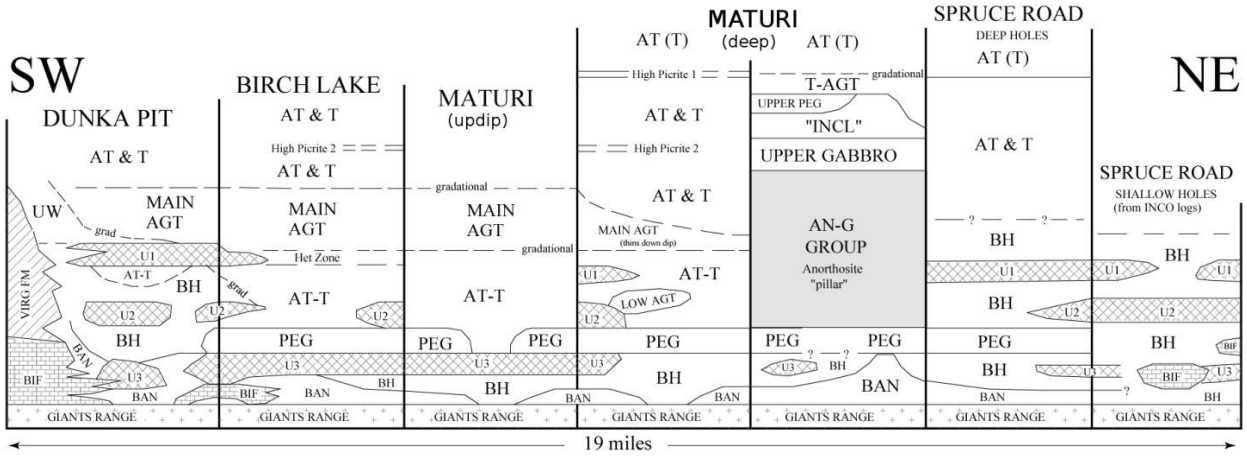


Figure 3-7. Generalized stratigraphy of the basal zone of the South Kawishiwi intrusion (modified from Severson, 1994; and included in Miller and Severson, 2002). The lowermost igneous units are: BAN = Basal Augite Troctolite and Norite; BH = Basal Heterogeneous; U3 = Ultramafic 3; PEG = Pegmatitic unit of Foose (1984); U2 = Ultramafic 2; U1 = Ultramafic 2; AT-T = Anorthositic Troctolite to Troctolite; UW = Updip Wedge; Main AGT = Main Augite Troctolite.

PART 3A: POLYMET NORTHMET DEPOSIT

By: the late Richard Patelke with modifications by Andrew Ware

NORTHMET PROJECT SUMMARY

NorthMet, located in the Partridge River intrusion of the Duluth Complex, is a large, disseminated sulfide deposit in heterogeneous troctolitic rocks associated with the 1,100 million year old Mid-Continent rift. Metals of interest are copper, nickel, cobalt, platinum, palladium, and gold. The majority of the metals are concentrated in four sulfide minerals: chalcopyrite, cubanite, pentlandite, and pyrrhotite, with platinum, palladium and gold also found in bismuthides, tellurides, and alloys. NorthMet is one of eleven copper-nickel-PGE deposits along the northern margin of the Complex (PGE: platinum, palladium, gold). All of these share grossly similar geologic settings–disseminated sulfides with minor local massive sulfides in heterogeneous rocks forming the basal unit of the Duluth Complex along the contact with older rocks.

The deposit is on the southern flank of the Mesabi Iron Range, which is host to six large operating taconite mines, the closest of which is less than two miles (3.2 km) north of the planned NorthMet pits (Figure 5A-1). Ore from NorthMet will be processed at a rate of 32,000 short tons per day through the former LTV Steel Mining Company iron ore concentration plant ("Erie Plant) with new facilities for processing of the NorthMet copper-nickel-PGE concentrates through a hydrometallurgical method to produce copper metal and various hydroxide and concentrate products of nickel-cobalt-PGE (Figure 5A-2).

PERMITTING and THE FINAL ENVIRONMENTAL IMPACT STATEMENT

After 10 years of environmental review, the Final Environmental Impact Statement (FEIS) for the NorthMet Project was released in November 2015. The Minnesota DNR deemed the FEIS adequate in March 2016, and this DNR decision initiated the permitting process. The two other regulatory decision documents on the FEIS (Records of Decision from the US Forest Service and the US Army Corp of Engineers) are expected in 2016. The timelines for submitting and obtaining permits will be different for each permit.

EXPLORATION and DEVELOPMENT

There have been four major drilling programs since 1969, re-sampling for PGE began in 1989, three PolyMet joint ventures were pursued and dissolved in the 1990's, processing technology was developed in the late 1990's, the former LTV Steel Mining Company concentrator and other property was optioned in 2003, and the metallurgical process was refined in 2005-2008.

Drilling programs have been conducted by United States Steel (USS, 1969-1974) and PolyMet Mining Inc. (Reverse Circulation or "RC" drilling and core drilling in 1998-2000 & two phases of core drilling in 2005 and 2007), plus two (actually two pairs of twins) holes by NERCO Minerals Company in 1991. This drilling encompasses 285,756 feet over 371 holes as of May 2008. Over 35,973 acceptable assays have been taken from this drilling (216,344 feet assayed). Table 3A-1 gives a breakdown of years, footages, and number of assays for all project drilling.

United States Steel (USS) began core drilling at NorthMet (as the Dunka Road project) in 1969. Drilling targeted a conductor that turned out to be in the footwall metasedimentary rocks, but the first drill hole hit massive sulfide in the Duluth Complex. Drilling continued over five years for 112 holes with 133,716 feet of intercept. The working assumption was to mine the deposit from underground, sampling was limited to the most continuous zones with strong visible copper-nickel mineralization, and only about 2,200 samples representing about 22,000 feet were taken. USS assayed only for copper, nickel, sulfur, and iron. PGE

presence was known from sampling on concentrates, but the economics of PGE recovery were apparently not pursued. Project work stopped while apparently incomplete and was not restarted.

USS did not do much follow-up, but kept their land ownership, core, pulps, coarse rejects, and records for the project. In the mid 1980's the Minnesota Department of Natural Resources (MDNR) began sampling various historic drill core intervals in the Duluth Complex for PGE and got some good, but localized, results. In 1989 Fleck Resources (Fleck) leased the Dunka Road property from USS and began a program of re-assaying USS pulps and coarse rejects with a much more extensive multi-element suite, as well as adding in some new samples from existing core through cooperative work with the Natural Resources Research Institute (NRRI). The results were very positive in showing elevated PGE values in the deposit and confirming the previous copper-nickel assays.

Fleck partnered with NERCO in 1991 for some bulk sample work, mine plans, environmental reviews etc., done through Fluor Daniel Wright engineers, but the partnership was eventually dissolved. In 1995 Fleck joined with Argosy Mining Corp. to do more work on the project, again with no major progress towards production. In June 1998, Fleck became PolyMet and focused their resources on Dunka Road, which was renamed NorthMet. Without partners, except for a brief venture with North Mining (North), PolyMet drilled and sampled 87 holes in 1998-2001, and sent two large bulk metallurgical samples to Lakefield Laboratories (now SGS) in Lakefield, Ontario for development and refinement of the PlatSol hydrometallurgical process and began some environmental background work.

In the summer of 2000, North was taken over by Rio Tinto. The joint venture agreement was terminated upon consideration that NorthMet appeared to be a low priority to Rio Tinto. However, much of the North funding was already in place and was used to partially finance the 2001 pre-feasibility study. After release of the pre-feasibility study (2001), a brief hiatus, and a major re-evaluation of how the project should proceed, PolyMet became active again in 2003 with new management and a new development plan.

This plan involves integrating the former LTV Steel Mining Company iron ore concentration plant (“Erie Plant) with new facilities for processing of the NorthMet copper-nickel-PGE concentrates through a hydrometallurgical method at rate of 32,000 short tons of ore per day to produce copper metal and various hydroxide and concentrate products of nickel-cobalt-PGE. Geologic work towards this end began in 2004 and first focused on a careful and total re-compilation of the historic NorthMet project drill hole related data. This effort organized and verified all drilling metadata, location, downhole survey, lithology, and assay data, and cataloged all paper (and digital) records for the project. Of note is that this resulted in an increase in the number of acceptable assays from 12,000 to around 17,200 and an improved geologic picture from careful consolidation of existing records.

This work was used as background for a revised resource estimate in January 2005 and planning of a drill program for 2005. The 2005 program entailed drilling and sampling 109 holes (77,000 feet), collection of a forty ton metallurgical bulk sample for pilot scale testwork, geotechnical (oriented core) drilling, in-fill sampling of previously drilled core, and extensive collection of waste characterization data. The 2005 drilling program added 13,450 multi-element assay records to the existing database. A PolyMet report covers the details of historic drilling and assaying (Patelke & Geerts, 2006).

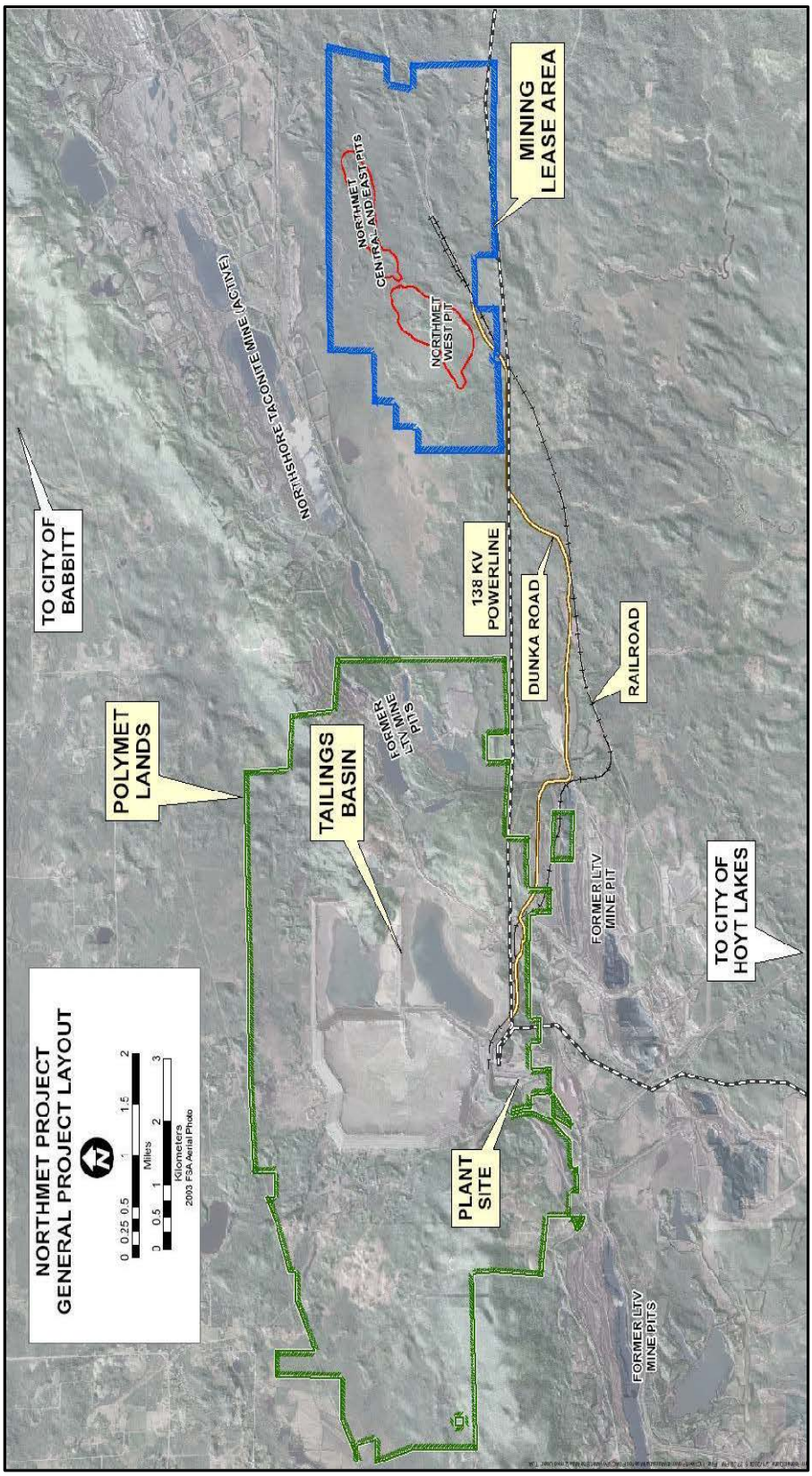


Figure 3A-1. PolyMet NorthMet project site.

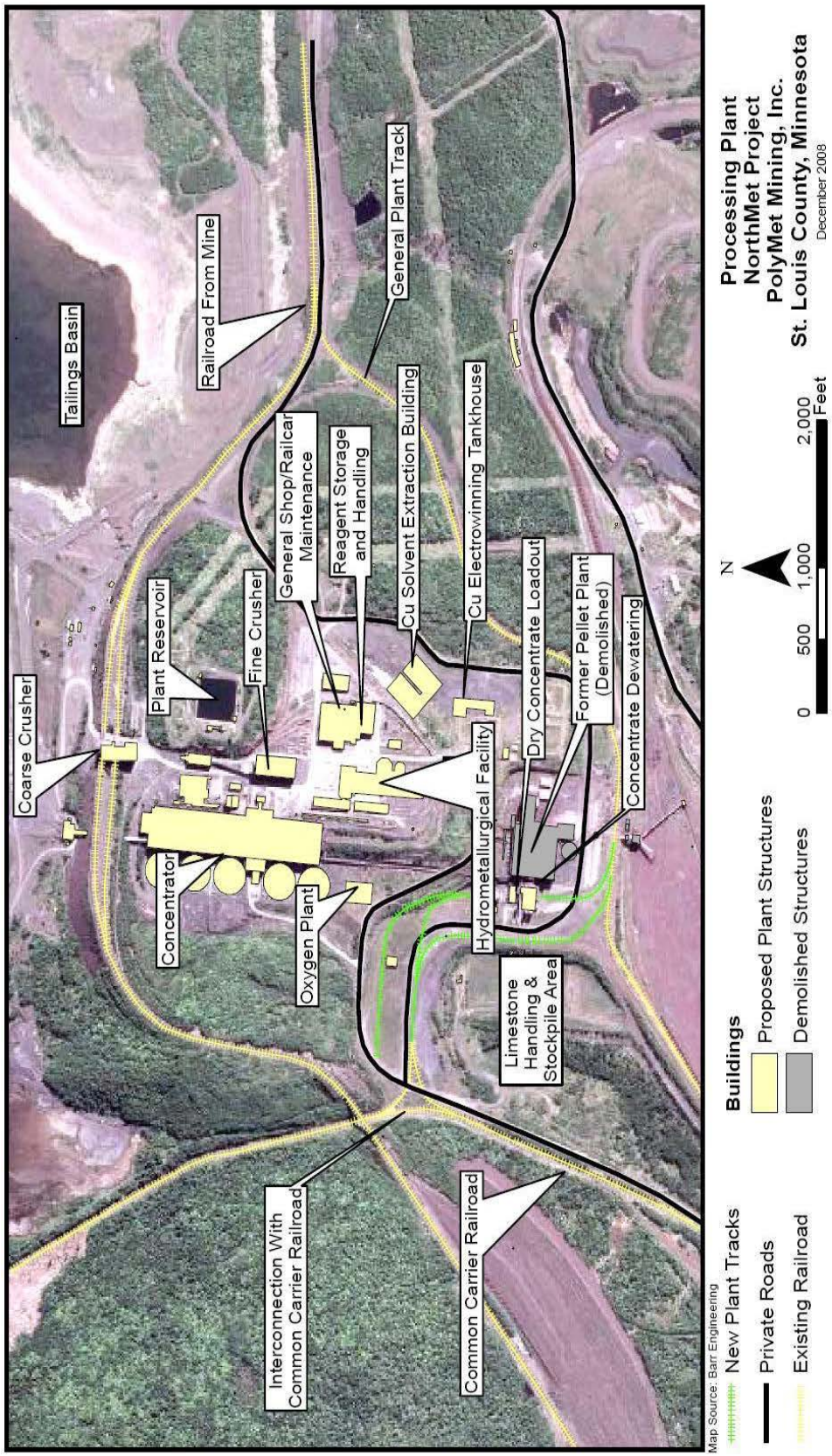


Figure 3A-2. Detail of Erie Plant site showing existing facility and new construction.

Drilling in 2007 for 24.530 feet with 3,546 assays concentrated on defining mineralization in the upper units in the west part of the deposit (the "Magenta Zone"). This drilling and the subsequent re-modeling of the deposit turned about 50 million tons of material previously classed as waste to ore. There is also over 34,000 feet of hydrogeology drilling and "stratigraphic holes" (drilling by other companies not done as part of the NorthMet project). No assays are in use from these 44 holes which are used for geologic control. Approximately 89.5% of Unit 1 and about 57% of the upper units have been sampled across the deposit. The sampled percentages are higher in the anticipated area of mining.

Table 3A-1. Total drilling and assaying for NorthMet project.

Company	Drilling years	Assaying years	No. of drill holes	Total footage for group	No. of assay intervals used in "accepted values" tables	Assayed footage used in final database	Assay Laboratories
US Steel	1969-1974	1969-1974, 1989-1991, 1999-2001, 2005-2006, 2008	112	133,716	11,259	73,303	USS, ACME, ALS-Chemex
NERCO	1991	1991	2 (4)	842	165	822	ACME
PolyMet reverse circulation drilling	1998-2000	1998-2000	52	24,650	4,765	23,767	ACME
PolyMet core drilling	1999-2000	2000-2001, few in 2005	32	22,156	4,058	20,727	ALS-Chemex
PolyMet RC drilling deepened with AQ core tail	2000	2000	3	2,696	524	2,610	ALS-Chemex
PolyMet core drilling	2005	2005-2006	109	77,166	11,656	71,896	ALS-Chemex
PolyMet core drilling	2007	2007	61	24,530	3,456	23,310	ALS-Chemex
Totals for Exploration Drilling:			**371**	**285,756**	**35,973**	**216,344**	
US Steel stratigraphic holes	1970's?	none	6	9,647	none	none	
INCO	1956	none	3	2,015	none	none	
Humble Oil / Exxon	1968-1969	none	3	9,912	none	none	
Bear Creek / AMAX	1967-1977	none	11	8,893	none	none	
PolyMet / Barr Engineering (hydrologic testing)	2005-2007	none	21+	3,459+	none	none	

Sampling in Unit 1 (the main mineralized zone) is now mostly continuous through the zone for all generations of drilling. The PolyMet RC and core holes have continuous sample through the upper waste zones (which do have some intercepts of economic mineralization). Work in 2005 through 2008

essentially completed the sampling of historic USS core within the area likely to be mined. This broad sampling limits the possibility of location bias in the sample set. The entire USS core footage has not been sampled, however there is no known un-sampled mineralized intervals.

Table 3A-2. Large metallurgical samples collected at NorthMet.

Bulk Sample	Year	Tons	Location of sample
USS Bulk sample pit No. 1	1971	Unknown, but small	Pit in center of property
USS Bulk sample pit No. 2	1971	300	Pit at east end of property
USS Bulk sample pit No. 3	1971	20	Pit at east end of property
NERCO PQ drill core	1991	Estimated at 4.5 tons or less by drill core size	One PQ drill hole from each end of property
Argosy Mining	1995	Unknown, but small	Composited from USS coarse rejects
PolyMet RC drill cuttings	1998	26	One composite, mostly from what is now considered east part of 10 year pits
PolyMet RC drill cuttings	2000	33	One composite, mostly from what is now considered east part of 10 year pits
PolyMet 4 inch and PQ core and coarse reject	2005	10.5, 21.5, and 10.7	Three composites from within ten year pits across property
PolyMet coarse reject	2006	4.2 and 4.94	One composite from 10 year east pit, one from 20 year pit across property
PolyMet ¼ core from 2005 and 2007 Drilling	2007	500 kg	One composite, from east and west pit areas
PolyMet ¼ core from 2005 and 2007 Drilling	2008	4.44	One composite, from east and west pit areas
PolyMet ¼ core from 2005 and 2007 Drilling	2008	4.48	One composite, from east and west pit areas

There have been numerous bulk samples taken at NorthMet. Samples have been representative by Unit and rock type. Agreement between calculated grades (based on core sampling) and analyzed grades of final sample has been excellent. Earlier bulk samples represented the first ten years of production, more

recent samples used material from across the deposit. Each bulk sample has built upon the previous, and work has progressed to the point where PolyMet has confirmed the ability to make separate, saleable, copper and nickel concentrates. This will allow the company to develop cash flow from sales much earlier in production while completing construction of the hydrometallurgical facility.

The planned hydrometallurgical process (PlatSol) was developed on NorthMet ores. The process uses pressure oxidation (225°C, over 30 atmospheres) in the presence of chloride to capture all base and precious metals in the concentrate. Hydromet process recoveries are all over 98%. Other geologic data collected includes: recovery and RQD measurements on all core, over 7,000 specific gravity measurements, over 900 whole rock analyses, over 300 Rare Earth Element packages and a large amount of microprobe data collected for waste characterization purposes.

GEOLOGY OF THE NORTHMET DEPOSIT

NorthMet consists of seven igneous units that dip southeast, with most economic sulfide mineralization in the top parts of the lowermost unit (Unit 1). The following is a summarized description of the geology of the deposit, based on observations from drill core and limited outcrop mapping.

Quaternary Geology

In general the Quaternary geology of the region is a thin (0-30 feet or 0-10 meters, but locally thicker) blanket of glacial deposits including till, lacustrine materials, and outwash. Low spots are usually peat bog or open wetland. Topography is subdued and drainage is poor. Site specific geologic studies of the drift have not been done, though a series of geophysical soundings were carried out in 2006 to better define drift thickness outside the area to be mined (Ikola, 2006).

Structural Geology

The general structure of the NorthMet deposit, as defined by igneous contact dips, foliation in serpentinized zones, bedding trends in the Biwabik Iron Formation (BIF) and in the Virginia Formation, is dominated by an overall dip ranging from 15-25° to the southeast, striking about N56°E. Dips in the seven igneous units are grossly similar, but dips of the mineralized zone are up to 60° in the east pit area. Dips in both the Animikie and the Duluth Complex rocks can be attributed to crustal loading, associated with the input of large volumes of magma originating from the Mid-continent Rift System (Sims and Morey, 1972).

Numerous faults have been proposed across the NorthMet Deposit, based largely on reconciling dips in the footwall rocks. There is insufficient evidence, based on drilling to indicate with certainty the exact location of offsets or faulting within the igneous rock units or the footwall rocks on a hole-to-hole basis.

Clearly however, pre-intrusion offset or faulting probably exists within the footwall rocks, due to substantial offsets in the BIF (assuming an average 20° dip) as evidenced between drill holes portrayed in cross-sections. Many of these same offsets can be correlated in adjacent cross-sections. Fault zones are apparent in drill core and show up as brecciated intervals (up to several feet thick), including gouge mineralization (clay, calcite, quartz, etc.), slickensides on serpentinized fracture faces, and/or severely broken (rubble) core. Extensive angle drilling in 2005 and 2007 (142 of 170 holes) brought no great clarity to this issue (virtually all previous drilling was vertical). The current geological model and working cross-sections are therefore constructed with minimal faulting influence, especially within the igneous rock units of the Partridge River intrusion.

Logging and Mapping Units

A summary of the general stratigraphy of the NorthMet Deposit is outlined below. Rock units and formations are listed in descending order, as would be observed from top to bottom in drill hole. NorthMet units are labeled as Units 1 through 7 (Units I through VII in Severson's terminology), bottom to top. Unit 3 is probably the oldest, the intrusion sequence of the other units is not clear.

The broad picture is of a regular stratigraphy of troctolitic to anorthositic rock units, dipping southeast at 20° to 25°, with basal ultramafic units defining the boundaries of some of these units. The basal ultramafic zones tend to have diffuse tops, sharp bases, and are commonly serpentinized and foliated. Geologists have generally picked the unit boundaries at the base of these ultramafics though there are local exceptions. Economic sulfide mineralization is ubiquitous in the basal igneous unit (Unit 1) and is locally present, but restricted, in the upper units.

Unit Definitions and Descriptions

Descriptions of the general igneous Stratigraphy for the NorthMet deposit is described below and presented in a stratigraphic column in Figure 3A-3.

Unit 7

Unit 7 is the uppermost unit intersected in drill holes at the NorthMet Deposit. It consists predominantly of homogeneous, coarse-grained anorthositic troctolite and troctolitic anorthosite, characterized by a continuous basal ultramafic subunit that averages 20 ft. thick. The ultramafic consists of fine- to medium-grained melatroctolite to peridotite and minor dunite. The average thickness of Unit 7 is unknown due to erosion removing the upper parts. Unit 7 is generally not mineralized.

Unit 6

Very similar to Unit 7, Unit 6 is composed of homogeneous, fine- to coarse-grained, troctolitic anorthosite to troctolite. It averages 400 ft. thick and has a continuous basal ultramafic subunit that averages 15 ft. thick. Overall, sulfide mineralization is minimal, although a number of drill holes in the southwestern portion of the NorthMet Deposit contain significant sulfides and associated elevated PGEs (Geerts 1991, 1994). Sulfides within Unit 6 generally occur as disseminated chalcopyrite/cubanite with minimal pyrrhotite. This mineralized occurrence, the "Magenta Zone", transitions into Units 3, 4, and 5, and is discussed in greater detail below.

Unit 5

Unit 5 exhibits an average thickness of 250 ft. and is composed primarily of homogeneous, equigranular-textured, coarse-grained anorthositic troctolite. Anorthositic troctolite is the predominant rock type, but can locally grade into troctolite and augite troctolite towards the base of the unit. The lower contact of Unit 5 is gradational and lacks any ultramafic subunit; therefore the transition into Unit 4 is a somewhat arbitrary pick. Due to the ambiguity of this contact, thicknesses of both units vary dramatically. However, when Units 5 and 4 are combined, the thickness is fairly consistent deposit-wide. Aside from Magenta Zone mineralization in the west, Unit 5 is not mineralized.

Unit 4

Being somewhat more mafic than Unit 5, Unit 4 is characterized by homogeneous, coarse-grained, ophitic augite troctolite with some anorthosite troctolite. Unit 4 averages about 250 ft. thick. At its base, Unit 4 may contain a local thin (usually no more than 6 inch) ultramafic layer or oxide-rich zone. The lower contact with Unit 3 is generally sharp. Unit 4 is rarely mineralized outside the Magenta Zone.

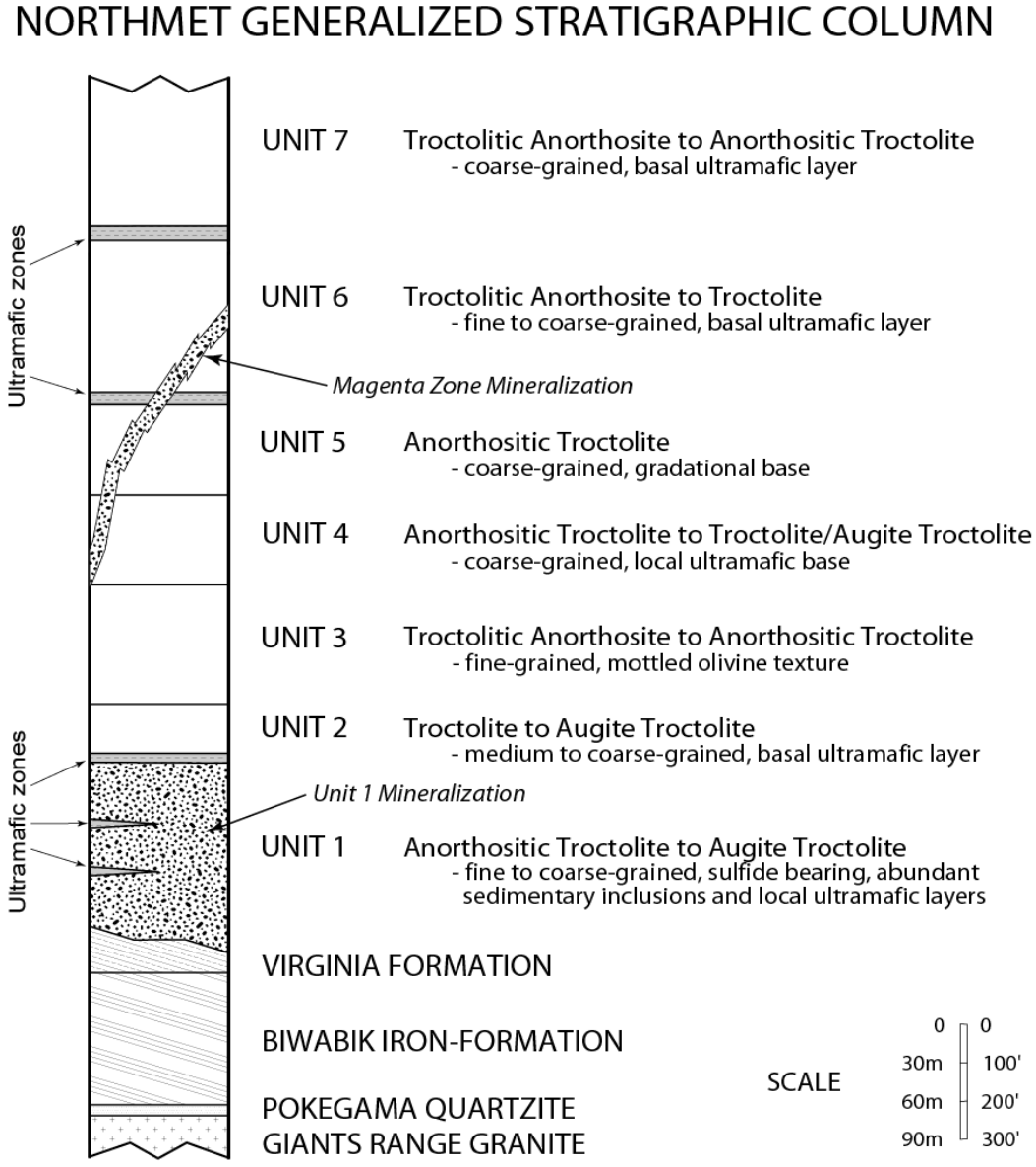


Figure 3A-3. Generalized stratigraphic column for NorthMet units (modified after Geerts, 1994)

Unit 3

Unit 3 is used as the major "marker bed" in determining stratigraphic position in the PRI. It is composed of fine- to medium-grained, poikilitic and/or ophitic, troctolitic anorthosite to anorthositic troctolite. Characteristic poikilitic olivine gives the rock an overall mottled appearance. On average Unit 3 is 300 ft. thick. As with Units 4 and 5, the thickness of Units 2 and 3 tend to be highly variable, whereas if combined into one unit, it is more consistent deposit-wide (though not as consistent as Units 4 & 5).

Unit 2

Unit 2 is characterized by homogeneous, medium- to coarse-grained troctolite and augite troctolite with a consistent basal ultramafic subunit. The continuity of the basal ultramafic subunit, in addition to the relatively uniform grain size and homogeneity of the troctolite, makes this unit distinguishable from Units 1 and 3. Unit 2 has an average thickness of 100 ft. The ultramafic subunit at the base of Unit 2 is the

lowermost continuous basal ultramafic horizon at the NorthMet Deposit, averages 25 ft. thick, and is composed of melatroctolite to peridotite and minor dunite.

Unit 1

Of the seven igneous rock units represented within the NorthMet Deposit, Unit 1 is the only unit that contains significant deposit-wide sulfide mineralization. Sulfides occur primarily as disseminated interstitial grains between a dominant silicate framework and are chalcopyrite > pyrrhotite > cubanite >pentlandite. Unit 1 is also the most complex unit, with internal ultramafic subunits, increasing and decreasing quantities of mineralization, complex textural relations and varying grain sizes, and abundant sedimentary inclusions. It averages 450 ft. thick, but is locally 1,000 feet thick and is characterized lithologically by fine- to coarse-grained heterogeneous rock ranging from anorthositic troctolite (more abundant in the upper half of Unit 1) to augite troctolite with lesser amounts of gabbro-norite and norite (becoming increasingly more abundant towards the basal contact) and numerous sedimentary inclusions. By far the dominant rock type in Unit 1 is medium-grained ophitic augite troctolite, but the textures can vary wildly. Two internal ultramafic subunits occur in drill holes in the southwest, and have an average thickness of 10 ft.

Footwall rocks are covered in the Partridge River intrusion description.

Inclusions

Two broad populations of inclusions occur at NorthMet: hanging wall metabasalts (Keweenawan) and footwall metasedimentary rocks. Basalts are fine-grained, generally gabbroic, with no apparent relation to any mineralization. Footwall inclusions may carry substantial sulfide (pyrrhotite) and often appear to contribute to the local sulfur content. Footwall inclusions are all Virginia Formation, no iron-formation, Pokegama Quartzite, or older granitic rock has been recognized as an inclusion at NorthMet. Sedimentary inclusions make up about 4% of the logged rock types, and basalt inclusions sum to less than 1% of the drilling footage.

Other Igneous Units

Quadrangle scale outcrop mapping indicates that other igneous stratigraphic units are present above Unit 7. These units are similar to Units 6 and 7 in that they consist of homogeneous-textured troctolitic rocks with basal ultramafic members. There are minor, mineralized, pre-Complex sills in both the Virginia Formation and Biwabik Iron Formation at NorthMet (VirgSill and BIF Sill in footwall descriptions above). In neither case is there any apparent relation to Duluth Complex mineralization.

Alteration

The vast majority of rock within the NorthMet Deposit would be considered fresh and is unaltered or only weakly altered. Types of alteration most commonly observed in NorthMet rocks are serpentinization / chloritization of olivine, sericitization and saussuritization of plagioclase, and uralitization of pyroxenes. Most alteration is related to close proximity of fractures and/or joints that cross-cut the troctolitic rocks. Likewise, on a microscopic level the center of alteration is focused around microfractures. This pattern suggests that both fracturing and accompanying alteration of the rock occur as a result of the migration of late-stage deuteric fluids during the cooling phase. The vast majority of sulfide mineralization is independent of alteration.

Nickel in Silicates (Lab Assay Nickel vs. Recoverable Nickel)

It has been characteristic of NorthMet and other Duluth Complex deposits to show lower nickel recoveries in process test work than would be expected from laboratory assays on drill core. Generally there is a loss of about 25-35% of the nickel compared to drill core assays when concentrating sulfides. From previous work, it is known that small amounts of unrecoverable nickel occur as a magnesium-iron-

nickel silicate [$(Mg,Fe,Ni)_2 SiO_4$] that is tied up in the mineral olivine, which is one of three significant gangue minerals that occur across the NorthMet deposit..

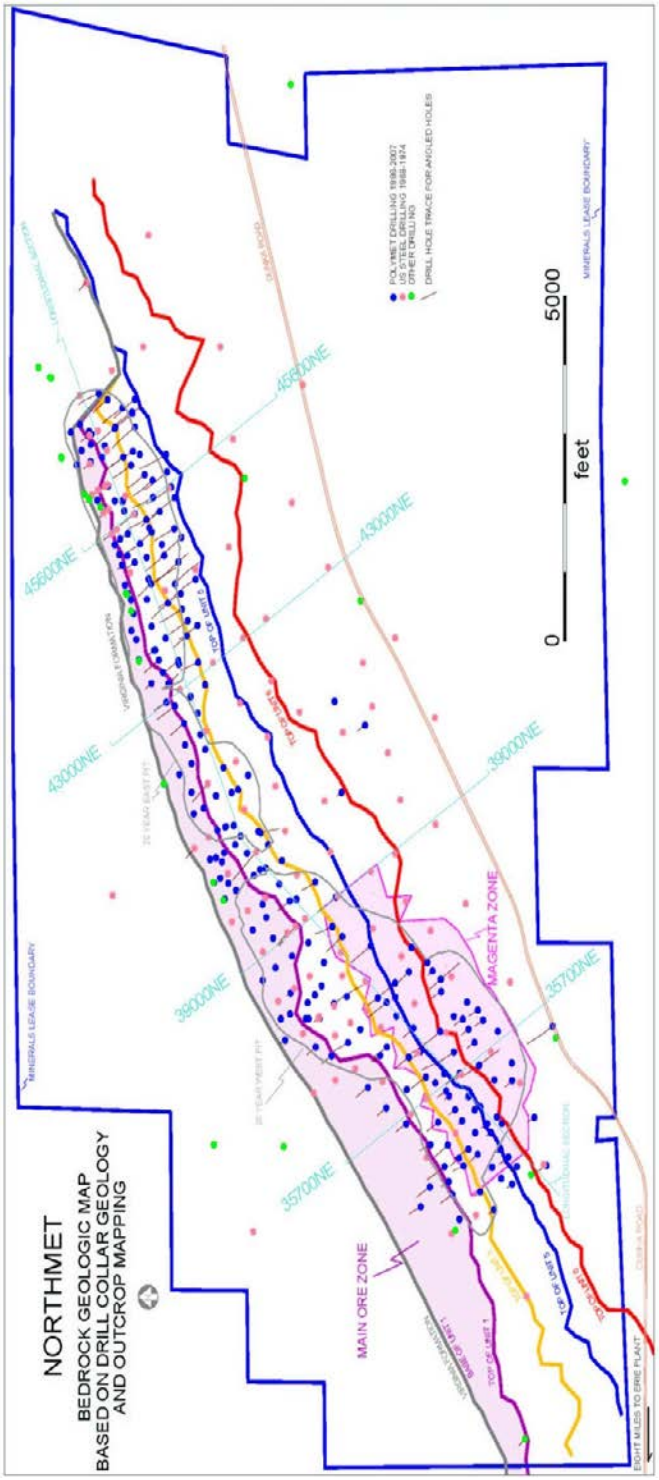


Figure 3A-4. Geologic map of NorthMet Deposit, all units dip southeast, Magenta Zone is projected upward, does not actually subcrop.

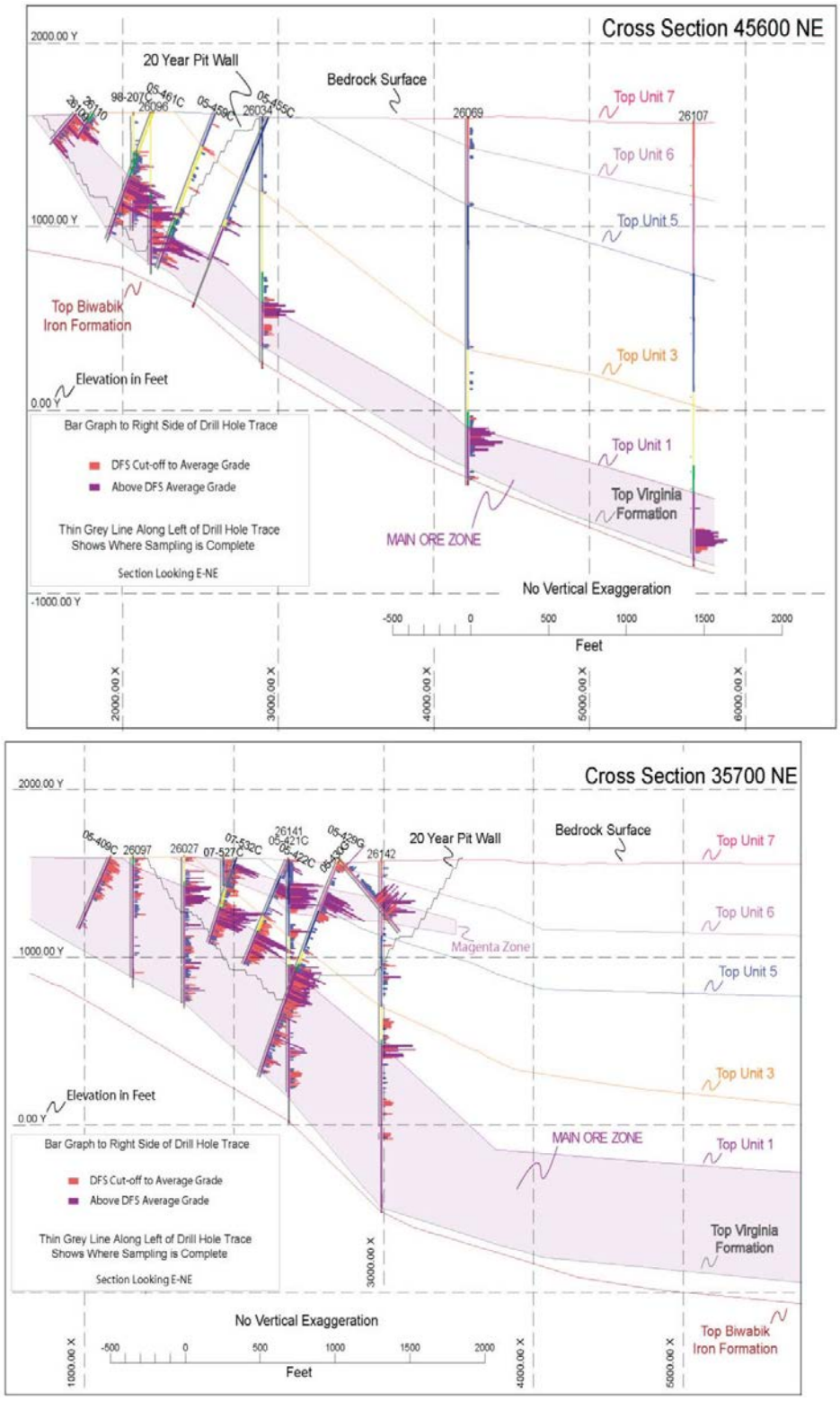


Figure 3A-5. Cross section 35700 at west end of property and 45600 at east end. Purple shading indicated ore zones, bar graphs along holes indicate grades expressed as dollar values, where red = $7.42 cut-off to average grade (~$14.39), and purple shows above average grade, blue are zones of potential lean ore should metals prices rise.

ECONOMIC MINERALIZATION

The majority of economic mineralization (copper, nickel, cobalt, platinum, palladium, and gold) at NorthMet occurs in the upper parts of basal Unit 1, with copper and nickel in chalcopyrite, cubanite, and pentlandite, all in the presence of pyrrhotite. Cobalt is contained in sulfides. Platinum, palladium, and gold, while showing good correlation with sulfur and the other metals, are also in a variety of tellurides, bismuthides, and alloys, as well as associated with the major and minor sulfides. Table 3A-3 shows correlation of metals values in drill core data.

Table 3A-3. Simple correlation ® table for economic metals and sulfur

	Cu %	**Ni %**	**S %**	**Pt ppb**	**Pd ppb**	**Au ppb**	**Pt+Pd+Au**	**Co ppm**	**Zn ppm**
Cu %	1.000								
Ni %	0.860	1.000							
S %	0.541	0.572	1.000						
Pt ppb	0.568	0.508	0.195	1.000					
Pd ppb	0.750	0.635	0.292	0.673	1.000				
Au ppb	0.591	0.472	0.250	0.482	0.699	1.000			
Pt+Pd+Au	0.760	0.645	0.292	0.778	0.983	0.755	1.000		
Co ppm	0.544	0.704	0.621	0.217	0.281	0.241	0.288	1.000	
Zn ppm	-0.021	-0.004	0.286	-0.041	-0.037	-0.017	-0.039	0.093	1

The simple correlation table above (number of samples=19,516) shows the strong relation of copper, nickel, and palladium, and a somewhat surprising relation of cobalt to sulfur. Zinc's low factor is probably related to its multiple origins as either magmatic or derived from assimilation of footwall rock, hence representing two populations of data. The sulfur vs. metal correlation is probably greatly affected by iron, the presence of which is not shown here, but is in excess in all rocks.

Grades are highest at the top of Unit 1 and fade going down hole. Grades appear to be higher down-dip though this may be an artifact of less dense sampling. There is a smaller zone of economic mineralization (about 50 million tons) at the western end of the property in the upper units, known as the "Magenta Zone." This zone is generally copper and PGE-rich (sulfur-poor relative to metals) and of "average" reserve grade.

The minerals of interest from a waste characterization perspective are the same as above, but pyrrhotite is expected to be the main mineral affecting water quality in regards to waste rock, though the traces of chalcopyrite, cubanite and pentlandite are studied for waste rock storage. Trace pyrite and pyrrhotite are the main sulfide minerals found in the tailings.

Most sulfide mineralization at NorthMet is thought to be of a distant source (magmatic?), some is locally modified by sulfur derived from footwall metasedimentary rocks (Virginia Formation). Minor veins and other cross-cutting relations indicate some movement of sulfides within the deposit, but there is no evidence recognized for large scale relocation of sulfides, nor any macroscopic evidence for any hydrothermal event that may have remobilized PGE's or sulfides.

Element distributions, on a single section through the west pit in figure 5A-6 are, located on a single page at the end of the PolyMet Section. The Magenta Zone mineralization cutting across upper intrusive units, is illustrated in this section.

RESOURCE

The PolyMet resource and reserve (Table 3A-4) models have been done in cooperation with several consultants, most recently PEG Mining of Toronto. PolyMet supplies the geologic solids model, database, and block model geometry. Geostatistics and population of the block model, and hence the resource estimate, are done in consultation, with finalized resource block models then sent forward to engineers for reserve calculation and mine planning.

Table 3A-4. The NorthMet resource and reserve values work was done by Wardrop Engineering 2007. Cut-off based on "Net Metals Value" per ton, accounting for grade, average flotation and Hydromet recovery, realization costs, metal prices, and other factors. See Desaultels and Patelke, 2008 for resource calculation details. Enough reserve has been shown for 20 years of permit constrained production.

RESERVES-2007								
	Cut-off value	**Million Tons**	**Cu %**	**Ni %**	**Co Ppm**	**Pt ppb**	**Pd ppb**	**Au ppb**
Proven	$7.42	118.1	0.30	0.09	75	75	275	38
Probable	$7.42	156.5	0.27	0.08	72	75	248	37
Proven and Probable	$7.42	274.6	0.28	0.08	73	75	260	37

RESOURCES-2007								
	Cut-off value	**Million Tons**	**Cu %**	**Ni %**	**Co ppm**	**Pt ppb**	**Pd ppb**	**Au ppb**
Measured	$7.42	202.5	0.285	0.083	74	71	258	36
Indicated	$7.42	491.7	0.256	0.075	70	66	231	34
Measured & Indicated	$7.42	694.2	0.265	0.077	71	68	239	35
Inferred	$7.42	229.7	0.273	0.079	56	73	263	37

ASSUMPTIONS						
Metal and Units	**Cu %**	**Ni %**	**Co Ppm**	**Pt ppb**	**Pd ppb**	**Au ppb**
Assumed Metal Price	$1.25 lb.	$5.60 lb.	$15.25 lb.	$800 oz.	$210 oz.	$400 oz.
Average % recovery, as used in DFS	92.33	70.34	40.75	75.74	72.69	67.04

In the center of the deposit the highest, near surface, Unit 1 grades transition into the middle of the unit, while in the east, mineralization is strong and vertically persistent throughout the unit. The top of the merged Unit 1 and Unit 2 mineralized domain (domain 1) forms a hard boundary that, combined with the bedrock ledge (depth to bedrock) surface, forms the bottom and top estimation boundaries for the upper units (exclusive of the "Magenta Zone", which is internal to this domain). There is no conclusive relation between specific Unit 1 specific rock type and presence or grade of mineralization except that noritic rocks are generally of lower grade.

Units 2 and 3: These units are treated as one unit in the geologic model, with PolyMet geologists considering them as a single package grading from an ultramafic base to an anorthositic top for modelling purposes. The thickness of the package stays relatively constant, though the thickness of the two individual units varies, primarily due to Unit 2 locally thinning. While generally barren, Unit 2 has mineralization at its base in the western half of the deposit. These zones may not be strictly equivalent to Unit 1 type mineralization. Copper and nickel values are lower, as is pyrrhotite, but behavior of other metals is inconsistent, with PGE (Pt + Pd +Au) content varying locally relative to nearby grades at the top of Unit 1. Above the basal zone of Unit 2 it is usually barren, medium-grained, and homogenous in texture. Average PGE in Unit 2 is slightly above that of Unit 1.

Unit 3 shows mineralization in the west, in the middle of the unit and near the top. This occurrence is merged into the Magenta Zone.

Units 4 and 5 are also modeled as a geologic package. There is no compelling geologic reason to fully separate these units, the boundary between them being an arbitrary pick based on overall changes in texture from homogenous to heterogeneous, grain size, and plagioclase content, but without a well-defined bounding horizon. The top boundary of Unit 5 is the basal ultramafic of Unit 6, which is an unused hard boundary in grade modelling. The bottom boundary of Unit 4 is a discontinuous ultramafic horizon. There are also discontinuous oxide-rich zones along the contact between Units 3 and 4.

Metals and sulfur grades in Unit 4 are proportional to Unit 1, but consistently lower. Unit 4 has few high copper or sulfur assay intervals. There is some near surface mineralization, modelled as a part of the Magenta Zone, described below. Otherwise there is only low grade, discontinuous material at the base.

Unit 6 and Unit 7: These units are very similar in nature. Both are homogenous anorthositic troctolite with well-defined ultramafic bases. No top for Unit 7 has been seen in drill hole.

Units 3, 4, 5 and 6 host a zone of mineralization, modeled as the Magenta Zone. Unit 6 mineralization was described by Geerts (1994) as the "Magenta Horizon" when originally found in six drill holes. Further drilling has extended these copper rich, sulfur poor zones (of moderate overall grade) into more than fifty drill holes in Units 3, 4, 5, and 6. The zone transitions across the ultramafic base of Unit 6 and into Units 3, 4 and 5, (i.e., does cross the igneous stratigraphy) which is problematic if the emplacement model of these units representing individual pulses of magma is correct. There is no gross evidence for this mineralization being hydrothermal, which could cross boundaries, but would presumably alter large masses of rock.

Unit 7 has a few good assay intercepts, but no apparent continuity for sulfides.

Copper, nickel, and sulfur values in Table 3A-5 are calculated after removing samples with less than 0.05% copper.

Table 3A-5. Average values for assays by unit after removal of the less than 0.05% copper intervals (drill core samples). Unsampled zones not accounted for here. Data complete through 2006.

	Cu %	Ni %	S %	Pt+Pd+Au ppb	Co ppm	Cu+Ni %	Cu/Ni	Cu/S	Total % of unit sampled	Average sample length-feet
Unit 1	0.3	0.09	0.83	349	76	0.39	3.35	0.43	90	5.3
Unit 2	0.2	0.07	0.39	365	73	0.27	2.74	0.61	80	5.6
Unit 3	0.19	0.05	0.5	286	62	0.25	3.19	0.53	71	7.2
Unit 4	0.21	0.06	0.58	269	66	0.28	3.40	0.44	51	7.6
Unit 5	0.27	0.07	0.54	398	65	0.35	3.64	0.54	41	7.8
Unit 6	0.33	0.08	0.48	532	69	0.41	3.74	0.69	27	7.2
Unit 7	0.2	0.06	0.32	330	83	0.26	3.60	0.72	11	8.4

- Gatehouse (North Mining) did report some geochemical cyclicity in unit 1, but this has not been revisited with the larger data set;
- Poor assay grades in the noritic rocks are related to footwall assimilation and contamination, otherwise there is little connection between grades and specific rock type. About 83% of the igneous rocks at NorthMet are troctolites, 6% anorthositic rocks, 4% ultramafic rocks, and 4% footwall inclusions. The remainder are norite, gabbro and others;
- Within Unit 1 copper:sulfur ratio tends to be highest at top, then diminishes with depth, following the pattern of PGE's;
- The upper units have higher copper:sulfur ratios than Unit 1 (i.e., more chalcopyrite rich), but lower overall copper values;
- Ratio of PGE to copper is lowest in Unit 1, but Unit 1 has greatest quantities of both;
- Chalcopyrite is the dominant sulfide in the upper units regardless of total sulfur content;

Sulfide (Ore) Mineral Proportions

Various metallurgical test programs have been conducted on NorthMet ores since the 1970's. Reported sulfide mineral proportions have not been entirely consistent between these tests. Sulfide mineralogy within the NorthMet Deposit has been described in detail through petrographic observations and microprobe analysis. Approximately 95-98% of all sulfide mineralization consists of 4 predominant species, in decreasing order of abundance: chalcopyrite (cp) > pyrrhotite (po) > cubanite (cb) > pentlandite (pn). In general, Po:Cp+Cb ratios increase towards the basal contact or in proximity to sedimentary inclusions. Likewise, Cp:Cb ratios increase with increased distance away from the footwall rocks. In core logging and other work, chalcopyrite is often not distinguished from cubanite.

Mining

Mining at NorthMet will begin with contractor clearing and overburden stripping of the pit and stockpile areas. Engineered stockpile bases and liner systems must be in place before mining begins, as does the overall water collection system for treatment and pumping to the tailings basin. Ore and waste production will start in the east pit, with production from the west pit ramping up soon afterwards. Up through about year 11 or 12 production from both pits will be equal until the east pit is mined out. At that point, backfilling of the east pit will begin, with the ultimate goal of constructing a wetland in that pit. The central pit area will be mined last.

Ore will be moved at a rate of 32,000 tons per day. Waste to ore strip ratio will be about 1.46:1. Ore will be moved by truck to the "superpocket" and loaded to 100 ton capacity side dump rail cars by pan feeder. There will be twenty trains per day of 16 cars each.

Ore and waste categorization ("ore control") will be by assay of core and / or blast holes and careful pit mapping. Waste material will be sorted to stockpiles, and stockpile liners will be built, according to the sulfur and metals content of the waste rock.

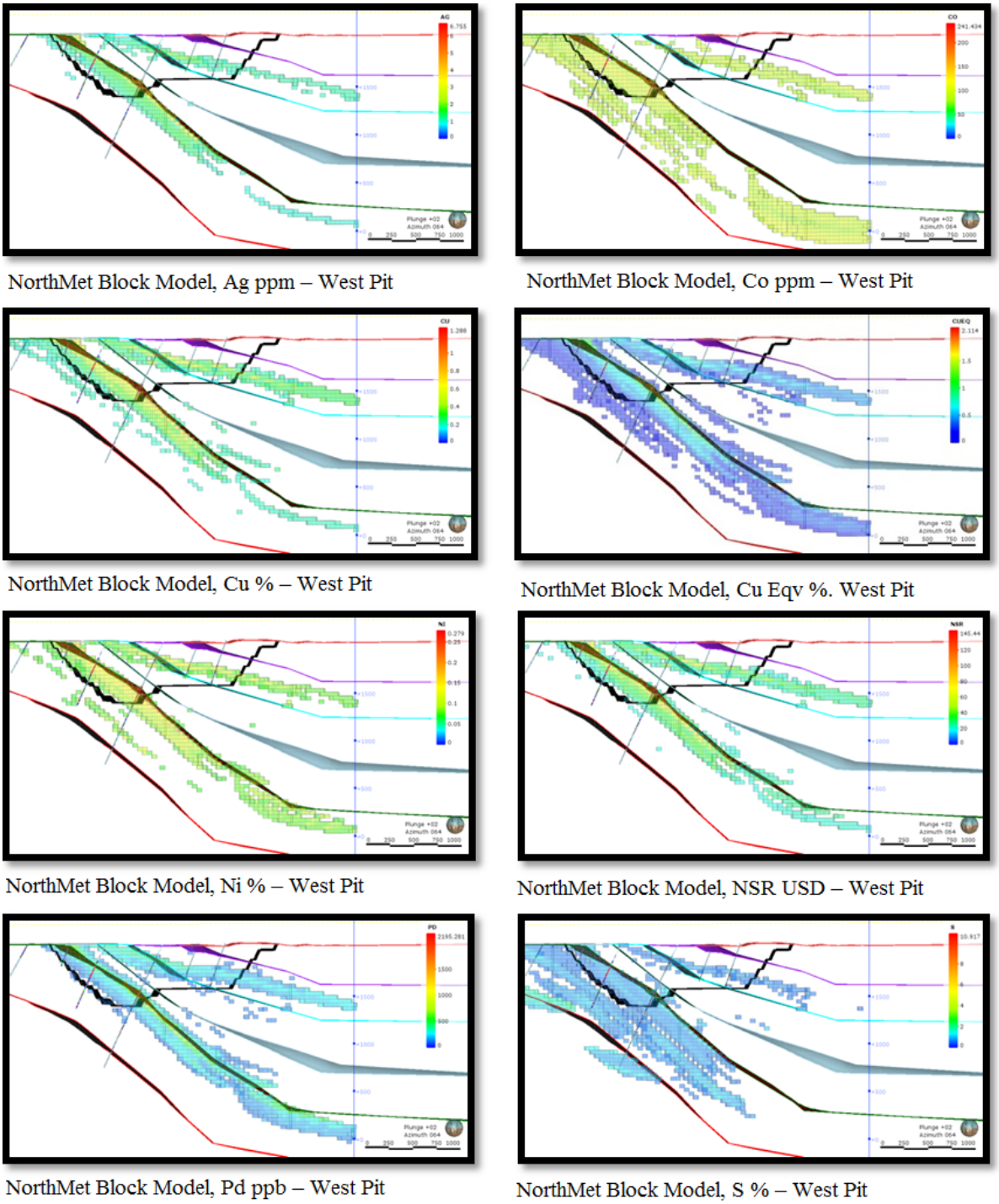


Fig. 3A-6. Economic element distribution, sulphur and NSR in the west pit. Section is orthoganal to the NE-SW strike of the Virginia Fm - Duluth Complex contact.

PART 3B: TECK AMERICAN MESABA DEPOSIT

By: Mark Severson (portions originally by Tim Jefferson)

BACKGROUND

Previous exploration and development work

The Mesaba deposit was first discovered along the base of the Duluth Complex in 1958 by Bear Creek Mining Company (BMC). Between 1958 and 1960, BMC completed 55 shallow drill holes for 43,000 feet (13,952 meters). BMC renewed drilling activities in 1967-1971 completing 149 additional holes. Drill hole B1-105 intersected substantial amounts of semi massive to massive sulfide mineralization between 1,400 and 1,800 feet (425 and 550 meters) below surface in footwall rock. Subsequent drilling defined a high grade zone appropriately named the Local Boy ore zone after BCM geologist Stuart Behling, the "local boy," who encouraged BMC to continue drilling this site.

In late 1973, AMAX Exploration, Inc. agreed to take over BMC's state and private leases. During the next four years (1974-1978) AMAX continued drilling the deposit (completing 228 drill holes). In particular their focus was drawn to the Local Boy ore zone (Watowich and others, 1981), and following successful permitting, they sank a shaft in 1976-1977. Four drifts totaling 3,800 feet (1,160 meters) were developed and 218 underground holes were completed. Based on this work, AMAX reported an overall underground estimate of 364 million tons (330.2 million tonnes) averaging 0.84% Cu and 0.19% Ni, with a Local Boy-only resource of 5 million tons (4.54 million tonnes) grading 1.89% Cu, 0.36% Ni (Watowich, 1978). Both underground resources were estimated based on a 0.60% Cu cut-off (Watowich, 1978). Due to weakening copper and nickel markets and the inability to produce separate high grade Cu and Ni concentrates, AMAX abandoned their plans to develop the deposit in late 1981. Rhude and Fryberger obtained leases and, along with the NRRI, evaluated the PGE potential of the Local Boy ore zone circa 1990.

Arimetco Inc., picked up the Babbitt deposit leases, renamed it the Mesaba deposit, and evaluated the property circa 1994-1996. They did not complete any drilling but collected two bulk samples for metallurgical test work. Arimetco reported a resource estimate to 3,300 million tons (2,993.7 million tonnes) grading 0.46% Cu, 0.12% Ni, cut-off 0.38% Cu (Miller et al, 2002). Arimetco Inc. declared bankruptcy in late 1996.

Present exploration and development work

Teck American Incorporated acquired a package of state and private leases covering the Mesaba deposit in 1998. Teck drilling began in 2007-2008 for a total of 67,430 feet (20,560 meters) in 64 drill holes (Fig. 3B-1). This drilling was concentrated on the western portion of the deposit to complete a 400 foot (120 meter) grid infill program. In 2012-2013, Teck conducted three additional drilling campaigns (Fig. 3B-1).

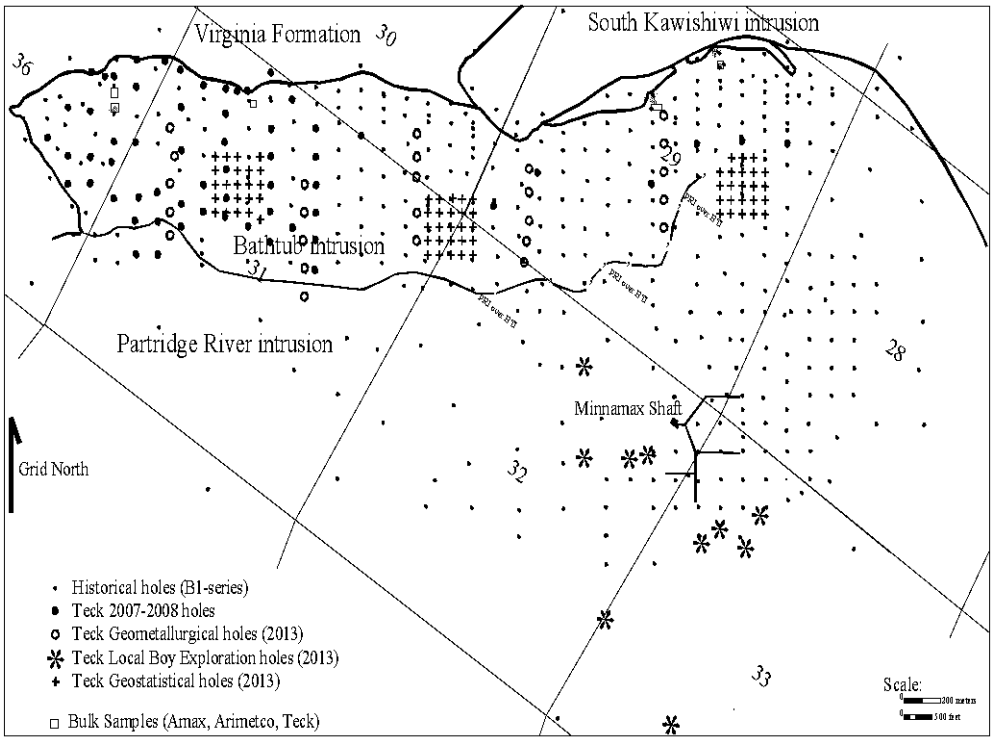


Figure 3B-1. Drill hole location map for Mesaba Deposit. Grid north is about 33° west of north.

Re-logging of historic holes at the Mesaba deposit over an 18 year period, in addition to information gained from logging of holes completed in 2007-2008 and 2012-2013, indicates that the deposit is primarily hosted by a previously unrecognized intrusion within the Duluth Complex (Severson and Hauck, 2008). It is believed that this intrusion, informally named the Bathtub intrusion (BTI) lies between the Partridge River intrusion (PRI) to the south, and the South Kawishiwi intrusion (SKI) to the north and east. This intrusion is believed to have been fed by a vent in the Grano Fault area on the east side of the Mesaba deposit. The BTI is believed to pre-date the SKI and to be coeval to slightly older than the PRI. It is further believed, based on drill hole evidence, that the upper igneous units of the PRI overlap specific BTI units. Supporting evidence for this new interpretation is based on igneous units that are unique to either the PRI or BTI, and different styles of sulfide mineralization between the two. The following geologic discussion is largely based on the work of Severson and Hauck (2008) but is condensed and summarized.

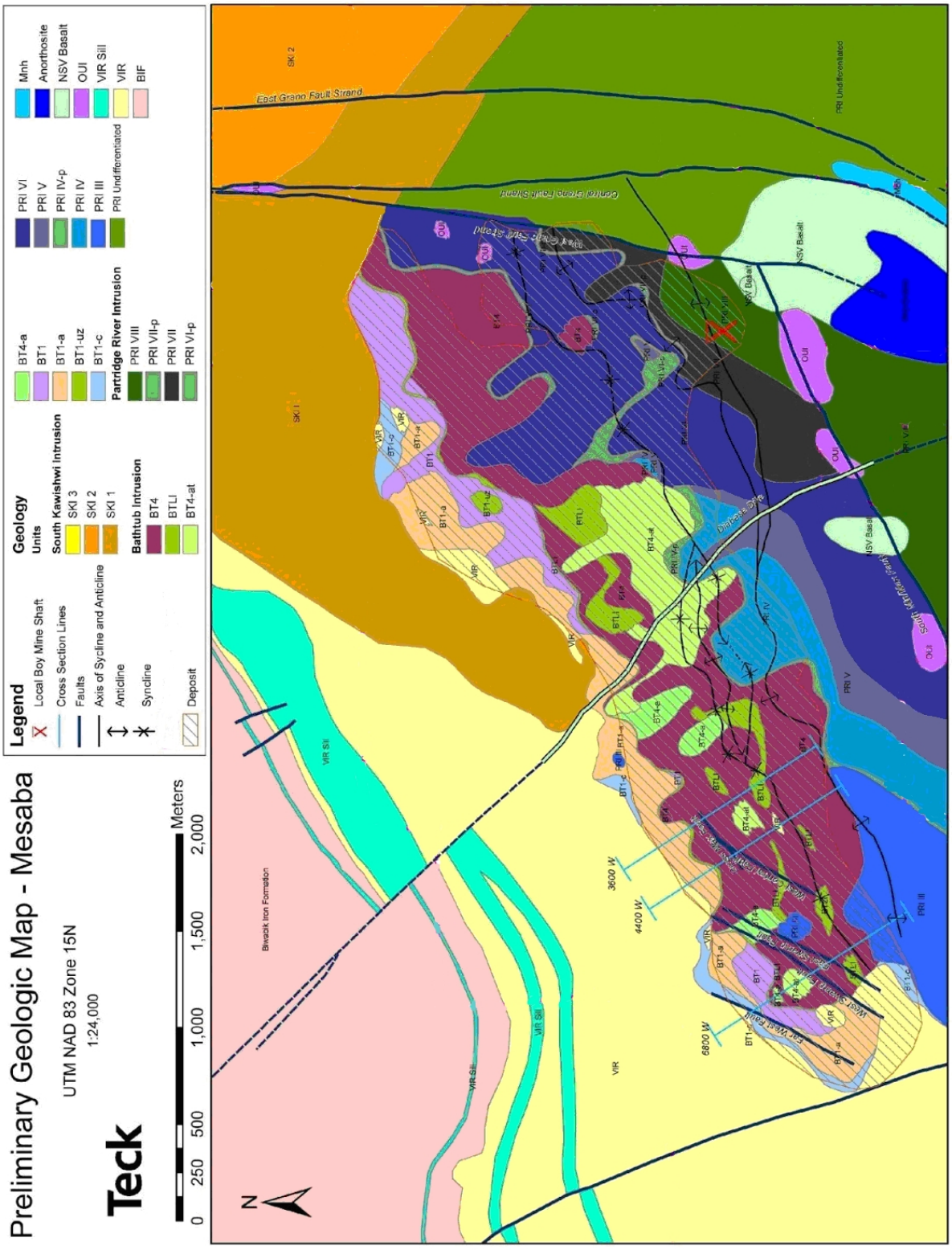


Figure 3B-2. Preliminary geologic map of the Mesaba deposit showing major geologic units of the Bathtub, Partridge River, and South Kawishiwi intrusions. Major structural features associated with the deposit are also shown.

GEOLOGIC SETTING

Footwall Rocks

As there is great commonality between the footwall rocks at the NorthMet Deposit and the Mesaba Deposit, they are discussed in the regional geology section.

Structure

As discussed earlier in this guidebook, there are three structural features that are pertinent to understanding the intrusive history of the BTI that include (Fig. 3B-2): 1. an east-west trending paired syncline and anticline in the footwall rocks referred to as the Bathtub Syncline and Local Boy Anticline; 2. a zone referred to as the "Hidden Rise" that separates the PRI and BTI; and 3. a north-trending fault zone, referred to as the Grano Fault, that has been postulated to have been the feeder zone for the BTI and footwall-injected massive sulfides of the Local Boy ore zone.

The "Hidden Rise," as discussed earlier, is a loosely-defined zone wherein scattered hornfels inclusions of footwall Virginia Formation are fairly common. When viewed collectively, the "Hidden Rise" defines an east-west trending "ridge" that is roughly positioned at the contact between the PRI and BTI.

Along the far eastern edge of the Mesaba deposit is the north-trending Grano Fault, so named for the abundant and sometimes voluminous amounts of late granitoid and oxide rich pyroxenitic lenses (OUIs) associated with the fault zone (Severson, 1994). The late intrusive lenses are interpreted to have vertical configurations and were injected along subsidiary fault zones parallel to, and immediately west of, the Grano Fault. The late OUI and granitoid bodies cut the troctolitic rocks and thus demonstrate that the fault was active during and after emplacement of the BTI and PRI.

BATHTUB INTRUSION

The newly named Bathtub intrusion (BTI) is wholly contained in the central portion of the Mesaba (Babbitt) deposit. The BTI has recently been singled out as a separate intrusion to explain the abrupt change from typical Partridge River intrusion (PRI) stratigraphy, in the southern part of the deposit, to a completely different stratigraphy to the north in the remainder of the deposit. The BTI has been divided into two major units, BT1 and BT4, each of which contain several subunits. These units, in addition to footwall rocks, and structural features, are portrayed in Fig. 3-5.

BT1 Unit

The lowermost unit of the BTI is referred to as the BT1 Unit. It is very similar to Unit I of the nearby PRI in that it is heterogeneous-textured at all scales, contains abundant hornfels inclusions near the basal contact, and is the main sulfide-bearing unit at Mesaba. However, there are some important differences between Units I and BT1 that include:

- Massive sulfide occurrences are more common near the basal contact in the BT1 than in Unit I (excluding the unique Local Boy ore zone) indicating that sulfide settling may have been a more important mineralization mechanism in the BTI;

- Coarse- to very coarse-grained disseminated sulfides (up to several centimeters across) are exceedingly common in the lowermost portions of BT1; whereas, this same relationship is not so obvious in Unit I – this again implies the importance of a sulfide settling origin, and;

- Ultramafic horizons and patches are very common in portions of the BT1; whereas, similar ultramafic horizons are not as common in Unit I of the PRI.

The BT1 Unit has been further subdivided into several internal subunits that are discussed below.

BT1-a
This subunit of the BT1 is a heterogeneous-textured augite troctolite grading to olivine gabbro. The BT1-a subunit is more common in the bottom half of the BT1 Unit and increases up dip (to the north) at the expense of most other subunits of the BT1.

BT1-c
At the base of the BT1 there is significant silica contamination of the magma, due to assimilation of the footwall rocks, and noritic rocks (norite to gabbro norite), with common hornfels inclusions, are the dominant rock types. Graphite occurrences are also commonly found in various rock types of BT1-c. The BT1-c subunit spatially occurs as a rind or coating along the basal contact.

BT1-uz
Wherever olivine-rich ultramafic rocks are common over appreciable intervals in the BT1 Unit, this subunit is used to designate ultramafic zones. The ultramafic rocks in these zones range from well-defined layers to zones where irregular ultramafic patches are presumably peppered throughout a troctolitic host rock.

BT1-at
This subunit of the BT1 is used to denote areas where anorthositic troctolite is the dominant rock type.

BT-sli
A few holes in the western end of the BTI exhibit well-defined modally-bedded rocks consisting of alternating troctolitic and ultramafic rocks. These intervals are designated as BT-sli for the Bathtub Side Layered Interval. The BT-sli subunit occurs about in the center of BT1 unit in close proximity to the "Hidden Rise."

BT4 Unit
The uppermost unit of the BTI is referred to as the BT4 Unit. It was originally correlated with Unit IV of the PRI. However, the BT4 Unit is distinctly different from Unit IV in that the BT4 Unit at Mesaba is:

- Often more heterogeneous-textured at all scales and composed of many alternating rock types;
- commonly contains local sulfide-bearing zones; whereas, Unit IV is mostly sulfide-barren – the sulfides in BT4 are generally chalcopyrite-rich in comparison to chalcopyrite/cubanite ores in the underlying BT1 Unit;
- floored by a semi-persistent ultramafic layer termed the "± Picrite" (see discussion below) in the central portion of the Bathtub ore zone; and
- ultramafic layers and modally-bedded zones, termed the Bathtub Layered Interval (BTLI), are common in the central portion of the Bathtub ore zone.

The BT4 Unit has been further subdivided into several internal subunits based on the presence of a dominant rock type. The various subdivisions of the BT4 Unit are briefly discussed below.

BT4-a
This subunit of the BT4 on the cross-sections denotes areas where heterogeneous-textured augite troctolite is the dominant rock type.
BT4-at

This subunit of the BT4 is used to denote areas where anorthositic troctolite is the dominant rock type.

"± Picrite"

At the base of BT4 is a semi-persistent olivine-enriched ultramafic horizon referred to as the "± Picrite." It is present in about 70% of the drill holes in the BTI-portion of the Mesaba deposit. The "± Picrite" is generally absent in the up dip direction (to the north) and is variably present to the south in the contact zone between the PRI and BTI. Where present, the "± Picrite" is about 1-15 feet thick, but exceptions are locally present. In some areas, the "± Picrite" consists of several stacked ultramafic horizons, or modal beds, that are interlayered with troctolitic rocks, and thus, the zone represents a collection of several cyclic layers. In other areas of the Mesaba deposit, the "± Picrite" is not always easily singled out as it occurs in close proximity to a downward thickening BTLI with similar ultramafic layers and modal beds. Therefore, in some instances it is difficult to pick the "± Picrite" out of a myriad of ultramafic horizons associated with either the BTLI or BT-sli.

Bathtub Layered Interval (BTLI)

In the vicinity of the Bathtub Syncline and the “Hidden Rise,” ultramafic layers and modal-bedded zones are extremely common within the BT4 Unit. In the eastern half of the Mesaba deposit the BTLI appears to be present in a subhorizontal saucer-shaped morphology. Conversely, in the western half of the deposit, the BTLI is confined to one or two cylinder-shaped zones, albeit with irregular edges, that is positioned in close proximity to the “Hidden Rise.”

Overall, the ultramafic rock types of the BTLI are characterized by alternating assemblages of either/or: melatroctolite (picrite), feldspathic peridotite, peridotite, dunite (minor), olivine-rich troctolite, and troctolite with modal beds of olivine-rich layers. One or more of these rock types may be stacked above the other in no particular order, and the thickness of this assortment may be highly variable between drill holes. The number of individual ultramafic layers present within the BTLI for any particular drill hole varies drastically. The range in thickness for each of the individual ultramafic beds also shows considerable variation, ranging from a few inches to over tens of feet thick. Although the BTLI can be correlated as a package of alternating troctolitic and ultramafic layers, each of the individual ultramafic layers cannot be correlated on a hole by hole basis. This situation indicates that the ultramafic layers either: 1) bifurcate/divide into many thin ultramafic layers; 2) pinch out or have very limited spatial extent; 3) some may actually represent dike-like features (filter pressed crescumulates?); or 4) combinations of the above. Further complicating the picture, the inclination of contacts and modal bedding associated with the ultramafic layers are highly variable, ranging from 5°-80° (with localized overturned beds). This variation in inclinations can even be present in a single drill hole. For the most part, the bedding and contact inclinations in the BTLI are steeper higher up in the drill hole and gradually shallow with depth. The shallow to steep angles exhibited by the BTLI may reflect that the ultramafic layers originated via a variety of mechanisms that include: 1) crystal settling to form subhorizontal layers (dominant in the eastern half of the deposit); 2) filter-pressing to form localized dike-like morphologies; 3) slumpage and folding of the beds took place before they were fully crystallized to form highly irregular and overturned beds; 4) compaction differences took place during lithostatic loading of the crystal pile to form steep and irregular beds; 5) cooling and crystallization, or size/density sorting, took place along, and parallel to, the southern wall of the BTI (up against “The Hidden Rise”); or 6) combinations of all of these mechanisms. Whatever their origin, the steep beds displayed by the BTLI in the western half of the Mesaba deposit are inordinately associated with the “Hidden Rise” and the southernmost edge of the BTI.

PARTRIDGE RIVER INTRUSIVE (PRI) AT MESABA

Many of the igneous rock units that are present at the nearby NorthMet deposit are also present along the southern edge of the Mesaba deposit and are believed to represent units of the Partridge River Intrusion (see previous geologic setting discussion). Additionally, Units IV through VI of the PRI appear to extend

northward and overlie the heterogeneous-textured BT4 Unit. This relationship, also depicted in Figure 3B-2, suggests that the BTI was eventually over-ridden/overlain by the upper units of the PRI. The overall timing of emplacement for the lower PRI units versus the BTI is unknown but correlations in cross-sections crudely suggest the following:

- Units I through III were intruded first along the southern edge of the Mesaba deposit with a vent area located somewhere to the southwest. The "Hidden Rise" generally marks the northern extent of this intrusive activity and originally formed as part of the floor to these units. Unit III may have been intruded as thin lenses across and north of the "Hidden Rise" – this may explain the local presence of Unit III-like inclusions in the BTI.

- Concurrent with or after the above activity, the BT1 Unit was intruded from a vent area located somewhere to the east, possibly from the Grano Fault area. The "Hidden Rise" formed the southern wall of this particular magma chamber.

- The BT4 Unit was intruded into the same magma chamber but was emplaced above the BT1 Unit.

- Concurrent with or after the above activity, Units IV through VII+ of the PRI were intruded from a vent area located somewhere to the southeast. These upper units were emplaced over the BT4 Unit.

MINERALIZATION AT MESABA

The Mesaba deposit is characterized by disseminated sulfide mineralization, which occurs most commonly as accumulations of chalcopyrite, cubanite, pyrrhotite, and pentlandite. Additionally, common occurrences of talnakhite have been noted in close proximity to the "Hidden Rise." Short intercepts of semi-massive to massive sulfide mineralization are locally encountered in the BT1-c. Sulfur isotope analyses have indicated that the source of the sulfur used in the formation of the sulfides at Mesaba is the Virginia Formation (Ripley, 1986). The model of sulfide deposition entails turbulent injection of units of the BTI wherein immiscible sulfide droplets coalesce within the silicate melts and attract the chalcophile elements (chiefly copper and nickel) through magma mixing. Thus, the most contaminated magma (from assimilation of footwall Virginia formation) hosts basal sulfides that contain excess sulfur and iron relative to intrusive units higher above the footwall. The sulfide content of the rock increases, often dramatically, as the footwall is approached. This sulfide content increase with depth is accompanied by the increasing presence of pyrrhotite and a subsequent change in the copper bearing sulfides (cubanite is dominant over chalcopyrite with depth). The disseminated mineralization is generally composed of 1-4% sulfides, but can reach upwards of 8-12 % sulfides as the footwall is approached.

The most important mineralized zone at Mesaba is the basal zone, starting at the footwall Virginia Formation contact, and ranges between 200 and 400 feet thick (60 and 125 meters thick). Higher up in the intrusive package, often overlapping the BT1-BT4 unit boundary, is a second zone of disseminated sulfide mineralization that is more erratic and discontinuous in nature but contains markedly lower amounts of cubanite and pyrrhotite.

The mineralized footprint of the Mesaba deposit is oblong to arcuate in shape, 3,000 by 13,000 feet (925 by 4,000 meters) in approximate dimensions, crops out at the surface on the northern/up-dip side and extends to approximately 1,650 feet (500 meters) below surface in the southern/downdip direction. The strongest basal mineralization is often localized within the Bathtub Syncline. Here, concentration of sulfides by gravitational settling into the footwall depression has likely occurred.

PGE Mineralization at Mesaba

Platinum group element (PGE) mineralization in the BTI at Mesaba occurs to a lesser degree than the other deposits and intrusions. Generally, the highest PGE values at Mesaba are associated with Cu-rich massive to semi-massive sulfides in the Local Boy ore zone. Analyses from sampled intervals (5-15 feet thick) record values as high as 11.1 ppm Pd, 8.3 ppm Pt, 13.1 ppm Au, and 62 ppm Ag in the sulfide-rich ores (Severson and Barnes, 1991; Hauck and Severson, 2000). The majority of the anomalous PGE values are spatially distributed along the axis of the Local Boy anticline with the highest Cu and PGE values occurring in the west half of Local Boy. The Grano Fault may have served as a feeder zone to the massive sulfides that were injected into the footwall rocks along the Local Boy Anticline as an immiscible sulfide melt. This melt fractionally crystallized in an east-to-west direction and progressively became enriched in PGE towards the west (see discussion below).

MASSIVE SULFIDES AT THE LOCAL BOY ORE ZONE OF THE MESABA DEPOSIT

Cu-rich massive sulfides near the basal contact of the Complex are locally present at the Mesaba deposit in a small zone referred to as the Local Boy ore zone. In 1976, AMAX Inc. completed a 1,700-foot-deep exploratory shaft (Minnamax shaft), and in 1977, completed four drifts (A, B, C, and D; Figures 3B-3 and 3B-4). Underground Fan drilling (217 holes) was completed in 1978 to further define the massive sulfide distribution. Sulfide minerals include pyrrhotite, pentlandite, chalcopyrite, talnakhite, cubanite, maucherite (nickel arsenide), sphalerite, bornite and late mackinawite, chalcocite, covellite, godlevskite, and native silver (Severson and Barnes, 1991).

Footwall Structures in the Local Boy Ore Zone

Several investigators have recognized that pre-existing structural conditions in the footwall rocks strongly influenced the basal contact of the Duluth Complex (Mancuso and Dolence, 1970; Watowich, 1978; Holst et al., 1986; Martineau, 1989; Severson and Barnes, 1991). Major irregularities in the basal contact are generally related to folds in the underlying country rock indicating that intrusion proceeded more or less along bedding planes in the footwall rocks (Holst et al., 1986). This is readily expressed by a major east-west -trending trough and ridge in the basal contact at Mesaba that coincides exactly with a syncline-anticline that is defined by the top of the Biwabik Iron Formation (BIF). The thickness of preserved Virginia Formation between the Complex and the BIF is variable due to the amount of material assimilated by the Complex.

The Local Boy ore zone is also situated over this anticlinal ridge. The majority of massive sulfide ore zones, hosted mainly by the Virginia Formation (Severson and Barnes, 1991), are broadly coincident with the axis of the anticline. The contoured top of the BIF in the Local Boy area is shown in Figure 3B-3 (left). Similar anticline geometries are also present for the basal contact as shown in Figure 3B-3 (right). All the data indicate that an EW-trending anticline is the major structural feature present within the footwall rocks of the Local Boy area.

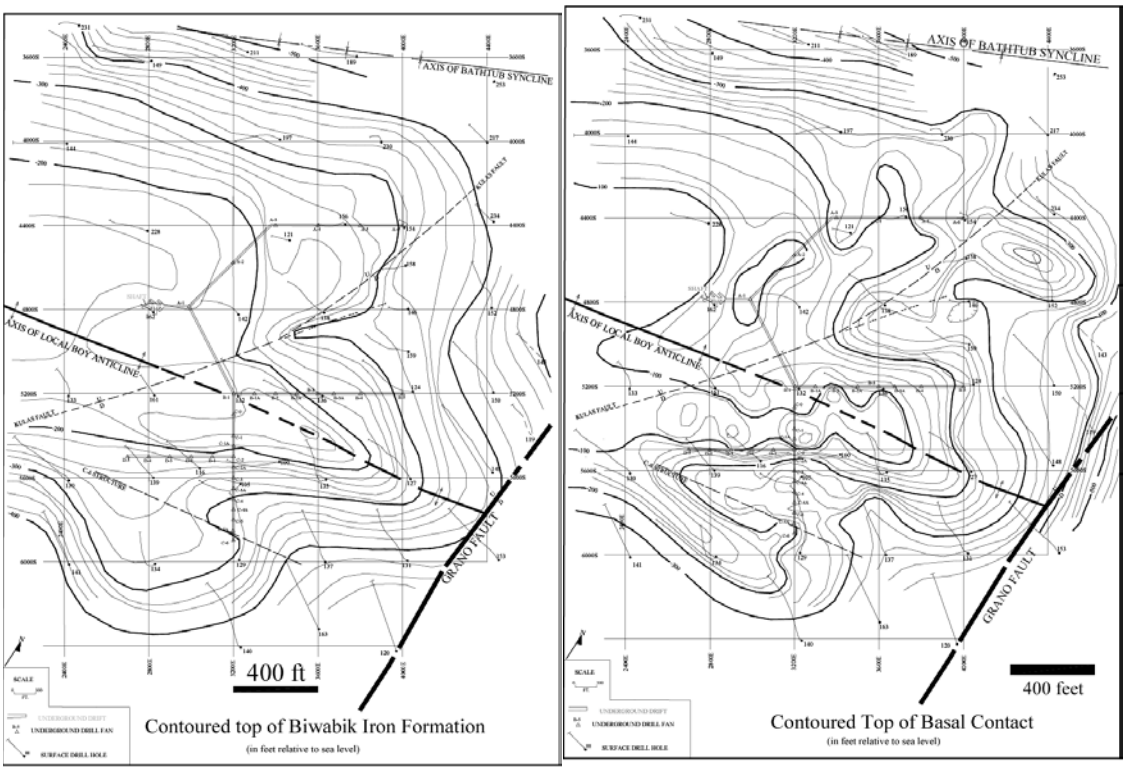


Figure 3B-3. Contoured top of the Biwabik Iron Formation at Local Boy (left), and the contoured top of the basal contact between the footwall Virginia Formation and the Partridge River intrusion at Local Boy (right). Diagrams from Severson and Hauck, 2008.

Mineralization Trends in the Massive Sulfide at the Local Boy Ore Zone

The vast majority of massive sulfides at Local Boy are contained within the Paleoproterozoic Virginia Formation. Even though the massive sulfides straddle the basal contact, most of the massive sulfides are associated with either hornfelsed sedimentary inclusions above the contact or with footwall rocks below the contact while the interfingering intrusive rocks are relatively barren of massive sulfides (Severson and Barnes, 1991). This suggests that the massive sulfide ores were not formed in this area by the gravitational settling of sulfides, but rather, the ores formed by injection of an immiscible sulfide melt into structurally prepared areas within the footwall rocks along the Local Boy anticline in a vein-like setting. A similar mechanism is proposed for the Norilsk-Talnakh deposits in Russia.

Even though the basal contact of the Complex with the Virginia Formation is highly undulatory, the massive sulfides exhibit a definite top and bottom. The ore is distributed such that most of it is contained within a zone between 20 feet and 300 feet above the top of the Biwabik Iron Formation. The geologic constraint for the bottom of the ore zone generally corresponds to the top of the VirgSill (a structurally competent unit). The constraints for the upper portion of the ore zone are unknown and may have been obliterated during emplacement of the Complex. Figure 5B-7 is an attempt to show, in a plan view, where massive sulfide zones are present. Also shown in the figure are the different massive sulfide types (ranging from pyrrhotite-dominant to Cu-rich) relative to structural features. The relationships shown in Figure 3B-4 indicate that the massive sulfides show a progressive change in an east-to-west direction from Cu-poor massive sulfides to Cu-rich massive sulfides in the vicinity of the Local Boy anticline. These relationships suggest that the injected immiscible sulfide melt underwent fractional crystallization

and progressively became more Cu and PGE enriched as it moved through the footwall rocks in an east-to-west direction.

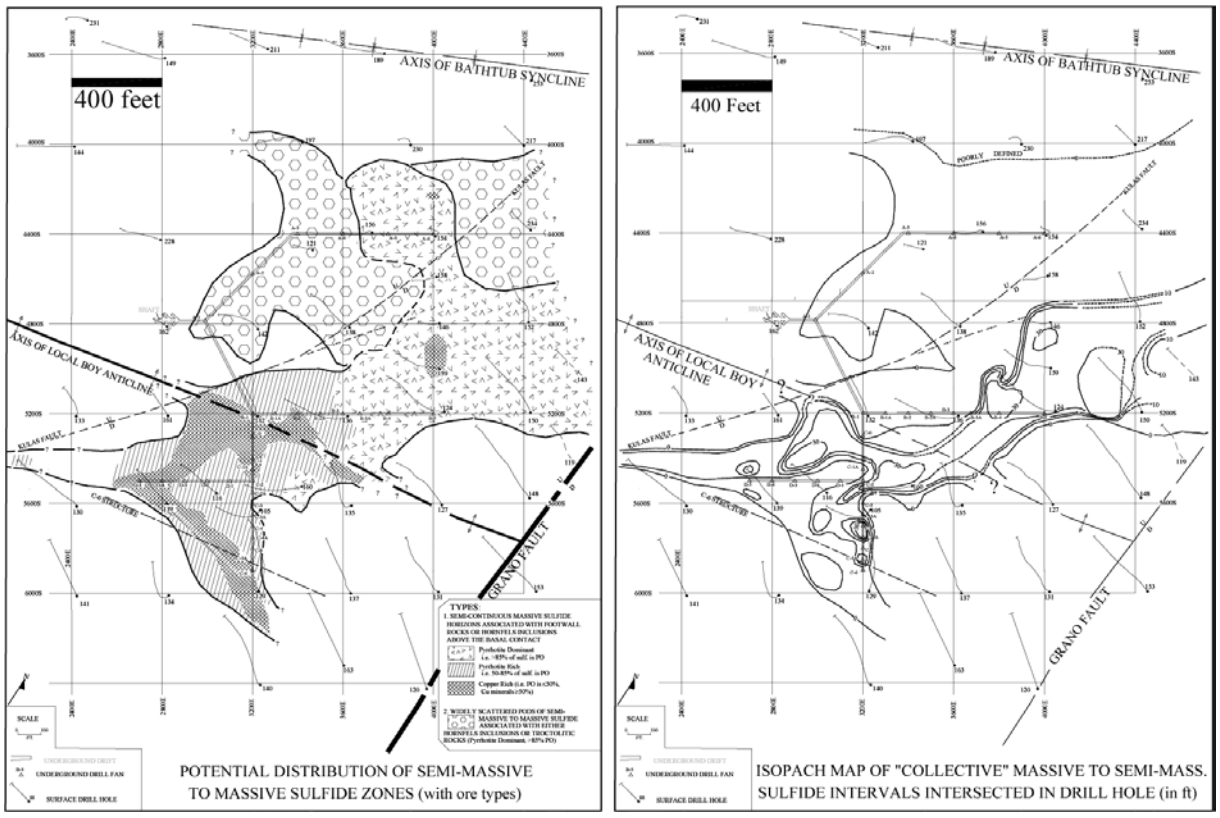


Figure 3B-4. Potential distribution of semi-massive to massive sulfide types (Cu-poor versus Cu-rich) at the Local Boy ore zone (left); and an isopach map of the cumulative thickness of the massive sulfide zones at the Local Boy ore zone (right). Note that the massive sulfides are not present as a continuous blanket, but rather, as one or more stacked disjointed/separated multiple horizons near the basal contact. Diagrams from Severson and Hauck, 2008.

A possible feeder vent for the sulfide injection event may have been the Grano Fault, which was repeatedly reactivated during emplacement of the Complex. Other data that indicates that the Grano Fault was a potential feeder vent include: 1) the massive sulfides are more common, and thicker (Figure 3B-4), close to the Grano Fault (feeder) and along the axis of the Local Boy anticline (structurally-prepared site); 2) the VirgSill rarely contains significant amounts of disseminated sulfides – except near the Grano Fault; and 3) the Biwabik Iron Formation rarely contains sulfides – except near the Grano Fault.

In summary, the massive sulfides at the Local Boy ore zone are interpreted to be structurally controlled in that they are situated along the axis of the Local Boy anticline. The massive sulfides are locally Cu-rich (5-25% Cu; Severson and Hauck (2008) – based on historical assay data on file at MDNR) and are almost exclusively hosted by the Virginia Formation. Sulfide textures suggest that the massive sulfides were injected as an immiscible sulfide melt into the footwall rocks. The overall pattern of sulfide types and PGE contents suggest that the sulfides formed via a process of fractional crystallization of an immiscible sulfide melt as it migrated into the footwall rocks. The Grano Fault is inferred to represent the potential feeder zone in this scenario.

PART 3C: TWIN METALS MINNESOTA'S MATURI DEPOSIT

Kevin D. Boerst – Twin Metals Minnesota

(Portions previously written by Dean M. Peterson – formerly with Duluth Metals Limited)

INTRODUCTION

Twin Metals Minnesota's Maturi deposit is the largest and highest-grade classified Cu-Ni-PGE deposit in the 1.1 Ga. Duluth Complex of northeastern Minnesota. The deposit is located near the north end of the South Kawishiwi intrusion (SKI) west-southwest of the junction of the Nickel Lake Macrodike (NLM) and the SKI (Peterson et al., 2006; Peterson and Albers, 2007; Tharlason et al., 2007; Peterson, 2008; Gal, 2008; and White, 2010). The deposit was discovered utilizing a genetic ore deposit model that identified channelized magma flow within the SKI under a large xenolith/pillar of anorthosite. The model led to exploratory drilling in 2006; deposit discovery and resource estimations in 2007 & 2008; a joint venture with Antofagasta plc in 2010; and significant resource expansion and classification upgrades in 2012 and 2014 (Fig. 3C-1). The company is currently optimizing its business case with the aim of completing a Mine Plan of Operation (MPO) in the future.

RESOURCES

The Mineral Resource estimate for the Maturi deposit (completed by AMEC) incorporate assay data from 564 drill holes totaling 1,466,641 feet (excluding wedges) drilled on the Maturi deposit that includes 75 legacy holes also in the geologic data base. The April 2014 Resource Estimates for the Maturi (as well as the Birch Lake and Spruce Road deposits) is based on a 0.3% copper cut-off grade to define the resource model. Based on AMEC`s review of metal prices, process recoveries, refining costs and underground mine operating costs likely to apply at the Twin Metals site, the 0.3% copper cut-off grade (highlighted) is considered the base case for the statement of Indicated and Inferred Mineral Resources at this time. The estimates at the cut-off grades higher and lower than the base case are provided to show sensitivity of the cut-off grade (Table 3C-1).

Table 3C-1. April 2014 resource estimate for TMM's Maturi Deposit.

	Cu%	Million	Cu	Ni	Pt	Pd	Au	Ag	Co
	Cut-off	Tons	%	%	ppm	ppm	ppm	ppm	ppm
Measured Resources	0.2	327	0.61	0.20	0.141	0.328	0.080	2.2	105
	0.3	308	0.63	0.20	0.146	0.339	0.083	2.3	107
	0.4	275	0.66	0.21	0.155	0.359	0.088	2.4	110
	0.5	237	0.70	0.22	0.165	0.383	0.093	2.5	113
	0.6	183	0.74	0.24	0.177	0.411	0.100	2.7	116
Indicated Resources	0.2	881	0.56	0.18	0.148	0.336	0.080	2.0	102
	0.3	822	0.58	0.19	0.155	0.350	0.083	2.1	104
	0.4	716	0.61	0.20	0.166	0.375	0.089	2.2	106
	0.5	547	0.66	0.21	0.186	0.420	0.099	2.4	109
	0.6	379	0.71	0.22	0.205	0.461	0.108	2.6	111
Inferred Resources	0.2	768	0.42	0.13	0.116	0.262	0.059	1.6	81
	0.3	531	0.49	0.16	0.138	0.314	0.070	1.8	98
	0.4	358	0.57	0.19	0.167	0.376	0.083	2.0	110
	0.5	235	0.63	0.20	0.202	0.449	0.099	2.3	112
	0.6	127	0.69	0.21	0.246	0.545	0.118	2.5	111

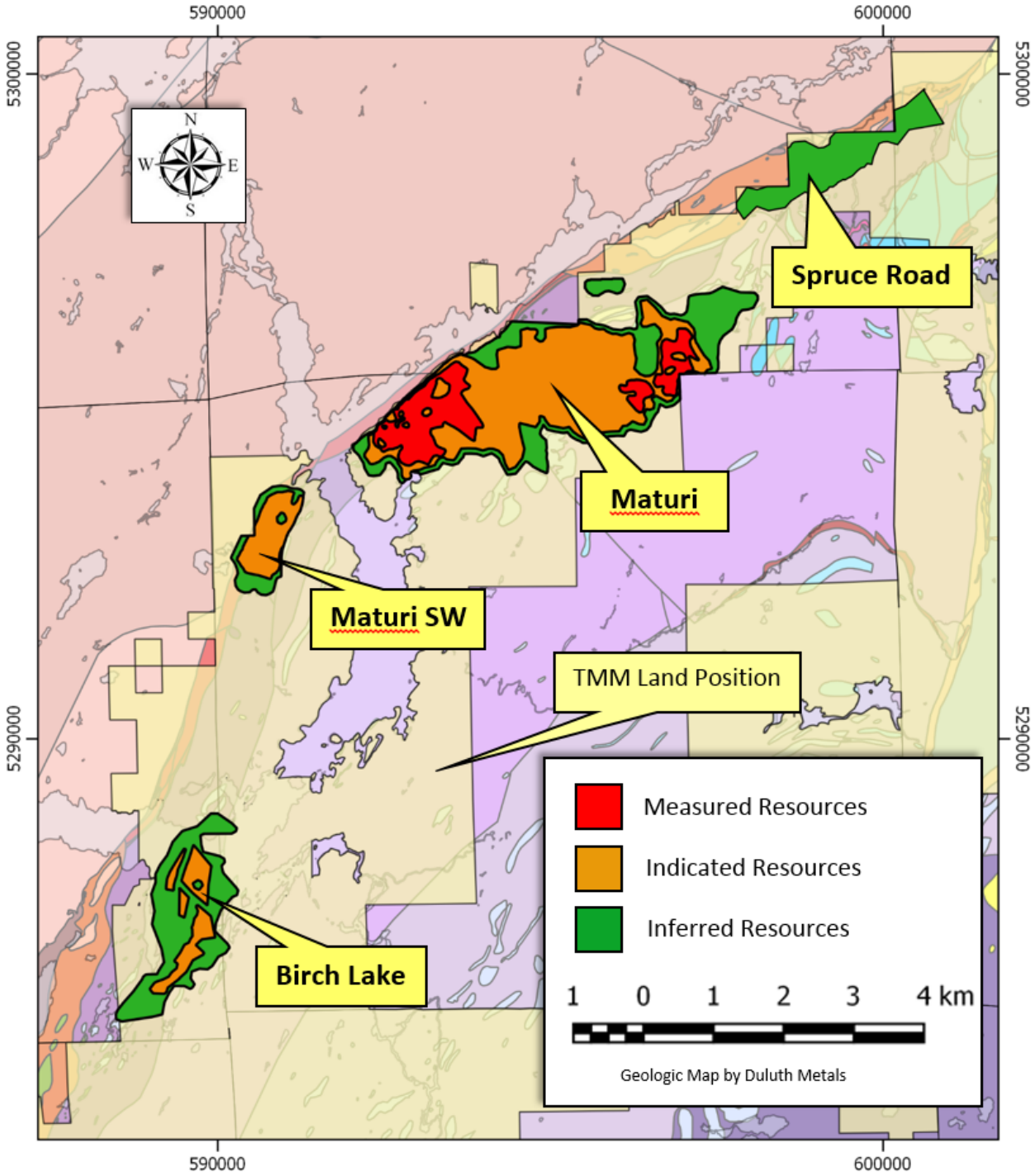


Figure 3C-1. Map of Twin Metals Minnesota's deposits and resource classification.

GEOLOGY OF THE MATURI DEPOSIT

The Maturi Deposit is located within the South Kawishiwi Intrusion (SKI), a shallow dipping (~24º east-southeast) sill-like troctolitic intrusion exposed in an 8- x 32-kilometer arcuate band along the northwestern margin of the Duluth Complex. Lithologic units within the Maturi deposit include Mesoproterozoic rocks of the SKI and Anorthositic Series of the Duluth Complex as well as basalt xenoliths of the North Shore Volcanic Group. At Maturi, SKI magmas intruded between hanging wall anorthositic rocks and footwall granitic rocks of the Neoarchean Giants Range batholith (Fig. 5C-1). Brief descriptions of the lithostratigraphic units within the Maturi Deposit are given in Table 3C-2.

Table 3C-2. Lithostratigraphic units within the Maturi deposit.

Duluth Complex and related rocks (1.1 Ga.)	
SKI	Anorthositic troctolite to troctolite **(ATA Series)** - Medium to coarse-grained, homogeneous, well-foliated and locally layered anorthositic troctolite, troctolite, and ophitic troctolitic rocks. In the field, this unit is commonly referred to as the "sea of troctolite".
	Augite-bearing troctolite **(Main AGT)** - Homogenous, coarse-grained, subophitic to ophitic, poorly foliated augite troctolite characterized by scattered augite-rich pegmatitic clots and patches. Commonly capped by hanging wall inclusions (HB & Ai) and interpreted to be the solidified basaltic liquid that carried the BMZ crystals and sulfides.
	Sulfide-bearing troctolite **(BMZ)** - Heterogeneous, sulfide-bearing, varitextured troctolite, augite troctolite, anorthositic troctolite, and olivine gabbro with 0.5 - 5% disseminated chalcopyrite, cubanite, talnakhite, pentlandite and pyrrhotite.
Xenoliths in the SKI	Anorthosite **(An-Series & Ai)** - Undifferentiated Anorthositic Series inclusions. Includes well-foliated very coarse-grained anorthosite, troctolitic-anorthosite, poikilitic troctolitic anorthosite, gabbroic anorthosite, gabbro, and locally troctolite. Inclusions range from a few cm's to elongate bodies measured in km's.
	Anorthositic gabbro to gabbro **(Upper Gabbro)** - Mixed group of Anorthositic Series rocks that occur in the central portion of the map area. Includes well-foliated anorthositic gabbro, gabbro, oxide gabbro, anorthosite, and augite troctolite.
	Basaltic hornfels **(Upper Basalt, HB)** - Fine-grained, granoblastic to poikiloblastic basaltic hornfels; consists of variable amounts of plagioclase, augite, olivine, hypersthene, and inverted pigeonite. Commonly associated with Anorthosite xenoliths (unit Ai).
Giants Range Batholith (2.68 Ga.)	
Footwall	Porphyritic quartz monzonite **(GRB)** - Pink, coarse-grained, hornblende-phyric, porphyritic quartz monzonite with large (1-2 cm) orthoclase phenocrysts. Also contains irregular zones of aplite, lamprophyre, and supracrustal xenoliths. Strongly recrystallized and partially melted locally adjacent to the contact with the SKI.

Early modeling of the Maturi Deposit was limited due to wider-spaced drill holes across the deposit area, though Severson (1994) did a remarkable job in defining the igneous stratigraphy of the SKI along a 19 mile strike length. Severson recognized the fact that the rocks below the lower pegmatite (PEG) unit typically contained sulfides and that rocks above the PEG unit were a monotonous sequence of sulfide-barren anorthositic troctolite to troctolite (AT/T), and augite-troctolite (Main AGT).

Two detailed geologic cross sections through the Maturi Deposit are presented in Figure 3C-2. These sections display the continuity of the basal mineralization as well as the differences in the hanging wall

stratigraphy from west to east through the deposit. In the east, the deposit is located under an extremely thick (>1,000m) megaxenolith of Anorthosite Series rocks, and in essence the basal SKI can be viewed as a thin sill-like body. To the west, the anorthosite xenolith ends and the immediate hanging wall rocks to the deposit are sulfide-barren troctolites of the Main AGT unit. We interpret that the Main AGT as the solidified troctolite melt that carried the crystals and sulfide droplets of the magmatic slurry.

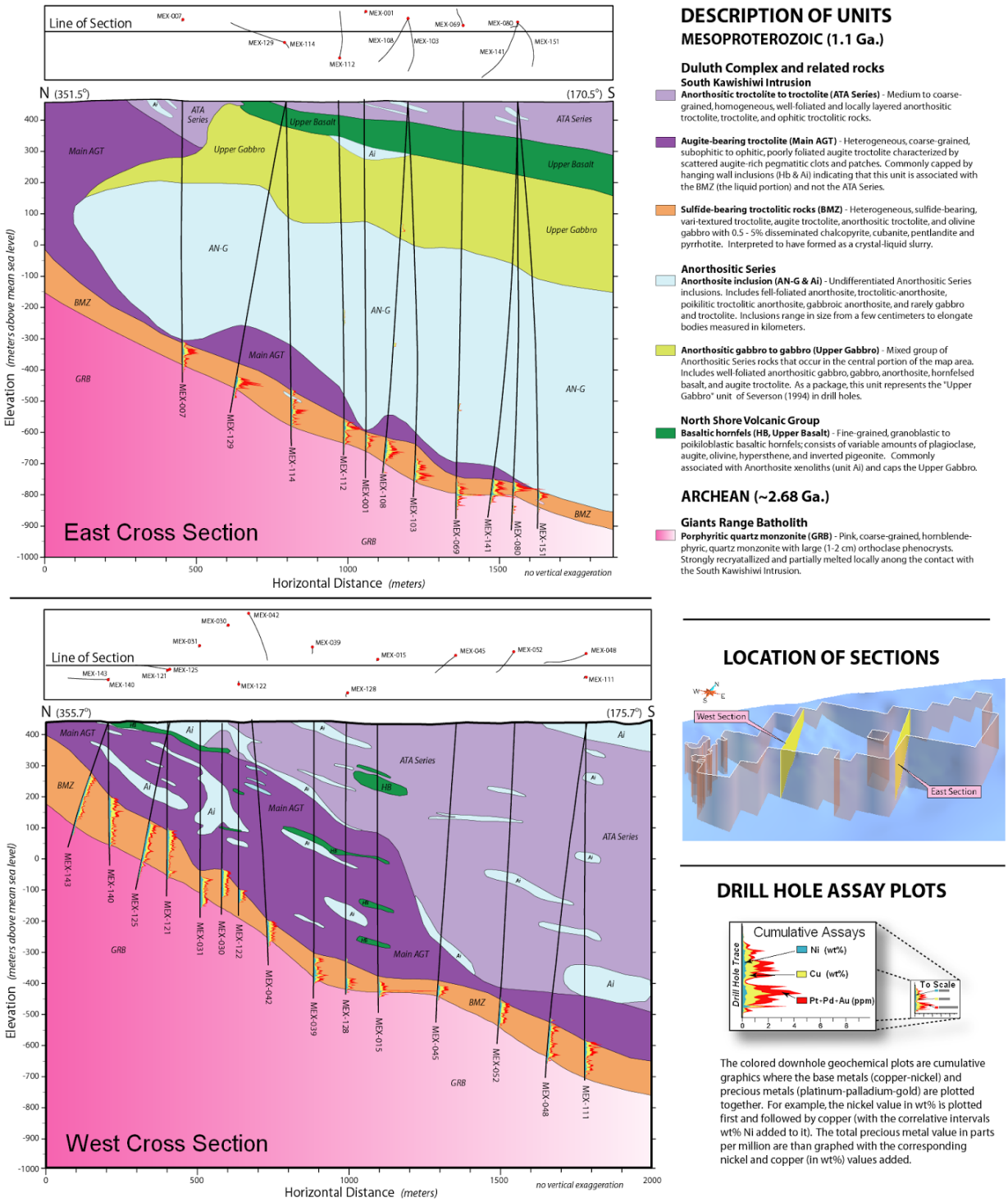


Figure 3C-2. Geologic cross sections through the Maturi Deposit.

In 2008, geologists from Duluth Metals came to the realization that the initial basaltic composition SKI magmas that ultimately solidified to create the Maturi deposit intruded as sulfide-bearing, crystal-laden (olivine and plagioclase crystals), magmatic slurries. Based on this new interpretation, the company reinterpreted Severson's (1994) regional basal stratigraphy (units U3, BH, BAN) of the SKI (Fig. 3C-3) at Maturi into the Basal Mineralized Zone, or BMZ. The company believes that the geometry of the system (sill-like sub-horizontal intrusion) and the inherent crystallinity of the basaltic melts (phenocrysts of plagioclase and olivine) led to crystal sorting and melting of the footwall granitic rocks to create the heterogeneous lithologies and textures of the BMZ.

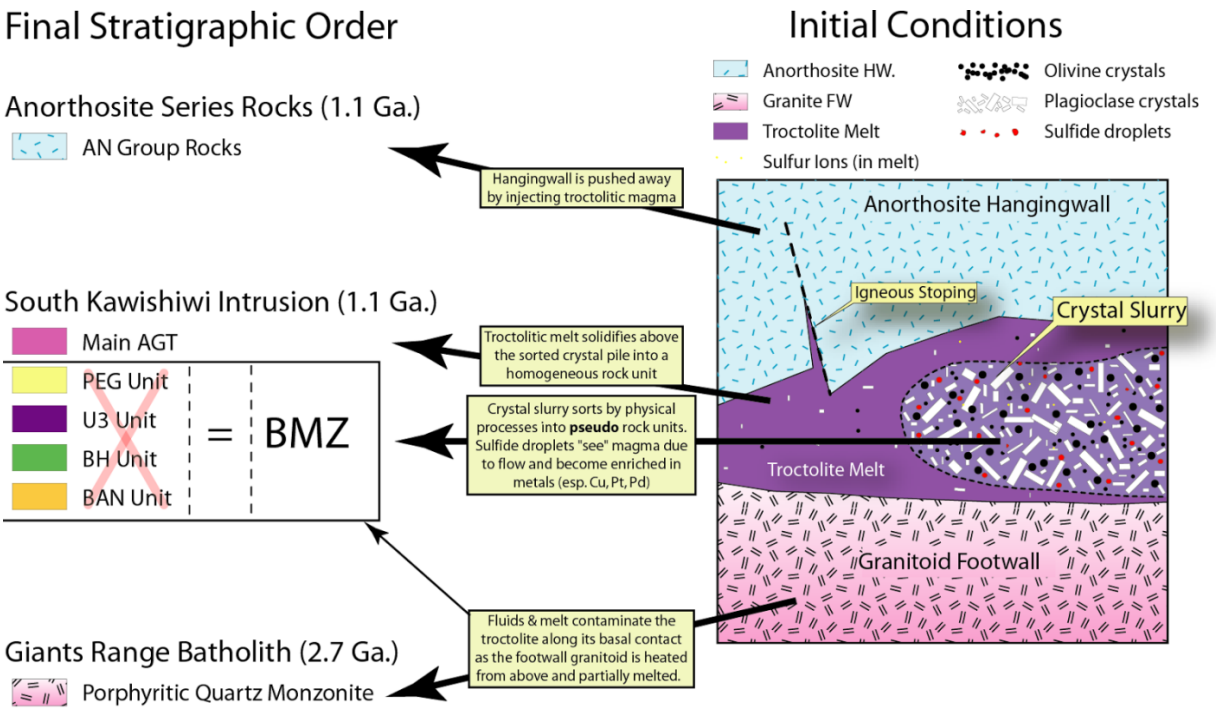


Figure 5C-3. Simplified crystal-liquid slurry model for the SKI in the Maturi area.

MATURI ORE DEPOSIT MODEL

In 2012, the geology of the mineralized portions (the BMZ) of the Maturi deposit were reevaluated by the geologic staffs of Duluth Metals, Twin Metals, and geologists from AMEC utilizing a significant volume of new, high-quality geochemical and geological data during the completion of an updated mineral resource classification by the consulting firm AMEC.

Mineralization in both the BMZ and footwall at Maturi were reclassified based on patterns in the physical distribution of mineralization as projected on down-hole plots. Sulfide mineralization is characterized by several distinct patterns, including (1) very low grade mineralized intervals showing low variability (Stage 1), (2) moderate grade mineralized intervals showing low variability (Stage 2), and 3) higher grade mineralized intervals showing higher variability and commonly bounded by low grade selvages (Stage 3) (Fig. 3C-5). Significantly, the contacts between different mineralized intervals are typically quite abrupt. A single hole might contain one or several distinct mineralized intervals within the BMZ, including higher grade intervals with the highest grade occurring at the top, middle, or bottom of the section. Based on these criteria, four intrusive subunits, characterized by common grade profiles, were defined in the BMZ. In addition, two distinct suites of mineralization were identified in the footwall

rocks, including Ni-Co enriched semi-massive to massive sulfide zones and disseminated Cu-PGE enriched zones deep in the footwall granitoids.

The classifications derived from this exercise were validated by multivariate statistical analysis of multi-element geochemical data, including principal component analysis (Fig. 3C-6) and factor analysis. This investigation revealed a significant correlation of multi-element geochemistry to mineralization within the BMZ as well as several possible subdivisions of the BMZ based on both the physical distribution patterns of mineralization and the geochemistry of the host rocks. The Maturi subunits so defined and validated were determined to occur in a consistent stratigraphic order, and are correlative across the deposit.

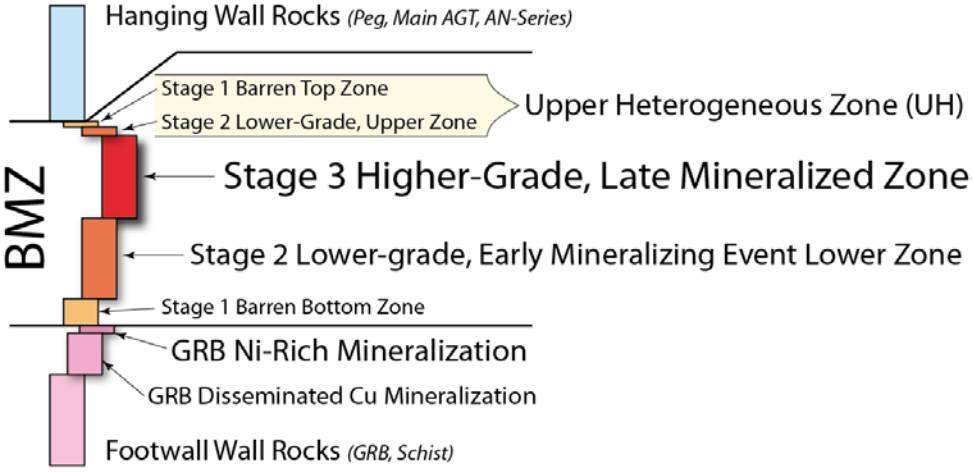


Figure 3C-5. Revised igneous stratigraphy of the BMZ and adjacent rocks within the Maturi deposit.

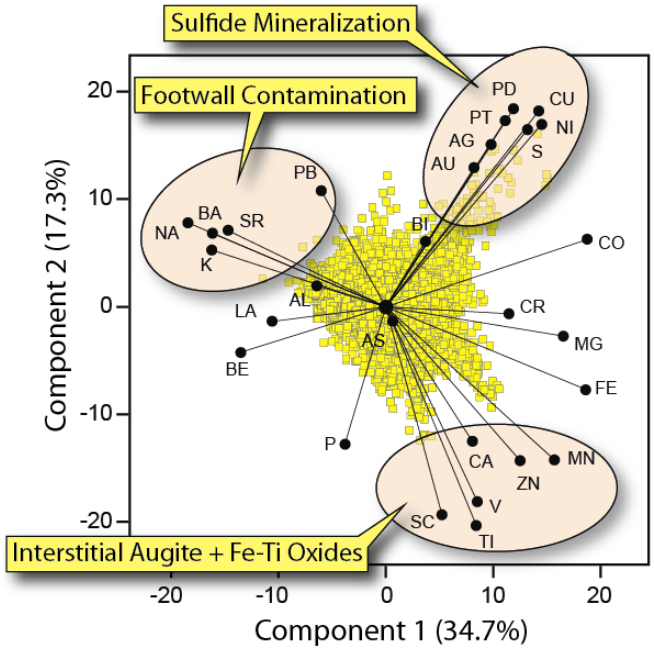


Figure 3C-6. Multi-element principal component analysis plot of MEX-Series drill hole geochemical data.

Typical geochemical plots of Maturi drill holes are presented in Figure 3C-7 and display several of the patterns that were originally identified in the development of the revised geological model of the Maturi deposit. As well, an idealized intrusive sequence model for the SKI in the Maturi deposit area is given in Figure 3C-8 and a NW to SE cross section of the modeled units of the BMZ is presented in Figure 3C-9.

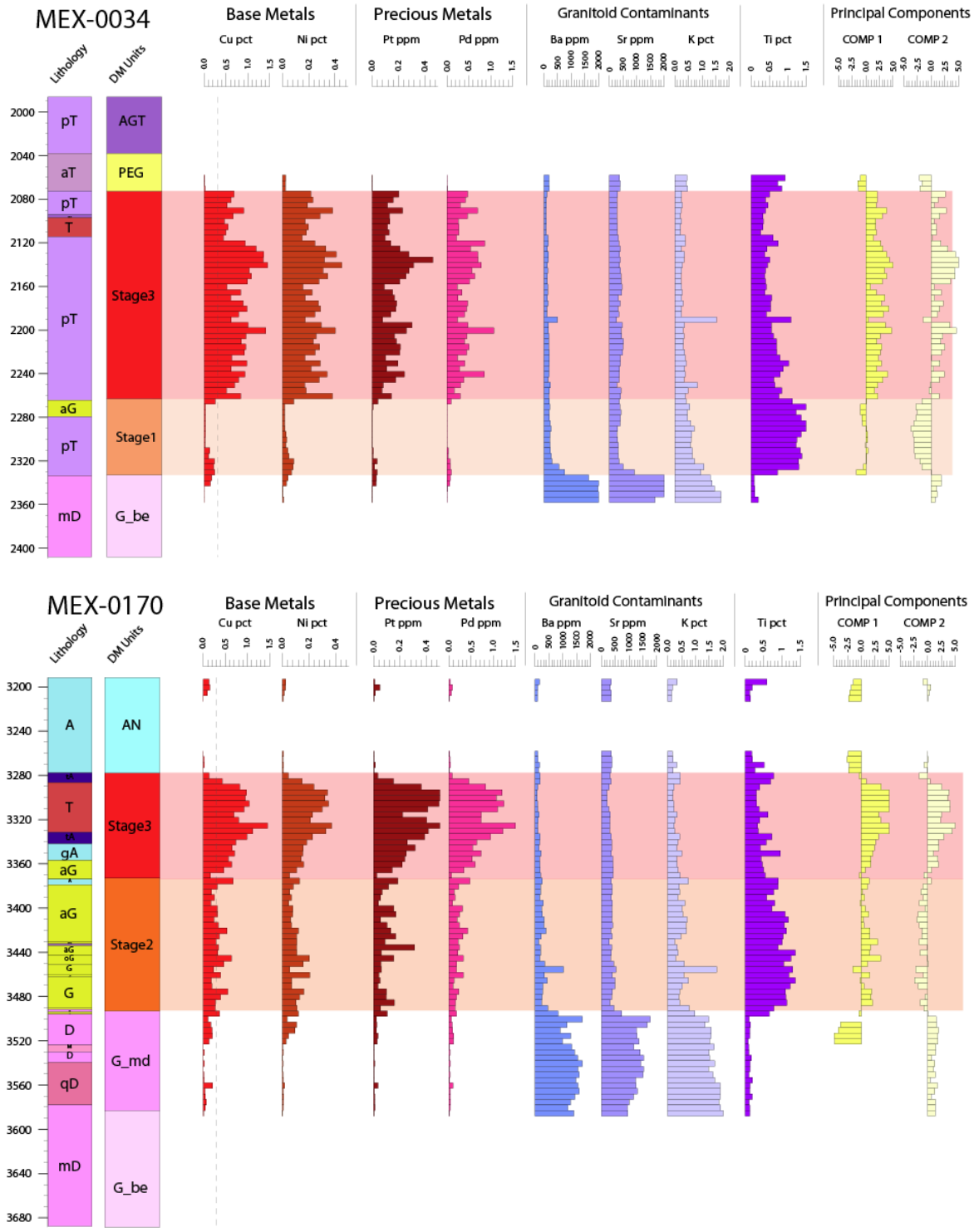


Figure 3C-7. Downhole geochemical and principal component plots of typical drill holes within the Maturi deposit.

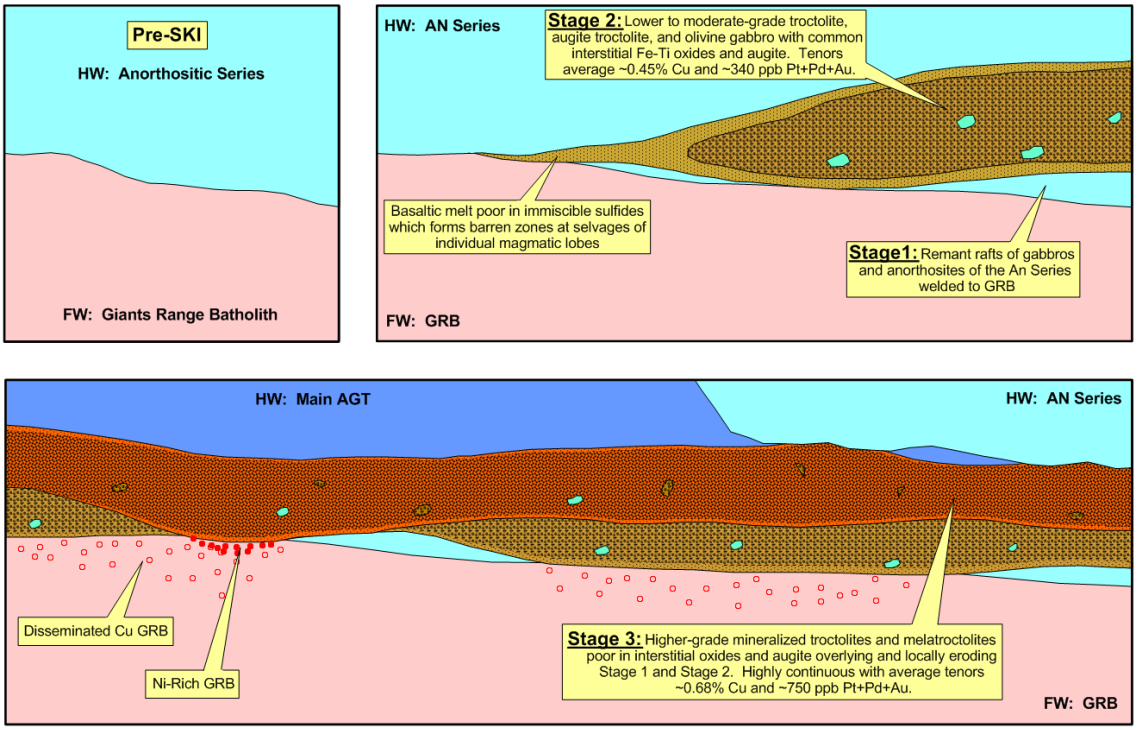


Figure 3C-8. Idealized intrusive sequence model of the SKI in the Maturi deposit area.

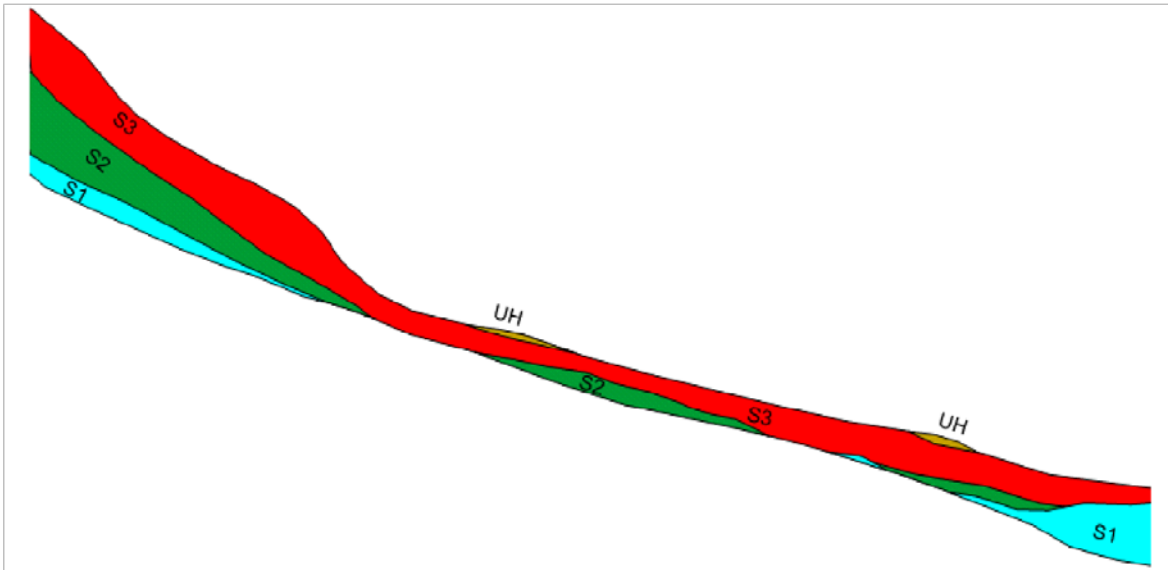


Figure 3C-9. Northwest (left) to Southeast (right) cross section through the Maturi deposit depicting the recently modeled geological units of the BMZ.

Detailed descriptions of the seven units modeled for the Maturi deposit is well beyond the scope of this field trip guidebook. However, brief descriptions are provided in Table 3C-3 below and geochemical plots of copper, nickel, and precious metals are given in Figure 3C-10.

One of the most important outcomes of the reinterpretation of the geology and mineralization within the Maturi deposit has been the identification of the higher-grade Stage 3 (S3) intrusive unit of the SKI (Table 3C-4). S3 has the highest grade and is the most widely distributed of the four BMZ units (Fig. 3C-11). Cu, Ni, and PGEs and are all significantly elevated in S3 relative to the other BMZ units and the

mineralized GRB. Stage 2 (S2) mineralization is overall much lower grade than S3, but locally S2 is well mineralized, and will likely contribute significantly to the deposit economics. Mineralization in the GRB is overall low grade and discontinuous. However, local zones of the unit G-N (where Cu and especially Ni locally occur as massive and semi-massive sulfides) are very high grade and may contribute to the resource.

Table 3C-3. Interpreted lithostratigraphic-chemostratigraphic units within and adjacent to the BMZ within the Maturi deposit.

Unit	Description
UH	Discontinuous, barren to low-grade, highly variable troctolite
Stage 3	Continuous, higher-grade, PGE-enriched, heterolithic troctolite and melatroctolite
Stage 2	Continuous, moderate-grade, heterolithic, oxide-bearing, augite-troctolite to troctolite
Stage 1	Discontinuous, barren to very low-grade, homogeneous troctolite, gabbro, anorthosite and/or norite
G-N	Irregular, locally high-grade, Ni- and Co-enriched semi-massive to massive sulfide pods and veins at or immediately below the basal SKI contact.
G-M	Discontinuous, low to moderate-grade, disseminated Cu and PGE enriched mineralization.
G-B	Continuous, barren granitoid footwall rocks

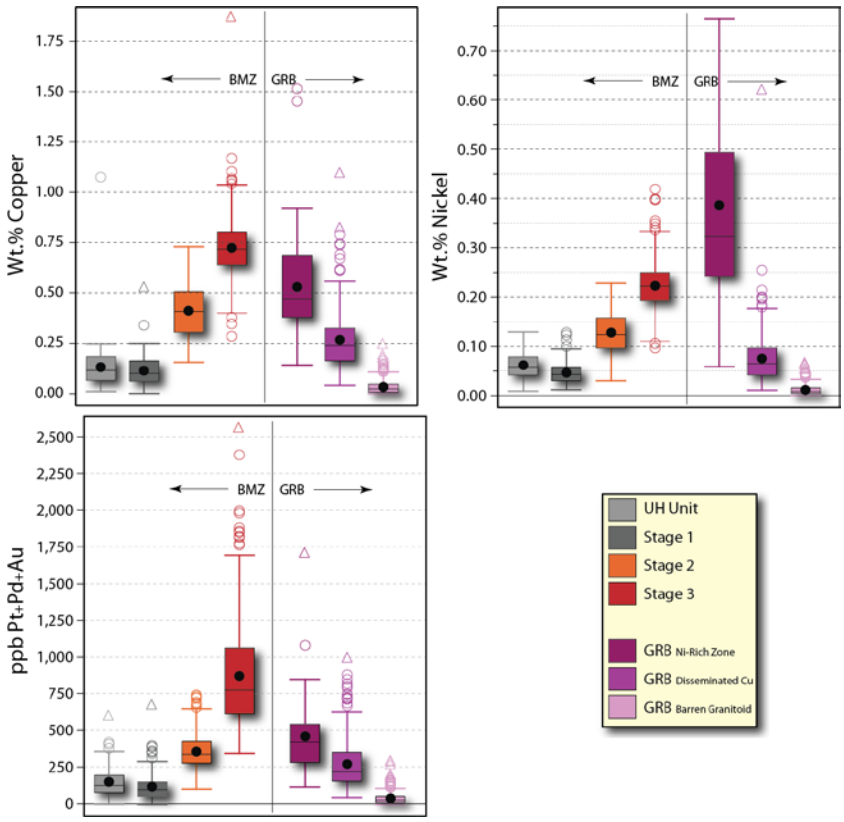


Figure 3C-10. Geochemical boxplots of composited drill hole geochemistry for units within and adjacent to the BMZ within the Maturi deposit.

The current lithostratigraphic model of the Maturi deposit effectively discriminates between higher- and lower-grade mineralization and provides a realistic geological model. The new data allowed correlation of units from hole-to-hole and section-to-section resulting in a very robust geologic model upon which to build mine plans and further our understanding of the magmatic processes that occurred to generate TMM's Maturi Deposit.

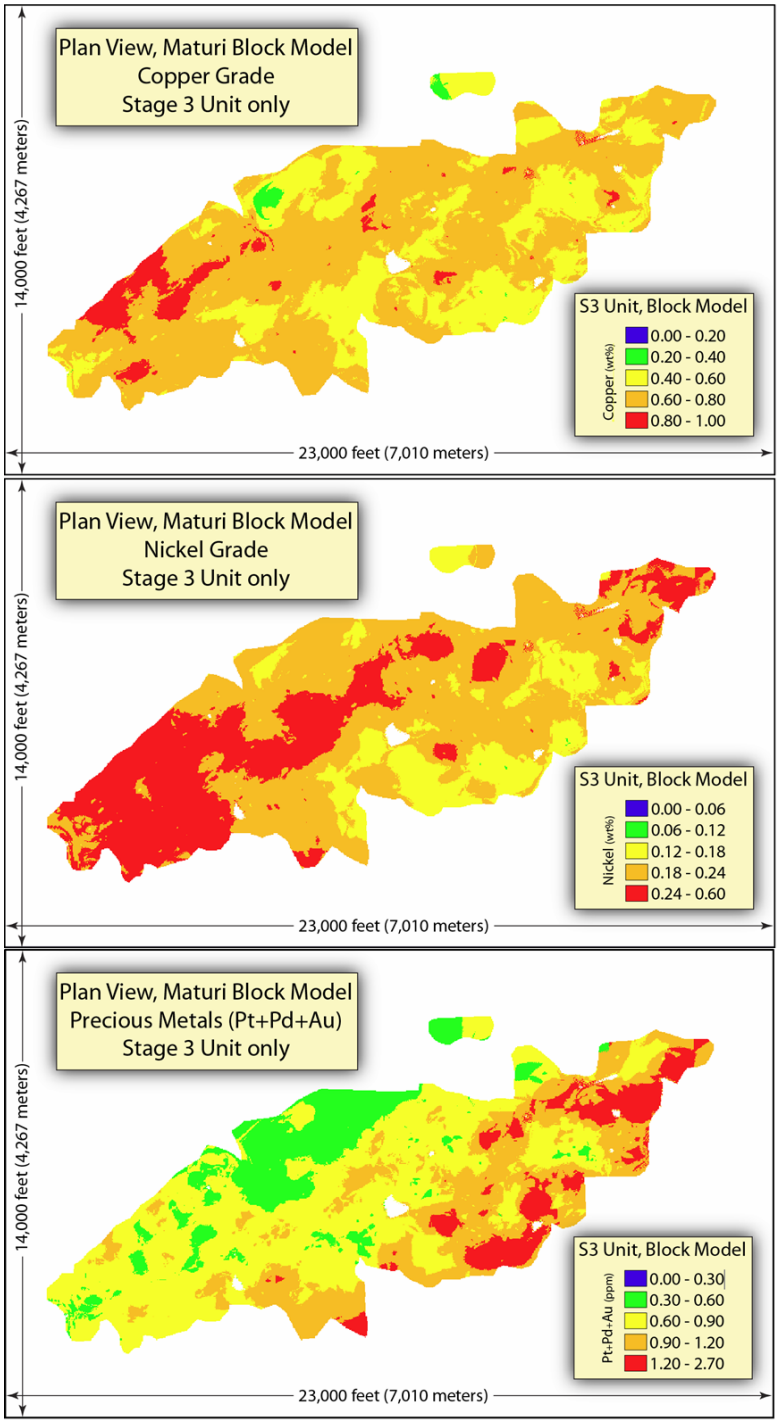


Figure 3C-11. Plan views of Stage 3 Cu, Ni, and TPM grades from the TMM Maturi deposit block model.

REFERENCES

Desaultels, P., and Patelke, R., 2008, Updated Technical Report on the NorthMet Deposit, Minnesota, USA, by Wardrop Engineering, (Toronto) for PolyMet, 109 p.

Duchesne, L., 2004, Partial melting in microstructures associated with the contact aureole of the Duluth Igneous Complex: Unpublished M.S. thesis [in French], University of Quebec at Chicoutimi, 217 p.

Foose, M.P., 1984, Logs and correlation of drill holes within the South Kawishiwi intrusion, Duluth Complex, northeastern Minnesota: United States Geological Survey, Open-file Report 84-14.

Gal, B., 2008, The South Filson Creek deposit, a Masters of geology thesis: Eotvos Lorand University, Budapest, Hungary.

Geerts, S. D., 1994, Petrography and geochemistry of a platinum group element-bearing horizon in the Dunka Road prospect, (Keweenawan) Duluth Complex, northeastern Minnesota: Unpublished M.S. thesis, University of Minnesota, Duluth, 100 p.

Geerts, S.D., 1991, Geology, stratigraphy, and mineralization of the Dunka Road Cu-Ni prospect, Northeastern Minnesota: Natural Resources Research Institute, Univ. Minn., Duluth, Tech. Rpt., NRRI/TR-91/14, 63 p.

Hauck, S.A., Severson, M.J., Zanko, L.M., Barnes, S.-J., Morton, P., Aliminas, H.V., Foord, E.E., and Dahlberg, E.H., 1997, An overview of the geology and oxide, sulfide, and platinum-group element mineralization along the western and northern contacts of the Duluth Complex, in Ojakangas, R.W., Dickas, A.B., and Green, J.C., eds., Middle Proterozoic to Cambrian rifting, central North America: Geological Society of America Special Paper 312, p. 137-185.

Hauck, S.A., and Severson, M.J., 2000, Platinum-group element-gold-silver-copper-nickel-cobalt assays primarily from the Local Boy ore zone, Babbitt deposit, Duluth Complex, northeastern Minnesota: An update: Natural Resources Research Institute, University of Minnesota, Duluth, Report of Investigations NRRI/RI-2000/01, 48 p.

Holst, T.B., Mullenmeister, E.E., Chandler, V.W., Green, J.C., and Weiblen, P.W., 1986, Relationship of structural geology to the Duluth Complex to economic mineralization: Minnesota Department of Natural Resources, Division of Minerals Report 241-2.

Ikola, R.J., 2006, Vertical Electrical Soundings - NorthMet Project - St. Louis County, Minnesota, Prepared for PolyMet Mining Corp.: R.J. Ikola and Associates, Inc., Hibbing, Minnesota, 115 p.

Jennings, C.E., and Reynolds, W.K., 2005, Surficial Geology of the Mesabi Iron Range, Minnesota: Minnesota Geological Survey, Miscellaneous Map M-164, scale 1:100,000.

Lehr, J.D., and Hobbs, H.C., 1992, Glacial geology of the Laurentian divide area, St. Louis and Lake Counties, Minnesota: Minnesota Geological Survey Field Trip guidebook series, 18, Prepared for the 39th Midwest Friends of the Pleistocene Field Trip, Biwabik, Minnesota, 1992, 73 p., map, 1:250,000.

Listerud, W.H., and Meineke, D.G.., 1977, Mineral resources of a portion of the Duluth Complex and adjacent rocks in St. Louis and Lake Counties, northeastern Minnesota: Minnesota Department of Natural Resources, Division of Minerals, Report 93, 74p.

Mancuso, J.D., and Dolence, J.D., 1970, Structure of the Duluth Gabbro Complex in the Babbitt area, Minnesota (abs.): 16th Annual Institute on Lake Superior Geology, Thunder Bay, Ontario, p. 27.

Martineau, M. P., 1989, Empirically derived controls on Cu-Ni mineralization: A comparison between fertile and barren gabbros in the Duluth Complex, Minnesota, U.S.A.: in Prendergast, M. D., and Jones, M. J., eds., Magmatic Sulphides - The Zimbabwe Volume: Inst. Min. Metall., London, p. 117-137.

Miller, J.D., Green, J.C., Severson, M.J., Chandler, V.W., and Peterson, D.M., 2001, Geological map of the Duluth Complex and related rocks, Northeastern Minnesota; Minnesota Geological Survey, Miscellaneous Map M119, scale 1:200,000.

Miller, J.D., Jr. and Severson, M.J., 2002, Geology of the Duluth Complex in Miller, J.D., Jr., Green, J.C., Severson, M.J., Chandler, V.W., Hauck, S.A., Peterson, D.M., and Wahl, T.E., 2002a, Geology and mineral potential of the Duluth Complex and related rocks of northeastern Minnesota: Minnesota Geological Survey Report of Investigations RI-58, p. 106-143.

Miller, J.D., Jr., Green, J.C., Severson, M.J., Chandler, V.W., Hauck, S.A., Peterson, D.M., and Wahl, T.E., 2002a, Geology and mineral potential of the Duluth Complex and related rocks of northeastern Minnesota: Minnesota Geological Survey Report of Investigations RI-58, 207 p.

Morton, P.M., and Hauck, S.A., 1987, PGE, Au and Ag contents of Cu-Ni Sulfides Found at the Base of the Duluth Complex, Northeastern Minnesota: Natural Resources Research Institute, University of Minnesota, Duluth, Technical Report NRRI/GMIN-TR-87-4, 94 p.

Muhich, T.G., 1993, Movement of titanium across the Duluth Complex–Biwabik Iron Formation contact at Dunka Pit, Mesabi Iron Range, northeastern Minnesota: Duluth, Minn., University of Minnesota Duluth, M.S. thesis, 154 p.

Park, Y.R., Ripley, E.M., Severson, M.J., and Hauck, S.A., 1999, Stable isotopic studies of mafic sills and Proterozoic metasedimentary rocks located beneath the Duluth Complex, Minnesota: Geochimica et Cosmochimica Acta, v. 63, no. 5, p. 657-674.

Patelke, R.L., 2003, Exploration drill hole lithology, geologic unit, copper-nickel assay, and location database for the Keweenawan Duluth Complex, northeastern Minnesota: Natural Resources Research Institute, University of Minnesota, Duluth, Technical Report, NRRI/TR-2003/21, 96 p.

Patelke, R.L., and Geerts, S.D.M., 2006, PolyMet NorthMet Drill Hole / Geological Database Recompilation: Location, Downhole Survey, Assay, Lithology, Geotechnical Data, and Related Information, 2004 to 2006, PolyMet Mining Inc. Internal report, 86 p.

Peterson, D.M. and Albers, P.B., 2007, South Kawishiwi Intrusion Cu-Ni-PGE mineralization in association with the Nickel Lake Macrodike, Institute on Lake Superior Geology, 53rd Annual Meeting, Field Trip Guidebook, Lutsen, Minnesota, Volume 53.

Peterson, D.M., 2001a, Development of a conceptual model of Cu-Ni-PGE mineralization in a portion of the South Kawishiwi Intrusion, Duluth Complex, Minnesota: Laurentian University – Society of Economic Geologists, Second Annual PGE Workshop, Sudbury, Ontario.

Peterson, D.M. and Severson, M.J., 2002, Chapter 4, Archean and Paleoproterozoic rocks forming the footwall of the Duluth Complex, in Geology and mineral potential of the Duluth Complex and related intrusions of northeastern Minnesota, Minnesota Geological Survey, Report of Investigations 58, pp. 76-93.

Peterson, D.M., 2008, Bedrock geologic map of the Duluth Complex in the northern South Kawishiwi intrusion and surrounding area, Lake and St. Louis Counties, Minnesota: Natural Resources Research Institute, Map Series NRRI/MAP-2008-01, scale 1:20,000.

Phinney, W.C., 1972, Duluth Complex, history and nomenclature, in Sims, P. K., and Morey, G. B., eds., Geology of Minnesota: A Centennial Volume: Minn. Geol. Survey, pp. 333-334.

Ripley, E.M., 1986, Origin and concentration mechanisms of copper and nickel in Duluth Complex sulfide zones – a dilemma: Economic Geology, v. 81, p. 974-978.

Sabelin, T., and Iwasaki, I., 1985, Metallurgical evaluation of chromium-bearing drill core samples from the Duluth Complex (Contract report of Minnesota Department of Natural Resources, Division of Minerals): Minerals Resources Research Center, University of Minnesota, Minneapolis, MN, 58 p.

Sabelin, T., and Iwasaki, I., 1986, Evaluation of platinum group metal occurrence in Duval 15 drill core from the Duluth Complex: Internal report, Minerals Resources Research Center, University of Minnesota, Minneapolis, MN, 23 p.

Severson, M.J., 1994, Igneous stratigraphy of the South Kawishiwi intrusion, Duluth Complex, northeastern Minnesota: Natural Resources Research Institute, University of Minnesota, Duluth, Technical Report NRRI/TR 93/34, 210 p. (with plates)

Severson, M.J., and Barnes, R.J., 1991, Geology, mineralization and geostatistics of the Minnamax/Babbitt Cu-Ni deposit (Local Boy area), Minnesota, Part II: Mineralization and geostatistics: Natural Resources Research Institute, University of Minnesota, Duluth, Technical Report, NRRI/TR-91/13b, 216 p.

Severson, M.J., and Hauck, S.A., 1990, Geology, geochemistry, and stratigraphy of a portion of the Partridge River intrusion: Natural Resources Research Institute, University of Minnesota-Duluth, Technical Report, NRRI/GMIN-TR-89-11, 236p. (with plates).

Severson, M.J., and Hauck, S.A., 2003, Platinum group elements (PGEs) and platinum group minerals (PGMs) in the Duluth Complex: University of Minnesota Duluth, Natural Resources Research Institute, Technical Report NRRI/TR-2003/37, 296 p.

Severson, M.J., and Hauck, S.A., 2008, Finish logging of Duluth Complex drill core (And a reinterpretation of the geology at the Mesaba (Babbitt) deposit): University of Minnesota Duluth, Natural Resources Research Institute, Technical Report NRRI/TR-2008/17, 68 p.

Severson, M.J., Miller, J.D., Jr., Peterson, D.M., Green, J.C., and Hauck, S.A., 2002, Mineral potential of the Duluth Complex and related intrusions in Miller, J.D., Jr., Green, J.C., Severson, M.J., Chandler, V.W., Hauck, S.A., Peterson, D.M., and Wahl, T.E., 2002a, Geology and mineral potential of the Duluth Complex and related rocks of northeastern Minnesota: Minnesota Geological Survey Report of Investigations RI-58, p. 164-200.

Severson, M.J., Patelke, R.L., Hauck, S.A., and Zanko, L.M., 1994a, The Babbitt copper-nickel deposit, Part B: Structural datums: Natural Resources Research Institute, University of Minnesota, Duluth, Technical Report NRRI/TR-94/21b, 48 p.

Severson, M.J., Patelke, R.L., Hauck, S.A., and Zanko, L.M., 1994b, The Babbitt copper-nickel deposit, Part C: Igneous geology, footwall lithologies, and cross-sections: Natural Resources Research Institute, University of Minnesota, Duluth, Technical Report NRRI/TR-94/21c, 79 p.

Sims, P.K., and Morey, G.B., eds. 1972, Geology of Minnesota: A Centennial Volume, Minnesota Geological Survey.

Tharalson, E., Sweet, G., Boisjoli, T., Lentz, B., Fellows, T., and Peterson, D., 2007, Geological Map of the Nickel Lake Macrodike and Northern Bald Eagle Intrusion, Lake County, Northeastern Minnesota: Precambrian Research Center Map Series PRC/MAP-2007-01, scale 1:10,000.

Watowich, S.N., Malcomb, J.B., and Parker, P.D., 1981, A review of the Duluth Gabbro Complex as a domestic source of critical and strategic metals: Society of Mining Engineers of AIME, preprint 81-351, 9 p.

White, C., 2010, The Nokomis Deposit, a Masters of Geology thesis: University of Minnesota, Duluth.

Wolff, J.F., 1917, Recent geologic developments on the Mesabi range, Minnesota: American Institute of Mining and Metallurgical Engineers Transactions, v. 56, p. 142-169.

Zanko, L.M., Severson, M.J., and Ripley, E.M., 1994, Geology and mineralization of the Serpentine copper-nickel deposit, Duluth Complex, Minnesota: Natural Resources Research Institute, University of Minnesota, Duluth, Technical Report, NRRI/GMIN-TR-93-52, 90p.

FIELD TRIP 4

May 4, 2016

DULUTH STREAM GEOMORPHOLOGY AND THE JUNE 2012 FLOOD

Karen Gran
Department of Earth and Environmental Sciences
University of Minnesota Duluth

~~FIELD TRIP CANCELLED~~

FIELD TRIP 5

May 4, 2016

GEOLOGY OF THE ENDION SILL EXPOSED ALONG DULUTH'S LAKEWALK

James D. Miller
Department of Earth and Environmental Sciences
and the Precambrian Research Center
University of Minnesota Duluth

Introduction

The Endion Sill is a mafic to felsic, hypabyssal intrusion that was emplaced into the North Shore Volcanic Group lavas during the 1.1 Ga Midcontinent Rift (Miller and Green, 2002). The sill is the lowest hypabyssal intrusion in the volcanic rocks overlying the Duluth Complex at Duluth. This gently east-dipping, approximately 425m-thick intrusion is semi-continuously exposed along a half-mile stretch of Lake Superior shoreline in wave-washed outcrops adjacent to Duluth's Lakewalk path between 16th and 28th avenues east. This field trip will highlight the mineralogic and textural attributes of the diverse lithologies exposed in these shoreline outcrops and consider the various ideas for its emplacement and crystallization history.

All who have studied the Endion Sill (Schwartz and Sandberg, 1940; Ernst, 1955, 1960; Oestrike, 1983; Gardner, 1987; and Jerde, 1991) have noted its being generally composed of a lower gabbroic zone and an upper intermediate to felsic zone. The sill was emplaced between basaltic to basaltic andesite flows comprising the upper part of the Leif Erickson Park Lavas (unit Mnb, Fig. 1) and the 300m-thick, Congdon Park rhyolite (unit Mnc, Fig. 1) which forms the lowermost flow unit of the Lakeside Lavas of the NSVG (Green and Miller, 2008). The emplacement of mafic intrusions beneath felsic lavas and intrusions is a commonly observed phenomenon in igneous rocks of the Midcontinent Rift and likely is triggered by the felsic rocks serving as a density barrier to mafic magma (Miller, 2015). The gradational contacts typically observed between of felsic rock types and underlying mafic intrusions further suggests partial melting and assimilation of the felsic hanging wall is involved in the evolution of the mafic intrusion. This contamination process appears to have occurred in the Endion Sill as well.

Previous Studies

Schwartz and Sandberg (1940) were the first to report on the petrology of mafic and felsic components of the Endion Sill and of related sills in the Duluth area, the Northland and Lester River sills. From their field observations and petrographic studies and major and minor element wet chemical analysis of seven samples, they considered five different hypotheses to explain the bimodal distribution of rock types, and particularly the occurrence of felsic rock types (commonly referred to as granophyre or "red rock"): 1) as a composite felsic intrusion, 2) by metamorphism of the rhyolite, 3) by hydrothermal alteration, 4) by a mix of assimilation and differentiation, and 5) by differentiation alone. They concluded "that many factors had some effect, but that differentiation within each sill accounts for the major part of the segregation of rock types into two distinct facies." Nevertheless, they acknowledge that simple fractional crystallization of the diabase could not produce the large amount of felsic material in the sills.

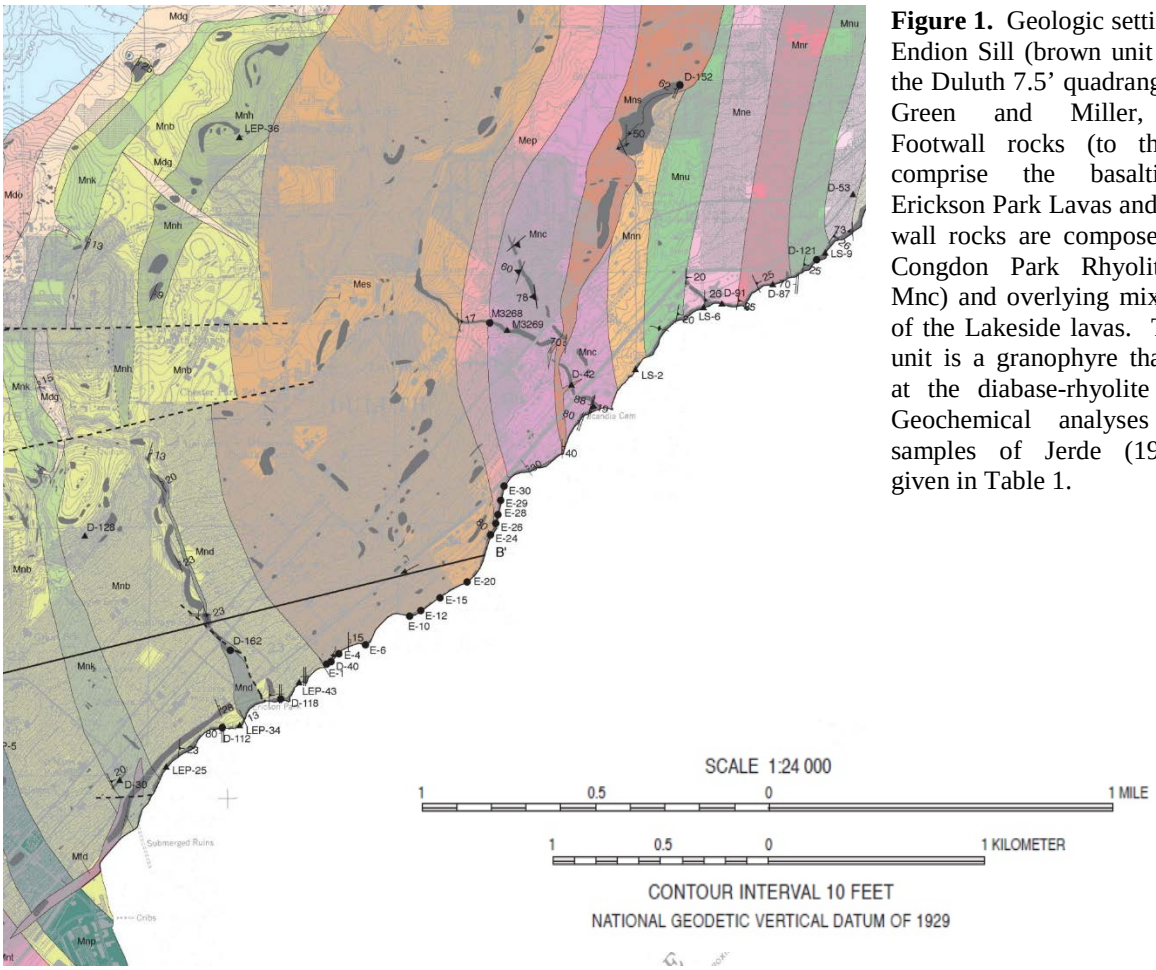


Figure 1. Geologic setting of the Endion Sill (brown unit Mne) in the Duluth 7.5' quadrangle (from Green and Miller, 2008). Footwall rocks (to the west) comprise the basaltic Leif Erickson Park Lavas and hanging wall rocks are composed of the Congdon Park Rhyolite (Unit Mnc) and overlying mixed lavas of the Lakeside lavas. The Mep unit is a granophyre that occurs at the diabase-rhyolite contact. Geochemical analyses of E-samples of Jerde (1991) are given in Table 1.

For his MS thesis at the University of Minnesota under the advisement of SS Goldich, Ernst (1955, 1960) conducted a detailed petrographic study of 27 samples collected from lakeshore exposures and streambed exposures up Tischer Creek (Fig. 2). Ernst (1955) defined several stratiform map units within the sill. The lower half of the sill is composed of medium-grained, subophitic to ophitic diabase. The diabase is overlain over a narrowly gradational contact by a medium-grained, intermediate "mottled" granodiorite which gradually transitions upward into granophyre/"red rock" which he calls a "sodalite-adamellite". This "medial granophyre" then abruptly grades upward into a fine-grained diabase. The upper 10 meters of the sill is capped by a fine-grained "upper granophyre" which is in sharp irregular contact with the diabase. The upper granophyre-Congdon Park rhyolite contact is observed to be abrupt in sea cliff exposures and in streambed outcrops along Tischer Creek (where it crosses East 2nd Street, Fig. 2). The transition into rhyolite is marked by the abrupt decrease in grain size.

Ernst (1955, 1960) concluded that much of the mafic and intermediate rock types in the lower part of the sill (about 40% of the total thickness) were likely related by fractional crystallization. However, like Schwartz and Sandberg (1940), he recognized that there was too much felsic material to have been produced by in situ differentiation. He offered two possible explanations for the large volume of granophryre in the upper part of the sill - 1) additional granophyre generated by differentiation from a downdip, thicker section of the sill had injected itself into an up-dip section of the sill, where it is currently exposed or 2) the granophyre represents a separate intrusion of felsic magma unrelated to the mafic component.

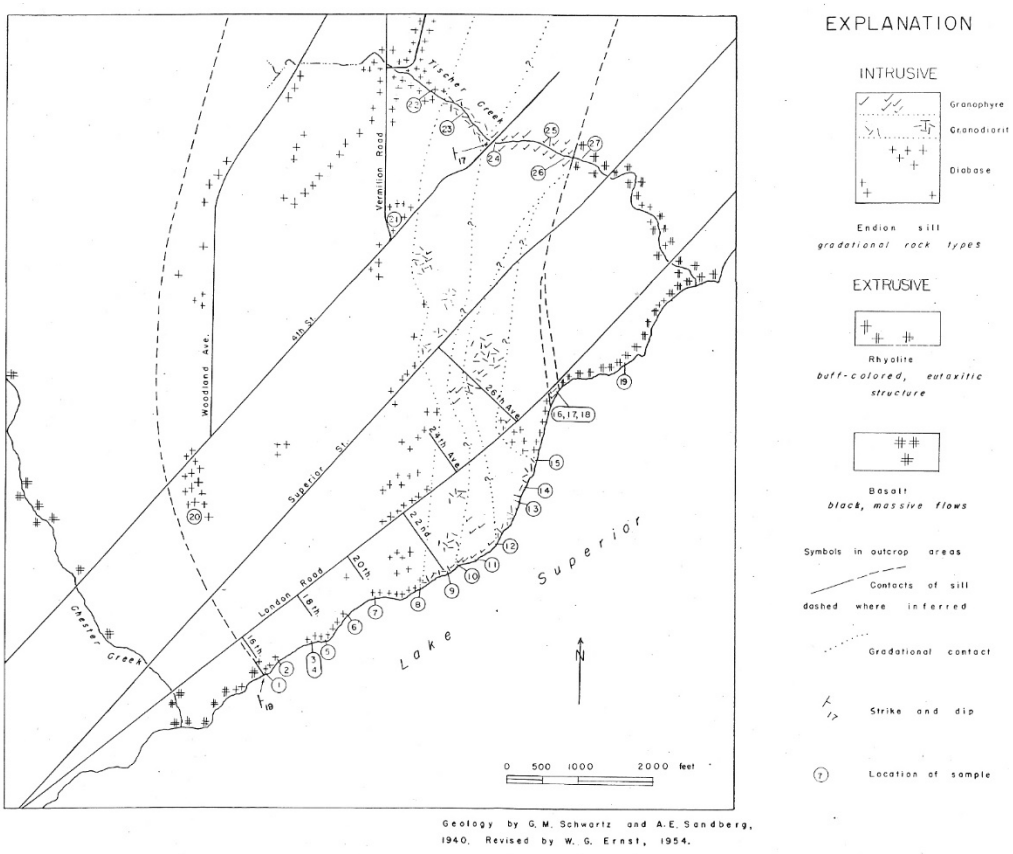


Figure 2. Geology of the Endion Sill from Ernst (1955) showing his sample locations.

For his University of Illinois MS thesis, Oestrike (1983) conducted a more thorough petrographic and mineral chemical study of the Endion Sill along the shoreline and Tischer Creek sections (Figs. 3 & 4). He subdivided the sill into 3 main units that he termed the Gabbroic Zone, the Acidic Zone and the Intermediate Zone. Grading abruptly up from a basal chill zone, the Gabbroic Zone is largely composed medium-grained, subophitic to ophitic, oxide gabbro to olivine gabbro with variable concentrations of "red spots" (interstitial concentrations of granophyre) and felsic dikelets. About 100 meters above the basal contact, Oestrike noted that the gabbro is in sharp contact with a medium-grained, subprimatic ferromonzodiorite – a rock type commonly found in the Acidic Zone. The next exposure upsection of the ferromonzodiorite is more subophitic gabbro, but the contact is not exposed. Oestrike calls this interval the Gabbroic Zone Acidic Layer (Figs. 3&4). The contact between the Gabbroic and Acidic Zone is about 220 meters above the basal contact and is gradational over several 10's of meters. It is marked by the transition from a subophitic to subprismatic pyroxene texture and an increase in interstitial granophyre to above 10%. Within the Acidic Zone this trend continue to where the rock becomes a subprismatic to prismatic quartz ferromonzonite and develops a very deep salmon red color. Oestrike notes that these rocks have tridymite paramorphs of quartz. The upper 50 meters of the sill, an interval Oestrike calls the Intermediate Zone, is largely composed of a gray, fine-grained ferrodiorite that locally contains granophyric clot and dikes. Its lower contact with the Acidic Zone s gradational over several meters and its upper contact is characterize by an irregular mixture of ferrodiorite and massive red granophyre over a 3 meter interval. This Intermediate Zone is not observed in the Tischer Creek section. The granophyre-rhyolite contact is inaccessible along the shore due to sea cliffs.

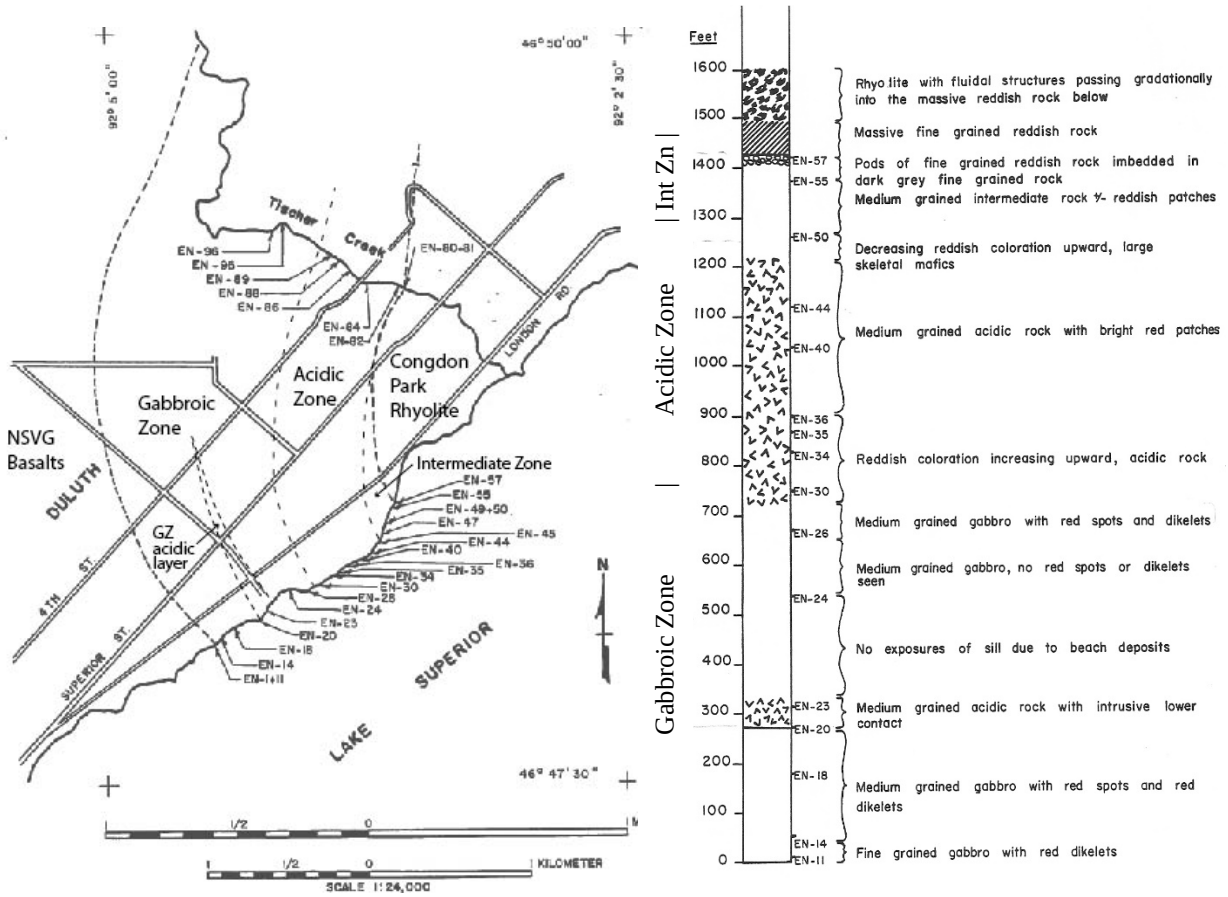


Figure 3. Geology and lithostratigraphy of the Endion Sill from Oestrike (1983) showing his sample locations.

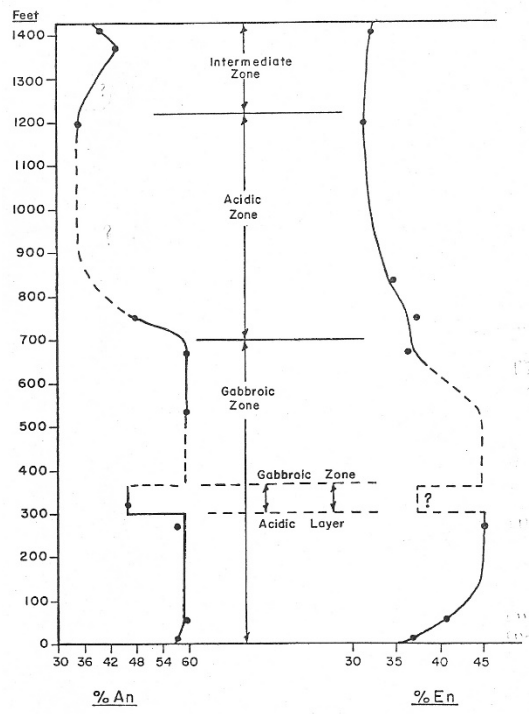


Figure 4. Cryptic variation of An content in plagioclase and En% (relative to Fs and Wo) in pyroxene through shoreline exposure of the Endion Sill. Mineral compositions were determined by electron microprobe (from Oestrike, 1983).

Citing constant and distinct mineral compositions within the Gabbroic and Acidic Zones (Fig. 4), Oestrike (1983) disagreed with the conclusions of Schwartz and Sandberg (1940) and Ernst (1955, 1960) that the compositional variations in the Endion Sill represent mostly the effects of magmatic differentiation. Instead, he concluded that the Endion Sill was formed by the composite emplacement of mafic and intermediate-felsic magmas in rapid succession. He speculated that the two magmas did not readily mix due to the effects of double-diffusive convection. He did not have a satisfactory explanation for the origin of the Intermediate Zone ferrodiorite.

A lithogeochemical study of the Endion Sill, including Sm-Nd isotopes, was conducted by Gardner (1987) for his MS thesis at Washington University. (*I have not been able to track down a copy of his 350 page thesis, so I will paraphrase the conclusions of his study from a Lunar and Planetary Science Conference Abstract (Gardner et al., 1987) and from a summary by Jerde (1991)*). Although Jerde reports that Gardner (1987) conducted 9 analyses of Sm-Nd isotopes for his thesis study, Gardner et al. (1987) reported Sm-Nd analyses of only one Gabbroic Zone sample and one Acidic Zone sample. Gardner's (1987) INAA analyses of 26 samples through the sill show incompatible trace element concentrations increasing uniformly through the sill. He notes that REE patterns and concentrations of Gabbroic Zone samples resemble andesitic NSVG compositions. He further notes that the 30m-thick granophyre interval, which he calls the altered rhyolite zone and which occurs between the top of the sill and the base of the unaltered rhyolite, is depleted in REE and other incompatible trace elements (Ta, Rb, Th) and enriched in more compatible elements such as Sr, Ba, Co, and Sc relative to unaltered rhyolite. He suggests that devolution of fluids from the rhyolite may have mobilized trace element into the underlying sill.

Gardner et al. (1987) reports ε^{Nd} (1100Ma) values for the Gabbroic Zone sample of -0.6 and -2.0 for the Acidic Zone sample (Fig. 5). Gardner concludes that if the Congdon Park Rhyolite has an ε^{Nd} value of <-8, its partial melting and assimilation along with fractional crystallization of the Endion sill may explain its Nd isotopic compositions. Gardner did not analyze the Sm-Nd isotopic compositions of the Congdon Park Rhyolite, but Vervoort and Green (1997) report a ε^{Nd} (1100Ma) value of -4.1 (Fig. 5).

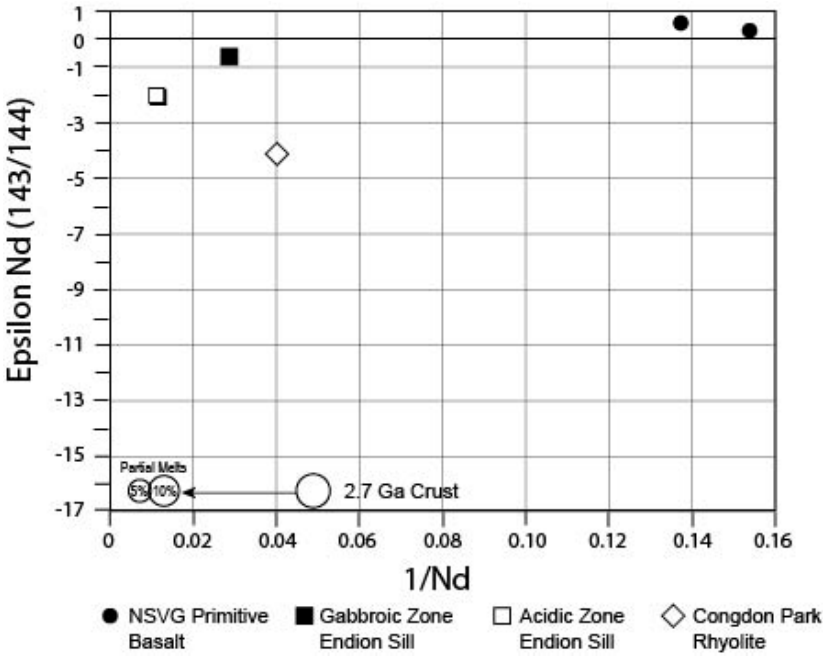


Figure 5. ε^{Nd} (1100Ma) and 1/Nd values for samples from the Gabbroic and Acidic zones of the Endion Sill compared to primitive NSVG basalt, the Congdon Park Rhyolite, and 5% and 10% model partial melts from Superior Province crust. The values show for the Congdon Park Rhyolite are from Vervoort and Green (1997). All other data are from Gardner et al. (1987).

Gardner (1987) conclude from his geochemical data that the Gabbroic and Acidic zones represent two separate intrusions into the sill and are not related by in-situ fractional crystallization. Both show contamination which may have been contributed by the Congdon Park rhyolite or by partial melts of Archean crust during the intrusion of mantle-derived magmas (Fig. 5). He interpreted the more contaminated Acidic Zone to have been intruded later and above the semi-molten gabbroic zone. Gardner (1987) further interpreted the upper Intermediate Zone to be a more contaminated upper contact of the Gabbroic Zone.

Jerde (1991) studied the lithogeochemistry of the Endion Sill as a part of a larger study of hypabyssal mafic intrusions into the NSVG for his PhD dissertation at UCLA. Locations of the 17 samples he analyzed by INAA and microprobe analyses of fused glass are shown in Figure 1 and the data are presented in Table 1. By his own admission, he conducted only reconnaissance field investigations and instead relied on the previous studies of Oestrike (1983) and Gardner (1987).

Table 1. Geochemical analyses of Endion Sill samples from Jerde (1991). Locations shown in Figure 1.

Sample	E-1	E-4	E-6	E-8	E-10	E-12	E-15	E-18	E-20
Strat Height (m)	5	41	95	196	220	241	288	327	352
SiO_2	48.86	48.60	49.02	47.55	50.06	50.22	58.13	62.88	61.37
TiO_2	4.61	3.62	2.88	3.96	2.47	3.71	2.00	1.30	1.29
Al_2O_3	13.42	14.98	13.99	14.15	16.47	11.70	14.05	14.54	14.55
FeO	14.98	13.40	13.94	15.82	11.44	15.79	11.00	8.95	9.08
MnO	0.30	0.29	0.20	0.23	0.17	0.28	0.27	0.23	0.20
MgO	5.17	7.43	6.68	6.84	4.21	5.01	4.16	2.97	2.59
CaO	7.37	6.32	8.34	6.11	8.16	7.32	1.95	1.47	1.90
Na_2O	2.14	2.33	2.18	2.47	2.63	2.64	2.61	2.88	2.65
K_2O	1.00	0.54	0.76	0.70	2.70	1.54	3.86	4.12	4.63
Total	97.9	97.5	98.0	97.8	98.3	98.2	98.0	99.3	98.3
mg#	38.1	49.7	46.1	43.5	39.6	36.1	40.3	37.2	33.7
TRACE ELEMENTS (ppm)									
Sc	35.70	25.20	27.80	25.60	33.50	32.40	18.60	13.20	13.40
Cr	60.50	48.30	90.40	57.40	29.60	2.73	3.12	1.97	0.79
Co	38.30	40.30	47.40	40.20	30.30	34.90	14.60	9.05	8.59
Ni	55.0	131.0	194.0	60.0	29.0	25.0	43.0	14.0	24.0
Zn	177.0	122.0	132.0	135.0	143.0	219.0	187.0	192.0	173.0
Ga	24.8	16.1	22.0	20.8	26.3	24.4	29.2	32.5	27.5
Rb	26.6	11.6	26.1	16.4	55.5	47.2	127.0	132.0	150.0
Sr	163	156	204	193	388	167	151	135	129
Zr	440	309	284	266	242	467	708	827	800
Ba	305	232	209	362	458	385	604	674	625
La	44.5	28.9	28.4	30.3	29.1	58.0	69.1	71.4	72.7
Ce	92.4	62.2	62.1	64.3	62.5	131.0	142.0	151.0	150.0
Nd	48.5	39.1	34.1	38.3	36.7	75.0	82.9	74.0	84.4
Sm	11.4	8.5	7.8	8.4	8.1	17.2	17.8	15.9	17.8
Eu	3.45	2.53	2.61	2.54	2.67	4.46	3.69	3.46	3.35
Tb	2.01	1.31	1.44	1.37	1.37	2.85	2.62	2.78	2.82
Dy	11.90	8.06	8.91	8.79	9.37	19.10	15.60	18.30	17.30
Tm	1.06		0.80	0.64	0.71	1.15	1.22	1.72	1.41
Yb	5.98	4.19	4.04	4.05	3.94	7.14	9.07	8.86	9.51
Lu	0.85	0.62	0.57	0.61	0.58	1.02	1.32	1.28	1.41
Hf	9.18	6.45	5.87	6.34	5.72	9.69	15.20	17.40	17.40
Ta	1.82	1.32	1.18	1.33	1.13	1.95	2.66	2.85	3.00
Th	5.55	4.03	3.62	4.28	3.72	7.10	12.50	13.90	14.80
U	1.51	1.11	0.99	1.43	1.30	2.16	3.97	4.30	4.74

Table 1 (cont.)

Sample	E-22	E-24	E-25	E-26	E-27	E-28	E-29	E-30
Strat Height (m)	377	419	435	442	449	457	467	474
SiO_2	60.47	59.84	52.30	52.54	64.70	65.10	70.19	75.20
TiO_2	1.65	1.94	3.05	2.95	1.58	1.18	0.69	0.17
Al_2O_3	13.99	13.41	13.05	12.90	13.84	13.85	13.32	11.75
FeO	8.99	10.59	14.70	15.36	7.39	6.60	4.29	3.89
MnO	0.18	0.19	0.23	0.25	0.15	0.10	0.07	0.03
MgO	2.17	2.77	3.76	3.96	2.42	1.34	0.77	0.08
CaO	3.68	2.96	4.88	5.32	1.93	3.12	1.54	0.05
Na_2O	2.27	2.07	2.56	2.39	3.08	3.04	3.06	2.81
K_2O	4.87	4.01	3.19	2.46	4.15	3.54	5.22	5.61
Total	98.3	97.8	97.7	98.1	99.2	97.9	99.2	99.6
mg#	30.1	31.8	31.3	31.5	36.9	26.6	24.2	3.5
TRACE ELEM								
Sc	15.70	16.20	23.10	19.90	12.30	8.71	5.24	0.76
Cr	2.47	1.63	4.42	1.81	13.40	14.40	13.30	3.32
Co	13.80	16.90	24.70	24.70	14.60	9.75	6.60	0.88
Ni	14.0	22.0	31.0	40.0	16.0	37.0	25.0	9.0
Zn	144.0	171.0	223.0	222.0	181.0	159.0	180.0	92.5
Ga	29.4	24.4	24.7	27.9	29.3	28.5	27.2	25.4
Rb	130.0	101.0	88.2	82.3	132.0	123.0	184.0	216.0
Sr	106	95	118	137	124	73	37	16
Zr	814	622	631	620	715	620	651	536
Ba	568	528	515	468	567	297	238	150
La	78.5	65.9	76.2	67.6	68.3	65.7	76.7	97.8
Ce	160.0	135.0	165.0	145.0	137.0	129.0	146.0	197.0
Nd	78.5	77.5	92.9	74.9	65.3	67.3	72.1	86.9
Sm	18.6	16.5	19.8	16.8	14.8	13.4	16.2	19.8
Eu	3.49	3.50	4.63	4.59	2.26	1.66	1.22	0.74
Tb	2.93	2.47	3.02	2.84	2.63	2.10	3.08	3.06
Dy	17.80	14.50	20.70	18.00	16.50	14.00	20.60	19.80
Tm	1.71	1.31	1.53	1.47	1.64	0.85	1.49	1.77
Yb	9.00	7.83	8.31	8.29	8.31	7.55	10.50	10.70
Lu	1.29	1.13	1.19	1.17	1.17	1.11	1.47	1.44
Hf	16.50	13.30	13.00	13.20	15.50	13.70	15.60	14.60
Ta	2.87	2.44	2.59	2.68	2.50	2.29	3.04	3.47
Th	13.30	10.70	9.96	9.30	14.40	13.50	18.60	21.40
U	4.45	3.31	3.29	2.71	4.67	4.18	5.24	4.56

The chemostratigraphic variations of major and trace elements of Jerde's (1991) data are shown in Figures 6 and 7, respectively, relative to the lithostratigraphy of Oestrike (1983). The major element data (SiO2, TiO2, mg# and Na2O+K2O) clearly show abrupt compositional changes between the gabbroic and acidic zones across 50 meter-thick interval that Jerde (1991) termed the transitional zone (AZ/GZ, Fig., 6). Oestrike (1983) recognized this hybrid transitional zone petrographically and interpreted this as a mixing zone between Acidic Zone magma that was compositely emplaced above the partially solidified Gabbroic Zone. Interestingly, the Intermediate Zone (IZ, Fig. 6) has major element compositions that are comparable with the transitional zone compositions suggesting that it is the upper hybrid chill zone of the Acidic Zone rather than a remnant chill of the Gabbroic Zone as interpreted by Gardner (1987). The transitional major element compositions of the recrystallized rhyolite (xRhy, Fig. 6) between the unaffected rhyolite and the Intermediate Zone rocks suggests that the recrystallized rhyolite has been contaminated by and provided contaminants to the Endion Sill as suggested by Gardner (1987).

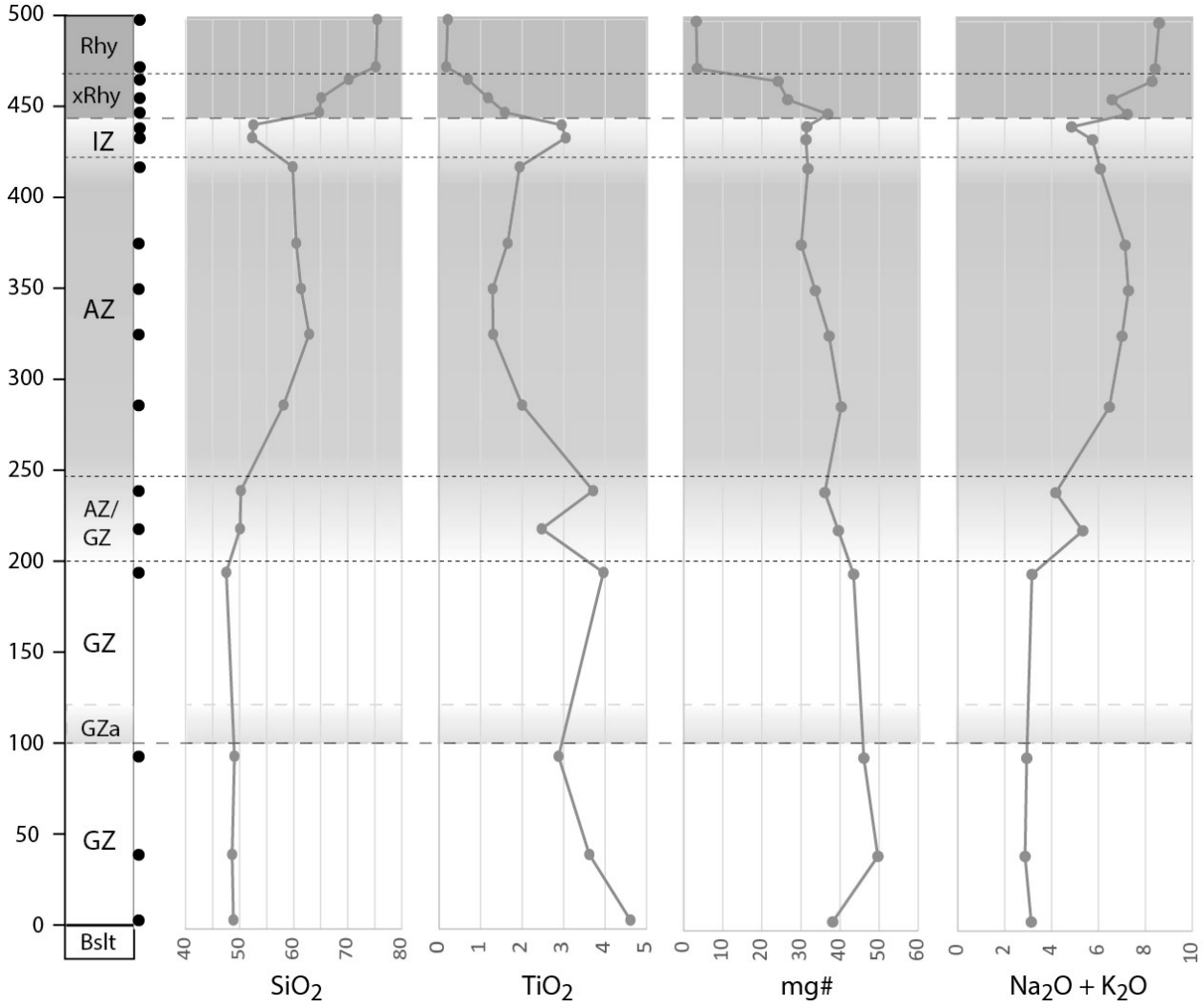


Figure 6. Chemostratigraphic variation of major elements through the Endion Sill. Lithogeochemical data from Jerde (1991), see Table 1. Lithostratigraphic units modified from Oestrike (1983); see Fig. 3 – GZ-Gabbroic Zone; GZa- acidic layer in the Gabbroic Zone; AZ/GZ – transitional zone between the Acidic and Gabbroic Zones; AZ – Acidic Zone; IZ – Intermediate Zone; xRhy – recrystallized rhyolite; Rhy – unaffected rhyolite. Darker shades indicate felsic compositions.

Jerde's (1991) trace element data (Zr, Ba, Ni, and Cr, shown in Figure 7) are more consistent with the Acidic and Gabbroic Zones being formed by composite intrusions, as opposed to in situ fractional crystallization. Moreover, the similarity of trace element abundances between the transitional zone (AZ/GZ, Fig. 7) with the Intermediate Zone is consist with the IZ being an upper hybrid chill of the Acidic Zone magma. However, the very uniform incompatible trace element ratios of Ce/Yb and Zr/Hf indicate that both zones were formed from a common parent magma which presumably differentiated at depth. The subtle increase in the Th/Hf ratio in the Acidic zone is consistent with Gardener's (1987) Sm-Nd isotopic data that implies contamination of the acidic zone magma by the overlying Congdon Park rhyolite. Most Midcontinent Rift rhyolites are interpreted from negative ε_{Nd} isotopic compostions to have formed by partial melting of Archean to Paleoproterzoic crust, which should also be enriched in Th (Vervoort and Green, 1997).

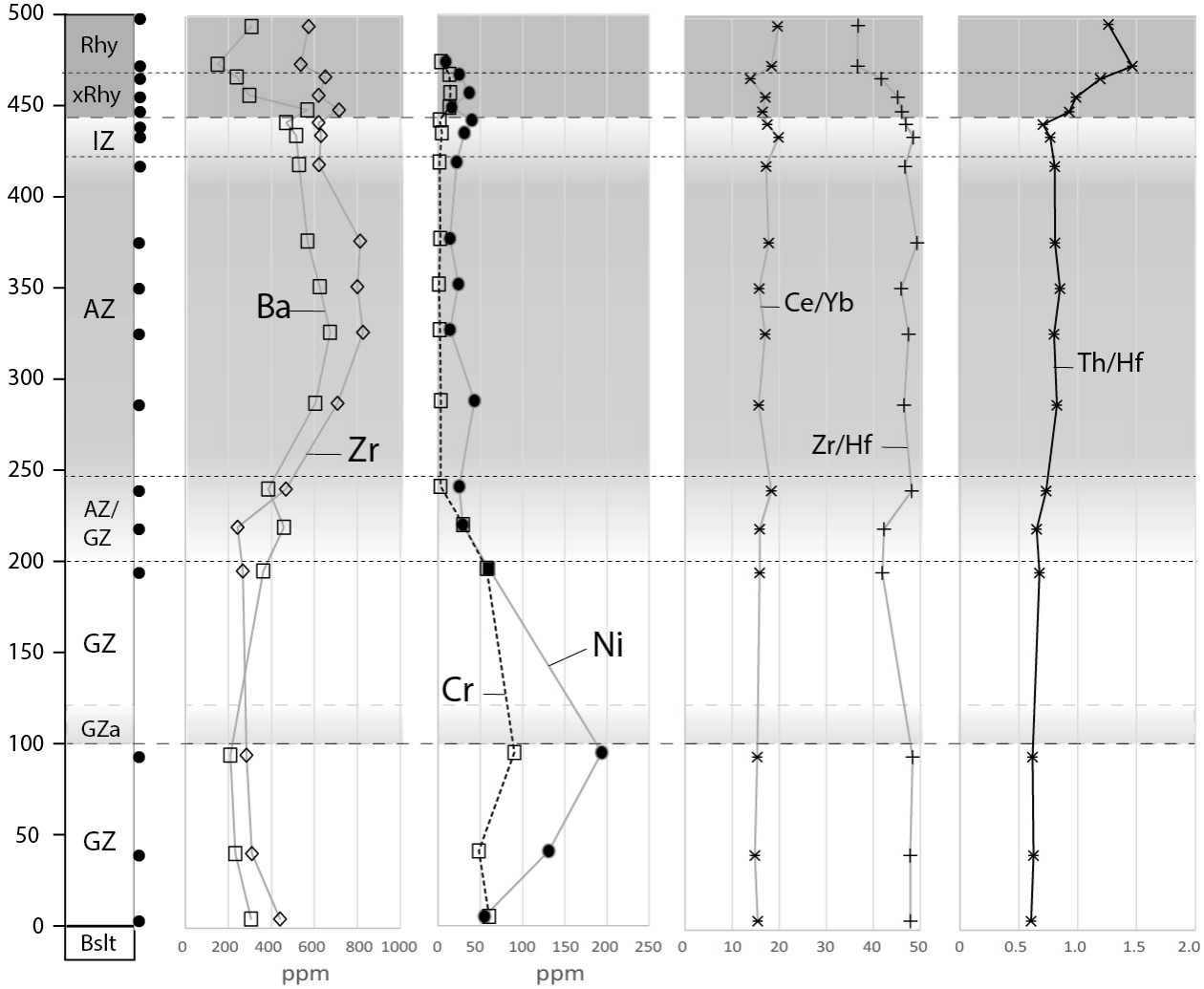


Figure 7. Chemostratigraphic variation of trace elements through the Endion Sill. Lithogeochemical data from Jerde (1991), see Table 1. Lithostratigraphic units modified from Oestrike (1983) – GZ-Gabbroic Zone; GZa- acidic layer in the Gabbroic Zone; AZ/GZ – transitional zone between the Acidic and Gabbroic Zones; AZ – Acidic Zone; IZ – Intermediate Zone; xRhy – recrystallized rhyolite; Rhy – unaffected rhyolite. Darker shades indicate more felsic compositions.

The REE data reported by Jerde (1991), and plotted in normalized spidergrams in Figure 8, also provide some insight into the petrogenetic relationship between the Gabbroic and Acidic Zones. That the general slopes of the REE curves from the Endion Sill samples are general coparallel are again consistent with the Gabbroic and Acidic Zones being evolved from a common magma. However, the GZ and AZ samples clearly cluster in two distinct REE abundance groups. The basal chill sample (black dot in Fig. 8) shows enriched REE abundances relative Gabbroic Zone samples, but show a similar trend and lack of Eu anomaly. This suggests that the gabbroic zone samples may have cumulate tendencies (i.e. concentrations of primocrysts over parental magma) as suggested by Jerde (1991) and supported by his noting higher than normal concentrations of olivine in his sample E6 from the Gabbroic Zone (Table 1). The Acidic Zone samples have distinctively higher REE concentration with a similar slope to the GZ samples, but a moderate negative Eu anomaly. Interestingly, two sample from the transitional (AZ/GZ) zone have distinctive compositions with one lining up with the Gabbroic Zone samples and the other similar to the Acidic Zone samples, though with a less pronounced negative Eu anomaly. Interestingly, the REE-enriched transitional zone sample is most similar to the REE compositions of the upper

Intermediate Zone. This lends additional evidence to the suggestions of Jerde (1991), Gardner (1987) and Oestrike (1983) that the acidic zone is a later composite intrusion above the semi-crystallized Gabbroic Zone and that the Intermediate Zone and transitional zone are upper and lower margins of that later impulse of intermediate magma. The REE patterns of the overlying Congdon Park Rhyolite and its recrystallized lower interval in contact with the Intermediate Zone are somewhat similar, but have steeper LREE slopes and a much more pronounced negative Eu anomaly. That Eu values for Acidic Zone straddle the range between Intermediate Zone and transition zone samples and those of the rhyolite and recrystallized rhyolite are also consistent with Gardner (1987) Nd isotope data that suggest that the Acidic Zone assimilated a modest amount of anatectic melt from the rhyolite.

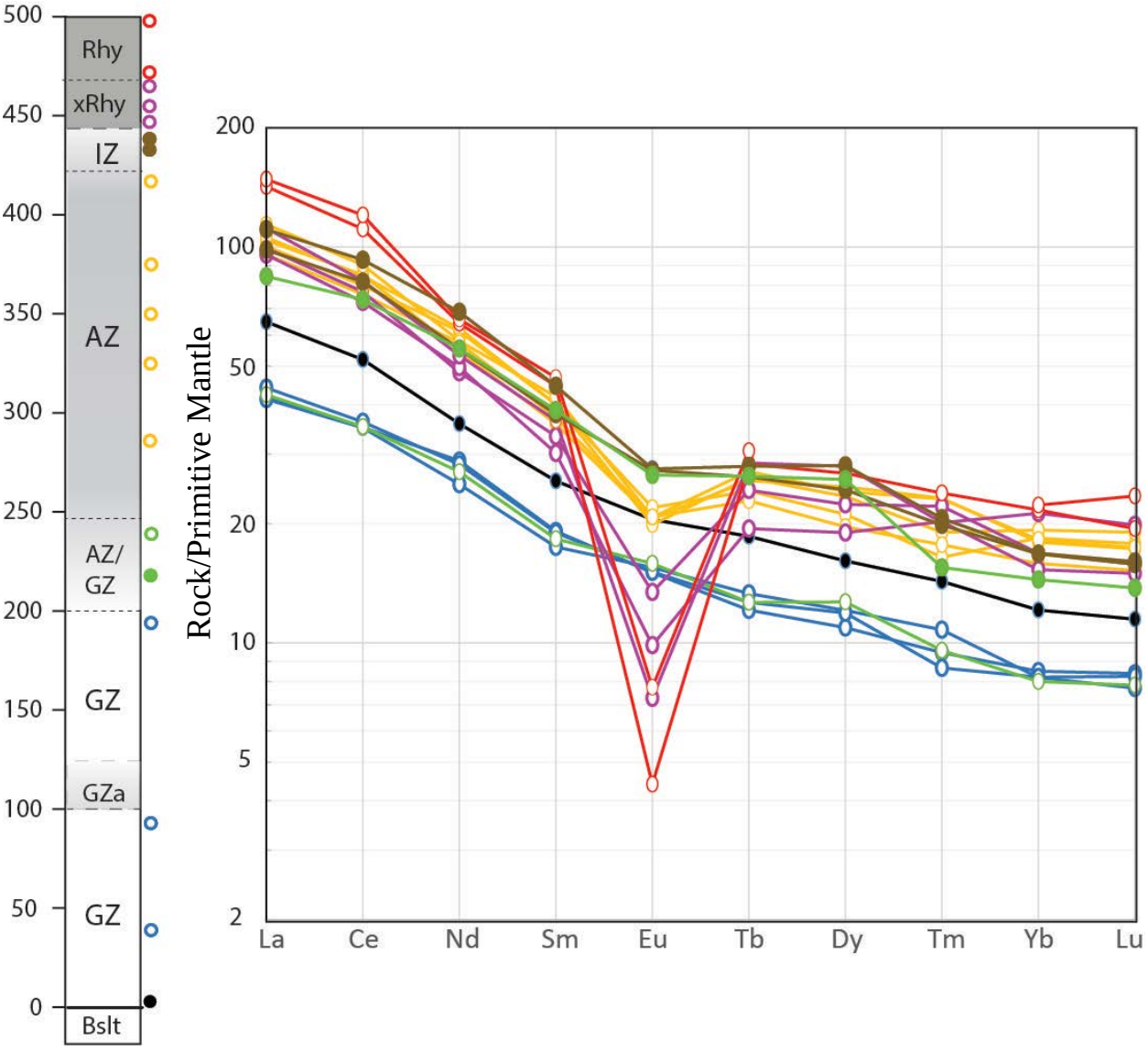


Figure 8. REE normalization plot of samples from the Endion Sill analyzed by Jerde (1991); see Table 1. Samples are color coded to the lithostratigraphic column modified from Oestrike (1983). REE abundance normalized to primitive mantle composition of Sun and McDonough (1989).

Recent Studies

The shoreline exposures of the Endion Sill, which will be the focus of this field excursion, were mapped in detail in September 2007 by the author as the final element of bedrock mapping integrated into the geologic map of the Duluth 7.5' quadrangle (Green and Miller, 2008); See Figure 1. A total of 27 sample were collected during the mapping and thin sections were made for 25 of these. These sections were only recently investigated and photographed earlier this year (*nothing like leading a field trip to finally getting around to it*). Field stop descriptions given in the next section will incorporate the field and petrographic observations and will be illustrated with field photos and photomicrographs from these recent studies.

Based on these field and petrographic studies, a revised lithostratigraphy for the Endion Sill is proposed and summarized in Figure 9. This figure highlights the textures, mineralogy and reddish hemitization of the various lithologies with thumbnail scans of thin sections and summary petrographic descriptions. The main differences with the stratigraphic column proposed by Oestrike (1983) is to expand the base of the AZ/GZ transition zone from 200 meters down to 100 meters. This corresponds to the sharp intrusive contact between gabbroic rocks and ferromonzodiorite of his "acidic layer in the Gabbroic Zone" (Fig. 3). Oestrike (1983) resumes the Gabbroic Zone over the acidic layer based on interpreting his sample E-24 as being gabbro. However, sample MD769 is observed to be varitextured oxide gabbro with about 10% granophyre and no evidence of olivine. Indeed olivine is only observed in the lower 100 meters of the sill. Field description of this outcrop notes that this sample was taken from the least granophyric sample. As such, it bears greater resemblance to the variably granophyric olivine-barren gabbros ranging in pyroxene texture from subophitic to intergranular to poikiloprismatic that are common in the transition zone. Unfortunately, Jerde (1991) did not sample this exposure to see if it maintains a Gabbroic Zone chemistry or starts to show evidence of mixing with the Acidic Zone magma. (*Don't know if Gardner (1987) sampled here*). Other elements of the lithostratigraphic column are as portrayed by Oestrike (1983).

Questions to Consider

As we progress up section through the excellent shoreline exposures of the Endion Sill, some questions to consider include:

- What is the petrogenetic relationship between the Gabbroic Zone and the Acidic Zone and particularly theAZ/GZ transition zone between them?
- Do the field relations (and geochemical data) give any indication that fractional crystallization is involved?
- What is the evidence for composite emplacement of the GZ and AZ, and what is the relative timing of their emplacement?
- What does the ferrodioritic Intermediate Zone represent? - an upper chill of the Acidic Zone? a remnant of the upper chill of the Gabbroic Zone? or something unrelated to either?
- What is the source of granophyric material in the sill? – partial melting of the overlying rhyolite or fractional crystallization in situ or in a remote staging chamber?

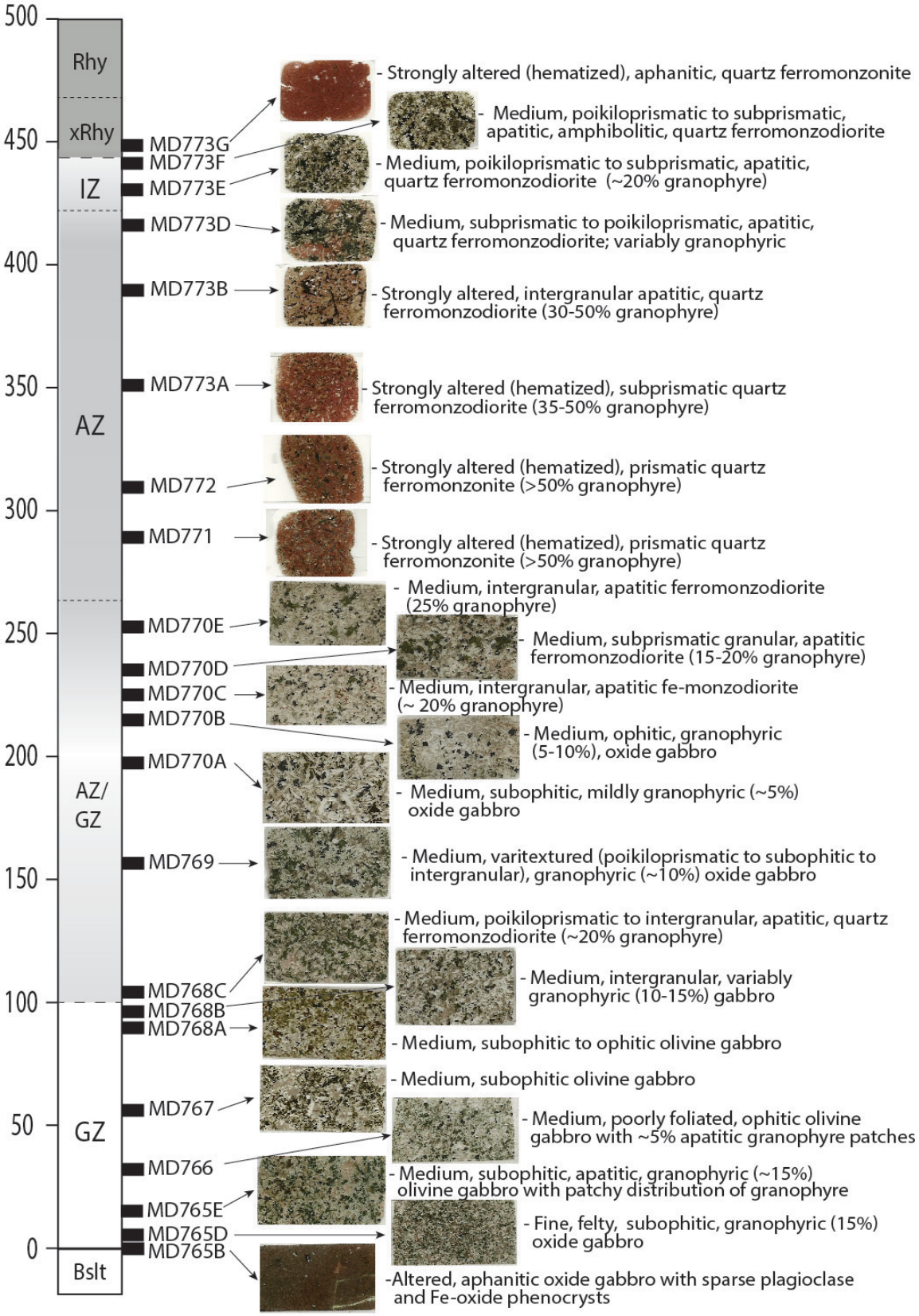
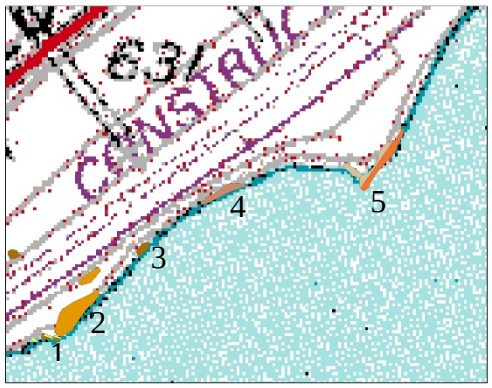


Figure 9. Revised lithostratigraphy of the Endion Sill based on recent field and petrographic studies.

Field Stop Descriptions

The field trip will start at a large glacially polished and striated outcrop (location 2) just several meters east of the Lakewalk where 17th Ave. East projects to the shore and an elevated walkway crosses the interstate highway. Proceed to the SW edge of the outcrop to observe the basal contact (Location 1).

Area A – Gabbroic Zone of the Endion Sill



Location 1: Basal Chill of the Endion Sill
UTM (NAD83): 570490_5183340

Description: Exposed here is a sharp contact between an intermediate volcanic (icelandite?) and an aphanitic gabbroic rock with sparse small phenocrysts of plagioclase and an altered mafic (olivine?). The volcanic occurs in an outcrop just SW of the fine gabbro and as a 0.5 m thick slab/septum of similar intermediate volcanic about 1 meter above the (unexposed) basal contact (Fig. 11). Fragments of the volcanic also occur as blocks in the fine gabbro. The contact between the volcanic slab and the very chilled hackly fractured surface of the gabbro has a strike and dip of N30°W/18°NE. A small (unexposed) fault is evidenced by an apparent left lateral offset of the volcanic slab across a N15E trending gap in exposure. Given the NE dip of the contact, this offset may also indicate east-side up displacement, which would imply it formed during late rift compression.

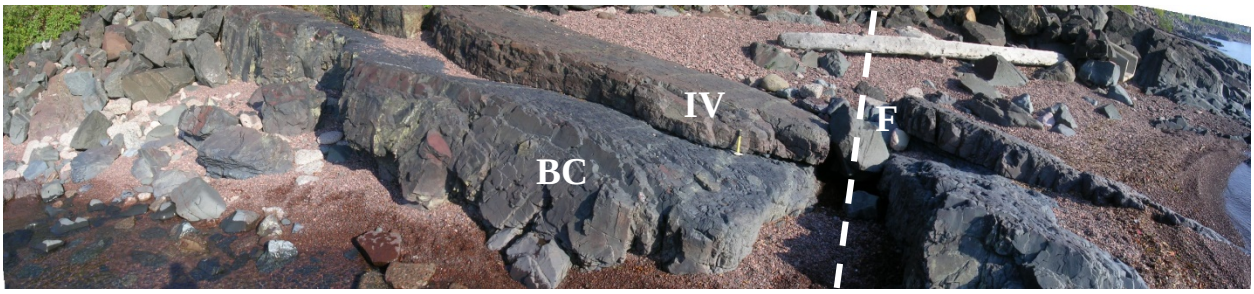


Figure 11. Panoramic photo of the basal chill (BC) of the Endion Sill with a slab/septum of intermediate volcanic (IV) offset by a reversed? fault (F).

Location 2: Glacially polished whale-back outcrop granophryic gabbro.
UTM (NAD83): 570620_5183305

Description: Progressing northeasterly across this glacially smoothed, polished, and striated outcrop, it is easy to observe the progressive coarseing in texture and the increase in granophyre clots, which stand out in relief, from about 5% to over 30% (Fig. 12A) Samples MD765D and MD765E (Fig. 10) show a transition from a medium fine-grained, felty subophitic slightly granophryic oxide gabbro to a medium-grained, ophitic apatitic, granophryric olivine gabbro with 1-2 cm clots of micrographic Ksp+Qtz and free quartz (Fig. 13). All igneous phase show moderate degrees of alteration to bowlingite (Ol), uralite (Cpx), and sericite (Pl).

Small inclusion of fine-grained, locally amygaloidal basalt occur in the gabbro and tend to concentrate granophyre at their margins (Fig. 12B). Also, the outcrop is cut by alteration veins trending N15E (parallel to the fault) along which liesegang redox bands are developed.

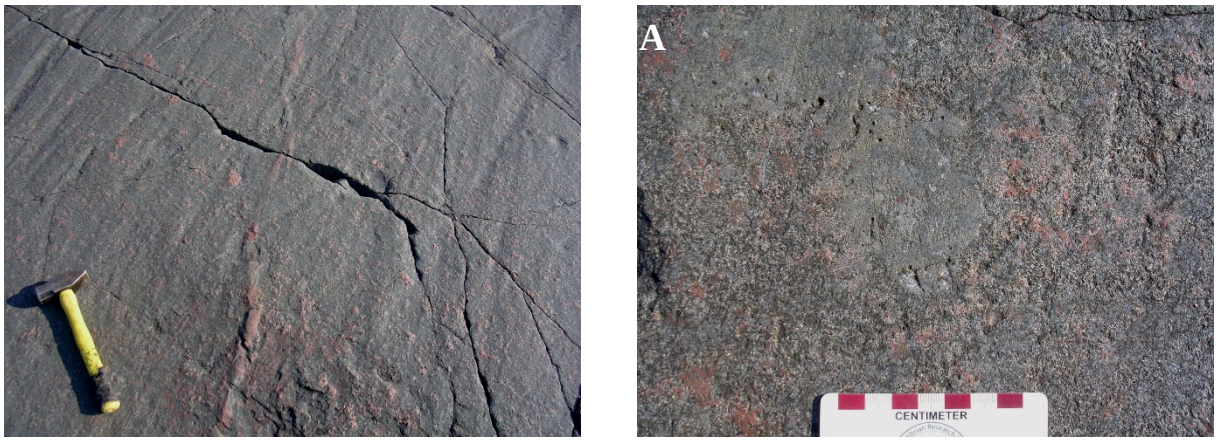


Figure 12. A) Glacially polished and striated subophitic gabbro with irregular granophyre clots standing out in relief; B) Basaltic inclusion with concentrations of granophyre in surrounding gabbro.

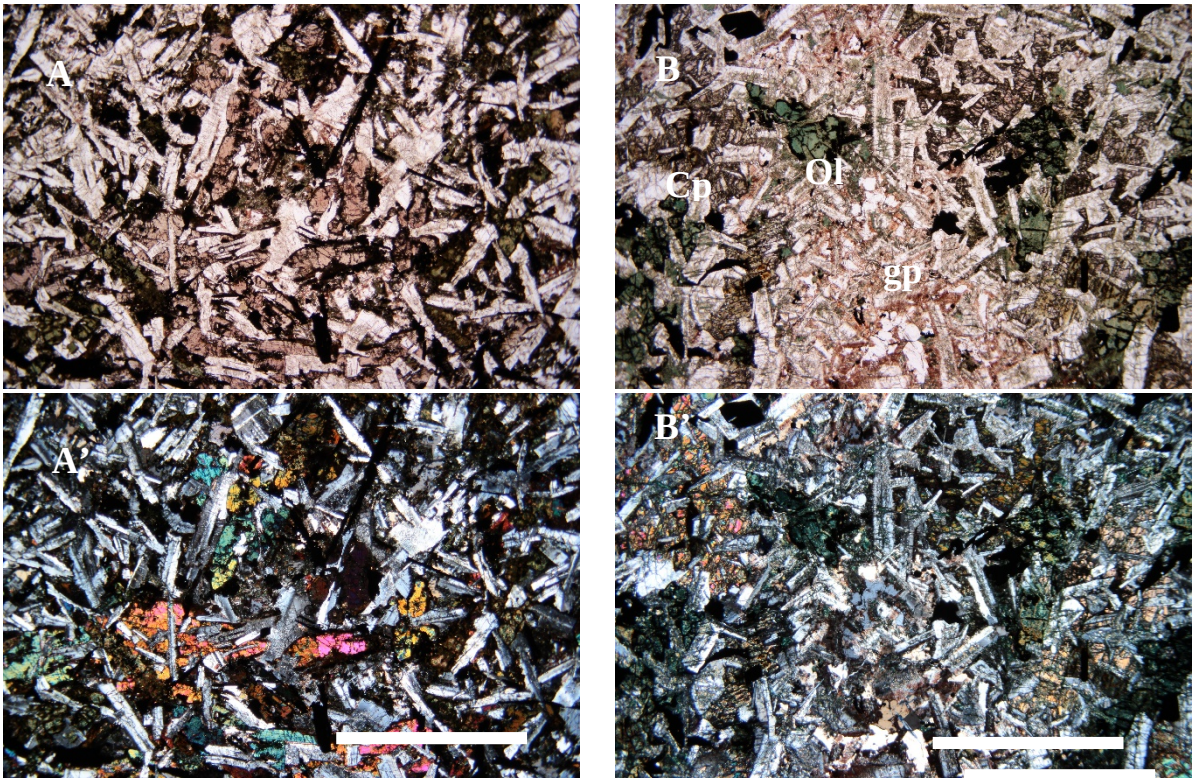


Figure 13. Photomicrographs of felty subophitic gabbro texture of sample MD765D (A & A') and subophitic granophyric olivine gabbro texture of MD765E (B & B'). Poikilitic augite (Cp), bowlingite-altered olivine (Ol) and granophyre-rich (gp) area noted in B. All photos at 1.25x, scale bar = 3mm

Location 3: Ophitic olivine gabbro
UTM (NAD83): 570665_5183350

Description: Medium fine-grained, poorly foliated, ophitic olivine gabbro. Augite oikocrysts are about 0.5cm diameter (Fig. 14A). Granular olivine tends to cluster in the inter-ophite areas (Fig. 14B) and preferentially weather out on the bedrock surface to form pits.

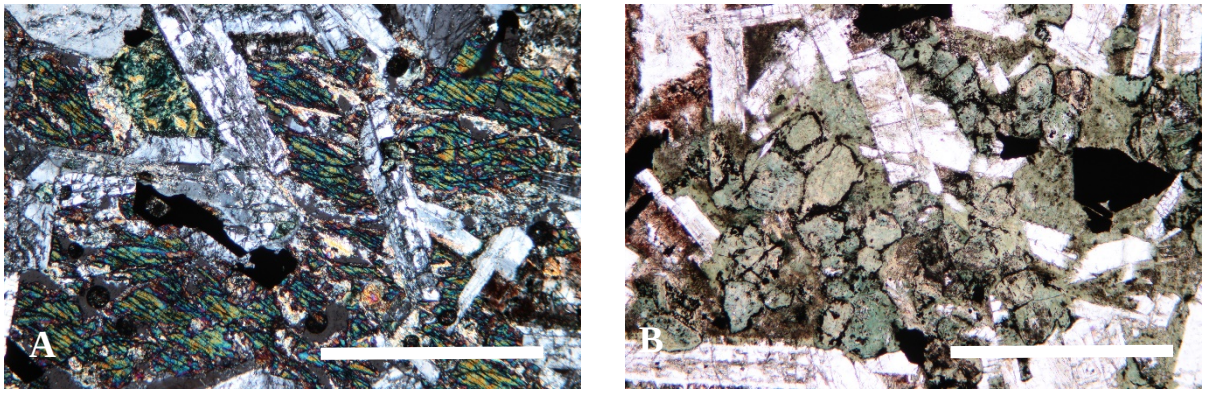


Figure 14. Photomicrographs from Sample 766. A) Ophitic augite with plagioclase chadacryts. B) Altered (bowlingite) olivine clusters in interophite areas. Both photos at 4x, scale bar = 0.5mm

Location 4: Columnar jointed, ophitic olivine diabase
UTM (NAD83): 570725_5183402

Description: The best developed columnar jointing in the Endion Sill are exposed here (Fig. 15A) as is obvious ophitic texture (Fig. 15B). Cpx oikocryts range from 0.5 to 2 cm diameter over the outcrop. Thin sections show this gabbro to contain less than 5% granophyric mesostasis.

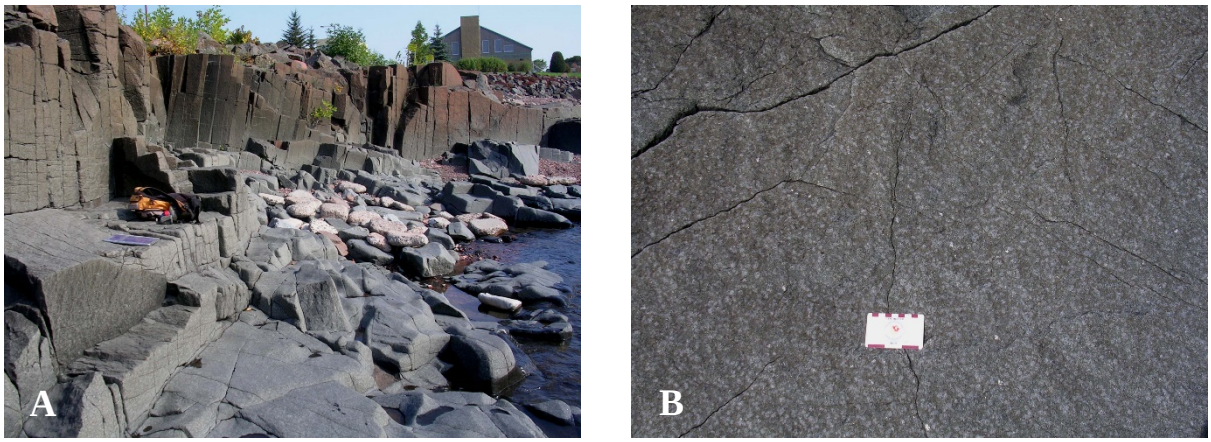


Figure 15. Field photos of Location 4 outcrop of ophitic olivine diabase displaying columnar jointing (A) and <1cm oikocrysts of pyroxene on a weathered surface (B).

Location 5: Contact between Gabbroic Zone and AZ/GZ Transitional Zone
UTM (NAD83): 570851_5183420

Description: Exposed in the outcrop at this point is a sharp contact between medium-grained, intergranular oxide gabbro and intergranular to subprismatic ferromonzodiorite (Fig. 16B). This contact has been recognize by all workers and marks the lower contact of Oestrike's acidic layer in the Gabbroic Zone (Fig. 3) . The gabbro near the contact is intergranular, moderately granophyric (5-10%) and devoid of olivine (Fig. 16C), but the westernmost exposures grade into a subophitic to ophitic, mildly granophyric (<5%) olivine gabbro typical of the Gabbroic Zone (Fig. 16D) . Given the textural zoning of the gabbro against the rather homogeneous ferromonzodiorite, one could argue that the gabbro is intrusive

into the ferromonzodiorite. This of course, is counter to interpretations of Oestrike (1983), Gardner (1987) and Jerde (1991) that the intermediate rocks intruded the gabbro.

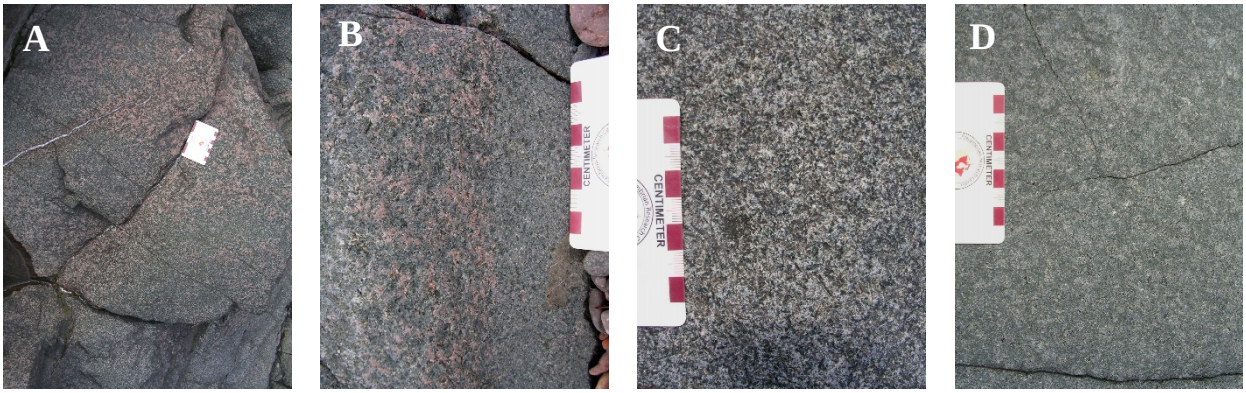
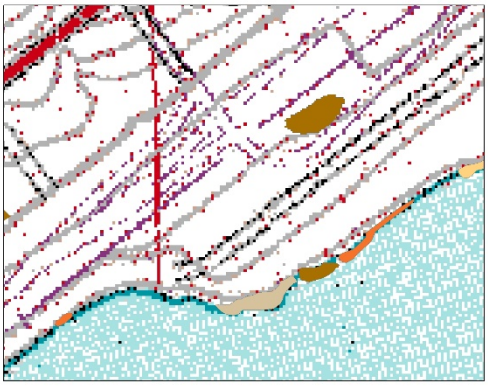


Figure 16. Progression of rock types at Location 5. A) subprismatic ferromonzodiorite, B) sharp contact between ferrodiorite and intergranular granophyric gabbro, C) intergranular oxide gabbro 1 meter form contact, subophitic olivine gabbro 5 meters from the contact.

Area B – Transitional AZ/GZ Zone of the Endion Sill



Location 6: Heterogeneous granophyric gabbro
UTM(NAD83): 570995_5183600

Description: Although Oestrike (1983) shows this exposure as belonging to the Gabbroic Zone, this medium-grained, variably granophyric (15-25%) and varitextured (poikiloprismatic to subophitic to intergranular) oxide gabbro seems better grouped in the transitional AZ/GZ zone (Fig. 17).

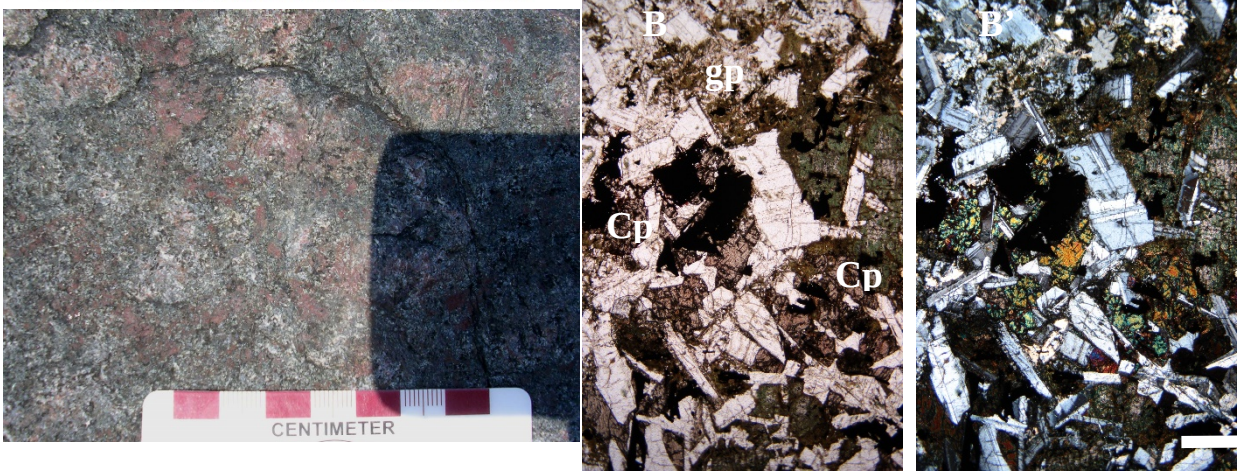


Figure 17. Field and petrographic photos of sample MD769 from Location 6. A) Field photo of the variably granophyric composition of this exposure. B) Plane and cross-polar images of intergranular to subophitic augite (Cp) and interstitial areas rich in K-feldspar and quartz (granophyre). Photomicrographs at 1.25x, scale bar = 3mm.

Location 7: Gradation from Granophyric Gabbro to Ophitic Gabbro

UTM(NAD83): 571125_5183608

Description: Across this point, a very gradational transition in rock type is observed. At the SW end of the exposure, the rock is a subprismatic to subophitic granophyric (5-10%) oxide gabbro (Fig. 18A) . Crossing the point to the southeast, the granophyre abundance drops to below 5% and an ophitic texture is clearly developed with Cpx oikocrysts up to 3 cm across evident (Fig. 18B). At one location, a softball-sized anorthosite inclusion is present. Plagioclase phenocrysts are present throughout the ophtic gabbro.

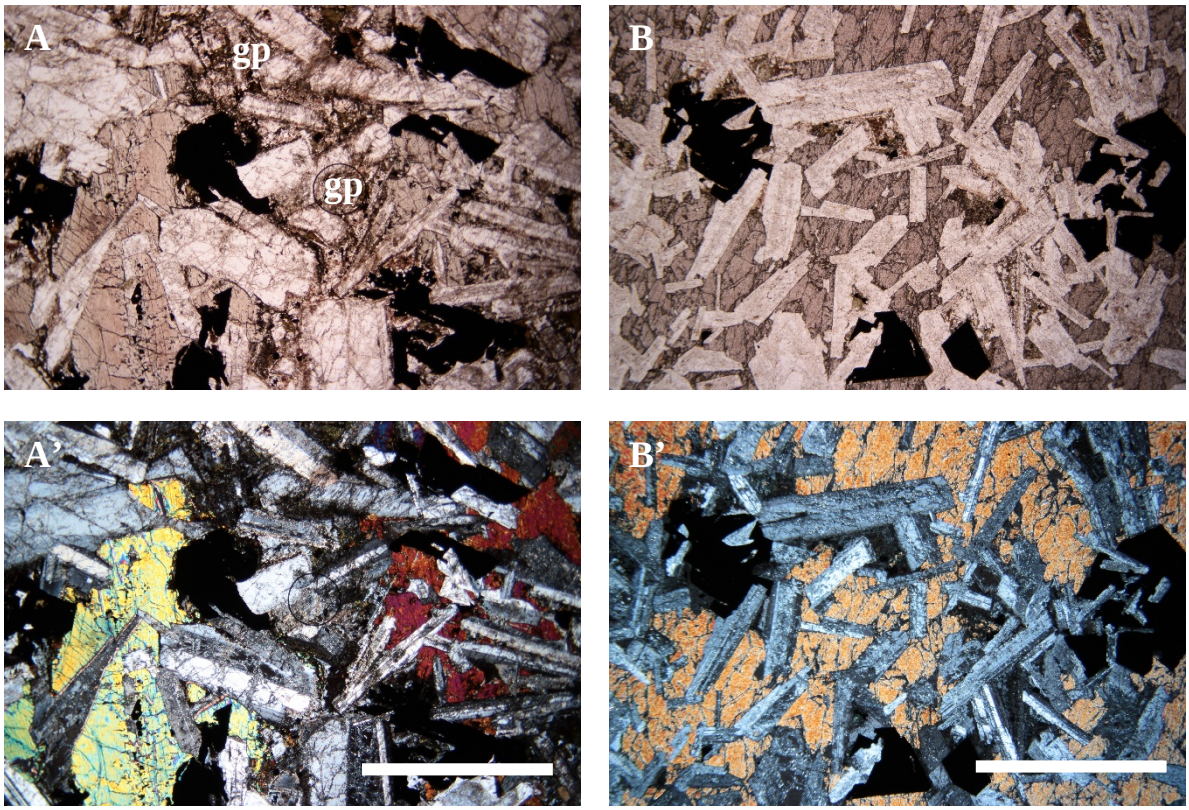


Figure 18. Photomicrographs from samples at Location 7. A) Subophitic granophyric oxide gabbro with granophyric mesostasis (gp) (Sample MD770A). B) Ophitic oxide gabbro (Sample MD770B). All photos at 1.25X; scale bar = 3mm.

Location 8: Foliated, Subprismatic, Apatitic Granophyric, Oxide Gabbro.

UTM (NAD83): 571185_5183635

Description: Across a 5 meter gap in exposure from the ophitic gabbro at the east end of Location 7, the rock type abruptly changes to a medium fine-grained, subprismatic to intergranular, apatitic oxide gabbro with up to 20% granophyre. Locally, the rock displays a crude foliation of plagioclase and pyroxene (Fig. 19). This is the first significant occurrence of more than 1% apatite as slender needles, which persists upsection throughout the Acidic Zone.

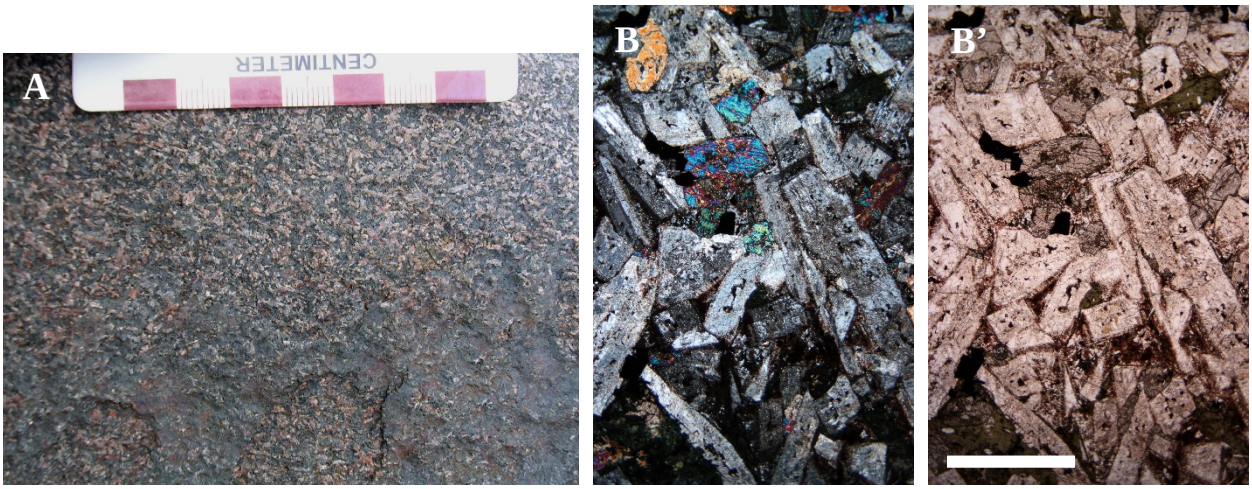


Figure 19. Textures of foliated intergranular granophric gabbro in outcrop (A) and thin section (B) at Location 8.

Location 9: Subprismatic Apatitic Quartz Ferromonzodiorite

UTM(NAD83): 571245_5183675

Description: The stretch of Endion ledges marks the consistent onset of subprismatic to prismatic texture of mafic phases, the increase in granophyric mesostasis to greater than 15%, the presence of quartz paramorphs after tridymite, and the occurrence of 2-3% apatite (Fig. 20). This interval marks the upper part of the AZ/GZ transitional zone. The rock has a pinkish hue, but its does not develop the deep red color characteristic of the Acidic Zone until the next outcrop at Location 10.

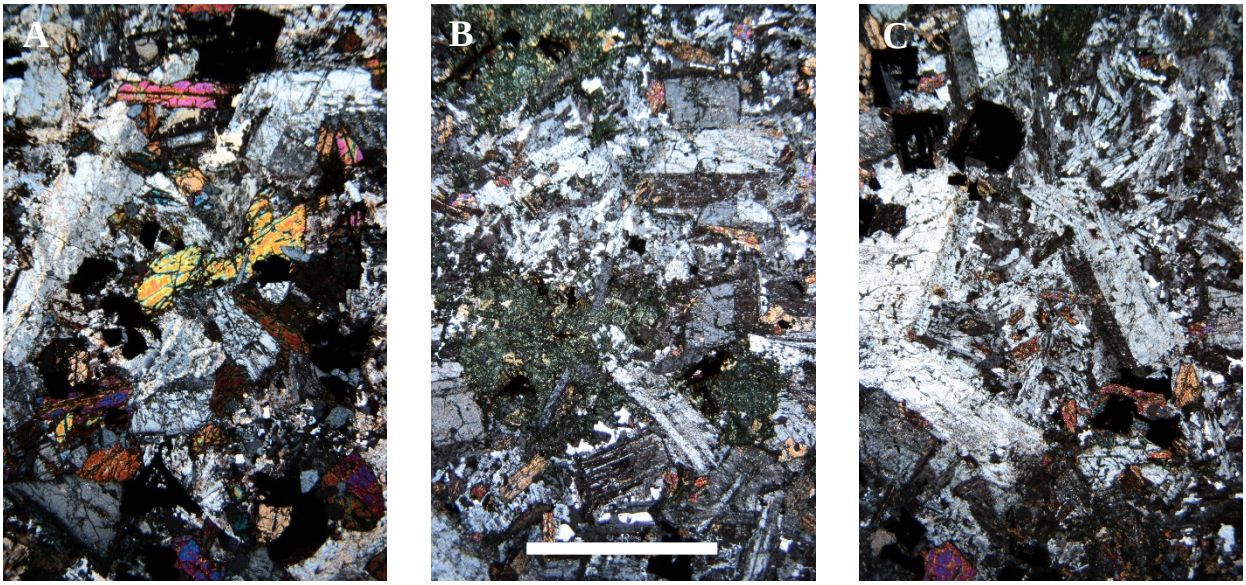
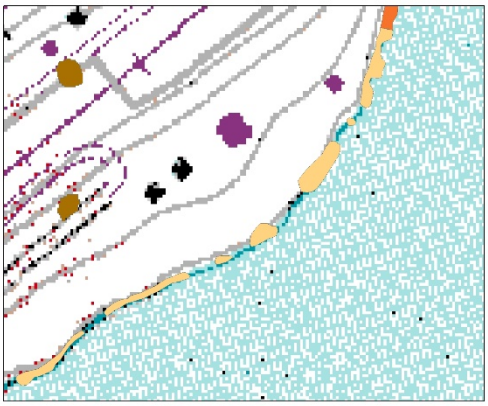


Figure 20. Photomicrographs of subprimatic, apatitic quartz ferromonzodiorite sample MD770D(A) and MD 770E(B & C). Quartz paramorphs of tridymite are commonly associated with granophyre patches. Scale bar = 3 mm.

Area C – Acidic Zone of the Endion Sill



Locations 10 - 13: Hematized Prismatic Quartz Ferromonzonite

UTM (NAD83): 571320_5183720 to 571607_5183960

Description: Homogeneous exposures along this stretch of shore display the strongly hematized rock that characterizes the Acidic Zone (or Red Rock of Schwartz and Sandberg, 1940). Granophyre content through this section is consistently between 30 and 50%, 20-35% plagioclase laths are commonly bleached white, and altered pyroxene becomes is consistently subprismatic to prismatic (Fig. 21). In thin section, tridymite paramorphs are ubiquitous. Apatite ranges from 0.5 to 2 %.

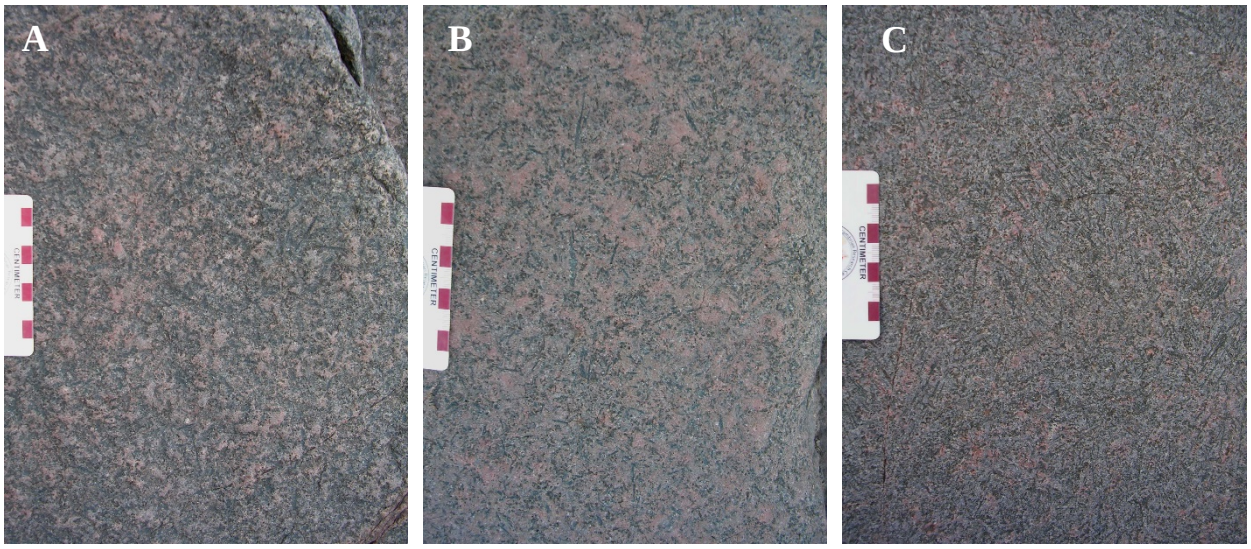


Figure 21. Prismatic to subprismatic textures of ferromonzonite exposures at Locations 10, 11 and 12.

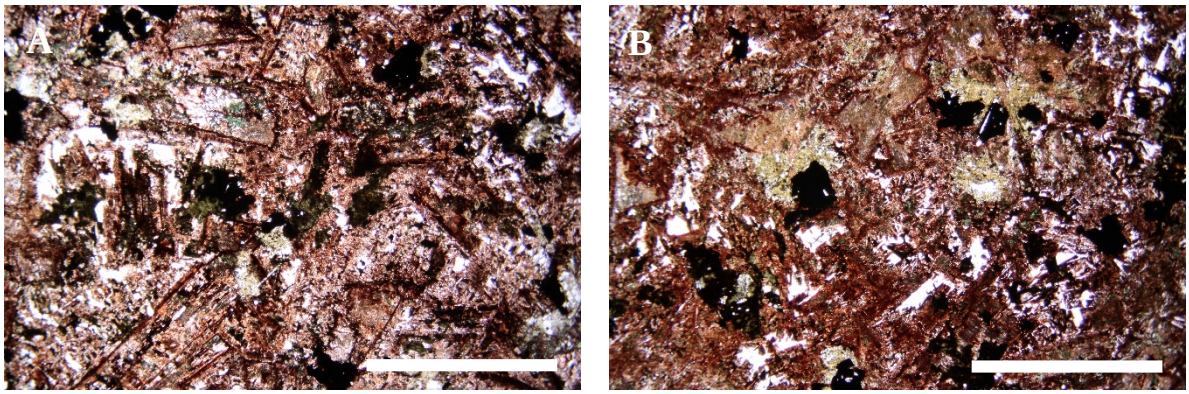
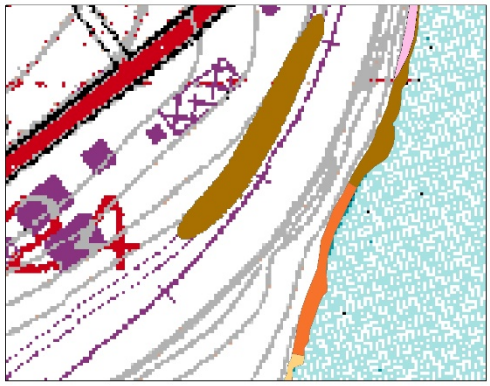


Figure 22. Strongly hematized and granophyre+tridymite mineralogy of samples MD771B (A) and MD772A (B) from locations 10 and 12, respectively. Scale bars = 3mm.

Area D – Intermediate Zone and Upper Contact of the Endion Sill



Location 14: Heterogeneous mix of ferromonzodiorite and granophyre

UTM (NAD83): 571615_5183990 to 571660_5184125

Description: Along this continuous stretch of shoreline outcrop, the prismatic quartz ferromonzonite grades into a less granophyric composition of ferrodiorite to ferromonzodiorite that becomes mixed with irregular-shaped masses of granophyre (Fig. 23). The host ferromonzodiorite still locally displays a very prismatic texture (Fig. 23A). Progressing north across this mixed zone, the granophyric and dioritic components become more strongly contrasted (Fig. 23B → Fig. 23C) with the intermediate component becoming dominant over granophyre and more ferrodioritic in composition (less granophyric mesostasis).

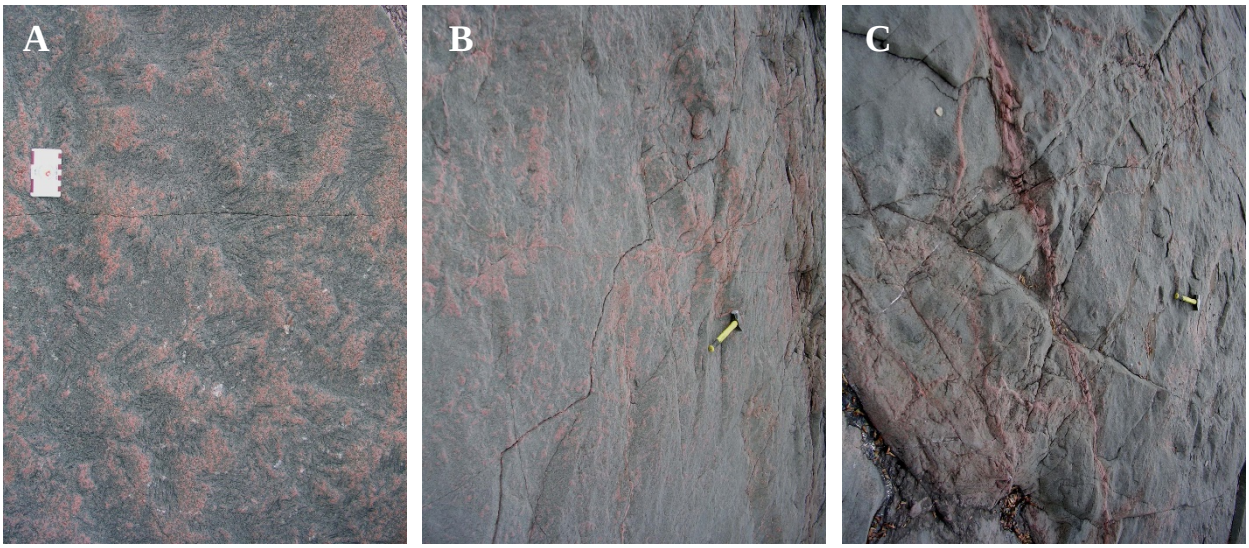


Figure 23. Exposures of complexly mixed granophyre and ferromonzodiorite observed at Location 14 progressing north. A) irregular masses of granophyre mixed with prismatic ferromonzodiorite. B) Broader scale view of complexly mixed granophyre with ferromonzodiorite. C) Granophyre occurring as irregular dikes and dikelets in more homogeneous ferrodiorite.

Location 15: Ferrodiorite of the Intermediate Zone

UTM(NAD83): ~ 571685_5184160

Description: At this point along the shore, the dominant rock is a dark ferrodiorite with only local occurrences of irregular granophyre masses. This is the main rock type of what other workers (Oestrike, 1983; Gardner, 1987; Jerde, 1991) have termed the intermediate zone. Petrographically, it is a medium-grained, subprismatic to poikiloprismatic quartz ferrodiorite to ferromonzodiorite with significant

amounts of apatite (4%), tridymite paramorphs (15%), and primary brown amphibole as rims on pyroxene prisms (Fig. 24). Strongly zoned pyroxene and plagioclase display preferentially altered cores and fresh rims (Fig. 24B).

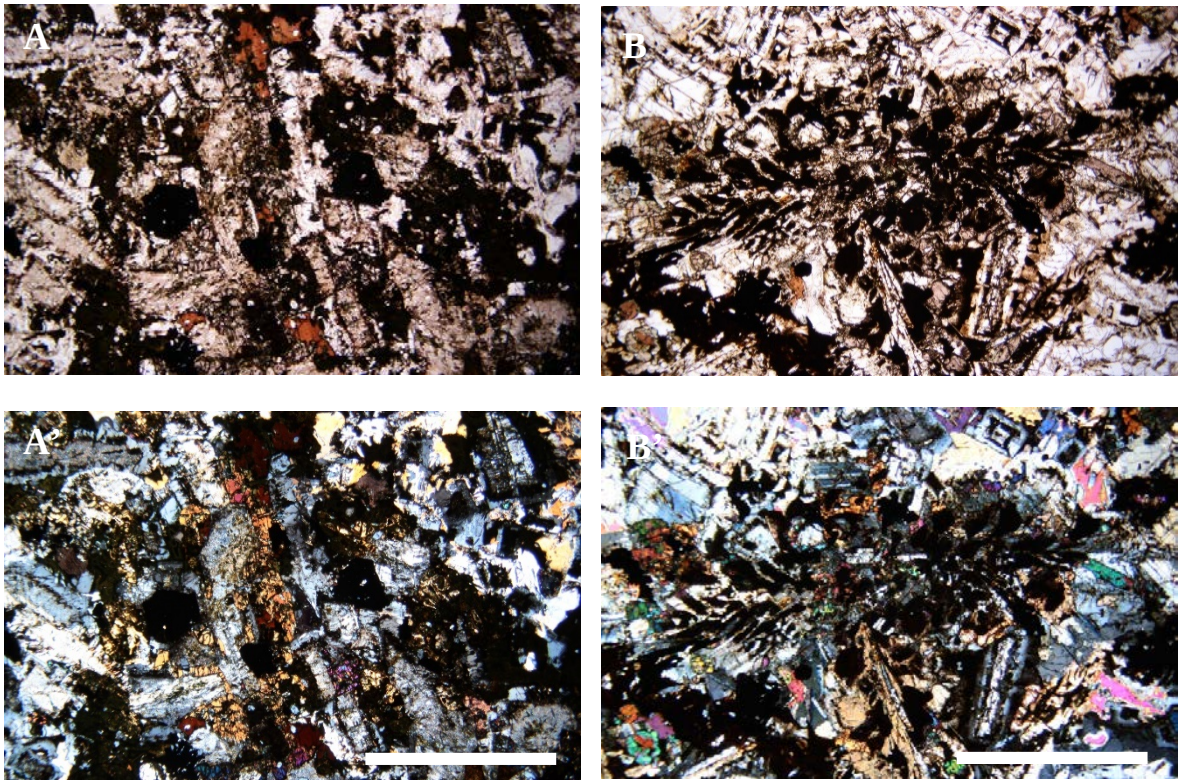


Figure 24. Photomicrographs of Samples MD773E (A) and MD773F (B) displaying the subprismatic to poikiloprismatic texture of the quartz ferromonzodiorite/ferrodiorite that forms the Intermediate Zone of the Endion Sill. Scale Bar = 3mm.

The ferrodiorite is cut here by a 0.5-1.5 meter wide diabase dike trending to the NE and dipping steeply to the NW. The diabase shows well-developed columnar joints that are curved indicating fault motion before the dike completely cooled (Fig. 25).



Figure 25. Columnar-jointed diabase dike cutting ferromonzodiorte at location 15.

Location 16: Contact of Intermediate Zone and Recrystallized Rhyolite

UTM(NAD83): ~ 571710_5184240



Figure 26. Panoramic view of the contact between ferrrodiorite and granophyre (recrystallized rhyolite) at Location 16.

Description: Exposed in the sloping ledge at this location is the subhorizontal (slightly NE-dipping) contact between the medium fine-grained ferrodiorite and medium fine-grained granophyre (Fig. 26). In detail, the contact is very irregular and interfingering with granophyre occurring as irregular masses to dike-like bodies in the ferrodiorite. In the overlying granophyre, some lobate masses of fine-grained ferrodiorite suggestive of two magma mixing textures.

The granophyre transitions into flow banded rhyolite in the seacliffs that line this bay (inaccessible except by boat). This transition is observed in Tischer Creek, where it is observed to occur over several meters (Ernst, 1955; Oestrike, 1983).

References

Ernst, W.G., Jr., 1955, Petrology of the Endion Sill. M.S. thesis, University of Minnesota-Minneapolis, 31p.

Ernst, W.G., Jr., 1960, Diabase-granophyre relations in the Endion Sill, Duluth, Minnesota. Journal of Petrology, v. 1, p. 286-303.

Gardner, J.E., 1987, Origin of the Endion Sill. M.A. thesis, Washington University, St. Louis, 359p.

Gardner, J.E., Haskin, L.A., Brannon, J.C., 1987, Possible assimilation by a mafic magma: the Endion Sill, Duluth, Minnesota. Lunar Planetary Science Conference Abstracts, v. 18, p. 312-313.

Green, J.C. and Miller, J.D., 2008, Bedrock geology of the Duluth quadrangle, St. Louis County, Minnesota. Minnesota Geological Survey Miscellaneous Map M-182, scale 1:24,000

Jerde, E. A., 1991, Geochemistry and petrology of hypabyssal rocks associated with the Midcontinent Rift, northeastern Minnesota; Appendix D – The Endion Sill. Ph.D. dissertation, University of California - Los Angeles, p. 278-288.

Oestrike, R.W., 1983, The Endion Sill, Duluth, Minnesota: mineralogy and petrology of a composite intrusion. M.S. thesis, University of Illinois, Urbana-Champaign, 141 p.

Schwartz, G.M. and Sandberg, A.E., 1940, Rock series in diabase sills at Duluth, Minnesota. Geological Society of America Bulletin, v. 51, p. 1135-1172.

Sun, S, -S. and McDonough, W.F., 1989, Chemical and isotopic systematics of oceanic basalts: implications for mantle composition and processes. In: A.D. Saunders and M.J. Norry (eds.), Magmatism in Ocean Basins. Geol. Soc. London, Special Publ., v. 42, p. 313-345.

FIELD TRIP 6

May 6, 2016

GEOLOGY AND TROUT FISHING ALONG AMITY CREEK, DULUTH

Dean Peterson
Peterson Geoscience LLC
George Hudak
UMD-NRRI

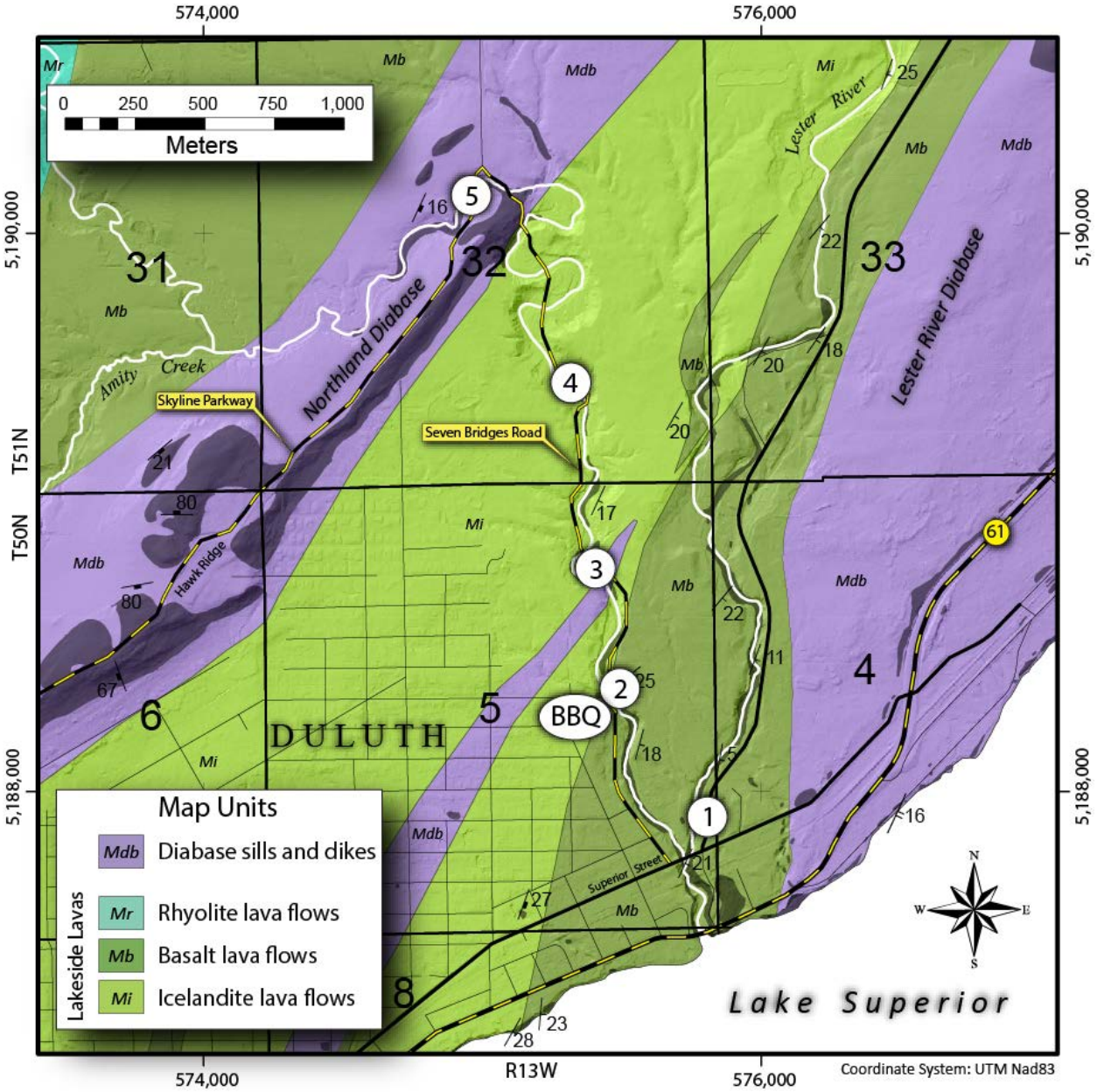


Figure 1. Bedrock geology and field trip stop map of Amity Creek, Duluth, Minnesota.

Introduction:
Circa 1985…. was the time, as seemingly all of the University of Minnesota Duluth (UMD) geology undergraduate and graduate students were aware, of monthly handouts of the infamous 5-pound bricks of government "eutectic" cheese as well as bags of rice and other edible things that we cannot remember. As a poor geology undergraduate student living on these government handouts and potatoes at the UMD, the first author spent many many days on Amity Creek fishing for meat (brook trout) for dinner after class. Most trips were successful back then and still are today. This short field trip will include the geology of the Seven Bridges Road portion of Amity Creek as well as trout fishing tips and perhaps some stories and seemingly tall tales from two proud products of the geology department of UMD. We will end our trip with a BBQ where additional tales may be told.

History of Seven Bridges Road:
This field trip largely follows the path of Duluth pioneer and former mayor Samuel Snively, who was instrumental in the development (late 1890s) and construction of our roadway, Seven Bridges Road. Seven Bridges Road is one of many parkways in Duluth, a city renowned for its parks and outdoor amenities. We will travel up Seven Bridges Road to Hawk Ridge and onto Duluth's famous hilltop boulevard, Skyline Parkway. Winding our way up Amity Creek through a mixed forest of pine, fir, maple, and birch you will see how the road intertwines and crosses with the creek over seven stone-arch bridges, and the reason for the road's current name. Each bridge is faced with local 1.1 billion year old basalt and diabase collected from the creek bed or blasted from nearby outcrops and the pink cap rocks consist of granite quarried in St. Cloud, Minnesota.

The following historical description of the development of Seven Bridges Road is modified from Ryan (1999). Work on the original section of the road was begun in 1899, and opened for use in the next year, though it took over three decades before the upper connection across Hawk Ridge was finally completed. The drive was built by Samuel Snively, a Duluth pioneer who owned a large 400 acre farm in the back country above Duluth suburbs of Lester Park and Lakeside. His hilltop farm was well-known for its thoroughbred stock and the beauty of its layout, which included a glimpse of Lake Superior through the nearby Amity Creek valley. Snively apparently often hiked the valley and explored the woods on both sides of the ridge line overlooking the east end of Duluth. During these strolls, Snively began to envision a park drive that would rival any other in Duluth. Donating sixty acres of his own property, Snively set to work contacting all the other landowners in the area, successfully garnering donations of the necessary rights-of-way for his road, as well as some of the necessary monies to build it.

A crew of workers from the surrounding countryside was hired and construction on Snively's road began in the late fall of 1899 and continued into the following summer. The road crew started its work at the junction of Oriental and Occidental boulevards near Lake Superior, two carriage paths that ran through and alongside the boundaries of Lester Park, a city park in east Duluth. Despite its popularity as a scenic parkway, the city of Duluth neglected to maintain Snively's road, and within a decade all the wooden bridges had fallen to ruin, making the road impassable to vehicle traffic.

In 1910, the road's destiny changed for the better when it was handed over to the Duluth's park commission, and a new plan for its rejuvenation was developed. The park board hired an architectural landscaping firm to design a new series of bridges for the road. In the fall of that year, the firm of Morell & Nichols of Minneapolis presented the park commissioners with sketches and blueprints for nearly a dozen new stone-arch bridges to replace the wooden ones Snively had built. During 1911, the roadway was regraded and graveled, and several first class stonemasons from the Duluth area were hired to build the bridges simultaneously. When completed, the newly refurbished road would become an official part of the Duluth's boulevard system. News of the park board's intentions delighted Snively, for the plans were exactly what he had in mind when he first built the road.

When Snively's road reopened on July 6th, 1912, it was renamed Amity Parkway and added nearly 6 miles to the city's growing boulevard system. The new Amity Parkway became a popular destination for tourists and locals alike. Winding its way up into the eastern hills, the route presented many scenic sights of the landscape and rushing creek. Flowers lined many of the drive's turns and curves, and in the autumn, the poplar and birch forests presented spectacular colors for the tourist.



"When the park board decided to take over and improve this roadway, it greatly pleased me, for it assured the consummation of the very purpose I had in view, the appropriation by the city for park and boulevard purposes of some of the scenic and natural park property in and about the city...Our possible park system rightly developed will be the city's greatest asset and advertisement."

Samuel Snively

Satisfied for the time being, Snively moved on again to other things in his life, but would return some two and a half decades later, (this time as the mayor of Duluth) to build the final leg to his road, the segment of the road leading to Hawk Ridge. Two of the bridges (#8 & #9) fell into disuse (by automobiles) when the eastern extension Winter Bridge to and along Hawk Ridge was completed in the thirties. Remnants of these two closely-built bridges still stand along a pedestrian pathway that shoots off from the main road near the last bridge crossed before the road ascends toward Hawk Ridge Nature Reserve. The remaining seven bridges are still used by vehicle traffic, but years of weather, combined with vandalism, and vehicle accidents had taken their toll.

In the mid-1990s the city of Duluth, realizing the historic significance of the bridges, initiated a program to repair and restore the structures. Bridge #2, just south of the Lakeview hockey rinks, being the most damaged of the lot, was the first to be restored. The original blueprints were consulted with the work beginning in late 1996, and completed the following summer. The bridge was restored to its original condition, and the project was hailed a success.

In the spring of 1998, the Duluth Preservation Alliance awarded the restoration with a plaque at its annual awards ceremony. Bridge #6 restoration work was begun the following year, a century after Samuel Snively began construction on the original road. Repairs to the remaining five bridges are slated to take place over the next few years.

Although in fairly rough condition and its paved section in need of resurfacing, Seven Bridges Road remains one of Duluth's more idyllic drives. Traveling the road, you'll often meet hikers and bicyclists, equestrians, and automobiles. **Fisherman can be spotted angling for trout** along the creek bank, and during the warmer days of summer, swimmers are often seen cooling themselves in pools such as the one situated just beneath the falls near Historic Bridge #6. During the winter months, snowmobilers share the route with hikers, cross-country skiers, and snowshoe enthusiasts.

One day, back in early November of 1934, Sam Snively stood along Hawk Ridge overlooking eastern Duluth and the blue expanse of Lake Superior. Much of his celebrated farm, less than a mile away, had been destroyed sixteen years before in a devastating forest fire that had swept through the area. He sold the property soon after. Now, as he stood there, fast approaching his 75th birthday, and well into in his last term as mayor, he contemplated his long life in Duluth.

"Sometimes, when I become discouraged, I say to myself, I should have gone to another city to seek my fortune. But when I look over these hills and see the great natural beauties of our community, I console myself and wonder--where in all this wide world could I find such a view as this?"

Samuel Snively

Geologic Setting:
As Amity Creek decends the steep hillside of Duluth to Lake Superior, it flows over mafic and felsic lava flow sequences and hypabyssal diabase dikes and sills of the 1.1 Ga. North Shore Volcanic Group as well as locally over red glacial rift. The variability in resistance to weathering and erosion of these rocks has lead to the varied character of Amity Creek and its most famous inhabitants, the brook trout. We will spend a late afternoon exploring the rocks, the character of the creek, and the possibility of hooking some trout.

The authors wish to let all of the field trip participants know that neither of us have ever formally mapped the geology we will be looking at during this short Duluth-centric field trip. The experts on the geology of this area are University of Minnesota Duluth geology professors Dr. John Green and Dr. James Miller, and thus we will be critiqueing their geology (**Fig. 1**) as shown on the Minnesota Geological Survey Miscellaneous Map M-182 (Green and Miller, 2008) during this field trip. However, as two experienced NE Minnesota geologists we can perhaps answer most questions and will explore the geologic details during the field trip simply along with all of the participants.

Angling Setting:
Unlike the trout fishery of southeastern Minnesota's driftless area, the streams of Minnesota's north shore of Lake Superior generally are only fair trout streams. These waterways depend on unstable runoff for their flow and surge after large rain events and during spring snowmelt which can dwindle to a trickle during drought and the winter season. In the summer some stretches (especially the upper portions of the stream systems) can get warmer than is best for trout.

The 1.1 Ga. volcanic bedrock over which the North Shore streams flow contain few of the water-soluble minerals that help keep the water alkaline and the aquatic invertebrate population large. Consequently, these streams tend to be soft, slightly acidic to neutral, and not particularly productive. Because they generally lack spring water, the streams get very cold in winter and can form "anchor ice" on the bedrock of the streambed, destroying aquatic life and habitat. However, North Shore streams have two things in their favor for the development of a trout fishery. The first is the cool Lake Superior-moderated climate and the second is the deep shade provided by the ubiquitous forest bank cover, which generally keeps these streams just cool enough to support trout.

Trout are not native to the upper reaches of the North Shore streams. Coaster brook trout occupied Lake Superior and ascended the rivers as far as the first barrier falls-usually less than a mile from the lake. Only during the last century have brook trout, rainbow trout, and locally brown trout been stocked above the barrier falls of North Shore streams.

FIELD TRIP STOP DESCRIPTIONS

NOTE: all UTM coordinates are given in NAD 83, Zone 15 and keyed to Figure 1.

STOP 1—*Lakeside lavas and the confluence of Amity Creek and the Lester River at Lester Park*

Location: UTM NAD83 coordinates 575795E, 5187900N

General description:

The confluence of Amity Creek and the Lester River occurs at Duluth's Lester Park, where these two stream systems flow on undifferentiated mafic flows of the Lakeside Lavas (Green and Miller, 2008). The lavas consist of dark gray to brown, aphyric to sparsely porphyritic basalt and basaltic andesite lava flows. Individual flows are generally 5 to 30 meters thick, with an amygdaloidal upper zone and smooth (rarely rubbly) upper surface. Phenocrysts, where present, are predominantly plagioclase, with minor altered olivine, magnetite, and augite.



Figure 2. The lower Lester River at Lester Park.

Angling tip:

Lester Park provides numerous angling opportunities (young steelhead and occasional brown or brook trout) with the best chances of success in pools immediately downstream of the massive interiors of lava flows. The park's streams also seasonally (spring and fall) receive runs of large adult salmon, steelhead, and kamloops rainbow from Lake Superior. Anglers should be aware that only lures with single hooks are allowed at Lester Park.

STOP 2—*Lakeside lavas waterfalls of Amity Creek at "The Deeps"*

Location: UTM NAD83 coordinates 575470E, 5188350N

General description:

A very short walk downstream from our parking spot leads us to numerous waterfalls and deep pools associated with the erosion of the Amity Creek diabasic basalt. This huge (100 meters thick) lava flow is a dark gray to brown, fine- to medium-grained, locally seriate to porphyritic, heterogeneously textured basalt flow. The flow contains up to 10 percent phenocrysts of thin plagioclase tablets and minor phenocrysts of ilmenite, magnetite, and oxidized olivine. Groundmass is intergranular/intersertal to ophitic to felty and locally diktytaxitic, and contains plagioclase, augite, oxidized olivine, tabular ilmenite, and magnetite, and a mesostasis including K-feldspar, quartz, apatite, and chlorite. Diktytaxitic cavities contain chlorite, quartz, calcite, and laumontite. The massive nature of the Amity Creek diabasic basalt has lead to the formation of numerous waterfalls and deep pools, which are favorite swimming/jumping/diving spots for local Lakeside area kids.



Figure 3. Waterfall of Amity Creek into "The Deeps".

Angling tip:
Within these pools prowl some of the largest stream-bound rainbow trout of the whole North Shore of Lake Superior in Minnesota. The summer angler must get up early in the morning (and bring a net) to fish these pools as swimmers always abound later in the day. The bridge we will cross and immediately park after is the Posted Boundary of Amity Creek. Below this bridge anglers are only allowed to fish lures with single hooks, while above the bridge treble hooks are allowed.

STOP 3—*Resistant diabase dike in icelandite lavas forming the "Rainbow Trout Pool"*

Location: UTM NAD83 coordinates 575410E, 5188000N

General description:
A steep hike down from Seven Bridges Road is needed to observe first hand the diabasic Lakeside intrusion. The intrusion here is a black, fine- to medium-grained, plagioclase-phyric, intergranular olivine diabase with abundant apatite, interstitial quartz, and K-feldspar. This exposure shows it to be a vertical dike cutting the Lester Park icelandite lava flow. On lakeshore exposures, the western contact is cross-cutting the Lester Park icelandite. These relationships are interpreted to indicate that the diabase came in along a high-angle reverse fault. The resistant diabase dike forms a beautiful waterfall and large pool in Amity Creek immediately downstream from the dike.



Figure 4. Subvertical diabase dike and the "Rainbow Pool".

Angling tip:
Small to moderate size (8-13 inches) rainbow trout are abundant in the pool and several casts of a 1/32 oz panther martin spinner into this pool should always be tried by anglers. Anglers should always remember to lower your rod tip when the hooked rainbow trout jumps out of the water. There have been days when the first author hooked rainbow trout on his first 12 casts.

STOP 4—*Flaggy weathering of icelandite lava and the meandering of Amity Creek*

Location: UTM NAD83 coordinates 575300E, 5189465N

General description:

A stop to observe the large Lester Park icelandite, a pink, red, or tan, porphyritic icelandite lava flow, about 180 meters (590 feet) thick. Mostly massive, but the upper part is strongly flow-laminated and folded, with local large, round vugs containing calcite, quartz, barite, and fluorite. Phenocrysts (5 to 10 percent) are of plagioclase, oxidized Fe-silicate, magnetite, zircon, and apatite. The groundmass contains poikilitic quartz (paramorphs after tridymite), K-feldspar, oxidized Fe-silicate, and magnetite, calcite, and chlorite.

Angling tip:

Perhaps we as a group we can locate the best brook trout pool since the first author has never had much luck in the past angling in this portion of Amity Creek.

STOP 5—*Waterfalls and pools off of the Northland Sill and the excellent brook trout fishing trail along the upper portions of Amity Creek*

Location: UTM NAD83 coordinates 574970E, 5190135N

General description:

Brook Trout Central!! This portion of Amity Creek is, in the opinion of the first author, the best place to first start angling on Amity Creek. The geology is dominated by the contact of the highly resistant Northland Sheet intrusion and the Amity Creek Icelandite lava flow, which culminates for the angler in a series of waterfalls and excellent brook trout pools. The Northland sheet is a brown, fine- to medium-grained, diktytaxitic intergranular/intersertal diabase grading to augite quartz ferromonzonite. The diabasic intrusion contains minor traces of low-Ca pyroxene, olivine, and primary hornblende and abundant magnetite, ilmenite, and apatite. The sheet-like intrusion is variable in thickness and cuts across more than 500 meters (1,640 feet) of volcanic flows of the Lakeside lavas.



Figure 5. His smile will last forever, Nathan's first trout, 2015 (nephew of Dean M. Peterson).

Angling tip:

At this stop, we'll investigate waterfalls and excellent brook trout fishing pools situated at the uppermost portions of the Amity Creek icelandite lava flow as well as those within the basal portions of the diabasic Northland Sheet. An excellent horse/hiking trail heads upstream from our parking spot and anglers should be aware that numerous large hook-jawed brook trout swim in these waters. If one is a believer in "take a kid fishing", then perhaps this is one place to begin (**Fig. 5**).

REFERENCES

Green, J.C. and Miller, J.D., 2008, Bedrock geology of the Duluth quadrangle, St. Louis County, Minnesota: Minnesota Geological Survey, Miscellaneous Map M-182, scale 1:24,000.

Ryan, Mark, 1999, The history of Duluth, Minnesota's Seven Bridges Road, Samuel Snively and the building of a Northern Minnesota parkway: http://www.amitycreek.com/sevenbridges/index.html.

FIELD TRIP 7

May 7-8, 2016

ARCHEAN AND PROTEROZOIC GEOLOGY OF THE WESTERN GUNFLINT TRAIL

Mark Jirsa
Minnesota Geological Survey

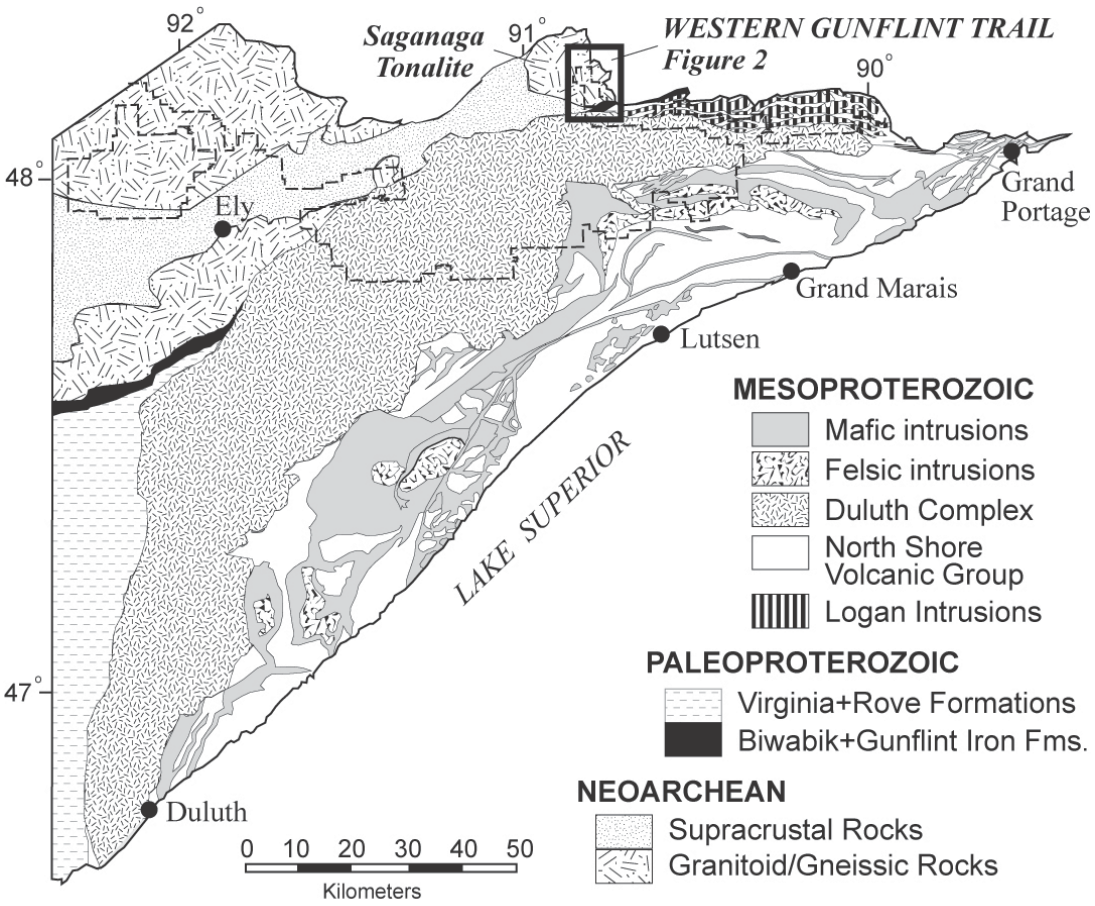


Figure 1. Regional geologic map of northeastern Minnesota showing the location of western Gunflint Trail area (modified from Jirsa and Miller, 2005). Inset box outlines **Figure 2**.

INTRODUCTION

This field trip along the western end of the Gunflint Trail explores Neoarchean, Paleoproterozoic, and Mesoproterozoic rocks, and a diversity of well displayed unconformable and intrusive contact relationships. The trip is modified from the ill-fated one attempted for the 2007 ILSG meeting in Lutsen (Jirsa and Weiblen, 2007) that was canceled due to outbreak of forest fire. For expediency, some of that field guide is repeated here. In addition, this guide borrows heavily from two other field trips: a

workshop on iron-formation hosted by the Precambrian Research Center (Jirsa and Fralick, 2010), and a Geological Society of America field guide that focused on the Sudbury Impact Layer (Jirsa and others, 2011). Readers should consult those publications for additional information and references. The order and number of stops that will be visited during this trip will be determined by time, weather, and access issues.

The bedrock geology of the field stops is portrayed on a recent map of the Western Gunflint Trail area published as Minnesota Geological Survey Miscellaneous Map M-191 (Jirsa, 2011; **Fig. 2**). In this area, the Neoarchean greenstone-granite terrane of the Wawa subprovince of Superior Province is represented by a succession of metavolcanic rocks (~2720 Ma) known informally as the Paulson Lake volcanic sequence, intruded by the Saganaga Tonalite (~2690 Ma) and Paleoproterozoic diabasic dikes. The Neoarchean and diabasic rocks are unconformably overlain by Paleoproterozoic sedimentary strata of the Animikie Group (~1870-1830 Ma), which includes the Gunflint Iron Formation. The stratigraphic top of the iron-formation is marked by seismically deformed and brecciated strata and ejecta—known collectively as the Sudbury Impact Layer—that resulted from a meteorite impact near Sudbury Ontario (~1850 Ma). A disconformity separates the impact layer from overlying siltstone and graywacke of the Paleoproterozoic Rove Formation (~1835 Ma). Mesoproterozoic rifting is manifest in hypabyssal dikes and sills of the Logan intrusions (~1115 Ma), and several phases of the Duluth Complex (~1100 Ma), emplaced into both the Archean and Paleoproterozoic rocks.

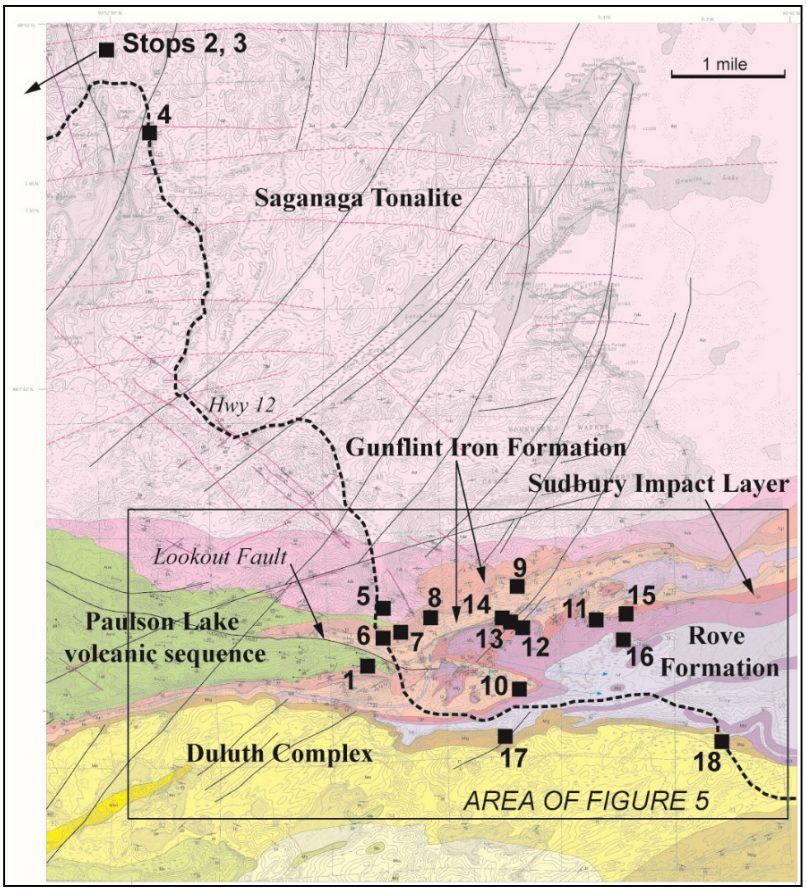


Figure 2. Geologic map (Jirsa, 2011) of the western Gunflint Trail (Highway 12 dashed), showing pertinent features of geology and field trip stops. Note that **stops 2** and **3** lie just off the northwest corner of the map. Sudbury Impact Layer is reddish; Proterozoic dikes are shown as thin red lines; Logan intrusions are shades of purple. Image reduced from 1:24,000 map scale.

GEOLOGIC SETTING

Neoarchean

The oldest rocks exposed in the region are Neoarchean metavolcanic and metasedimentary strata that are part of the Wawa subprovince of the Superior Province. They are probably equivalent to, but not demonstrably continuous with, the Ely Greenstone and Newton Lake Formation. Although the supracrustal successions are dissected by faults and intrusions, some correlation can also be made with adjacent terranes in Ontario. Most recent regional mapping in this terrane was conducted by Jirsa and Miller (2004) in the 1:100,000-scale, Ely-Basswood Lake map sheet that lies just west of the Gunflint Trail. A more detailed map of the Cavity Lake forest fire area that lies just west of the Gunflint is still in review and production (Jirsa and others, in prep.). Rocks of the terrane are divided into a number of fault-bounded segments, each having distinct geologic characteristics that cannot be easily correlated from place to place. The Gunflint Trail area exposes the eastern edge of what Gruner (1941) referred to as the Gabimichigami segment. Supracrustal rocks in this segment include an older suite of variably pillowed, mafic to ultramafic flows and hypabyssal intrusions of the Paulson Lake volcanic sequence (**stop 1**), and a younger suite of hornblende-bearing andesitic to dacitic pyroclastic and volcaniclastic rocks that comprise the Knife Lake Group that are exposed just east of **Fig. 2**. Based on stratigraphic facing directions established from pillowed metabasalt flows, the Paulson Lake sequence forms an east-trending and steeply south dipping and younging homocline. The Saganaga Tonalite (**stops 2-6**) was emplaced into metabasaltic rocks and defines the northern edge of the supracrustal succession. The metamorphic grade of greenstone along this contact is locally increased from greenschist facies that is typical of much of the belt, to amphibolite grade, and foliation in both tonalitic and volcanic rocks is well-developed near the contact. The western edge of the Gabimichigami segment is terminated by a north-northeast-trending fault that juxtaposed greenstone against sedimentary and volcanic rocks of the Knife Lake Group. The Knife Lake Group includes the informally named "Ogishkemunce conglomerate" that contains detrital clasts of the Saganaga Tonalite, along with clasts of iron-formation, metabasalt, metagabbro, and gneiss. This distinctive sequence of conglomerate, sandstone, and alkalic rocks is interpreted to have been deposited in a complex array of successor basins developed along early-formed faults at some time after emplacement of the Saganaga Tonalite at ca. 2690 Ma (Driese and others, 2011; Jirsa, 2016).

Lacking detailed geochronologic data for this immediate area, much of the temporal distinction between various geological elements of the Neoarchean bedrock is based on the correlation of U-Pb zircon dates acquired elsewhere with regionally developed fabrics and structures that resulted from three major phases of deformation, denoted D_1, D_2, and D_3. All three deformation events are the result of N-S- to NW-SE-directed compression. The timing of D_1 deformation is bracketed between deposition of the metabasaltic and associated rocks of the Wawa subprovince at ca. 2722 Ma (Peterson and others, 2001), and emplacement of the Saganaga Tonalite at ca. 2690 Ma. Folds attributed to D_1 deformation in the Ely Greenstone and related rocks are truncated by faults associated with Knife Lake strata, indicating that the latter is synchronous with or post-dates deposition and early deformation of the Ely. As such, the Knife Lake Group is inferred to be a Timiskaming-type extensional basin sequence temporally equivalent to the Shebandowan assemblage exposed in adjacent parts of Ontario (Lodge and others, 2013; Jirsa and others, 2016). D_2 deformation and metamorphism affected all of the Archean supracrustal units and can be crudely bracketed by U-Pb dates of intrusions in the Giants Range batholith to the southwest that place the regional deformation and metamorphic event between about 2674 Ma and 2685 Ma (Boerboom and Zartman, 1993). Thus, the age of sedimentary and volcaniclastic rocks is confined to a 10 million year duration between the emplacement of tonalite at ca. 2690 Ma and D_2 metamorphism and deformation at ca. 2680 Ma. In this region, D_3 deformation is manifest as crenulations and faults in rocks affected by D_2.

Paleoproterozoic

Mafic dikes

Mafic dikes emplaced into the Saganaga Tonalite are prominent on aeromagnetic maps as positive linear anomalies trending northward and eastward. Exposures mapped along the magnetic trajectories (thin red lines on **Fig. 2**) indicate that the dikes vary from diabasic to lamprophyric, and from a meter or less in width, to more than 30 meters. The roadcut at **stop 4** exposes diabase inferred to lie along one of the anomalies. The precise age of the dikes is unclear, and there may be suites representing more than one age. At least one of the northwest-trending dikes is unconformably overlain by, and shed fragments into conglomeratic strata of the basal Paleoproterozoic Animikie Group, indicating a syn- to pre-Paleoproterozoic age.

Animikie Group

Sedimentary rocks of the Paleoproterozoic Animikie Group are exposed in an east-trending belt that extends from Thunder Bay on Lake Superior to a point 12 miles (19km) west of the Gunflint Trail, where the belt is truncated by the Mesoproterozoic Duluth Complex (**Fig. 1**). The Animikie Group in this area consists of locally developed basal conglomerate and sandstone, and iron-bearing strata of the Gunflint Iron Formation. The stratigraphic top of the iron-formation is marked by a major unconformity and ejecta that resulted from a meteorite impact near Sudbury Ontario ca. 1850 Ma (Krogh, 1984; Davis, 2008). Of the 188 known and scientifically verified terrestrial impacts, the Sudbury event is the third largest (based on crater size) and forth oldest (www.unb.ca/passc/ImpactDatabase). The resulting ejecta blanket has been identified in Ontario (Addison and others, 2005), Michigan (Pufahl and others, 2007; Cannon and others, 2010), and here in Minnesota near Gunflint Lake (Jirsa and others, 2011), and in drill core along the Mesabi Iron Range (Addison and others, 2005). The overlying Rove Formation—a mudstone and turbiditic sandstone unit—was deposited directly on the ejecta. The sequence is broadly correlative with Animikie strata exposed to the southwest along the Mesabi Iron Range. The rocks form a homocline that dips gently southward, except where deformed by folding, faulting, and emplacement of Mesoproterozoic intrusions. For example, local folding, inferred to be associated with emplacement of the Logan intrusions, may be the product of magmatic delamination and shouldering of the sedimentary country rocks. Sequence "inflation" by the Logan sills may explain the observation that the dip of Paleoproterozoic rocks increases from 10º away from the contact with Duluth Complex, to 60º in some places near it. Faults are present locally, but few have displacements greater than 50 feet. A notable exception is the Lookout fault (**Fig. 2**) that crosses the Gunflint trail. As much as 200 feet of uplift on the west and south is speculated (Morey and others, 1981; Jirsa, 2011). In addition, the dip of Animikie strata on the west side of the fault is much steeper than that on the east, which explains in part the difference in the widths of map units apparent from the geologic map. Much of the complex-looking fold pattern east of the fault is an artifact of moderately high topographic relief and shallowly dipping units. The Lookout fault displaces Animikie strata; however the relationship between faulting and the emplacement of Logan and Duluth Complex intrusions is unclear.

Gunflint Iron Formation (field trip **stops 7-10**)

As on the Mesabi Iron Range, the Gunflint Iron Formation has historically been subdivided into so-called cherty (granular) and slaty (argillaceous) informal subunits or members. The members are denoted lower cherty, lower slaty, upper cherty, and upper slaty (Wolff, 1917). Although this terminology has some descriptive utility in the field, the subdivision employed here is based instead on a sedimentalogical model (after Pufahl and Fralick, 2004). In this model, depicted in **Figure 3**, the lower cherty and parts of the lower slaty members represent deposition during a single marine transgression. This was followed by a regression that deposited the lower part of the upper cherty member—the resulting sedimentary strata are collectively and informally termed lower sequence here. The upper part of the upper cherty represents the onset of a second transgression that continued through deposition of the thick upper slaty member,

and is collectively termed the upper sequence here. The contact between the two sequences is a diastem inferred to represent a period of maximum regression. The initial stages of the second transgression is marked by intraformational conglomerate containing oncoliths, fragments of what appear to have been semi-lithified grainstone derived from the lower sequence, and both in-place and dislodged stromatolites. The uppermost strata of iron-formation are variably brecciated and/or chaotically folded, carbonate-bearing, and capped by granular ejecta from the ca. 1850 Ma Sudbury meteorite impact event, collectively termed Sudbury Impact Layer here. More detailed descriptions are given below:

Lower sequence—Irregularly graded sequence recording marine transgression, followed by regression. It grades from conglomerate and sandstone at the base, unconformably overlying Neoarchean bedrock; to locally stromatolitic, siliceous grainstone; to interlayered, laminated to massive chert, to iron-rich mudstone, and finally to siliceous grainstone. Total thickness is approximately 50 m. The basal part of the sequence is marked by discontinuous conglomerate and minor fine- to medium-grained quartzofeldspathic sandstone that is typically thinner than 1 m. Conglomerate contains pebbles to small cobbles of quartz, Saganaga Tonalite, metabasalt, and diabase. Thicker sections of this facies exposed in Canada are known as the Kakabeka Conglomerate. The uppermost siliceous grainstone forms prominent ridges. It appears to have been partially lithified prior to deposition of, and contributed grainstone fragments to, the basal part of upper sequence.

Upper sequence—Siliceous grainstone and laminated chert; locally contains stromatolitic and intraclastic conglomerate at base of the sequence; which grades irregularly up-section to increasingly mudstone-rich; and typically parallel-laminated to wavy-bedded. Total thickness is approximately 45-55 m. Reworked volcaniclastic zircons from the upper sequence exposed in Ontario yielded a U-Pb age of 1878±1 (Fralick and others, 2002).

Sudbury impact layer *(SEE Discussion below)*—Brecciated and complexly deformed iron-formation as much as 10 m thick, overlain locally by less than 1 m of mesobreccia and granular ejecta. Both deformed (seismically shattered and chaotically folded) iron-formation and ejecta are inferred to be related to the Sudbury meteorite impact event (Jirsa, and others, 2011). The macroscopically most apparent feature of ejecta is the presence of 0.1-1.0 cm, concentrically zoned spheres inferred to be accretionary lapilli. Microscopic evidence that this material has an impact origin includes rare occurrence of quartz fragments marked by planar deformation features. Metamorphism here in the contact aureole of the superjacent Duluth Complex presumably has obscured or obliterated other diagnostic attributes (e.g., French and Koeberl, 2010).

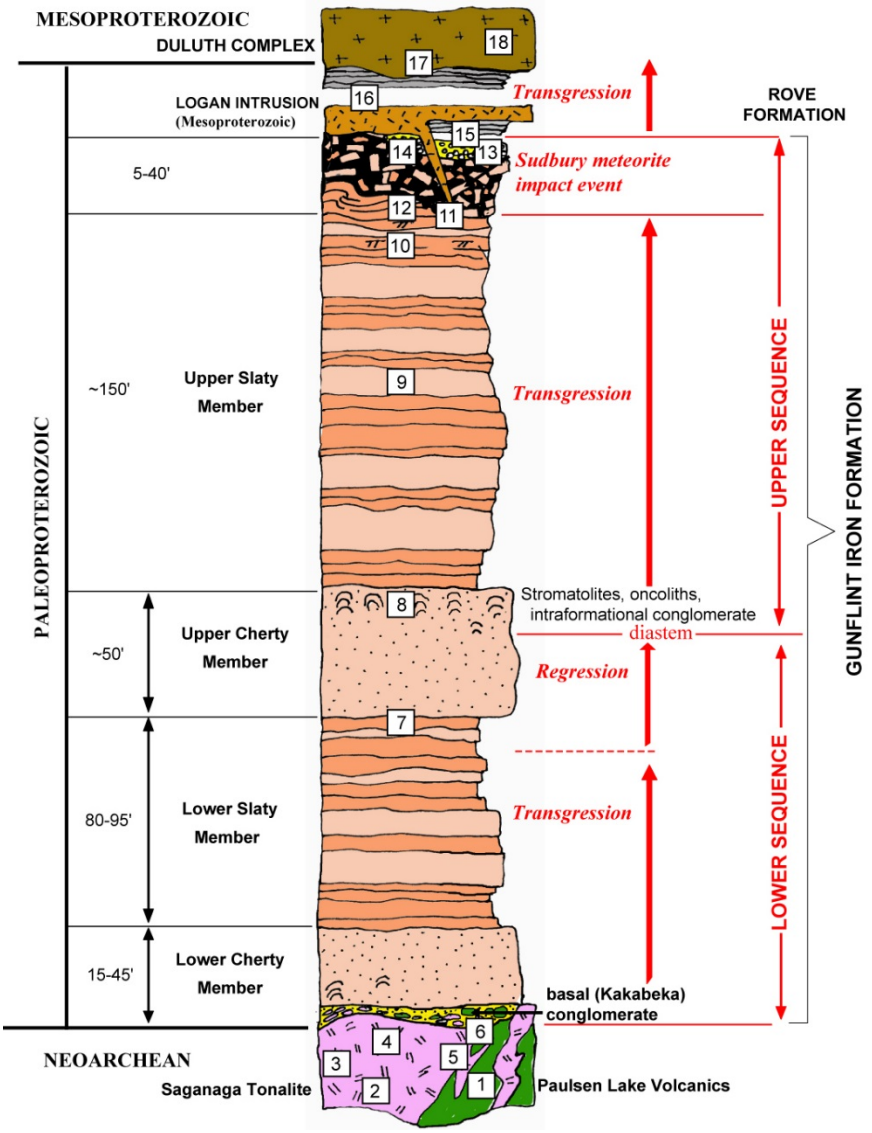


Figure 3. Schematic stratigraphic section of Gunflint Iron Formation and adjacent rocks comparing older stratigraphic nomenclature in left column with that used informally here on right. Siliceous grainstone (cherty) units in the iron-formation are represented by pale color; iron-rich mudstone is darker. Approximate stratigraphic positions of field trip stops are shown in boxes.

DISCUSSION OF SUDBURY IMPACT LAYER
(Field Trip **stops 11-15**)

The Gunflint Lake exposures lie some 480 miles (770 km) west of Sudbury, making this one of the most distant sites known to contain what is considered “proximal ejecta” from the ca. 1850 Ma Sudbury meteorite impact event. Similar deposits have been discovered in Thunder Bay, Ontario, and Michigan that are well documented by Addison and others (2005), Cannon and others (2010), and Pufahl and others, (2007). Deposits near Gunflint Lake appear to be consistently thicker than in other areas, even though these sites are more distal than those in Michigan and Ontario. The impact deposits at sites further away from the crater than Gunflint Lake are much thinner and lapilli are only rarely present. This has led Addison and others (2010) to hypothesize that the Gunflint Lake deposits may represent thick ramparts,

as described for end-of-flow Martian base-surge deposits (Kenkmann and Schonian, 2006; Osinski, 2006; Mouginis-Mark and Garbeil, 2007; Fralick and others, 2012). It should be noted at the onset, that only a small portion of the material described here can be considered true ejecta; i.e., air-borne detritus derived from the impact site. The great majority of the 7 meter-thick deposit is breccia that consists of thoroughly disheveled fragments that appear to have been derived from subjacent iron-formation. Like the deposits near Thunder Bay, the breccia is sandwiched between Gunflint Iron Formation and sedimentary strata of the Rove Formation. Unlike deposits near Thunder Bay, the breccia lies within the metamorphic aureole of the Mesoproterozoic Tuscarora and Poplar Lake Intrusions of the Duluth Complex (ca. 1100 Ma), and is intruded by diabasic sills of the Logan Intrusions (ca. 1115 Ma; Heaman and Easton, 2005). Pervasive carbonate mineralization and metamorphism has overprinted and obscured much of the original, delicate mineralogic features, but macroscopic textures and geochemical content that convey information about protolith and depositional mechanisms are preserved.

In the following discussion, the term Sudbury Impact Layer (SIL) is applied to all facies of sedimentary rocks inferred to have been *formed or deformed* in response to the ca. 1850 Ma Sudbury meteorite impact. By that definition, it includes autochthonous material interpreted to be seismically folded and shattered iron-formation (ejecta-absent), and overlying strata composed largely of allochthonous material derived from the impact site (ejecta-bearing). In no single outcrop are all facies present; however, an approximation of temporal relationships can be inferred from the juxtaposition of two or more facies in individual outcrops (**Fig.4**).

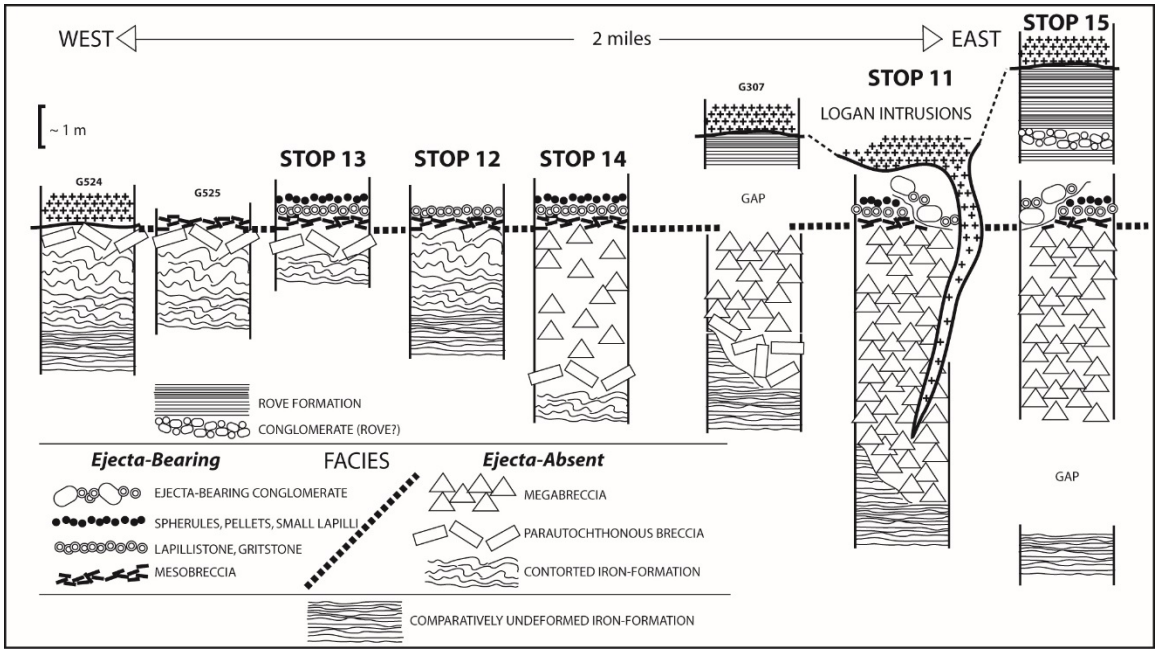


Figure 4. Stratigraphic framework derived from 8 exposures along a 2 mile strike-length near Gunflint Lake; hung from the contact (bold dashed line) between ejecta-bearing (upper) and ejecta-absent (lower) facies of the Sudbury Impact Layer.

Facies below are described in apparent stratigraphic order from oldest to youngest:

Ejecta-Absent

Contorted iron-formation facies: The uppermost layers of iron-formation are chaotically folded and exhibit both ductile and brittle behavior in close proximity at the scale of individual outcrops. The rheologic response depends on the apparent rigidity of material at the time of deformation. Silica-rich layers display brittle, shattered to semi-ductile, boudinage-like textures. By contrast, much of the iron-silicate mudstone layers behaved in a ductile fashion, locally showing evidence of

fluidization and injection into superjacent strata. Folds are non-systematic in trend and style, and multiple hinge detachments occur. These attributes counter-indicate a regional tectonic origin, and instead are best viewed in the context of impact-generated seismicity imposed on *semi-lithified* substrate.

Parautochthonous breccia facies: At several locations, straight-bedded iron-formation passes laterally along strike into irregular zones in which the silica-rich layers have been broken and disheveled, while still retaining some semblance of jigsaw-puzzle fit.

Megabreccia facies: This term is used for breccia composed of unsorted slabs (as large as 5 m), blocks, and smaller fragments of iron-formation. The fragments are angular and in most places have random orientations. Fragments of green, iron-silicate mudstone typically show some evidence of semi-ductile behavior, and locally this material was fluidized to form irregular matrix and clastic (muddy) dikes.

Ejecta-Bearing

Mesobreccia facies: This is fragmental rock containing angular, subrounded, and amoeboid clasts (up to 5 cm long) of dark green material and scattered accretionary lapilli. Petrography shows that much of the original structure of the clasts has been metamorphically recrystallized and annealed; however, relicts of amygdaloidal and fluid-looking textures remain—implying a glassy protolith.

Lapillistone-gritstone facies: Accretionary lapilli as large as 1.5 cm occur as irregular masses and layers interbedded with sandy to silty gritstone. In areas least affected by metamorphism, several grains of shocked quartz with planar deformation features have been identified in thin section.

Spherule, pellet, small lapilli facies: The upper parts of ejecta horizons locally contain layers, lenses, and interbeds of accretionary or relict glass grains that are smaller than typical lapilli and generally lack concentric zonation. These apparently accreted particles may represent waning ejecta plume deposition.

Ejecta-bearing conglomerate facies: In a few localities, the uppermost part of impactite deposits consist of conglomerate containing subrounded fragments of iron-formation (in contrast to anglular fragments typical in breccias described above), and matrices containing variably abraded lapilli.

The apparent contrast in rheologic response to seismicity between siliceous and interbedded "muddy" strata indicates that the relative competancy of the two sediment types was significantly different at the time of impact. One explanation is that the silicification process occurred very early, perhaps just beneath the sediment/water interface, and produced the more cohesive (but not yet fully lithified) siliceous layers. Seismic deformation brecciated those layers selectively, while folding and liquefacting the interbedded muds. This interpretation is relevant to the understanding of depositional environment. It implies that upper layers of the iron-formation were either in a shallow submarine setting or only recently emergent at the time of impact.

The arrangement of facies described above and depicted on **Figure 4** can be interpreted in the context of experimental evidence and observations from lunar and smaller terrestrial impacts. Using calculations from Collins and others (2005), based primarily on estimated crater dimensions, one can predict arrival times for various effects of the impact here, some 480 miles west of the impact site as follows:

EVENT	APPROXIMATE ARRIVAL TIME
1) Fireball	13 seconds (the modern equivalent of 3rd degree burns)
2) Earthquake	2-3 minutes (>10.9 at epicenter)
3) Ejecta Ground Surge	5-10 minutes (predicts ejecta 1-3 meters thick, grain sizes ~1cm)
4) Air blast	40 minutes (sonic boom)
5) Tsunami *	1-3 hours

[*The latter is speculation, as the arrival time and effects of tsunami are dependent on pre-impact position relative to strand line, and basin bathymetry which is nearly impossible to establish.]

Intuitively, only three of these events are likely to have produced a record in the rocks: earthquake, ejecta surge, and tsunami. Nearly all contacts between individual facies are gradational, with one very important exception—in all exposures, the boundary between ejecta-absent and ejecta-bearing facies is extremely sharp. This is inferred to reflect a fundamental shift in geologic processes from intense seismic perturbation of uppermost iron-formation represented by the ejecta-absent facies, to deposition by the passing ejecta plume. The uppermost conglomerate facies is inferred to represent mixing of local and exotic detritus, presumably by tsunamis or other post-impact fluvial or marine processes.

Rove Formation

The Rove Formation consists of carbonaceous, thinly bedded argillite to slate, and fine- to medium-grained graywacke (**stops 15** and **16**). Primary sedimentary structures indicate turbidity current flow was dominantly to the south. The basal several meters of the formation are irregularly bedded, carbonate-rich, and locally conglomeratic (**stop 15**). Detrital zircons taken from lower parts of the formation in Ontario yielded ages as young as1827±8 (Addison and others, 2005), indicating some considerable hiatus separated deposition of the Rove from that of the underlying 1850 Ma Sudbury Impact Layer.

Contact metamorphism

The iron-formation, SIL, and overlying argillaceous strata of the Rove Formation were variably replaced by carbonate and metamorphosed by the Duluth Complex to amphibole and pyroxene hornfels. Floran and Papike (1978) delineated irregularly northwest-striking metamorphic zones recognized on the basis of the dominant iron-silicate mineral present in iron-formation. From least metamorphosed on the northeast, to most metamorphosed on the southwest, these indicator minerals are greenalite+minnesotaite, grunerite, hedenbergite, fayalite, and ferrohypersthene. Despite this metamorphism, macroscopic sedimentary textures are well preserved in most outcrops. Metamorphic effects adjacent to the Logan Intrusions are minor.

Mesoproterozoic

Mesoproterozoic mafic intrusions comprise the remaining exposures in the Gunflint Trail area. The rocks represent early magmatic stages of the Midcontinent Rift. The apparently earliest of these are diabasic sills and dikes emplaced into the Animikie strata and collectively referred to as the Logan intrusions. A baddeleyite age of 1115 ± 1 Ma is reported from a sample of a Logan sill near Thunder Bay (Heaman and Easton, 2005). The sills are intruded, with slight angular discordance, by medium to coarse-grained gabbro and troctolite of the Poplar Lake and Tuscarora intrusions of the Duluth Complex. The Poplar Lake is part of the early gabbroic series of the complex. A basal gabbroic unit of the intrusion yielded a date of 1106.9 ±.8 (Miller and Severson, 2002). Field relationships indicate that the Poplar Lake is intruded by the Tuscarora intrusion, which is considered to be part of the layered series of Duluth Complex. This is consistent with a U-Pb age of 1098.81±0.32 from a sample just west of the Gunflint Trail area (Hoaglund and others, 2010).

Logan Intrusions

The Logan intrusions (**stops 11**, **15**, **16**) are exposed along a series of prominent, east-trending ridges formed by the differential erosion of diabase sills and sedimentary rocks, particularly the Rove Formation. Individual sills are as much as 1100 ft (33m) thick, and can be traced along strike for several kilometers. Branching and merging of individual sills is common, and many sills thicken and thin down-dip. Some

sills terminate against joints and inferred faults. Locally, fractures in the Rove Formation are occupied by thin dikes, which give a box-work configuration to the hypabyssal intrusions. Rock types include aphyric basalt, fine- to medium-grained diabase with ophitic clinopyroxene enclosing plagioclase, plagioclase cumulates, and granophyre (Jones, 1984). Outcrops in the field trip area commonly have plagioclase-phyric phases (**stop 11**). Chilled margins form sharp contacts with, and locally contain inclusions of, the country rocks. Diabase coarsens to medium-grained near the center of individual sills, and clinopyroxene is ophitic throughout. Minor differentiation is manifest in accumulations of plagioclase or granophyric intergrowths (quartz, sodic plagioclase, and orthoclase) in upper parts of sills.

Duluth Complex

The Duluth Complex (**Fig. 5**) is a sequence of generally discordant plutonic rocks consisting of many separate intrusions. Two of these intrusions, the Poplar Lake and Tuscarora, are exposed along the Gunflint Trail. The Poplar Lake intrusion, formerly referred to as Nathan's layered series, consists of interlayered gabbroic cumulates, with minor amounts of troctolitic and anorthositic cumulates. Rocks of the Poplar Lake have reversed magnetic polarity, and thus are broadly correlative with lower lavas of the North Shore Volcanic Group and with the Logan intrusions. The Poplar Lake intrusion is composed of at least 27 sheet-like units of mafic cumulates and intermediate to felsic rocks (the so-called Nathan's layered series). The Tuscarora intrusion irregularly cuts across the layered gabbro of the Poplar Lake intrusion (Morey and Nathan, 1978). The basal part of the Tuscarora intrusion consists of a fine-grained, augite-poikilitic, olivine gabbro (**stops 17** and **18**). Within 0.3 mi (0.5km) of the basal contact, fine-grained troctolite coarsens to medium-grained. The troctolite units consist of 65-70 percent plagioclase and 10-15 percent olivine. Relative amounts of poikilitic augite and iron-titanium oxides vary locally. Orthopyroxene mantles olivine and occurs in symplectic intergrowth with plagioclase. Biotite is locally present in association with iron-titanium oxides. Modal layering is well developed and generally concordant with unit boundaries that dip gently to the south—typically more steeply dipping than the subjacent Animikie Group strata. The basal part commonly contains chalcopyrite, pyrrhotite, and minor pentlandite interstitial to plagioclase and olivine. The sulfide concentrations are subeconomic, but locally form mappable zones (**stop 18**).

FIELD TRIP STOP DESCRIPTIONS

NOTES:

1) *Many of these outcrops are scientifically important—the subjects of on-going research, and all are on private or National Forest lands. For these reasons, we ask that you refrain from hammering and sampling without first checking with the leader.*
2) *This group is unlikely to visit all of the stops described below during this trip. A number of stop descriptions are included in this guide to provide context and for future visits to the region.*
3) *The stops are presented in general geochronologic order from oldest to youngest.*
4) *At the time of this writing, many of these stops had not been visited for several years. Regrowth after forest fires and other factors may preclude visiting some stops, and alternative locations may be substituted.*
5) *Some descriptions below show locations on images extracted from published 7.5-minute U.S.G.S. quadrangles.*
6) *All locations are given in NAD 83, Zone 15N UTM coordinates.*

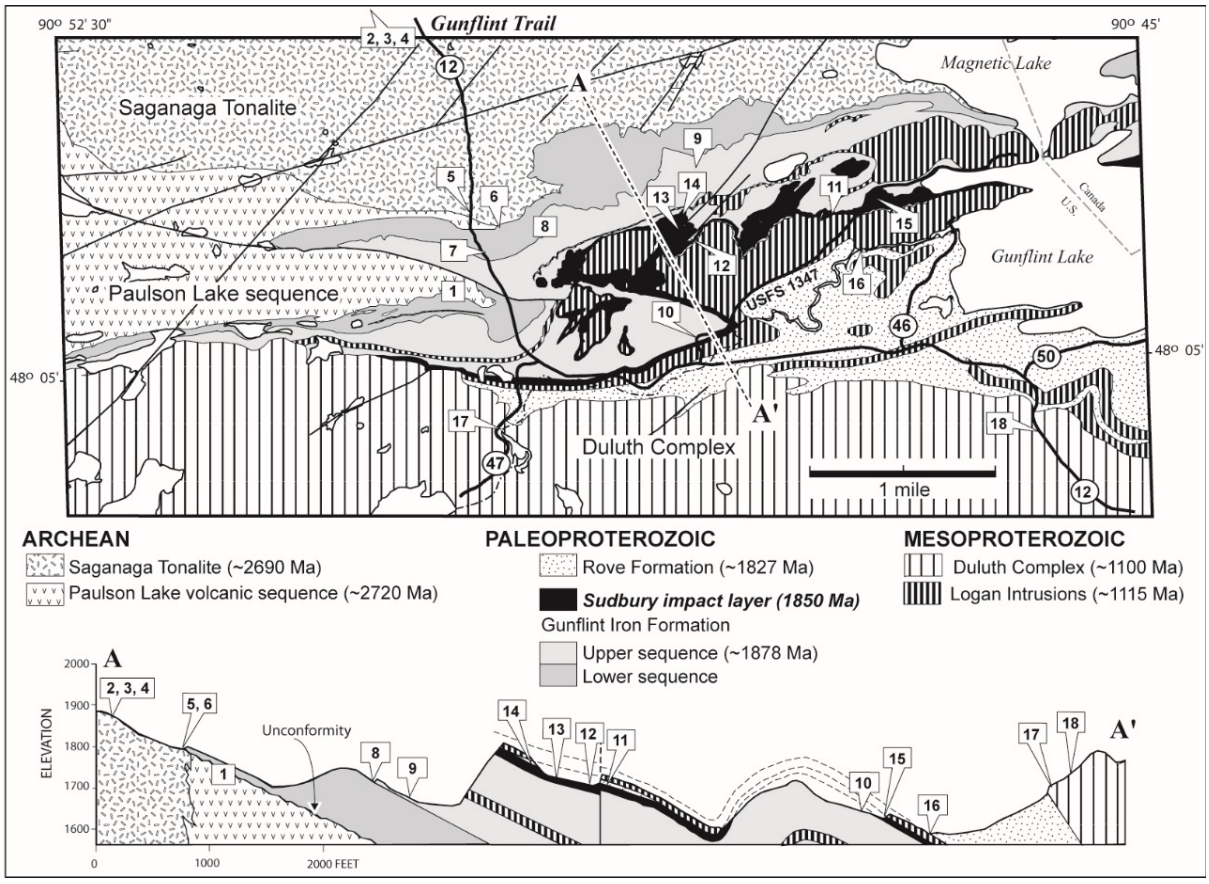


Figure 5. Geologic map and schematic cross-section (A-A') showing the *approximate* geographic and stratigraphic positions of field trip stops (geology modified from Jirsa, 2011). Note that the horizontal distances on the cross section are much greater than those on the map, and the section is vertically exaggerated by 3.5 X, resulting in apparent dips of contacts steeper and units thicker than true.

STOP 1—*Neoarchean pillowed basalt and basal Gunflint Iron Formation*
Location: UTM locations of several substops along the Kekekabic Hiking Trail west of Hwy 12—Gunflint Trail (**Fig. 5**) are given below:
1a = Outcrops along the irregular unconformable contact between metabasalt and iron-formation in the vicinity of UTM 661970E/5328460N
1b = Outcrops near the junction of Kekekabic and Lookout trails at UTM 661230E/5328410N
1c= "Paulson Mine" at UTM 660980E/5328320N; about 900 feet west of junction of Kekekabic and Lookout trails

General description: Follow the Kekekabic Hiking Trail from the parking lot, westward to several stops listed above, and perhaps others enroute. The Kekekabic trail parallels the base of the Gunflint Iron Formation where it rests unconformably on Neoarchean metabasalt. Several small outliers of the lower sequence (lower cherty member) of the iron-formation containing iron-silicates and magnetite can be found along the route, implying that this gently south-dipping surface is very near the unconformable contact between Neoarchean and Paleoproterozoic rocks. Exposures of metabasalt vary from massive to pillowed, autobrecciated, and locally variolitic. Analyses of a fine-grained hypabyssal intrusion associated with the metabasalt indicate that it has a komatiitic composition (Jirsa and Weiblen, 2007). Intrusions of this composition are also found in the Newton Lake Formation, some 30 miles to the southwest, and high-Mg tholeiitic basalt flows and pyroxenitic to peridotitic sills were described by Vervoort (1987) in the JAP Lake area two miles along strike to the west. Pillow shapes indicate moderate flattening by regional D_2 deformation. Bedding trends to the east-northeast, and is steeply southward dipping and facing.

The steep north-facing slope immediately south of the trail contains exposures of the lower sequence (lower slaty member). The iron-formation has been strongly metamorphosed in this area and now consists of various assemblages of quartz-grunerite-fayalite-magnetite and quartz-cummingtonite-grunerite-pyroxene-magnetite. Several test pits and shafts can be seen along more than a mile of the trail, including one that is fenced and labeled "Paulson Mine 1893" (**stop 1c)**. In reality, this and other scattered shafts collectively made up the Paulson "mines." They are developed in the lower sequence of iron-formation, and waste piles contain abundant pyrrhotite, other sulfide minerals, and magnetite. Despite construction of a rail line to Port Arthur (now Thunder Bay), only one train car of "ore" was ever shipped. Presumably the low iron and large sulfide content precluded further work, though the 1893 "financial panic" may also have played a role.

STOP 2—*Felsic phase of the Neoarchean Saganaga Tonalite cut by a small mafic dike.*
Location: UTM: 656333E/5335730N; End of the Trail Campground; Campsite #18



Description: Most of the outcrops in this area consist of gray, massive to trachytoid-foliated, medium to coarse-grained tonalite, having plagioclase in much greater abundance than microcline. Large quartz phenocrysts, or eyes, as much as 1 cm in diameter are characteristic of this phase, which is typical of 90% of the batholith (**Fig. 6**). Quartz eyes are polycrystalline aggregates, in which each crystal has a different optical orientation. Quartz also occurs as an interstitial mineral to subhedral plagioclase (An20-28). Small amounts of microcline occur as antiperthitic exsolution in plagioclase, as rims on plagioclase, and as small interstitial grains. Hornblende is the dominant ferromagnesian mineral, together with minor amounts of augite, biotite, epidote, and chlorite.



Figure 6. Texture typical of the Saganaga Tonalite, including lineated quartz "eyes" (medium gray, trachytoid-aligned).

The small dike of aphanitic mafic rock in this exposure has not been analyzed, but is inferred to be related to larger north-trending diabasic and lamprophyric dikes that form prominent north-trending anomalies on aeromagnetic maps.

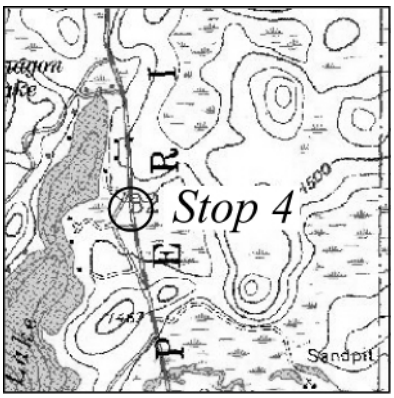
The pronounced foliation in the Saganaga Tonalite was inferred by Grout (1933) as a primary flow fabric (trachytoid). The tonalite is inferred to have been emplaced into Archean metavolcanic rocks shortly after early (D_1) deformation, based a U-Pb date of 2689±1 Ma in Canadian exposures (Corfu and Stott, 1998), and 2690.83±0.26 Ma (Driese and others, 2011) just west of the Gunflint Trail. As such, it experienced major regional metamorphism and transpression associated with D_2 deformation at ca. 2680 Ma. As with many large plutons in such terranes, the debate remains unresolved about whether the fabrics are wholly magmatic, wholly tectonic, or some hybrid of the two.

STOP 3—*Neoarchean Saganaga Tonalite with rounded dioritic to granodioritic inclusions*
Location: UTM: 656219E/5336079N; Campsite #13.



Description: Equigranular tonalite with characteristic quartz eyes, containing a wide variety of inclusions. The term "inclusion" has a tortured usage—we prefer to use the term to apply to material that has a contrasting composition or appearance from its host, regardless of origin, size, shape, degree of assimilation, or extent of equilibration with the enclosing host magma. Inclusions may represent blocks of county rock (xenoliths) incorporated into the Saganaga Tonalite, or cognate phases of the intrusion (autoliths). Note that each inclusion contains the same mineralogic components (hornblende, plagioclase, quartz), but the components occur in varied proportions. Although these inclusions have not been studied in detail, field work in the region has identified multiple phases of the intrusion that are compositionally identical with the inclusions, and they are therefore considered autholiths.

STOP 4—*Granodioritic phase of Neoarchean Saganaga Tonalite with inclusions; cut by diabase dike*
Location: UTM 658575E/5335837N; Roadcuts on both sides of Gunflint Trail (**Fig. 2**)

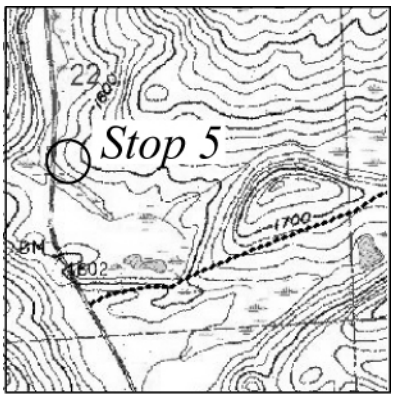


Description: Exposures on the west side of the road consist of pinkish to gray hornblende granodiorite to granite inferred to be a border phase of the Saganaga Tonalite and containing inclusions that are both more felsic and more mafic than the enclosing rock (**Fig. 7**). For example, the large angular block shown in the photo consists of quartz-eye-bearing tonalite, much like rock that is typical of the main phase of the intrusion. Foliation is poorly developed and likely magmatic in origin. This exposure demonstrates that the Saganaga is a composite intrusion that, despite its apparent homogeneity, consists of quite varied magmatic phases, particularly near its border. Tonalite on the east side of the road is cut by a fine-grained diabasic dike several meters in width. Although this location lies some distance east of the prominent north-trending aeromagnetic trends associated with dikes that are described in the text above, the dikes presumably are related.



Figure 7. Granodioritic phase of Saganaga Tonalite, containing many and varied inclusions. Large, lighter colored block in center of exposure is inferred to be an autolith of quartz-eye-bearing tonalite similar to the major phase of the batholith.

STOP 5—*Border phase Neoarchean Saganaga Tonalite with flattened inclusions and well-developed foliation in contact zone with Neoarchean metabasalt*
Location: UTM 661834E/5329257N; Roadcut on east side of Gunflint Trail (**Fig. 5)**



Description: This location exposes the border phase of the Saganaga batholith, characterized by a granodioritic composition, general lack of quartz eyes, and an abundance of dioritic inclusions consisting of varied proportions of hornblende, pyroxene, biotite, plagioclase, and minor quartz (**Fig. 8**). The irregular ovoid and discoid shape of inclusions is oriented subparallel to well developed, steeply dipping and east-trending foliation. Hornblende crystals and aggregates define a prominent lineation plunging shallowly to the east. Petrology indicates that much of this fabric appears magmatic, yet foliation may be a hybrid of approximately coaxial magmatic flow and regional tectonic deformation (D_2). This is typical of the border zone of the intrusion against Archean metabasaltic country rocks, which presumably lie in the low ground just to the south.

A preliminary comparative geochemical study, summarized in Jirsa and Weiblen (2007), indicates that the mafic inclusions are not partially assimilated, recrystallized, and tectonically deformed country rock volcanic xenoliths as implied by some earlier workers. They have the common chemical characteristics of the sanukitoid suite of Archean granitoid rocks. Thus, we infer that the inclusions studied are autoliths derived from a separate, primitive sanukitoid-magma.



Figure 8. Granodioritic border phase of Saganaga Tonalite containing mafic inclusions.

STOP 6—*Contact zone of Neoarchean Saganaga Tonalite and metabasalt; unconformably overlain by Paleoproterozoic Kakabeka conglomerate and lower sequence of Gunflint Iron Formation*

Location: 3 exposures along bush path off Gunflint Trail [individual UTM coordinates given below] (**Fig. 5**)



Description:

Stop 6a [UTM 661925E/5329065N] Archean metavolcanic rocks containing abundant granitic sheets and dikes, presumably related to border phases of Saganaga Tonalite (**Fig. 9**). The boundary between tonalite and metabasalt has been mapped in many places as a fault (Weiblen and others, 1971). These exposures do not preclude that possibility, but they imply that passive emplacement of the intrusion has also occurred, at least locally.



Figure 9. Outcrop of border zone of Saganaga Tonalite. Dark gray material probably represents various phases of the intrusion; lighter gray, wedge-shaped area in the foreground is inferred to be metavolcanic country rock.

Stop 6b [UTM 661965E/5329062N] Conglomerate developed at the gently southward dipping unconformity between Neoarchean intrusive and metavolcanic rocks and the overlying basal part of the Paleoproterozoic Animikie Group. The unit, regionally known as the Kakabeka Conglomerate, is present only locally on the western end of the Gunflint. In most places, the Lower cherty member of iron-formation lies directly on eroded Archean surfaces. This small outcrop is one of the few places where the conglomerate is exposed and accessible along the contact. The conglomerate is greenish gray, poorly bedded, and contains subangular to subrounded fragments of Saganaga Tonalite and related granitoid rocks, metabasalt, and quartz, in a granular siliceous matrix.

Stop 6c [UTM 661965E/5329037N] Walking southward from the basal conglomerate is a low "step-up" onto southward dipping strata of the Lower cherty member of Gunflint Iron Formation.



Figure 10. Outcrop photograph of Kakabeka conglomerate lying unconformably on vertically foliated and eroded Archean Saganaga Tonalite (uniform light gray area on right side of photo). Note diversity of fragment types, including Archean metabasalt (dark) and tonalite (light), quartz pebbles (light, subrounded), and Paleoproterozoic diabase (dark gray).

STOP 7—*Lower Sequence of Gunflint Iron Formation.*
Location: UTM 661844E/5328896N; Road cut on Gunflint Trail (Highway 12) just north of parking lot for west end of Magnetic Rock Hiking Trail.

Description: Gently southward-dipping, thinly interbedded granular and argillaceous iron-formation typical of the lower sequence. In earlier parlance, this stratigraphic position is the lower part of the Upper Cherty member of the Gunflint Iron Formation (**Fig. 3**).

STOP 8—***Stromatolitic grainstone at the diastem separating lower and upper sequences of Gunflint Iron Formation.***
Location: 3 exposures—specific coordinates given below; all adjacent to Magnetic Rock Hiking Trail (**Fig. 5**).
CAUTION and ADVICE: This is a fairly long hike, approximately 1 mile round-trip; please be prepared with water and other field needs. Although this is not in the BWCAW, it does lie within Superior National Forest and is frequented by hikers. For this reason, and to preserve scientific value, please be respectful in matters of hammering and sampling.

Description:
Stop 8a [UTM 662034E/5328885N] Thin-bedded, fine-grained, chert-amphibole-magnetite-bearing strata assigned to the upper part of the lower sequence of Gunflint Iron Formation ("Lower slaty member"). Beds strike ENE and dip generally less than 8 degrees southward.
Stop 8b [UTM 662401E/5329093N] Stromatolites lie within and just above a major regression-transgression boundary (diastem) that is marked by intraformational conglomerate containing fragments of the underlying granular chert that appear to have been cohesive (though likely not lithified) at the time of incorporation, and in-situ and dislodged stromatolites. Irregular domal and laminar stromatolite forms are present. Note the presence of granules, intraclasts, and oncoliths—the latter consist of intraclasts coated with what likely was biogenic material, now composed largely of silica.
Stop 8c [UTM 662583E/5329257N] Crest of ridge exposes the same boundary described above, here with abundant 3-dimensional views of stromatolites, intraformational conglomerate, and stromatolite "hash," all in a peloidal to ooidal, siliceous grainstone matrix. Given the apparent mineralogic replacement and moderate metamorphic grade, little of the original carbon-based material is likely present. Despite this, examples of nearly all morphological forms of stromatolites can be found, including columnar-digitate, domal, and laminar (**Fig. 11**).

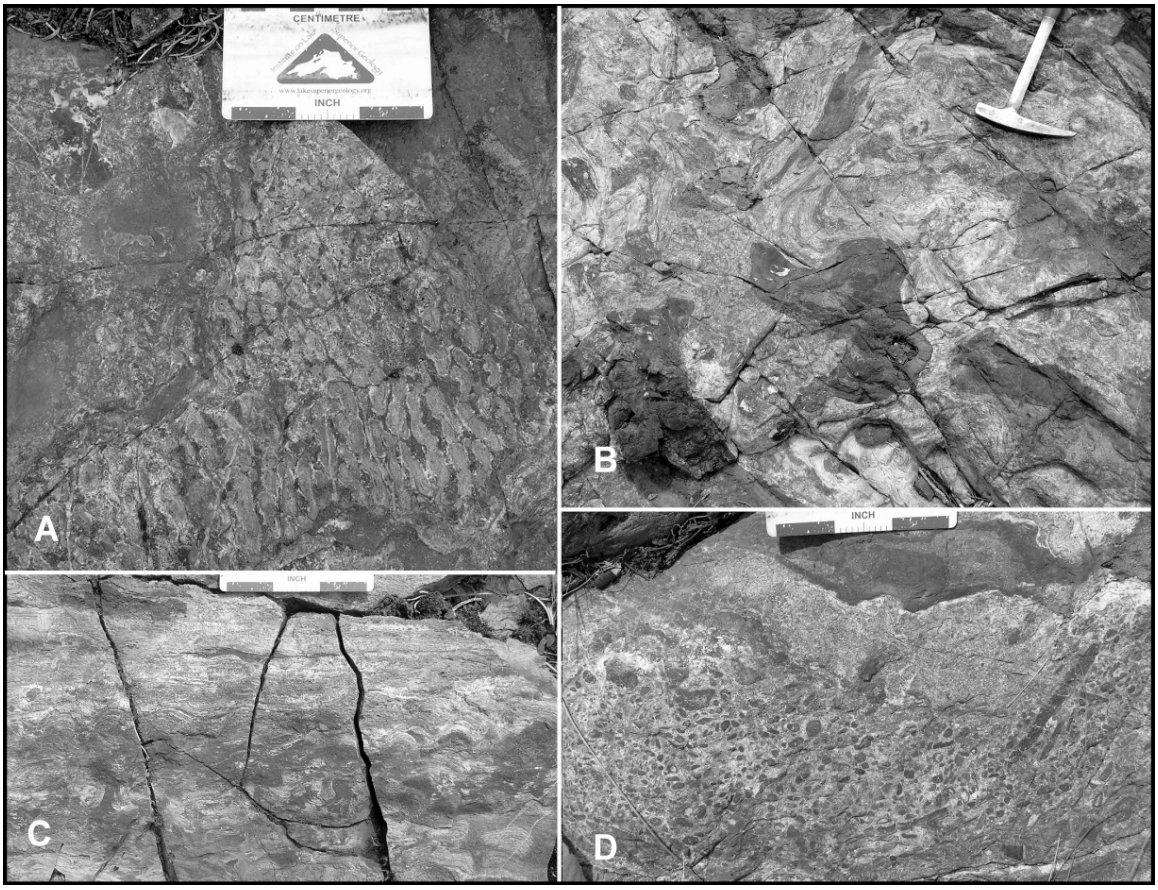


Figure 11. Cherty, stromatolitic Gunflint Iron Formation. **A**=Oblique surface of small columnar-digital stromatolites; B=Horizontal surface of irregular domal or laminar stromatolites; C=Vertical section of laminar stromatolites; **D**="Stromatolite hash."

STOP 9—*The "Magnetic Rock"*
Location: UTM 0663740E/5329670N; approximately 1 mile walk east of **stop 8** on the Magnetic Rock Hiking Trail (**Fig. 5**)



Description: Although most of the trail has magnetic iron-formation underfoot, the trail's actual namesake lies about a mile walk to the east. The "Magnetic Rock" is a slab of iron-formation in which bedding is essentially vertical and standing nearly 30 feet above the surrounding land surface (**Fig. 12**). The appearance of this tombstone-shaped block raises the question of how glaciers could have up-ended it, but left the delicately balanced slab intact during ablation. My answer invokes glacial rotation of a "cube" of rock, followed by spalling along bedding planes during repeated cycles of freeze/thaw (frost-heaving).

Figure 12. Slab of iron-formation. (Blue-handled hammer against lower 1/3rd of the rock is 40 cm long).

STOP 10—*Upper-most, largely argillaceous, Gunflint Iron Formation*
Location: UTM 663754E/5328212N; Gravel pit north of Gunflint Trail on U.S. Forest Service road #1347 (**Fig. 5**).

Description: This dip-slope exposure consists of interbedded granular (cherty) and laminated (slaty) strata of the uppermost Gunflint Iron Formation. The slope defines the southern limb of a large, shallowly east-plunging anticline. The gentle dip of this limb illustrates the observation that open folding and moderate-relief topography are responsible for the complex map pattern. Note that large ridge visible to the south represents the basal Mesoproterozoic Duluth Complex.

The bedding surface is marked by what have been referred to in earlier literature as "syneresis cracks". The cracks, now filled with quartz, occur both concentrically and radially around a central, apparently raised core within a single granular layer of siliceous iron-formation **(Fig. 13**). Syneresis cracks are defined generally as shrinkage cracks formed by dewatering in a gel or colloidal suspension. They differ from septarian cracks that may develop in a similar way, in that the latter typically occur in concretions. Surprisingly diverse interpretations can be found in the literature about syneresis cracks (summarized in Pratt, 2001). There is, however, general agreement that they represent localized tensional failure during sediment dewatering. The explanation for localized semi-brittle response to what likely were formation-wide stresses—caused by compaction or vibration due to syn-sedimentary earthquakes—is more contentious. It has been ascribed variously to the localization of cements, locally increased pore pressure, or zones of granular sediment made coherent by "microbial glue." It is interesting to note that syneresis structures are more prevalent in Precambrian and Cambrian rocks than younger ones. This may be due in part to more uniform organic bonding of clays in younger strata, which reduced the occurrence of stress-localization.



Figure 13. Polygonal quartz veining on eroded bedding surface of thinly bedded Gunflint Iron Formation.

Recent mapping by the author (Jirsa, 2011) indicates that these quartz-filled cracks occur only in some granular siliceous layers that lie near the stratigraphic top of the iron-formation. This stratigraphic position, and their enigmatic structural attributes, may indicate an origin by impact-induced seismic wave passage through cohesive, semi-rigid chert during the Sudbury meteorite impact event.

STOP 11—*Paleoproterozoic ejecta and breccia from the Sudbury meteorite impact, intruded by sill and dikes of the Mesoproterozoic Logan Intrusions.*
Location: UTM 664785E/5329200N

Description: This traverse provides a cross-section through diabase of the Logan Intrusions and underlying deposits of iron-formation, breccia, and ejecta. The diabase is medium- to coarse-grained in its core to the south, and grades to finer grained and more porphyritic near its base to the north. The northernmost outcrops lie along a steep cliff that exposes the upper Gunflint Iron Formation overlain by a

thick sequence of iron-formation breccia that represents the ejecta-absent facies (**Fig. 14.A**) of the Sudbury Impact Layer. This is overlain by irregular lenses of bedded lapillistone, mesobreccia (**Fig. 14.B**), and reworked breccia containing rounded fragments of iron-formation in a matrix composed largely of accretionary lapilli that collectively represent the ejecta-bearing facies. The precise stratigraphic position of the latter two rock types is not entirely clear, though the strata containing accretionary lapilli (true ejecta) appear to lie near the top of the deposit.

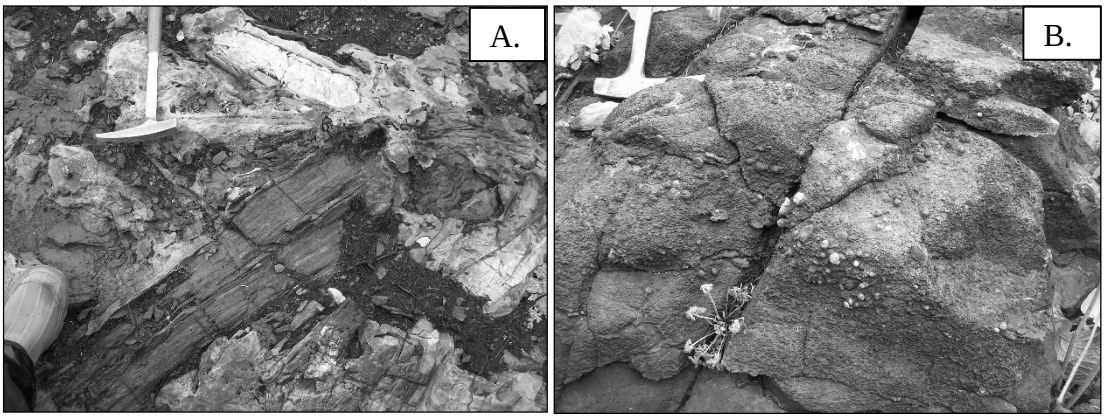


Figure 14. A. Large-fragment breccia (ejecta-absent); **B**. Bedded lapillistone and mesobreccia (ejecta-bearing).

STOP 12—S*udbury Impact Layer—folded iron-formation overlain by ejecta.*
Location: UTM 663700E/5328967N Off Magnetic Rock Hiking Trail

Description: Folded siliceous and argillaceous iron-formation overlain by a thin, discontinuous layer of mesobreccia containing scant accretionary lapilli. Note the structural detachment at the base of the outcrop that separates gently dipping, planar-bedded iron-formation layers from the overlying meter or so of folded strata. The chaotic fold style (**Fig. 15A**) indicates soft-sediment deformation prior to deposition of ejecta, which lends credence to the inference that iron-formation was not yet fully lithified at the time of impact.

The walk from here to **Stop 11** crosses several exposures of variably deformed iron-formation, all considered part of the ejecta-absent facies of SIL. These outcrops demonstrate the rheologic contrasts of substrate during deformation, and highlight the interpretation that at least some components of iron-formation were unlithified at the time of impact deformation (**Fig. 15B and 15C**).

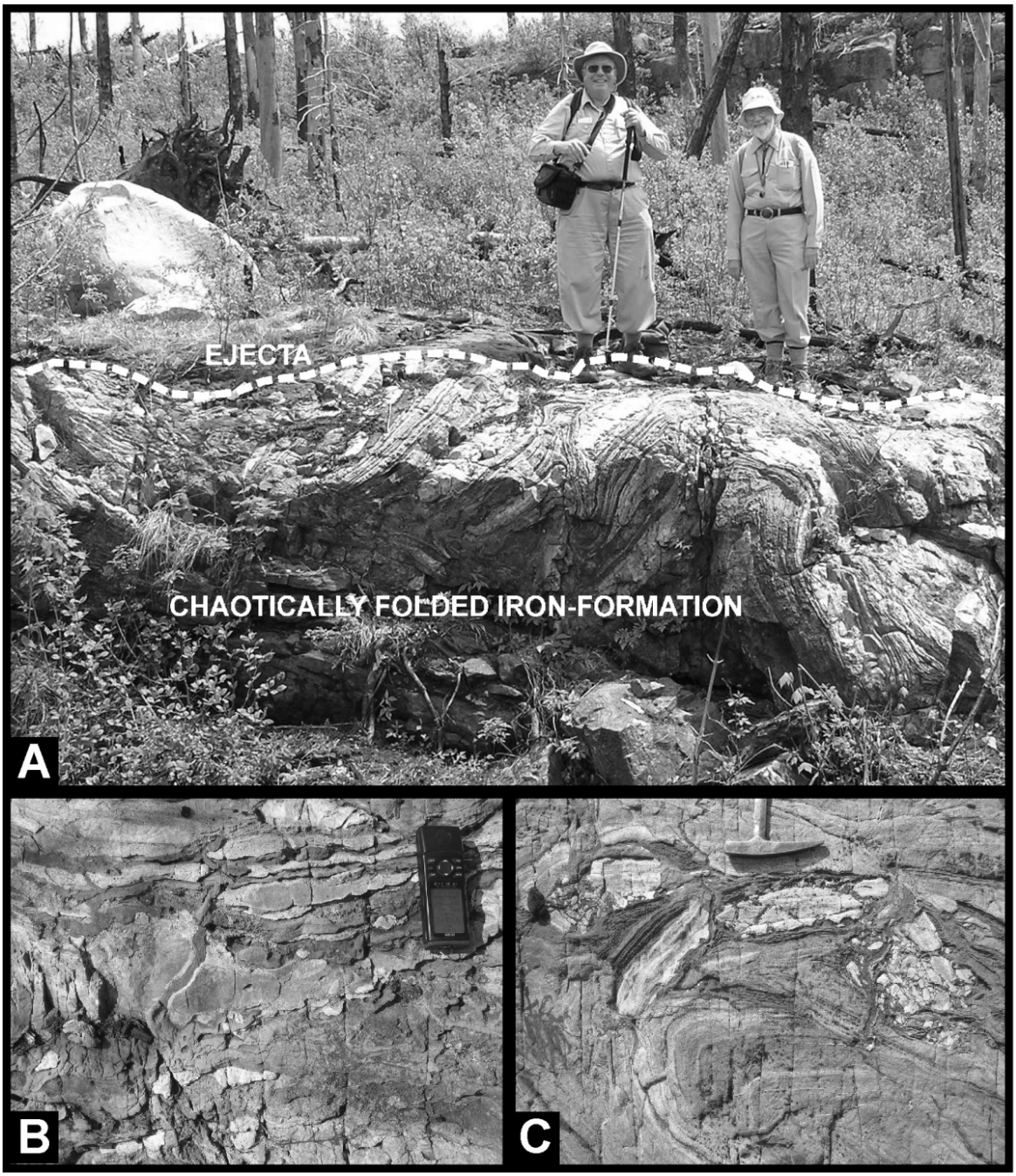


Figure 15. Outcrop photographs of soft-sediment deformation in the ejecta-absent facies of SIL, locally overlain by ejecta, and demonstrating that deformation occurred during and after silicification of mudstones, but prior to complete lithification. **A.** Folded siliceous (light-colored) and iron-silicate (darker) iron-formation overlain by thin skin of ejecta containing accretionary lapilli (Bill Addison and Bevan French for scale). **B.** Irregularly layered siliceous and iron-silicate mudstone cut by a mudstone "clastic" dike (darkest narrow feature running up-down in center of photo). **C.** Folded and brecciated iron-formation, in which the siliceous layer (light gray) is attenuated and shattered in contrast with the enclosing iron-silicate mudstone that is ductily folded.

STOP 13—*Sudbury Impact Layer—deformed substrate, mesobreccia, gritstone and lapillistone.*
Location: UTM 663535E/5329100N Off Magnetic Rock Hiking Trail

Description: This small outcrop provides a complete cross section of the SIL, and some unique sedimentalogical features not seen elsewhere**.** The stratigraphic sequence is shown in **Fig. 16A**. Of particular importance are the scoured (channelized) appearance at the base of lapillistone, and the presence of larger fragments of gritstone in lapillistone (**Fig. 16B**). Both indicate moderately high energy delivery of detritus—presumably by the passing ejecta plume or ground surge.

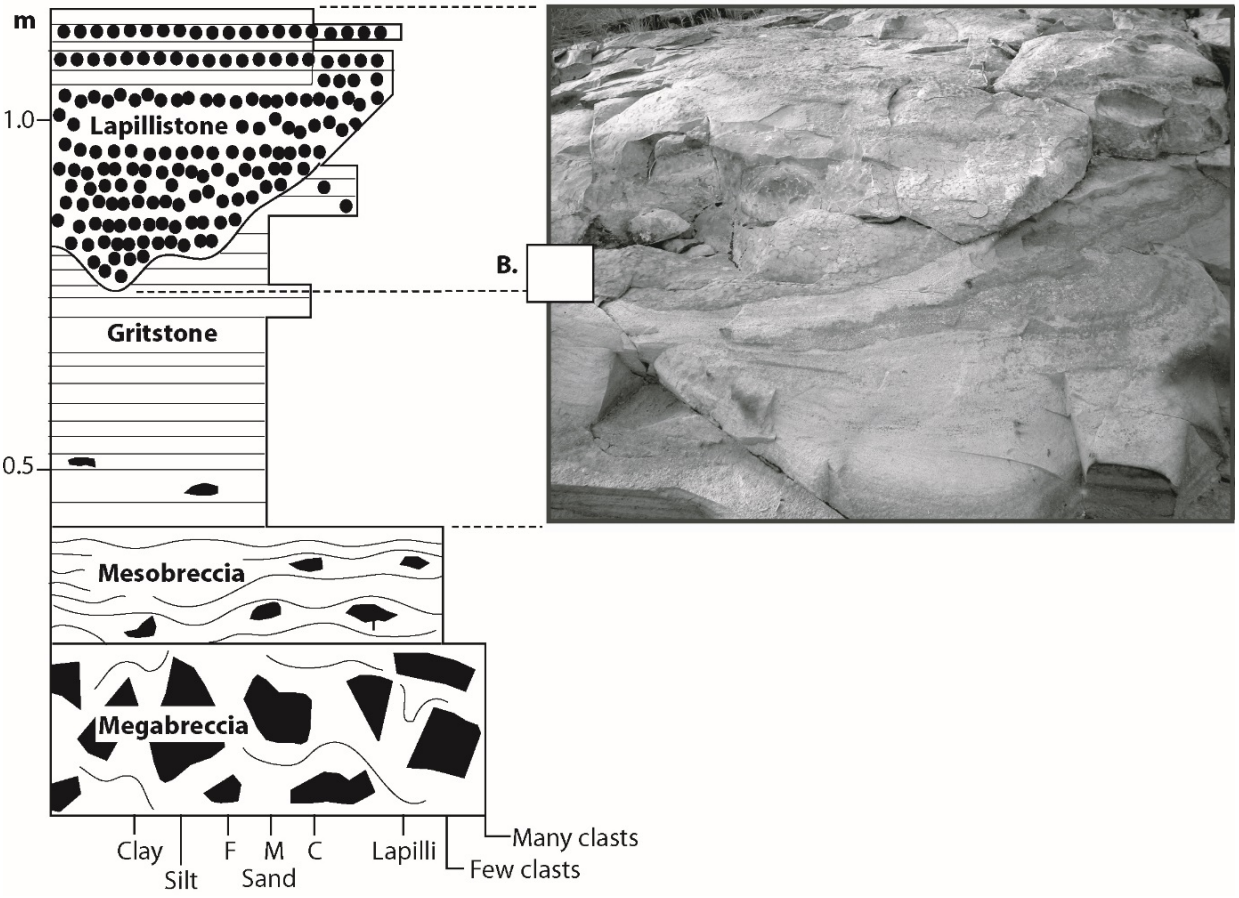


Figure 16A. Photograph and graphic sedimentological analysis of **stop 13**. Black angular polygons represent fragments of iron-formation; black circles represent lapilli. White box shows approximate location of photo **Fig. 16B**.

In detail, the basal part of this deposit consists of disorganized-bedded boulder "megabreccia", with clasts composed of rock types characteristic of the underlying Gunflint Iron Formation. The megabreccia is overlain by a decimeters-thick, matrix-supported, pebble "mesobreccia" and massive, pebbly sandstone—here termed gritstone due to its content of moderately sorted, but primarily angular grains. Scattered accretionary lapilli occur in this unit locally, implying that it may be a mixture of ejecta and locally derived detritus. The mesobreccia and gritstone are overlain by lapillistone, composed of tightly packed accretionary lapilli. These fill shallow scours in the top of the mesobreccia and gritstone, or deeper scours that remove strata all the way down to megabreccia locally. The bases of the scours are commonly overlain by a one-centimeter-thick wisp of coarse-grained gritstone, followed vertically by the accretionary lapilli. The scours give a paleocurrent direction of 260 degrees—the bearing from Sudbury



to Gunflint Lake is 280 degrees. At other locations, where individual smaller scours at the base of the lapillistone are not present, the basal, clast-supported lapillistone bed drapes shallow erosive scours. The lowermost accretionary lapillistone is massive-textured, as are overlying accretionary lapilli-rich beds, except where rare, small-scale, low-angle cross-stratification dipping towards 060 degrees is visible. The diameter of accretionary lapilli in the bed at the base of the lapilli-rich interval average 0.7 to 0.8 cm, and those higher in the section and interbedded with sandstone range from 0.2 to 0.4 cm. Gritstone beds become more dominant in the upper few decimeters. Here they are medium- to fine-grained with stringers and patches of small accretionary lapilli. Some beds are massive with abundant, isolated lapilli. Parallel lamination to undulating parallel lamination is common in the non-massive beds. Approximately 10 cm of thinly laminated siltstone caps the impact deposit.

Figure 16B. Close-up view of lapillistone containing entrained fragment of layered gritstone.

STOP 14—*Sudbury impact layer—deformed Gunflint Iron Formation overlain by thin ejecta layer that includes small spherules.*
Location: UTM 663628E/5329186N Off Magnetic Rock Hiking Trail

Description: This cliff and ridge-top exposure includes a 7m-thick breccia, abruptly overlain by mesobreccia (**Fig. 17A**), and capped by strata composed of small (2-5mm) accretionary pellets and slightly larger, concentrically zoned lapilli (**Fig. 17B**). Some of these small particles may be relict glass spherules; however, metamorphism precludes definitive identification.

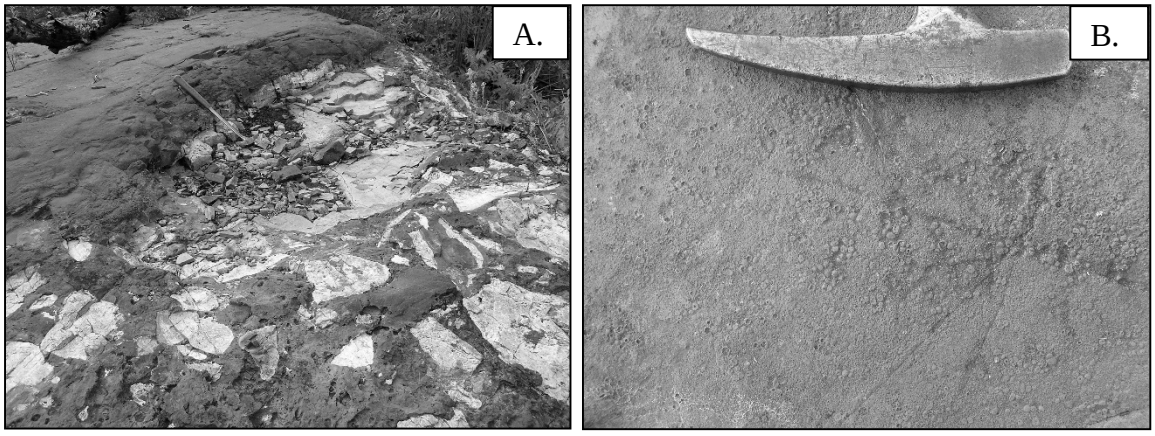


Figure 17. **A.** Megabreccia sharply overlain by mesobreccia and other ejecta. **B.** Layers composed of accretionary pellets, small lapilli, and inferred relict spherules.

STOP 15—*Paleoproterozoic Sudbury impact layer, basal Rove Formation, and Mesoproterozoic Logan Intrusion.*
Location: UTM 665200E/5329300N

Description: This outcrop affords a great number and variety of views of the ejecta and breccia (**Fig. 18**) because the exposed surface is nearly parallel with strike and dip of formations. The stratigraphic sequence is similar to that at **Stop 11**; however, this site lies along the top of the deposit, showing the relationship between ejecta and breccia more clearly. Just to the south is the eastern extension of the Logan sill traversed at Stop 11. In the intervening 0.25 mi., the basal contact of the sill cross-cut stratigraphic units to here overlie about 10 feet of slate and graywacke inferred to be the basal section of the Rove Formation.



Figure 18. Breccia irregularly overlain by a "skin" of lapillistone.

STOP 16—*Mesoproterozoic Logan sill and Paleoproterozoic slate of the Rove Formation at Cross River*
Location: UTM 0665120E/5328890N

Description: Outcrops on the north shore of Cross River and in it lie at the top of the same Logan sill that capped basal Rove Formation at **stop 15**. The cliff on the south shore exposes thinly bedded graywacke and mudstone of the Rove. Crossing the river may not be possible at this time.

STOP 17—*Mesoproterozoic Tuscarora intrusion of Duluth Complex—atypical border phase*
Location: UTM 662074E/5327457N; Roadcut on Cross Lake road (CR#47) south of Hwy 12

Description: A confusing exposure of the lower units of the Tuscarora intrusion. The outcrop consists of intergranular to ophitic gabbro and augite troctolite, with pods and veinlets of coarse mafic pegmatite and shear bands containing sulfide mineralization. Spheroidal weathering produced "core stones" locally.

STOP 18—*Mesoproterozoic Tuscarora intrusion of Duluth Complex*
Location: UTM 666638E/5327433N; roadcut on Gunflint Trail east of CR#50. (**Fig. 5**)

Description: Just south of the parking pull-off is the rather poorly exposed intrusive contact between Paleoproterozoic Rove Formation and the Mesoproterozoic Tuscorara Intrusion (**Fig. 5** explanation; Morey and others, 1981). The basal unit is a typical example of Cu-sulfide mineralized augite troctolite that is found at the base of the Duluth Complex here and in the Hoyt Lakes-Kawishiwi area to the southwest. It contains disseminated pyrite, pyrrhotite, and chalcopyrite. In the 1970's, International Nickel Company (INCO) drilled 7 holes in the basal Duluth Complex (Tuscarora and western Poplar Lake intrusions) to evaluate potential for Cu-Ni mining. All of these holes lie along the basal part of the intrusion within a few miles east and west of this stop. The archived drill cores were studied by Mogessie (1976) and Mogessie and others (1976).

REFERENCES

Addison, W.D., Brumpton, G.R., Davis, D.W., Fralick, Philip W., and Kissin, S.A., 2010, Debrisites from the Sudbury impact event in Ontario, north of Lake Superior, and a new age constraint: Are they base-surge deposits or tsunami deposits? Geol. Soc. Am., Special Paper 465.

Addison, W.D., Brumpton, G.R., Vallini, D.A., McNaughton, N. J., Davis, D.W., Kissin, S.A., Fralick, P.W., and Hammond, A.L., 2005, Discovery of distal ejecta from the 1850 Ma Sudbury impact event: Geology: **33**:193-196.

Boerboom, T.J., and Zartman, R.E., 1993, Geology, geochemistry, and geochronology of the central Giants Range batholith, northeastern Minnesota: Canadian Journal of Earth Sciences, **30**:2510-2522

Cannon, W.F., Schulz, K.J., Horton, J.W. Jr., Kring, D.A., 2010,The Sudbury impact layer in the Paleoproterozoic iron ranges of northern Michigan, USA: Geological Society of America Bulletin v. 122, p. 50-75.

Corfu, F., and Stott, G.M., 1998, Shebandowan greenstone belt, western Superior Province: U-Pb ages, tectonic implications, and correlations: Geological Society of America Bulletin **110**:1467-1484

Davis, D.W., 2008, Sub-million-year age resolution of Precambrian igneous events by thermal extraction-thermal ionization mass spectrometer Pb dating of zircon: Application to crystallization of the Sudbury impact melt sheet: Geology, v. 36, p. 383-396.

Driese, S.G., Jirsa, M.A., Ren, M., Sheldon, N.D., Brantley, S.L., Parker, D., and Schmitz, M., 2011, Neoarchean paleoweathering of tonalite and metabasalt: Implications for reconstructions of 2.69 Ga early terrestrial ecosystems and paleoatmospheric chemistry: Precambrian Research, v. 189, p. 1-17.

Floran, R.J., and Papike, J.J., 1978, Mineralogy and petrology of the Gunflint Iron Formation, Minnesota-Ontario: Journ. Petrology, **19**:215-288.

Fralick, P.W., Davis, D.W., and Kissin, S.A., 2002, The age of the Gunflint Formation, Ontario, Canada: single zircon U-Pb age determinations from reworked volcanic ask: Can. J. Earth Sci., 39:1085-1091.

Fralick, P., Grotzinger, J., and Edgar, L., 2012, Potential recognition of accretionary lapilli in distal impact deposits on Mars: A facies analog provided by the 1.85 Ga Sudbury impact deposit: Society for Sedimentary Geology Special Publication 102, p.211-227.

French, B.M., and Koeberl, Christian, 2010, The convincing identification of terrestrial meteorite impact structures: what works, what doesn't, and why: Earth Science Reviews, v. 98, p. 123-170.

Grout, F.F., 1933, Structural features of the Saganaga granite of Minnesota-Ontario: Report of XVI International Geological Congress, Washington, p. 255-270.

Gruner, J.W., 1941, Structural geology of the Knife Lake area of northeastern Minnesota: Geological Society of America Bulletin **52**:1577-1642.

Heaman, L.M., and Easton, R.M., 2005, Proterozoic history of the Lake Nipigon area, Ontario: Constraints from U-Pb zircon and baddeleyite dating: *in* Easton, M., and Hollings, P., eds., Institute on Lake Superior Geology Proceedings, 51st Annual Meeting, Nipigon, Ontario, Proceedings and Abstracts, v. 51, part 1, p. 24-25.

Hoaglund, S.A., Miller, J.D., Crowley, J.L., and Schmitz, M.D., 2010, U-Pb zircon geochronology of the Duluth Complex and related hypabyssal intrusions: Investigating the emplacement history of a large multiphase intrusive complex related to the 1.1 Ga Midcontinent rift: Institute on Lake Superior Geology Proceedings, v. 56, part 1, p.25-26.

Jirsa, M.A., 2011, Bedrock geology of the western Gunflint Trail area, northern Minnesota: Minnesota Geological Survey Miscellaneous Map M-191, scale 1:24,000.

Jirsa, M.A., 2016, Nine years of capstones: A summary of Precambrian Researcch Center field camp capstone mapping projects in the Newoarchean Knife Lake Group and associated rocks, central Boundary Waters Canoe Area Wilderness, Minnesota: (abs.) *in* Institute on Lake Superior Geology, Part 1—Abstracts and Program; abs., *this volume.*

Jirsa, M.A., Boerboom, T.J., and Radakovich, A.L., 2016, Neoarchean geology of the western Vermilion District: Field Trip 2 *in* Institute on Lake Superior Geology, Part 2—Field trip guidebook; *this volume*.

Jirsa, M.A., and Fralick, P.W., 2010, Field Trip 4: Geology of the Gunflint Iron Formation and Sudbury Impact Layer, in Field Guide to the Geology of Precambrian Iron Formations in the western Lake Superior region, Minnesota and Michigan: Precambrian Research Center Guidebook 10-01, p.77-92.

Jirsa, M.A., Fralick, P.W., Weiblen, P.W., and Anderson, J.L.B., 2011, Sudbury impact layer in the western Lake Superior region, *in* Miller, J.D., Hudak, G.J., Wittkop, C., and McLaughlin, P.I., eds., Archean to Anthropocene: Field Guides to the Geology of the Mid-Continent of North America: Geological Society of America Field Guide 24, p. 147–169.

Jirsa, M.A., and Miller, J.D., Jr., 2004, Bedrock geology of the Ely and Basswood Lake (U.S. portion) 30' x 60' quadrangles, northeastern Minnesota: Minnesota Geological Survey Miscellaneous Map Series M-148, scale 1:100,000.

Jirsa, M.A., Starns, E., and Schmitz, M.D., *in prep.*, Bedrock geology of the 2006 Cavity Lake fire area: Minnesota Geological Survey Miscellaneous Map M-193, scale 1:24,000. [in preparation; in the interim, refer to Open-File Report OF-08-05]

Jirsa, M.A., and Weiblen, P.W., 2007, Geology along the Gunflint Trail: Field Trip 6 in Miller, J.D., and Peterson, D.M., compilers; Institute on Lake Superior Geology, Part 2-Field Trip Guidebook; p. 143-168.

Jones, N.W., 1984, Petrology of some Logan sills, Cook County, Minnesota: Minnesota Geological Survey Report of Investigations **29**, 40p.

Kenkmann, T., and Schonian, F., 2006, Ries and Chicxulub: Impact craters on Earth provide insights for Martian ejecta blankets: Meteoritics and Planetary Science, v. 41, p. 1587-1603.

Krogh, T.E., Davis, T.W., and Corfu, F., 1984, Precise U-Pb zircon and baddeleyite ages for the Sudbury area: *in* The geology and ore deposits of the Sudbury Structure, E.G. Pye, A.J. Naldrett, and P.E. Giblin, eds, Ontario Geological Survey Special Volume 1, p. 431-446.

Lodge, R.W.D., Gibson, H.L., Stott, G.M., Hudak, G.J., and Jirsa, M.A., and Hamilton, M.A., 2013, New U-Pb geochronology from Timiskaming-type assemblages in the Shebandowan and Vermilion greenstone belts, Wawa subprovince, Superior Craton: Implications for the Neoarchean development of the southwestern Superior Province: Precambrian Research v. 235, p. 264-277.

MillerJ.D., Jr., and Severson, M.J., 2002, Geology of the Duluth Complex: in Miller, J.D., Jr., Green, J.C., Severson, J.J., Chandler, V.W., Hauck, S.A., Peterson, D.M., and Wahl, T.E., Geology and mineral potential of the Duluth Complex and related rocks of northeastern Minnesota: Minnesota Geological Survey Report of Investigations 58, p. 106-143.

Mogessie, A., 1976 Petrologic study of copper-nickel mineralization in the Tuscarora intrusion Duluth Complex, northeastern Minnesota: M.S. thesis, University of Minnesota, Twin Cities, 137p.

Mogessie, A., Stumpfl, E.F., and Weiblen, P.W., 1976, The role of fluids in the formation of platinum-group minerals, Duluth Complex, Minnesota: Mineralogic, textural, and chemical evidence: Econ. Geol. **86**:1506-1518.

Morey, G.B., and Nathan, H.D., 1978, Geologic map of the Gunflint Lake quadrangle, Cook County, Minnesota: Minnesota Geological Survey Misc. Map **M-42**, scale 1:24,000.

Morey, G.B., Weiblen, P.W., Papike, J.J., and Anderson, D.H., 1981, Geologic map of the Long Island Lake quadrangle, Cook County, Minnesota: Minnesota Geological Survey Misc. Map **M-46**, scale 1:24,000.

Mouginis-Mark, P.J., and Garbeil, H., 2007, Crater geometry and ejecta thickness of the Martian impact crater Tooting: Meteoritics and Planetary Science, v. 42, p. 1615-1625.

Osinski, G., 2006, Effect of volatiles and target lithology on the generation and emplacement of impact crater fill and ejecta deposits on Mars: Meteoritics and Planetary Science, v. 41, p. 1571-1586.

Peterson, D.P., Gallup, C., Jirsa, M.A., and Davis, D.W., 2001, Correlation of Archean assemblages across the U.S.-Canadian border: Phase I geochronology, (abstract): Institute on Lake Superior Geology Proceedings, 47th Annual Meeting, Madison, WI, 2001, Part 1, p.77-78.

Pratt, B.R., 2001, Syneresis cracks: subaqueous shrinkage in argillaceous sediments caused by earthquake-induced dewatering: Sedimentary Geol., **117**:1-10.

Pufahl, P.K., and Fralick, P.W., 2000, Depositional environments of the Paleoproterozoic Gunflint Formation: in Institute on Lake Superior Geology Proceedings, 46th Annual Meeting, Thunder Bay, Ontario, Part 2 Field Trip Guidebook, v. 51.

Pufahl, P.K., and Fralick, P.W., 2004, Depositional controls on Paleoproterozoic iron formation accumulation, Gogebic Range, Lake Superior region, USA: Sedimentology 51:791-808.

Pufahl, P.K., Hiatt, E.E., Stanley, C.R., Morrow, J.R., Nelson, G.J., and Edwards, C.T., 2007, Physical and chemical evidence of the 1850 Ma Sudbury impact event in the Baraga Group, Michigan: Geology **35**:827-830.

Vervoort, J.D., 1987, Petrology and geochemistry of the Archean of the JAP Lake area, northeastern Minnesota: M.S. Thesis, University of Minnesota-Duluth, 193 p.

Weiblen, P.W., Morey, G.B., and Mudrey, M.G., 1971, Guide to the Precambrian rocks of northwestern Cook County as exposed along the Gunflint Trail: *in* Davidson, D.M., Darby, D.G., Green, J.C., and Grant, J.A., eds., Technical Sessions, Abstracts and Field Guides, 17th Annual Institute on Lake Superior Geology, Annual meeting, Duluth, Minnesota, p.97-127.

Wolff, J.F., 1917, Recent geologic developments on the Mesabi Iron Range, Minnesota: American Institute of Mining and Metallurgical Engineers Transactions, v. 56 p. 229-257.

FIELD TRIP 8

Saturday, May 7, 2016

KEWEENAWAN GEOLOGY OF THE HOVLAND AREA

Terry Boerboom (Minnesota Geological Survey

John Green (University of Minnesota-Duluth Emeritus)

INTRODUCTION

This field trip will show several examples of the varied types of volcanic rocks within the Northeast sequence of the North Shore Volcanic Group (NSVG), beginning in the upper part of the lower, reversely-polarized sequence and working up the stratigraphic section into the upper, normally-polarized sequence (table 1). It also includes some stops in the Hovland sill, a layered intrusion that is subconformable to the host volcanic rocks, and some small hybrid intrusions. The trip will start NE of Hovland, and work back southwest toward and past Grand Marais (Figure 1). Although brief driving directions are given, the UTM coordinates should provide the most accurate locations. Some of the easternmost UTM coordinates (for stops 1-7) are given using NAD 83, Zone 16N, the rest (stops 7-21) use NAD 83 Zone 15N. It is likely that more stops are described here than can reasonably be covered in a single day. Stops missed during this excursion can be visited by individuals using the guide, with the caveat that some stops may require permission from land owners.

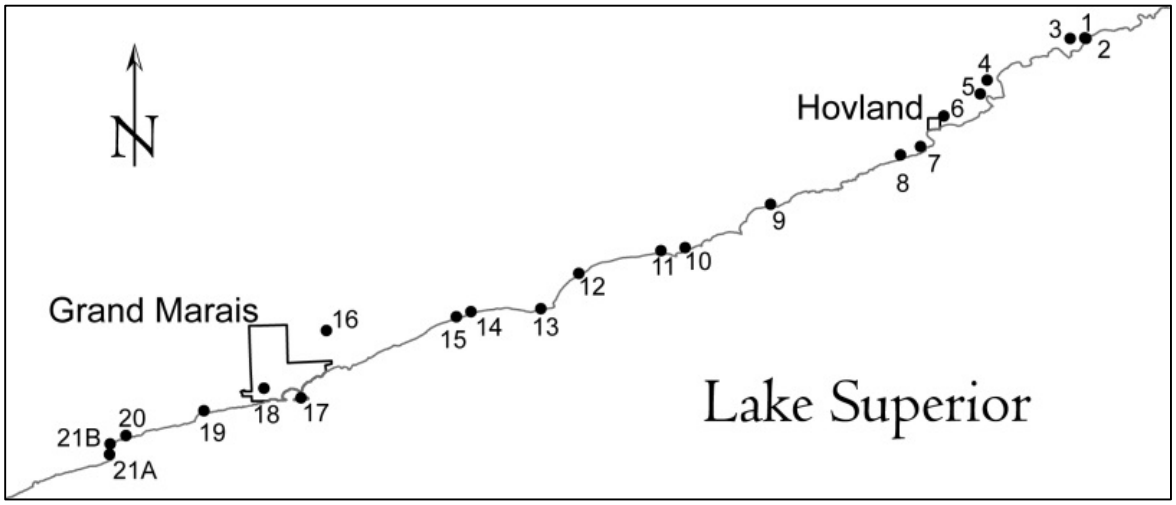


Figure 1. General stop locations with respect to the towns of Grand Marais and Hovland. Almost all the stops are along Highway 61, which parallels the shore**.**

The North Shore Volcanic Group (Figure 2), part of the Mesoproterozoic Midcontinent Rift System, is well described in a multitude of publications. Some of these include the Geological Society of America Special Paper 312 (Ojakangas, Dickas, and Green, editors, 1997); Minnesota Geological Survey Report of Investigations 58 (Green, 2002); and field trip number 7 in the Geological Society of America Field Guide 24 (Green and others, 2011). These are just a few examples, and within those publications numerous references to other publications on the topic are listed. Given the widespread background descriptions already available, the interested user is referred to those publications, and to the references therein.

A series of detailed geologic maps, based on 1:24,000-scale quadrangles, are available for almost all of the quadrangles that intersect the shoreline of Lake Superior. These maps as well as all Minnesota

Geological Survey publications are available for free download at the Minnesota Geological Survey website (***www.mngs.umn.edu***) under the 'search or browse' link. The geologic maps pertinent to the stops for this field trip are listed below.

Published Minnesota Geological Survey bedrock geology maps (all 1:24,000 scale) pertaining to this field trip:

Stops 1-10, MGS Map M-195, Marr Island and Hovland quadrangles (Boerboom and Green, 2013)

Stops 11-15, MGS Map M-190, Kadunce River (Boerboom and Green, 2011)

Stop 16, MGS Map M-189, Grand Marais (Boerboom and Green, 2010)

Stops 17-21, MGS Map M-179, Deer Yard Lake – Good Harbor Bay (Boerboom and Green, 2008)

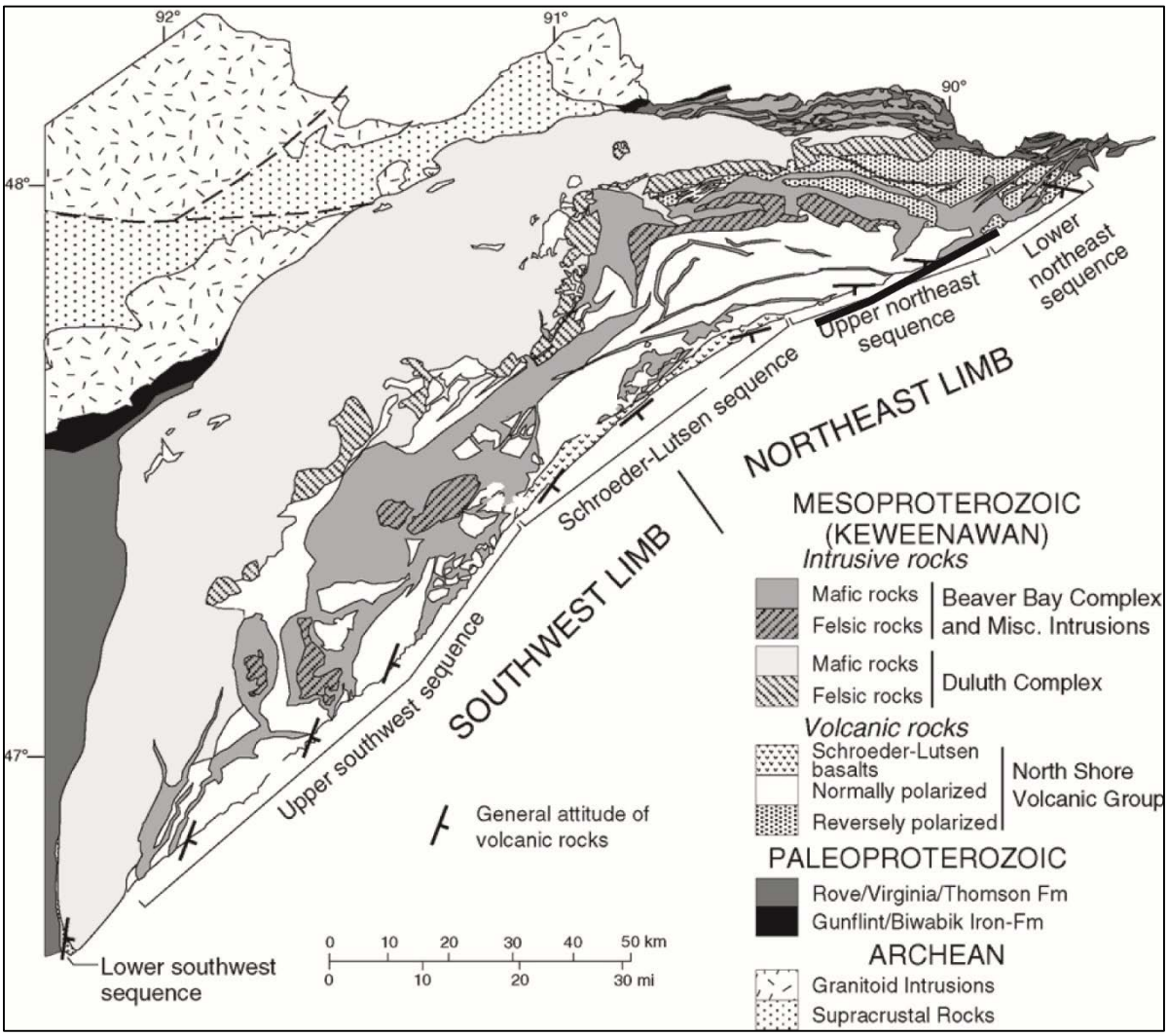


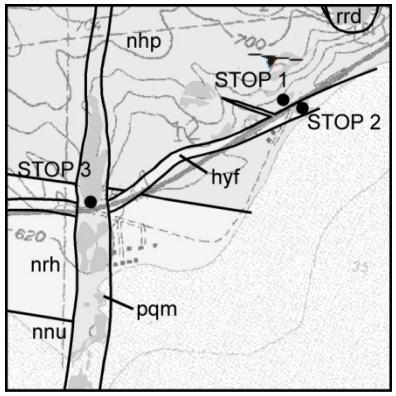
Figure 2. Generalized geology of the Mesoproterozoic rocks of northeastern Minnesota showing the major subdivisions of the North Shore Volcanic Group. The black bar denotes the general traverse of this field trip.

Table1. Generalized stratigraphy of the northeast limb of the North Shore Volcanic Group showing U/Pb ages (Davis and Green, 1997; Green and others, 2001; Boerboom and others, 2014). Positions of intrusions denote approximate stratigraphic level affected and not age of emplacement, except rocks of the Beaver Bay Complex affect multiple stratigraphic levels.

Thickness(m)		Lithostratigraphic units	Lithologic character	U/Pb ages
7359	**Total section**			
325	**Schroeder–Lutsen sequence (normal polarity)**			
		Lutsen basalts	olivine tholeiite; includes Indian Camp sandstone and thin conglomerate.	
	angular unconformity			
3998	**Upper northeast sequence (normal polarity)**			
	130	Terrace Point basalt (within Good Harbor Bay andesites) **(Stop 21)**	ophitic, olivine tholeiite basalt	
	100	Cut Face Creek sandstone **(Stop 21)**	red, laminated, ripple-marked sandstone	
	131	Good Harbor Bay andesites **(Stop 20)**	brown, porphyritic basaltic andesites	
	Beaver Bay Complex – Beaver River diabase, Leveaux ferrodiorite, etc. ***(Stops 2, 3, 5 & 6)***			
	122	Breakwater basalt **(Stop 17, 19)**	brown, columnar-jointed basalt flow	
	348	Grand Marais felsites **(Stop 18)**	pink to gray porphyritic rhyolite and felsite	1097.26±0.67
	335	Croftville basalts **(Stop 16)**	intergranular basalt and andesite flows, thick interflow sandstone	
	250	Devil Track rhyolite **(Stop 15)**	aphyric, intergranular rhyolite flow	
	70	Maple Hill rhyolite **(Stop 14)**	porphyritic rhyolite flow	
	274	Red Cliff basalts **(Stop 13)**	ophitic olivine tholeiite flows, some plagioclase-phyric	
	366	Kimball Creek felsites (rhyolite and icelandite) **(Stops 11 & 12)**	Porphyritic Kimball Creek rhyolite flow; Kadunce icelandite.	
	539	Marr Island lavas **(Stops 9 & 10)**	mixed basalt, tholeiitic andesite, and icelandite flows	
	198	Naniboujou basalts	intergranular basalt flows	
	235	Devil's Kettle rhyolite	porphyritic ash-flow tuff	1097.7±1.7
	900	Brule River lavas **(Stop 4)**	interbedded basalt and rhyolite flows	1100.2±1.9
	Brule Lake gabbro, Hovland sill, (of the Beaver Bay Complex) ***(Stops 7 & 8)***			1095.94±0.62 (Hovland sill)
3036	**Lower northeast sequence (reversed polarity)**			
	1932	Hovland lavas (**Stop 1**)	mostly plagioclase-phyric basalt flows, some rhyolite and andesite	1107.7±1.9
	67	Red Rock rhyolite	red/tan, porphyritic rhyolite	1107.9±1.8
	92	Deronda Bay andesite	tan/brown, porphyritic andesite	
	945	Grand Portage lavas	basalt lava flows, pillowed at base	
BASE				
60	60	Puckwunge Sandstone	Cross-bedded quartz sandstone	
	slight angular unconformity			
		Rove Formation (Paleoproterozoic)		

FIELD TRIP STOPS

STOP 1 – Porphyritic andesitic lavas – lower reverse sequence



***Location*:** UTM (NAD 83, Zone **16**T): 0284488E/5305983N, Hovland quadrangle, Milepost 133.2.

Park along Highway 61 just beyond the Axtell mailbox.

Note: This is private property except for the roadside outcrops.

Index map: rrd – Reservation River diabase; hyf – hybrid dike (stop 2); pqm; ferromonzonitic dike (stop 3); nnu – NSVG undivided, normally-polarized; nrh – Hovland lavas rhyolite; nhp – Hovland lavas porphyritic andesite (stop 1). Relationship between hyf and pqm modified from M-195. The gray areas on this and subsequent index maps denote mapped outcrops.

Description: Strongly porphyritic basaltic andesite lava flow with as much as 35% large plagioclase phenocrysts (An_{46}) up to 5 cm in length which show a subparallel flow alignment. There are also a few small phenocrysts of magnetite and altered olivine. Upper amygdaloidal portions of the flows contain amygdules filled with epidote and chlorite.

The lava flows at this stop are part of the Hovland lavas (mainly basalts and basaltic andesites), which are near the top of the reversely-polarized Lower Northeast sequence of the North Shore Volcanic Group. U-Pb ages for rhyolites within the Lower Northeast sequence include the 1107.7 ±1.9 Ma Tom Lake rhyolite (located inland to the northwest), and the 1107.9 ±1.8 Ma Red Rock rhyolite, which is located further northeast up the shore (Davis and Green, 1997).

DIRECTIONS: Cross the highway and proceed to the lake shore in the small cove by the boat house. *Note: This is private property and permission from the house across the road is needed to access.*

STOP 2 –Hybrid ferromonzonite to ferrodiorite dike

***Location*:** UTM (NAD 83, Zone **16**T): 0284647E/5306009N, Hovland quadrangle, Milepost 133.3 (see inset map under stop 1 for location). This is just across the highway and slightly east of the last stop, outcrops in a small cove on the lake shore.

Description: Pink to gray, variably porphyritic, intermingled rhyolitic (finely granophyric) to basaltic rock types that exhibit mutually cross-cutting relationships. Contacts between the phases vary from sharp to gradational. Plagioclase phenocrysts vary from few to abundant; also present are small phenocrysts of apatite, pyroxene, oxides, and possible altered olivine. Viewed from the proper perspective this dike appears to be curvilinear in form.

This dike can be traced to the west-southwest, subparallel to the shore, for nearly two miles. Other similar small hybrid dikes and intrusions have been mapped to the southwest in the Marr Island, Kadunce River, and Devil Track Lake quadrangles. These dikes commonly contain resorbed quartz and feldspar xenocrysts, implying that they may be the product of mafic magmas having melted porphyritic rhyolite flows at depth, and comingling with the felsic melts as they were emplaced.

The hybrid dike at this stop was shown to be reversely-polarized (K.G. Books, unpub. Data); it is considered to be part of the reversely-polarized Grand Portage dike swarm (Green and others, 1987). On the published bedrock geologic map (M-195) this information was overlooked, and this hybrid dike was mistakenly portrayed as cross-cutting the larger ferromonzodiorite dike that we will visit at the next stop.

DIRECTIONS: From the driveway near Stop 1, proceed back southwest approximately 0.5 mile to an outcrop along the north side of the highway and park on the edge of the road

---

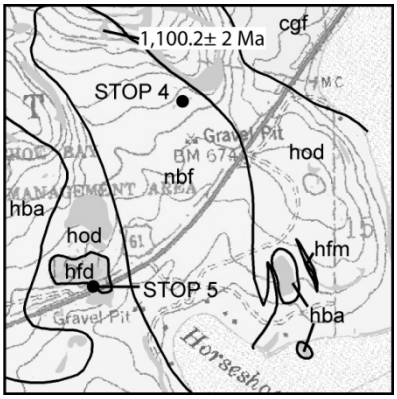
STOP 3 –Ferromonzodiorite dike

Location: UTM (NAD 83, Zone **16**T): 0283964E/5305764N, Hovland quadrangle (see inset map under stop 1 for location).

Description: Medium-coarse grained pyroxene-quartz ferromonzodiorite dike – gray, but weathers to a pinkish color, due to granophyre in the mesostasis, and cm-sized clots of granophyre are commonly visible on weathered faces. Contains an average of 49% plagioclase, 20% micrographic felsic mesostasis, 22% blocky to prismatic augite, 6% Fe-Ti oxides, up to 3% altered pigeonite, and trace amounts of apatite and possible altered olivine. This north–south vertical dike averages 328 feet (100 meters) in width and forms a prominent topographic ridge that makes a point out in the lake and extends inland about one mile from the shore. Its full extent, or how it relates to other hypabyssal diabase intrusions to the north, is not known as that area is incompletely mapped.

DIRECTIONS: Go back to Highway 61 and drive southwest approximately 2.5 miles to small road leading to a gravel pit, directly across from Big Bay Point road. Veer left at the first intersection on this road and proceed into an old gravel pit which has outcrops in the pit floor.

STOP 4 –Porphyritic rhyolite (Big Bay rhyolite; 1,100.2± 2 Ma)



Location: UTM (NAD 83, Zone **16**T): 0280325E/5304581N, Hovland quadrangle.

Index map: hfd – Hybrid ferromonzonite (stop 5); hfm – Hybrid ferromonzonite and remobilized rhyolite; hod– ophitic diabase; cgf – augite ferromonzodiorite; hba – coarse-grained amygdaloidal basalt; nbf – porphyritic rhyolite (stop 4).

Description: Maroonish-pink, feldspar-phyric rhyolite that is quite vesicular (drusy) at the western-most outcrops, but going east passes through a less vesiculated, spherulitic zone and farthest east into a dense, grayish-pink more massive zone; speculatively passing from the upper to lower part of a flow. The western-most outcrops contain possible relict fiamme features, and the eastern/speculatively lower part of the flow may be a welded tuff. Small garnets are locally present, presumably due to contact metamorphism by the surrounding diabases. A sample from here gave a U-Pb zircon age of 1,100.2 ± 2 Ma (the Big Bay rhyolite of Davis and Green, 1997). This rhyolite was determined by Val Chandler (Minnesota Geological Survey, pers. comm.) to have normal magnetic polarity, and thus must be very near the base of the Upper Northeast sequence.

Based on the phenocryst assemblage and flow characteristics, this rhyolite is grouped with other disparate occurrences of similar rhyolite in the area, but which are separated by one of the many intrusions.

DIRECTIONS: Go back to Highway 61 and drive southwest approximately 0.4 miles to roadcut on both sides of the highway, just past a right bend in the road. NOTE: There is a small pull-off on the north side of the highway just past/west of the outcrop roadcut where one could park a car. The highway is narrow and dangerous – please be careful!

STOP 5 – Hybrid ferromonzonite phase within ophitic diabase

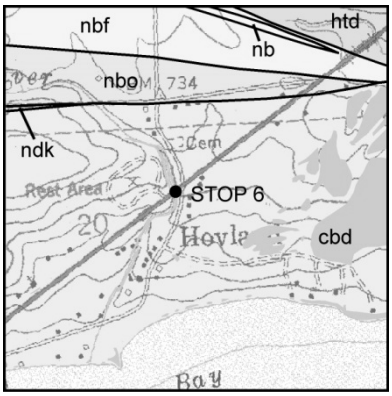
Location: UTM (NAD 83, Zone **16**T): 02799459E/5304014N, Hovland quadrangle (see inset map for stop 4 for location).

Description: This outcrop shows a gradation from ophitic olivine diabase (the Horseshoe Bay ophitic diabase – Beaver Bay Complex) into a plug-like body of prismatic pyroxene-quartz ferromonzonite. The western-most outcrop is spheroidally-weathered diabase with normal cm-sized pyroxene oikocrysts; going east the oikocrysts transition into bronzy clotted ophites, then to prismatic pyroxene grains; concurrently the diabase texture grades from ophitic, to intergranular and weakly granophyric, into increasingly coarse-grained, granophyric, and prismatic ferromonzodiorite, and ultimately into very coarse-grained ferromonzonite with large curved-prismatic clinopyroxene and plagioclase laths greater than 1cm in size. At the east end within the monzonite the pyroxene prisms and plagioclase laths are aligned into a vertical to steeply east-dipping flow structure. One petrographic sample of the ferromonzonite contains 40 percent strongly zoned plagioclase, 20 percent variably uralitized prismatic augite, 8 percent Fe-Ti oxide minerals, 20 percent felsic mesostasis that is dominated by micrographic quartz/alkali feldspar but also includes independent quartz and sanidine, 10 percent red-brown secondary clay-type minerals, 1 percent hornblende, and nearly 1 percent apatite.

This ferromonzonite body is one of several similar bodies that occur within or marginal to the Horseshoe Bay ophitic diabase (unit hod). Some of the marginal bodies may have formed as partial melt segregations from the underlying rhyolite.

DIRECTIONS: Continue southwest on Highway 61 for approximately 1.1 miles, to the Flute Reed River in the town of Hovland. Park near the river at a safe place along the highway or on the street parallel to the river and find your way down to the river. The water level must be sufficiently low to access the outcrops.

STOP 6 – Chicago Bay ophitic olivine diabase



Location: UTM (NAD 83, Zone **16**T): 0278355E/5303179N, Hovland quadrangle.

Index map: cbd – ophitic diabase (stop 6); htd – troctolitic ophitic diabase; ndk– Devil's Kettle rhyolite; nbo – ophitic basalt; nbf – feldspar-phyric rhyolite; nb – sparsely porphyritic basalt.

Description: This ophitic olivine diabase (part of the Beaver Bay Complex) exhibits strong sheet joints that dip more or less 10 degrees toward Lake Superior. It locally verges on augite troctolite; and in general contains 60 to 65% plagioclase (dominantly labradorite but includes andesine and bytownite; average $An_{66}Ab_{33}Or_1$), 11 to 20% ophitic augite ($Wo_{38}En_{43}Fs_{19}$, Mg# 70), 2 to 3% Fe-Ti oxides, 7 to 20% partially iddingsite-altered olivine (average Fo_{60}), trace to 5% felsic mesostasis and quartz, up to 2% hypersthene, up to 1.5% fine-grained chlorite and/or clay mesostasis, and trace amounts of pigeonite, apatite, hornblende, and biotite.

This typical ophitic olivine diabase is thought to be a sill-like body that underlies the Hovland sill, but it is not clear whether or not they are related. The extent of this unit is well established in the Hovland quadrangle by outcrops, water well cuttings, and topography; but the extension to the west in the Marr Island quadrangle below the Hovland sill is based on only one set of water well cuttings. This unit is of normal polarity (H.C. Palmer, unpub. data, 1972).

DIRECTIONS: From the Flute Reed River continue southwest on Highway 61approximately 1.3 miles to a set of outcrops on the uphill side of the road next to a small pull-off.

Overview of the Hovland Sill, Stops 7 and 8 (actual stops below)

The Hovland sill, previously mapped in part by Jones (1963), is a gently-dipping (approximately 15° S-SE), subcordant body composed of a basal massive ferrogabbro (stop 7), a middle zone of cumulate-foliated granophyric ferrogabbro to ferromonzodiorite (stop 7), and an upper coarse-grained felsic cap (stop 8). Overall the sill is estimated to be at least 984 feet (300 meters) thick. This sill is very similar to a less well exposed unit a few miles north that has informally been named the Lookout sill, which dips approximately 15° S-SE, and like the Hovland sill, has a cumulate portion with abundant coarse ilmenite plates and an upper felsic cap that contains fayalitic olivine. Both of these evolved intrusions are broadly similar to the 'Silver Bay ferrogabbro' type of zoned intrusions that are late intrusions associated with the Beaver Bay Complex (e.g. Miller and Green, 2002).

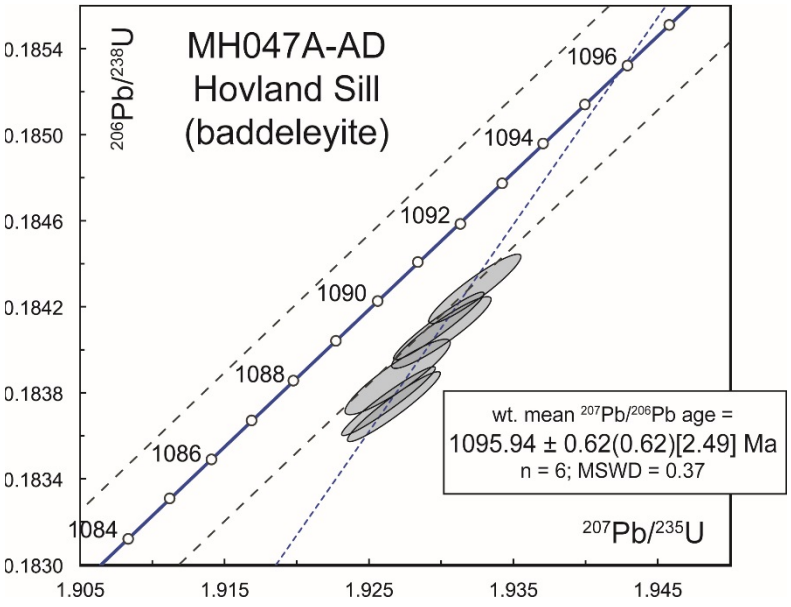


Figure 3. Isochron diagram for sample MH047A-AD.

A sample (MH047A-AD) of coarse prismatic olivine-pyroxene ferromonzonite from the upper felsic phase (**Stop 8**) was submitted for age dating to Dr. Mark Schmitz at the Boise State Isotope Laboratory. No zircon was separated from the sample, however relatively abundant, although small (approximately 100 microns in long dimension), flattened, light brown baddeleyite crystals were recovered. Six baddeleyite crystals selected for dissolution were all variably discordant, but gave equivalent $^{207}Pb/^{206}Pb$ dates with a weighted mean of 1095.94±0.62 (n=6; MSWD 0.37; Figure 3; Boerboom and others, 2014). This age falls within the range of published ages for various other units of the Beaver Bay Complex, including the Wilson Lake ferrogabbro (1095.75±0.92; Hoaglund and others, 2010), Sonju Lake intrusion (1096.1±0.8; Paces and Miller, 1993), Silver Bay ferrogabbro (1095.8±1.2; Paces and Miller, 1993), Pine Mountain granophyre (1095.3±3.8; Vervoort and others, 2007), as well as others. The sample was collected from a roadcut on Highway 6, 1.3 miles northeast of the Brule River near Hovland. (*UTM zone 15T 722714E, 5301024N*).

Figures 4 and 5 demonstrate various aspects of chemical differentiation trends within the Hovland sill, and Figure 6 shows examples of the varied textures between the phases.

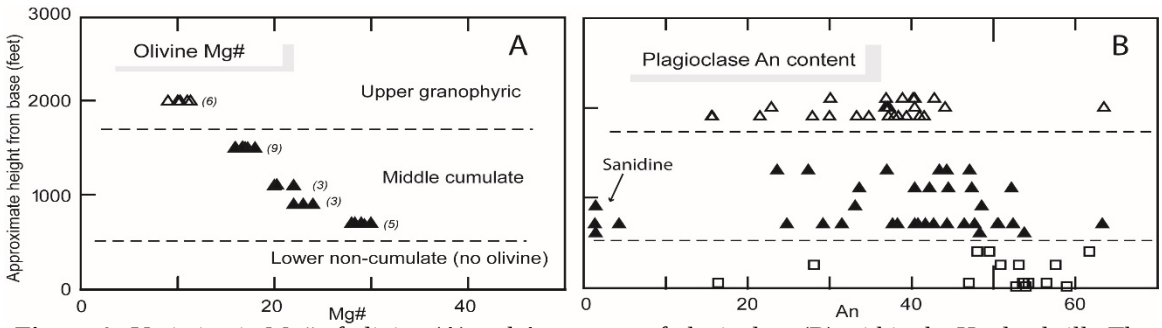


Figure 4. Variation in Mg# of olivine (A) and An content of plagioclase (B) within the Hovland sill. The olivine Mg plot shows the number of points analyzed for each individual sample in parentheses. The An diagram is from many samples which are not differentiated. Semi-quantitative SEM analyses were provided by Jeff Thole, Macalester College.

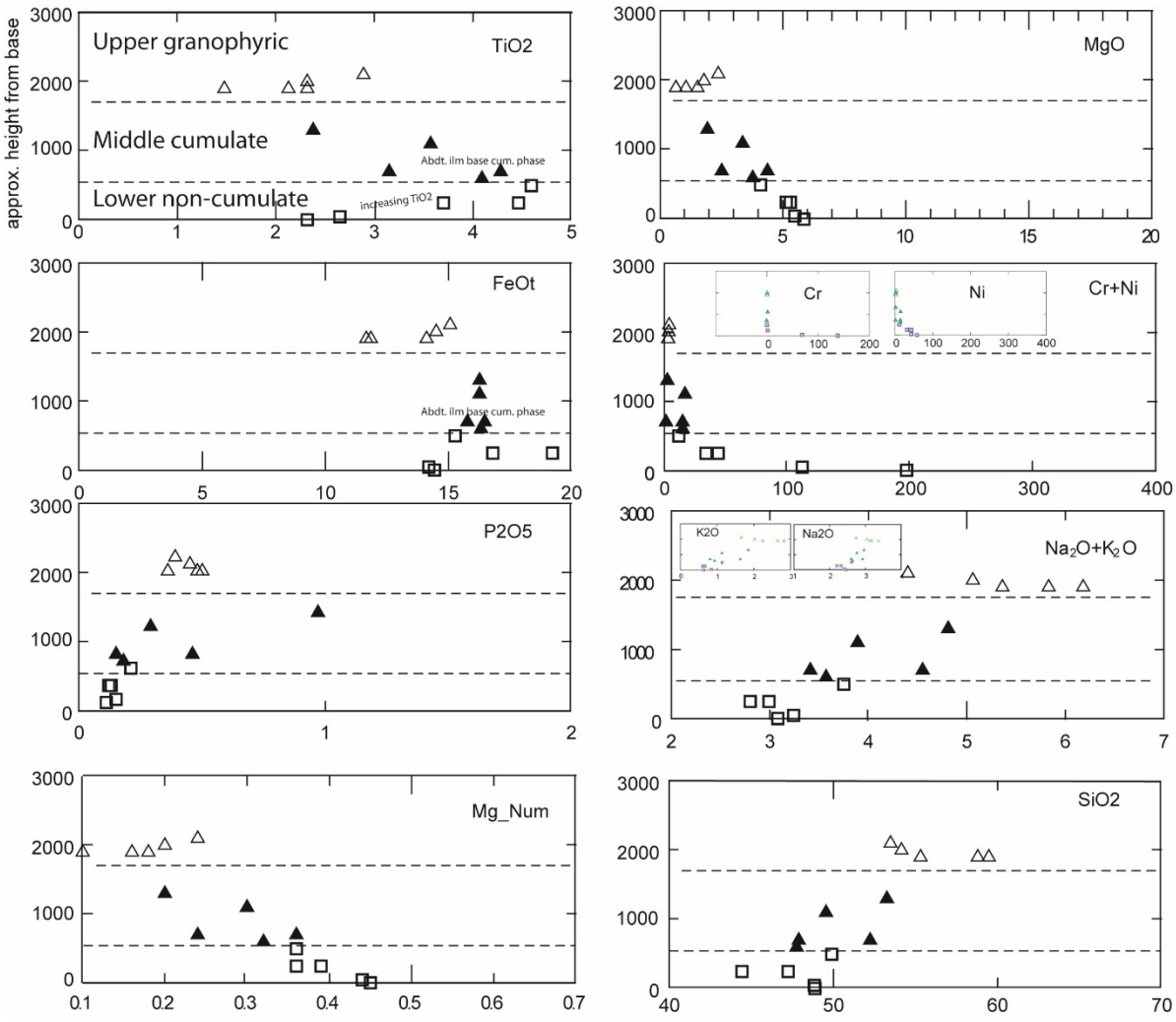


Figure 5. Whole-rock compositional variations through the Hovland sill. Note the increase in TiO_2 near the transition from the lower to middle zone, which is reflected by abundant cumulate ilmenite plates near the bottom of the cumulate zone. Analyses provided by Karl Wirth, Macalester College.

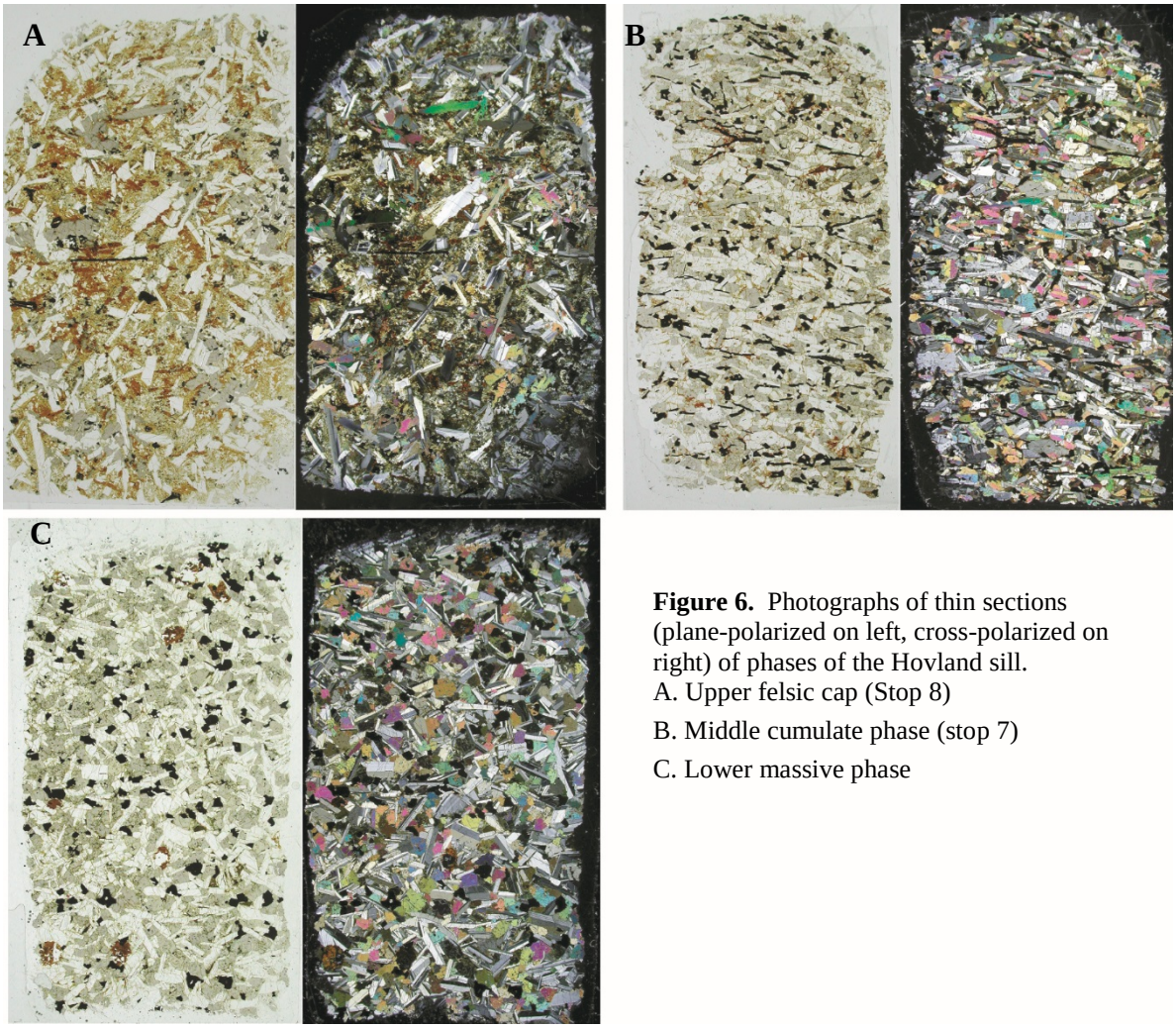
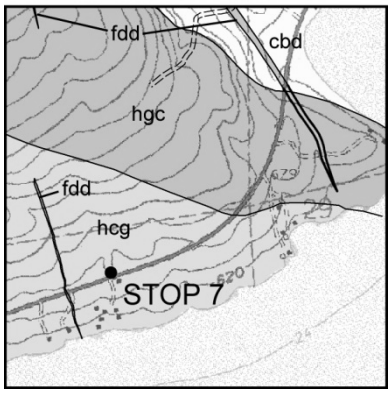


Figure 6. Photographs of thin sections (plane-polarized on left, cross-polarized on right) of phases of the Hovland sill.
A. Upper felsic cap (Stop 8)
B. Middle cumulate phase (stop 7)
C. Lower massive phase

STOP 7 – Strongly foliated cumulate ferromonzodiorite of the Hovland sill



Location: UTM (NAD 83, Zone **16**T): 0276907E/5301831N, Hovland quadrangle.

Index map: fdd – small ferrodiorite dikes; hcg – Hovland sill cumulate ferromonzodiorite (stop 7); hgc– Hovland sill ferrogabbro); cbd – ophitic diabase.

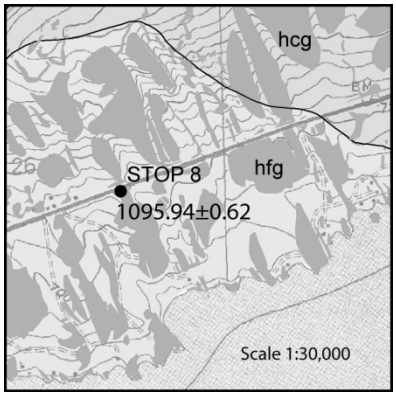
Description: This stop is within the middle cumulate zone of the Hovland sill. The cumulate ferromonzodiorite is strongly foliated, and granophyric, with abundant magnetite and plates of ilmenite plates (Figure 6B). The cumulate phases consist of plagioclase, augite, Fe-Ti oxides, olivine, and minor apatite. Prismatic augite crystals up to 2 centimeters in length are randomly oriented within the foliation plane. Olivine content (mostly altered) is generally low, around 2-4% in most of the intrusion. Pigeonite ($Wo_{13}En_{49}Fs_{38}$, Mg# 49) occurs as thin discontinuous rims on augite and as small post-cumulate grains within the felsic mesostasis. Samples from this unit examined petrographically contain 45 to 55% strongly zoned plagioclase, 16 to 33% augite, 0 to 3% pigeonite, 5 to 11% Fe-Ti oxides, 2 to 10% mostly

altered olivine, 8 to 15% felsic mesostasis, minor apatite, and near the top, rare hornblende. The felsic mesostasis is composed of a mixture of quartz paramorphs of tridymite, euhedral sanidine, micrographic to granophyric quartz and alkali feldspar, and abundant secondary iddingsite and clay minerals. Based on limited SEM semiquantitative analyses, average Fe/Mg ratios of augite increase from the base (augite; $Wo_{35}En_{38}Fs_{27}$, average Mg# 57) to the top (ferroaugite; $Wo_{37}En_{22}Fs_{41}$, average Mg# 35). Mg numbers for olivine (Figure 4A) range from Fo_{29} near the base, to Fo_{17} near the top; olivine is typically altered to reddish-brown iddingsite and/or green bowlingite (saponite). Limited feldspar analyses (Figure 4B) indicate that plagioclase becomes increasingly sodic, ranging from labradorite to mainly andesine at the base (average $An_{51}Ab_{47}Or_2$), and andesine to oligoclase near the top (average $An_{41}Ab_{56}Or_3$). Sanidine is common within the felsic mesostasis (average $An_2Ab_{45}Or_{53}$).

The basal **ferrogabbro** (Figure 6C) is poorly exposed along the highway to the east and will not be visited by this trip. It is dark greenish-gray with a rusty-weathered surface, medium- to coarse-grained, non- to weakly-foliated, and typically contains evenly distributed 3- to 4-millimeter, reddish-brown altered olivine spots. Based on several point counts this lower unit contains 48 to 55% plagioclase (labradorite), 25 to 35% granular augite ($Wo_{37}En_{41}Fs_{22}$, Mg# 59 at the base and $Wo_{32}En_{37}Fs_{32}$, Mg# 54 at the top), up to 2% pigeonite ($Wo_{10}En_{37}Fs_{53}$, Mg# 41), up to 5% altered olivine clots, 5 to 8% Fe- Ti oxides, 6 to 8% felsic mesostasis, 1% reddish-brown clay-like material, and traces of apatite.

DIRECTIONS: Continue towards Grand Marais for about 2.2 miles; pull over near the auto repair shop and go to outcrop on lake side of highway under powerline, just east of driveway marked by 4300. **Be careful** if you walk across highway! NOTE: Entering UTM zone 15 (NAD 83).

STOP 8 – Upper felsic phase of the Hovland sill



Location: UTM (NAD 83, Zone 15T): 722453E, 5300915N; Marr Island quadrangle.

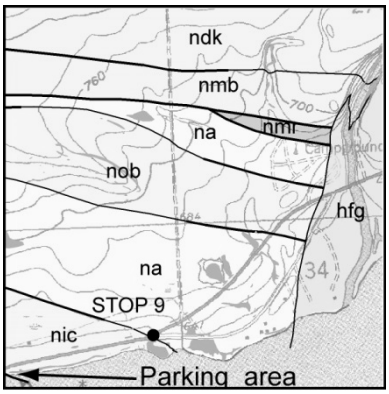
Index map: hfg – upper felsic cap of Hovland sill (stop 8); hcg – Hovland sill cumulate ferromonzodiorite (stop 7)

Description: Very coarse-grained, prismatic ferromonzonitic upper felsic portion of the Hovland sill; location of age date sample MH047A.AD (Figure 3). Note prismatic to trellis-shaped pyroxene, incomplete fayalitic olivine trellises, and brownish granophyric matrix. Overall description of this unit taken from published geologic bedrock map (M-195) below: Figure 6A shows the typical texture of this unit.

Prismatic olivine-pyroxene ferromonzodiorite to ferrogranite—Rusty reddish-brown where weathered, dark brownish- to greenish-gray where fresh, coarse-to very coarse-grained, granophyre-rich, prismatic. Contains 30 to 50 percent strongly zoned andesine (average $An_{39}Ab_{58}Or_3$) to oligoclase, 8 to 15 percent variably prismatic ferroaugite ($Wo_{22}En_{41}Fs_{37}$, Mg# 35), 10 to 15 percent fayalitic olivine (Fo_{10}) that is mostly altered to reddish-brown iddingsite and varies from irregular coarse prismatic grains and clots to acicular trellises up to30 centimeters in length, 2 to 8 percent Fe-Ti oxides, 30 to 40 percent felsic mesostasis (combinations of micrographic quartz and alkali feldspar, crystalline quartz, and sanidine crystals), 1 to 2 percent apatite, trace amounts of rutile within quartz, and rare fine-grained bornite. The felsic mesostasis also contains abundant reddish-brown iddingsite-like needles interpreted to be former fine-grained masses and prisms of Fe-olivine. Outcrops at the border zone along the Brule River are generally darker in color, slightly more fine-grained, and locally contain small round chlorite amygdules. This unit is of normal polarity (K.G. Books, unpub. data, 1972).

DIRECTIONS: Continue towards Grand Marais for about 2.5 miles to where the beach nearly touches the highway. Pull over and park along the small pull off near the beach. Walk back east along the beach to low outcrops, or park farther east along the edge of the highway.

STOP 9 – Icelandite of the Marr Island lavas



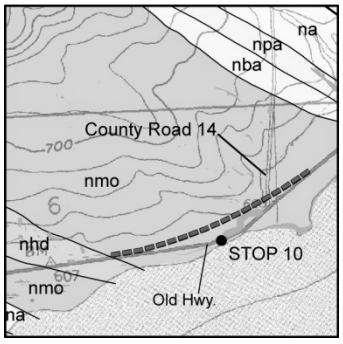
Location: UTM (NAD 83, Zone 15T): 719901E, 5299658N; Marr Island quadrangle.

Index map: hfg – upper felsic cap of Hovland sill (stop 8); nic – icelandite (stop 9) na – pigeonitic andesite; nob – ophitic basalt; nmr – aphyric rhyolite; nmb – strongly amygdaloidal basalt; ndk –Devil's Kettle rhyolite. All volcanic units are part of the Marr Island lavas. The volcanic units shown here are also known as the Naniboujou basalts; this unit has been incorporated into the larger Marr Island lava package on M-195 (Boerboom and Green, 2013).

Description: Low outcrops along the beach are fine-grained, sparsely porphyritic icelandite, with phenocrysts mainly of plagioclase but also some phenocrysts of magnetite, pyroxene, and apatite in a matrix of fine felty plagioclase and brownish-weathered alkali feldspar mesostasis. As you work east along beach there are zones that are variably amygdaloidal, but it is difficult to demarcate flow contacts.

Icelandite is a felsic rock characterized by 62-66% SiO_2, high FeO (~7%), and $Na_2O + K_2O$ (6.5-9%) (Carmichael, 1964, as summarized in Green and Fitz, 1993). Icelandites characteristically contain a few percent of small rectangular plagioclase phenocrysts that bleach white on an otherwise pinkish-brown weathered surface. Icelandite can be hard to differentiate from plagioclase-phyric rhyolite; however icelandite typically is brownish in color, has a fine felty texture, is weakly magnetic, and has small apatite phenocrysts compared to rhyolite which is more pink, saccharoidal in texture, non-magnetic, and lacking in apatite phenocrysts. Icelandite in some exposures has a strong flaggy parting which forms slabs about 6-10 cm thick (which would make ideal paving stones!).

DIRECTIONS: Continue towards Grand Marais for about 2 miles to County road 14, and directly across from it, turn left towards the lake onto an old section of the highway (Fire number 3500) and park. Walk west on the old highway and cut down to the beach to outcrops of ophitic basalt.



STOP 10 – Ophitic basalt of the Marr Island lavas, and another small hybrid intrusion.

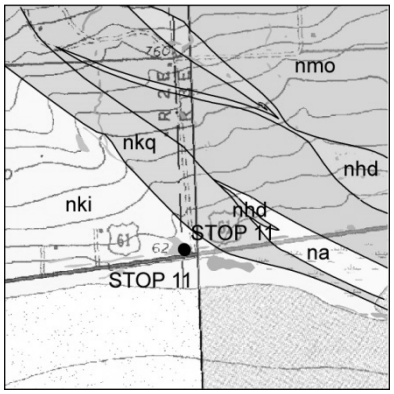
Index map: nhd – hybrid ferromonzonite (stop 10); na – pigeonitic andesite; nmo – ophitic basalt (stop 10);nba –basaltic andesite; npa – strongly porphyritic andesite. All volcanic units are part of the Marr Island lavas. Dashed red line is path of newer Highway 61.

Location: UTM (NAD 83, Zone 15T): 716788E, 5297938N; Marr Island quadrangle.

Description: Typical ophitic basalt, not only of the Marr Island lavas but of the North Shore Volcanic Group in general. Examine old road cuts and beach outcrops. Note scattered plagioclase phenocrysts.

DIRECTIONS: Continue towards Grand Marais for about 1 mile to the intersection with Kelly's Hill Road. Outcrop at the northwest corner of the intersection.

STOP 11 – Rangeline icelandite of the Kadunce icelandites.



Location: UTM (NAD 83, Zone 15T): 715255E, 5297698N; Kadunce River quadrangle.

Index map: nhd – hybrid ferromonzonite; nki – Kadunce icelandite (stop 11); nkq – porphyritic rhyolite; na – pigeonitic andesite; nmo – ophitic basalt.

Description: The roadcuts along the north side of the highway expose the Rangeline icelandite, which is typical of the icelandites of the NSVG. It is brownish, with ~15% phenocrysts of mainly plagioclase but also altered Fe-olivine, Fe-augite ($En_{15}Wo_{42}Fs_{43}$), magnetite, and apatite in a fine-grained groundmass of mainly plagioclase, alkali feldspar, and quartz (Figure 7).

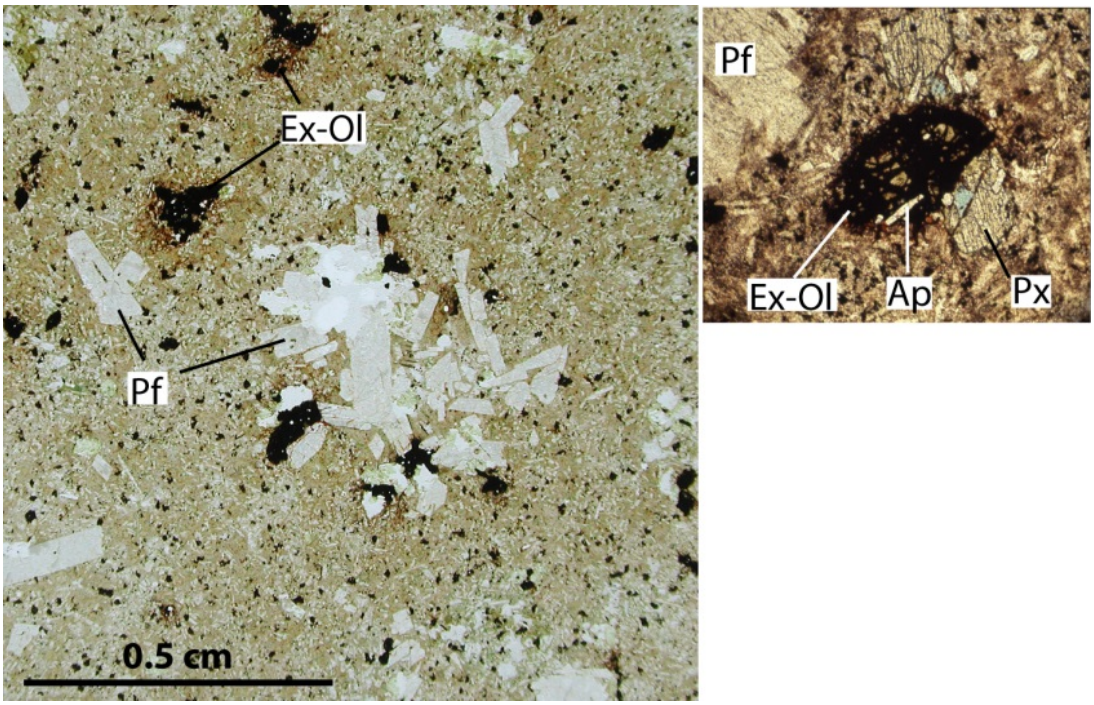
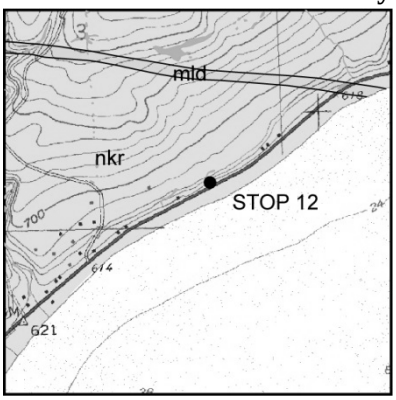


Figure 7. Photomicrographs (plane-polarized light) of the Rangeline icelandite showing phenocryst assemblage. The glomerophenocryst in the center of photo on left includes pale green-altered pyroxene; the brownish matrix is alkali feldspar. Pf – plagioclase; Ex-Ol – altered olivine; Px – ferroaugite; Ap – apatite.

DIRECTIONS: Continue towards Grand Marais for about 2.3 miles and park just beyond mile marker 118 at base of trail going up the hill on north side of the highway. *Note: this is private property so please use discretion and stay near the road. The loose pieces of rhyolite at the base of the cliff are identical to those on the cliff face, which is dangerous.*

STOP 12 – Kimball Creek Rhyolite Rheoignimbrite



Location: UTM (NAD 83, Zone 15T): 711750E, 5296730N; Kadunce River quadrangle.

Index map: mld – Monker Lake diabase; nkr – Kimball Creek rhyolite (stop 12).

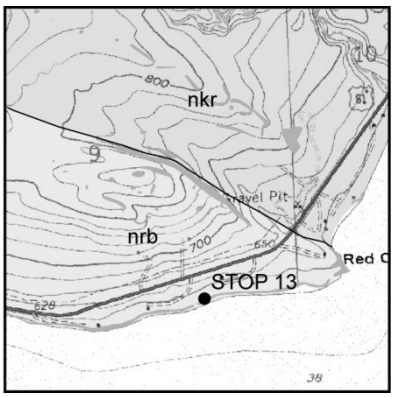
Description: The Kimball Creek rhyolite is thought to be the second largest felsic flow in the NSVG. It is ~350 m thick and extends at least 20 miles/32 km to the west (Green and Fitz, 1993).

The composition of this rhyolite is midway between typical rhyolites and typical icelandites. It contains 5-10% small phenocrysts, mostly plagioclase but also magnetite, zircon, apatite, quartz, and altered Fe-augite. The fine-grained groundmass is composed mainly of alkali feldspar and variably poikilitic quartz, much of which occurs as paramorphs after tridymite tablets. As in the Devil Track rhyolite, the size of these 'ex-tridymite' tablets increases toward the flow center from the top and the base, implying emplacement as a single cooling unit.

At both the top and bottom of this flow, outcrops show pyroclastic texture, with flattened fiamme and shards in a dense, probably originally vitric-ash groundmass. Near the base, these stretched fiamme are involved in the flow-folds (Green an Fitz, 1993). These observations imply that this flow was emplaced as a high-temperature ignimbrite that consolidated and underwent bulk flow.

DIRECTIONS: Continue toward Grand Marais for about 1.4 miles to mailbox #2524. Walk down the driveway toward the lake to outcrop on the shore below house. ***NOTE:*** *This is private property – please obtain permission of the owner before proceeding to the shore! NO HAMMERS! Alternate outcrops of this unit can be viewed at roadcuts along the highway, but they are not as strongly porphyritic.*

STOP 13 – Porphyritic basalt flow of Red Cliff basalts



Location: UTM (NAD 83, Zone 15T): 710132E, 5295236N; Kadunce River quadrangle.

Index map: nrb – Red Cliff basalts (stop 13); nkr – Kimball Creek rhyolite (stop 12).

Description: The Red Cliff basalts are a series of olivine tholeiite flows sandwiched between large rhyolite flows in this section of the Upper Northeast sequence. This group of basalt flows is approximately 300 m thick, and can be traced inland to the west for at least 18 mi / 30 km.

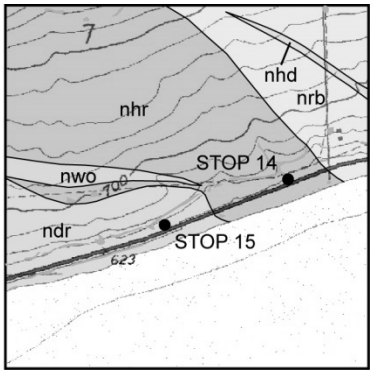
The thick ophitic to subophitic flow at this stop is remarkable for its concentration of large plagioclase phenocrysts (~An_{70}) near its top; the phenocrysts apparently floated in the lava after eruption. Locally it also contains dm-sized, angular inclusions of coarse-grained anorthosite. It appears as though some of the phenocrysts may have floated away from disaggregating anorthosite inclusions (Figure 8)



Figure 8. Photograph of Red Cliff basalt flow with coarse-grained anorthosite inclusion and plagioclase phenocrysts that appear to have disaggregated and floated away from it. Hammer is 40 cm long.

DIRECTIONS: Continue towards Grand Marais for about 1.9 miles and park along the edge of the highway near outcrops on the uphill side of the road.

STOP 14 – Maple Hill rhyolite



Location: UTM (NAD 83, Zone 15T): 707109E, 5295074N; Kadunce River quadrangle.

Index map: nhd – hybrid ferromonzonite; ndr – Devil Track rhyolite (stop 15); nwo – Woods Creek basalt; nhr – Maple Hill rhyolite (stop 14); nrb – Red Cliff basalts.

Description: The Maple Hill rhyolite varies from 260 to nearly 400 feet in thickness, and extends west for at least 12 mi / 20 km and possibly as far as 25 mi / 40 km. Structures such as lineated vesicles and folded vesicle trains, coupled with the lack of pyroclastic textures, indicate that this rhyolite erupted as a lava flow rather than a rheoignimbrite (Green and Fitz, 1993).

The upper part of the flow has quartz-lined stretched vesicles and amygdules of quartz and calcite, and local veinlets of purple fluorite. Below the upper vesiculated zone the rhyolite commonly shows tightly folded flow layering, and locally contains abundant spherulites and lithophysae as large as 3 centimeters. In general, this unit contains 4 to 6 percent alkali feldspar phenocrysts, 2 to 4 percent quartz phenocrysts, and rare microphenocrysts of zircon in a groundmass of fine-grained quartz and feldspar with minor fluorite (Fitz, 1988), as well as phenocrysts of plagioclase, altered Fe-olivine and Fe-augite, and Fe oxides (Green and Fitz, 1993). This rhyolite, in contrast to the aphyric Devil Track rhyolite (stop 15), contains abundant phenocrysts.

An enigmatic thin flow of ophitic basalt (Woods Creek basalt; now on inset map), which is exposed a couple miles inland to the west and also intersected in water wells, appears to have erupted at the same time as the Maple Hill rhyolite, or more likely between the Maple Hill and Devil Track rhyolites. Remarkably, the same stratigraphic relationships are noted over 40 km to the west in the Lutsen quadrangle (Boerboom and others, 2007), where a thin basalt flow overlies the western extension of the Maple Hill Rhyolite and in turn is overlain by the Devil Track rhyolite.

DIRECTIONS: Continue towards Grand Marais for about 0.25 miles and park along the edge of the highway near outcrops at the abandoned wave-cut cliff on the uphill side of the road.

STOP 15 – Devil Track rhyolite

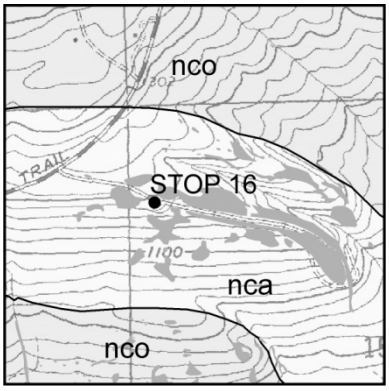
Location: UTM (NAD 83, Zone 15T): 706718E, 5294928N; Kadunce River quadrangle (see inset map for stop 14 above for location).

Description: The Devil Track rhyolite is the largest known flow of felsic volcanic rocks in the North Shore Volcanic Group and is inferred to have been either a hot superliquidus lava flow or possibly a thick, hot rheoignimbrite that flowed and underwent complete crystallization after deposition (Green and Fitz, 1993). Basal outcrops just northeast of here show strong lamination containing a marked flow lineation. This rhyolite varies from 750 to over 950 feet / 230-300 meters) in thickness, and extends west for at least 25 mi / 40 km from the mouth of the Devil Track River (and an unknown distance to the east, beneath Lake Superior).

This rhyolite is light pink to grayish-pink, fine-grained and saccharoidal textured, essentially aphyric, and contains abundant small, tabular paramorphs of quartz after primary tridymite. Grain size increases toward the center of the flow (Green and Fitz, 1993). Flaggy parting is typical, as well as a planar flow layering that is gently warped and is generally not parallel to the flaggy parting; neither parting nor flow layering provide consistent measured structural orientations. A well that penetrates the top of this rhyolite to the southwest of here shows that the upper part of the flow is perlitic, and is overlain by a thin, discontinuous sandstone.

DIRECTIONS: Drive to Grand Marais, and at the east edge of town, follow signs to go up the Gunflint Trail (Cook County Highway 12). Drive up the Gunflint Trail for approximately 2.5 miles, and turn right on the road to Pincushion Mountain ski trails. Drive this road to the parking lot.

STOP 16 – Andesitic Croftville lavas – Pincushion Mountain overlook



Location: UTM (NAD 83, Zone 15T): 701012E, 5294305N; Grand Marais quadrangle.

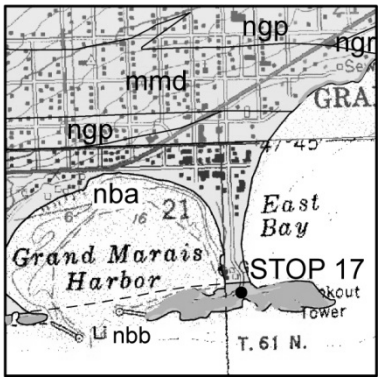
Index map: nco – ophitic to intergranular pigeonitic basalt; nca – andesite (stop 16). Both are part of the Croftville lavas.

Description: Artists' point and the breakwater that forms the enclosure around the Grand Marais Harbor visible below are formed by the Breakwater basalt flow, which will be the next stop. This landform, with an island tied to the mainland by a gravel bar, is a classical tombolo. The rubbly outcrops here below this overlook are fine-grained, sparsely porphyritic andesite which is part of the

Croftville lava sequence. Exposures on the dipslope and in creek valleys below the overlook show the andesite flows contain thick rubbly Aa-type flow tops, typical of lava flows of this composition.

DIRECTIONS: Drive back down the Gunflint Trail to Grand Marais, turn right (west) on Highway 61, and proceed to Broadway Avenue. Turn left on Broadway and drive to the parking lot next to the harbor just before the Coast Guard station, and continue walking toward the lake to the breakwater.

STOP 17 – Breakwater basalt – Artist's Point



Location: UTM (NAD 83, Zone 15T): 699945E, 5291458N; Good Harbor Bay quadrangle.

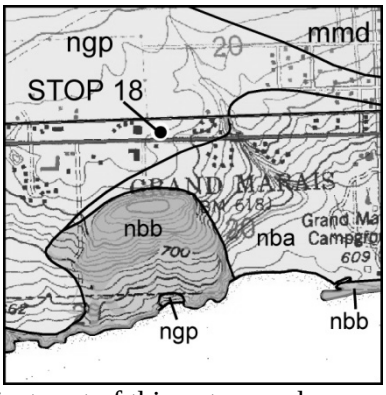
Index map: mmd – Murphy Mountain diabase; nbb – Breakwater basalt (stop 17); nba – Amygdaloidal porphyritic basalt; ngp –Grand Marais porphyritic rhyolite (stop 18); ngr – Grand Marais aphyric rhyolite.

Description: The broad ledges here that help form the Grand Marais harbor are made of a thick (>100 m) flow of transitional basalt called the Breakwater basalt. It has distinctive texture and columnar jointing, and forms some of the ridges of the 'Sawtooth Range' visible to the west from the Breakwater. The western end of the breakwater has well-preserved glacial striations and well-developed joint-plucking. This is the tombolo seen from the last stop.

The basalt is massive, gray to maroon, and fine- to medium- grained, with abundant small clustered plagioclase phenocrysts and minor augite, altered olivine, and magnetite in a felty-intergranular groundmass. The Breakwater basalt can be traced at least 7.5 mi/12 km to the west, where it apparently pinches out. It is not present in the Cascade River, which is approximately 10.5 mi / 16 km to the west.

DIRECTIONS: Drive back to Highway 61, turn left (west) and go 1 mile up the hill to small roadcut on the right (north) side of the road opposite the lake shore. It might be best to pull into the Harbor Light parking lot and walk back to outcrop.

STOP 18 – Porphyritic Grand Marais rhyolite (1097.26±0.67 Ma)



Location: UTM (NAD 83, Zone 15T): 698364E, 5291847N; Good Harbor Bay quadrangle.

Index map units same as stop 17.

Description: This outcrop (underneath large billboard) is the location of age date sample DG073-AD, porphyritic rhyolite ($^{207}Pb/^{206}Pb$ age of 1097.26±0.67). This strongly porphyritic rhyolite contains in general 2-4% each of quartz and feldspar phenocrysts, as well as minor magnetite and altered mafic silicate phenocrysts.

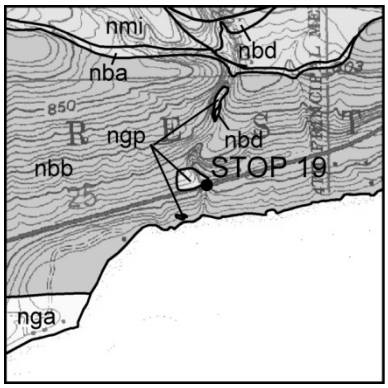
The rhyolite varies from massive to flow-banded, and is commonly strongly blocky-fragmental, a texture well-exhibited in the small creek just east of this outcrop where angular, flow-banded rhyolite blocks up to 1.5 m in size are evident; mapping in the vicinity indicates that loose blocks of rhyolite were overrun by the Breakwater basalt (see next stop for more description).

Age dating on rhyolite from this outcrop was performed by Dr. Mark Schmitz at the Boise State Isochron lab. Six zircon crystals were selected for CA-TIMS (*Chemical Abrasion Thermal Ionization Mass Spectrometry*) analysis, from which five grains produced concordant isotopic ratios, with a weighted mean $^{206}Pb/^{238}U$ date of 1095.00±0.33 (MSWD (*Mean Square Weighted Deviation)* = 0.07) and a weighted mean $^{207}Pb/^{206}Pb$ age of 1097.26±0.67 (n=5; MSWD 1.47).

Using the $^{207}Pb/^{206}Pb$ weighted mean date, this age is only slightly younger than the Devil's Kettle rhyolite (1097.7±1.7; Davis and Green, 1997), which lies roughly 8,000 feet stratigraphically below and is separated by several thick mafic to felsic volcanic units. The nearly identical ages for these two units indicates rapid and voluminous volcanic activity in the upper part of the northeast limb of the North Shore Volcanic Group.

DIRECTIONS: Continue southwest on Highway 61 approximately 1.7 miles to the Fall River. Park on wide spot at edge of Highway near river. First cross highway and follow trail along east side of river to the shore, then cross the river (if possible) to outcrops on the west.

STOP 19 – Breakwater basalt and Grand Marais rhyolite, Fall River



Location: UTM (NAD 83, Zone 15T): 695809E, 5290906N; Good Harbor Bay quadrangle.

Index map: nga – Good Harbor Bay andesites; nbb – Breakwater basalt; nba – amygdaloidal Breakwater Basalt; ngp – Grand Marais porphyritic rhyolite; nbd – inclusion-rich basalt sill or dike; nmi – icelandite (outcrop not shown).

Description: Outcrops of porphyritic rhyolite cross-cut and/or overrun by the Breakwater basalt. Dikelets of basalt intruded into fractures in the rhyolite contain abundant small chips and slivers of rhyolite, and larger inclusions of rhyolite or possibly more andesitic rocks with stretched vesicles are contained in the basalt.

Although the rhyolite here may be as inclusions in the basalt, farther up Fall Creek and also along the shoreline there are several 'windows' through the Breakwater basalt where the underlying rhyolite is exposed. In all cases, it appears as though the rhyolite was a 'loose breccia' that was overrun by the Breakwater basalt.

Figure 9 is a photograph taken along the shore towards Grand Marais, which shows a block of rhyolite that is draped by the Breakwater basalt; evidence for a loose, blocky rhyolite surface having been overrun by a basalt flow.



Figure 9. Block of porphyritic rhyolite overrun by the base of the Breakwater basalt flow, lakeshore west of Grand Marais (see map for stop 18, small unit labeled 'ngp' along shoreline due south of stop 18. Chilled, finely amygdaloidal margin of the basalt drapes over the block of rhyolite.

----Hike back up to the highway and climb down into the river just upstream of the highway-----

Exposed here (on the east side of the river) is another contact between the Breakwater basalt and rhyolite, which in this case has only feldspar phenocrysts. The basalt in general becomes increasingly amygdaloidal near the rhyolite, but the relationships are somewhat ambiguous because there are also inclusions of identical-appearing amygdaloidal basalt within the rhyolite. Another example of this can be found farther upstream, where the rhyolite is extremely brecciated, with fragments from 1 m or more to as small as 1 cm, and the fragments are intruded by the Breakwater basalt, or a possibly a feeder dike to the basalt.

DIRECTIONS: Continue southwest on Highway 61 for about 2.3 miles and park along the road edge adjacent to a long roadcut.

STOP 20 – Good Harbor Bay andesites



Location: UTM (NAD 83, Zone 15T): 692225E, 5289747N); Good Harbor Bay quadrangle.

Index map: ngs – Cut Face Creek sandstone (stop 21); nga – Good Harbor Bay andesites (stop 20); nbb – Breakwater basalt.

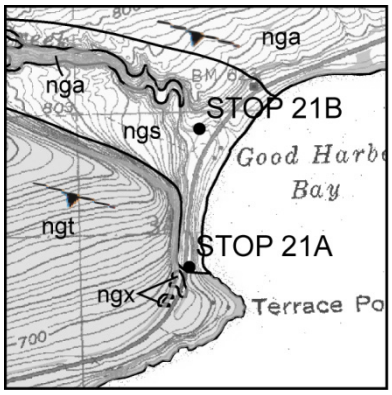
Description: The Good Harbor Bay andesites extend west from this location for nearly 20 mi\32 km, to beyond the Onion River, where they are terminated by the Leveaux Porphyry. The unit is at least 200 ft / 60 m thick. It overlies the Breakwater basalt and is overlain by the Cut Face Creek Sandstone, which in turn is overlain by the Terrace Point basalt flow (Stop 21). However, approximately 22 km to the west of here the sandstone pinches out, and the Good Harbor Bay andesites are in direct contact with the Terrace Point basalt.

This locality is typical of the Good Harbor Bay andesites – fine-grained, fresh, sparsely porphyritic, and moderately to strongly magnetic. This roadcut exposes a flow contact where a lower rubbly amygdaloidal Aa flow-top is overlain by a massive flow base. A discontinuous, meter thick bed of sandstone locally overlies the rubbly flow-top breccia. The flow-top breccia can be recognized by blocks of strongly amygdaloidal/vesicular andesite infilled by sandstone, and the base of the overlying flow contains abundant amygdules that are highly stretched parallel to the flow contact. The sandstone between the two flows can be identified by its red-spotted appearance (oxidation spots).

Just east of this outcrop is a small creek that crosses the highway. If the water is low enough to traverse up the creek, there are excellent fresh exposures of the Good Harbor Bay andesites. Approximately 200 m upstream is a small waterfall formed by an approximately N20°E, 20° north dipping, 30 cm wide sharply bounded brittle fault that has pink zeolite minerals infilled around the fault breccia clasts. Other small, flat faults, some with slickensides, may be visible in the stream bed.

DIRECTIONS: Continue southwest on Highway 61 about ¾ of a mile to the scenic overlook across from the high road cut.

STOP 21A – Terrace Point basalt flow and Cut Face Creek sandstone (Cut Face Creek Road cut)



Location: UTM (NAD 83, Zone 15T): 691780E, 5289170N Good Harbor Bay quadrangle.

Index map: ngt – Terrace Point basalt flow; ngx – basaltic breccia; ngs – Cut Face Creek sandstone; nga – Good Harbor Bay andesites.

Description: Thick interflow sandstone with ripple marks, deformation features in sandstone at base of flow, shale rip-up chips, and desiccation cracks. At the west end is a fragmental/scoriaceous phase of the Terrace Point basalt intruded and overrun by the main basalt flow. In high roadcut on northwest side of highway is an obvious contact between the Cut Face Creek Sandstone and the overlying Terrace Point basalt flow. The sandstone overlies the Good Harbor Bay andesites (stop 20).

Basalt – The Terrace Point basalt, which overlies the sandstone, is a major ridge-forming unit from here to the southwest, forming 'sawtooth mountains'. It is a distinctive flow characterized by a dark green color, white thomsonite amygdules, uniform 3-4mm ophitic texture, and scattered small glassy plagioclase phenocrysts. In general the contact with the sandstone is sharp and straight, but in places the sandstone has been slightly deformed, though not appreciably metamorphosed, by the basalt flow.

Near the south end of the road cut is a unit of scoriaceous, fragmental basalt that is intruded and overrun by the Terrace Point flow. Similar rock types and relationships have been observed to the southwest, also near the flow base. The breccia contains 1-100 cm angular basalt fragments that are both massive and amygdaloidal, and scattered large blocks of massive basalt. At this locality and others, sub-volcanic dikes of Terrace Point basalt that intrude the fragmental basalt are slightly chilled, and contain small amygdules stretched parallel to, and columnar joints perpendicular to, curvilinear dike margins. The fragmental unit is interpreted as a cinder cone or lahar-type deposit that may have formed by interaction between a basalt feeder and water-saturated sediment.

Sandstone –Jirsa (1984) measured approximately 73 meters of sandstone and 3 meters of shale in this section of the Cut Face Creek sandstone, but reported overall that nearly 30 percent of it is composed of thinly bedded, graded layers of fine-grained sand, silt, and clay. He reports both symmetrical and asymmetrical ripple marks, and bimodal paleocurrent distribution, and concluded that the Cut Face Creek sandstone was deposited in a fluvial-lacustrine environment. Unlike nearly all the other exposed interflow sandstones within the NSVG, planar cross-bedding is predominant, but some trough cross beds are present near the top of the section. Other features that may be visible in the sandstone are desiccation cracks filled with sandstone or coarse pink zeolite minerals, and rip-up textures. Compositionally it is predominantly a lithic arkose composed mostly of plagioclase feldspar and mafic rock fragments, with lesser amounts of quartz, altered clinopyroxene, and opaque grains; cemented by calcite and zeolite.

The base of the sandstone is exposed to the north in the Cut Face Creek valley, where it overlies the Good Harbor Bay andesite (see stop 21B). The Cut Face Creek Sandstone was earlier considered to represent clastic deposition during a significant hiatus in volcanism prior to eruption of the Terrace Point/Schroeder-Lutsen basalts. It was also considered to be somewhat unique in that it was one of the few thick sandstone units in the northeast limb of the North Shore Volcanic Group, along with the 68 meter thick Indian Camp sandstone (which is within the Schroeder-Lutsen basalts). However, recent remapping has shown that there are likely at least three more substantially thick sandstone units that occur within the lower series of lava flows to the north of the Good Harbor Bay lavas. Thus, it is now recognized that the Cut Face Creek and Indian Camp sandstones, exposed because of more active erosion near the Lake Superior coast, are only one part of a larger set of thick sandstone units (Figure 10), some of which are located over 5 miles inland and at least 500 and possibly more than 1,000 meters down-section from here.

The recognition of thick interflow sandstones throughout several different series of lava flows at different stratigraphic levels implies active sedimentation during a prolonged period of volcanism. Fragmental flow tops in the Good Harbor Bay Lavas contain abundant sandstone infillings, and thin, discontinuous, layers and crack fillings (clastic dikes) of sandstone are common in the Schroeder-Lutsen basalts. Elevated levels of clastic deposition during active volcanism may account for the relative abundance of sand at the tops of the lava flows, and the thick interflow sandstones may have formed during periods of relative volcanic quiescence, but continued basin subsidence. Available data indicate that the thicker sandstones may vary in thickness along strike, consistent with deposition onto an irregular lava surface.

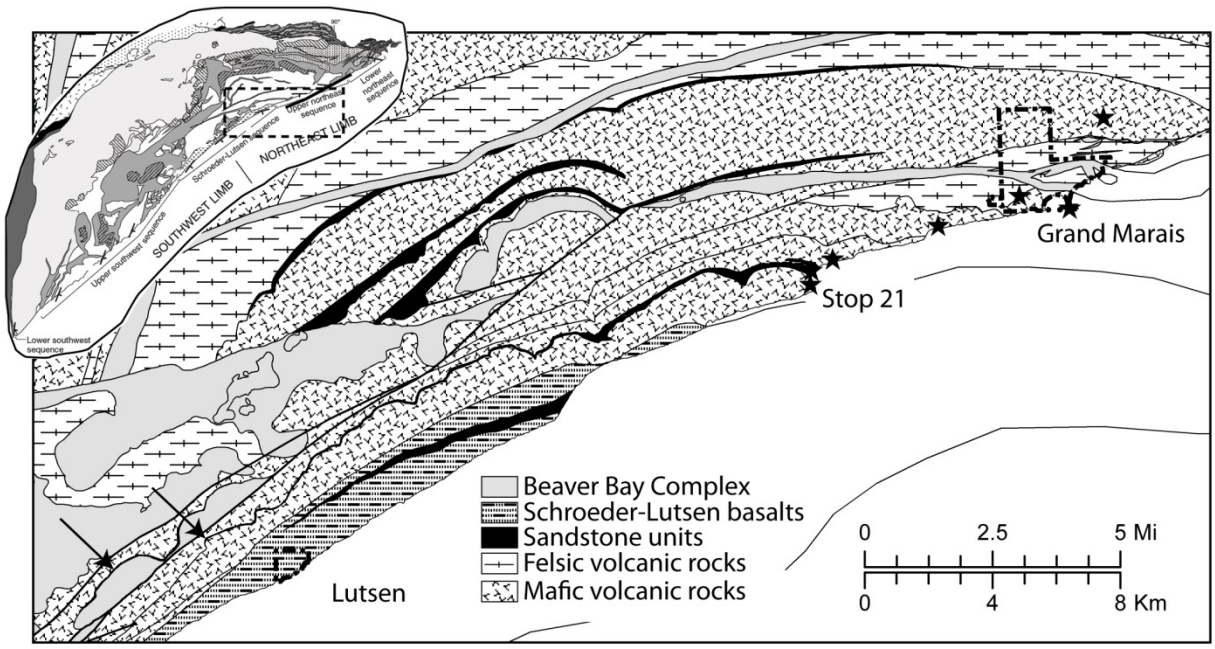


Figure 10. Simplified geologic map showing the distribution of sandstone units in the northeast limb of the NSVG. The black arrows at the lower left indicate thin sandstone units (one of which is the southwestern extension of the Cut Face Creek Sandstone at stop 21).

DIRECTIONS: Drive back towards Grand Marais a short distance to the wayside rest parking area on the lake side of the highway.

STOP 21B – Traverse up Cut Face Creek; Good Harbor Bay andesites, Cut Face Creek sandstone

Location: UTM (NAD 83, Zone 15T): 691953E, 5289526N Good Harbor Bay quadrangle. See index map for stop 21A.

Description: Small outcrop directly across highway from parking area and to northeast, and outcrops at the mouth of Cut Face Creek are fine-grained, brownish-gray, sparsely porphyritic Good Harbor Bay andesite. The andesite here is overlain by the Cut Face Creek sandstone, and the contact is exposed in numerous locations in the meandering Cut Face Creek valley. The basal contact appears to be conformable with the flat-surfaced, uneroded, amygdaloidal andesite. Small pebbles of massive to amygdaloidal andesite are common in the lower 3 meters of the sandstone, typically in 3-25 cm thick planar cross-bedded pebbly beds. The upper part of the andesite typically contains stretched amygdules, and has cracks filled with sandstone (Figure 11).

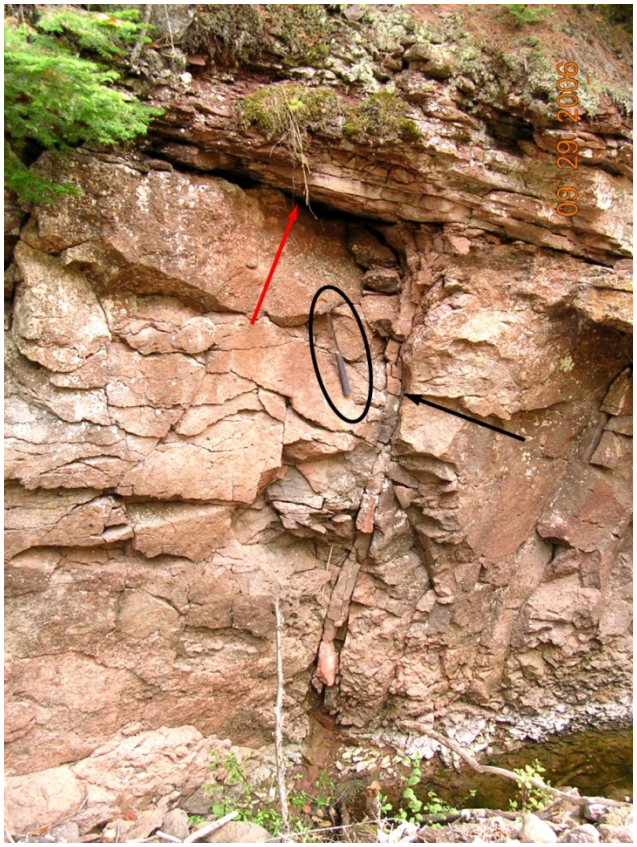


Figure 11. Photograph of base of Cut Face Creek sandstone (red arrow and above), showing clastic dike (black arrow) filling a crack in underlying andesite. Hammer in ellipse is 45 cm long.

REFERENCES

Boerboom, T.J., Wirth, K., 2014, and Evers, J.F., 2014, Five newly acquired high-precision U-Pb ages in Minnesota, and their geological implications [abs]: Institute on Lake Superior Geology, May 14-17, 2014, Proceedings Volume 60, Part 1 – Programs and Abstracts, p.13-14.

Boerboom, T.J., and Green, J.C., 2013, Bedrock geology of the Marr Island and Hovland quadrangles, Cook County, Minnesota: Minnesota Geological Survey Miscellaneous Map Series Map M-195, scale 1:24,000.

Boerboom, T.J., and Green, J.C., 2011, Bedrock geology of the Kadunce River quadrangle, Cook County, Minnesota: Minnesota Geological Survey Miscellaneous Map Series Map M-190, scale 1:24,000.

Boerboom, T.J., and Green, J.C., 2010, Bedrock geology of the Grand Marais quadrangle, Cook County, Minnesota: Minnesota Geological Survey Miscellaneous Map Series Map M-189, scale 1:24,000.

Boerboom, T.J., and Green, J.C., 2008, Bedrock geologic map of the Deer Yard Lake and Good Harbor Bay quadrangles, Cook County, Minnesota: Minnesota Geological Survey Miscellaneous Map Series Map M-179, scale 1:24,000.

Boerboom, T.J., Green, J.C., and Albers, P.B., 2007, Bedrock geology of the Lutsen quadrangle, Cook County, Minnesota: Minnesota Geological Survey Miscellaneous map M-174, scale 1:24,000.

Carmichael, I.S.E, 1964, The petrology of Thingmuli, a Tertiary volcano in eastern Iceland: Journal of Petrology 5, p. 435-460.

Davis, D.W., and Green, J.C., 1997, Geochronology of the North American Midcontinent Rift in western Lake Superior and implications for its geodynamic evolution: Canadian Journal of Earth Sciences, v. 34, no. 4, p. 476-488

Fitz, T.J., III, 1988, Large felsic flows in the Keweenawan North Shore Volcanic Group in Cook County, Minnesota: unpubl. M.S. thesis, University of Minnesota-Duluth, Duluth, MN; 165 p.

Green, J.C., Boerboom, T.J., Schmidt, S.Th., and Fitz, T.J., 2011, The North Shore Volcanic Group: Mesoproterozoic plateau volcanic rocks of the Midcontinent Rift System in northeastern Minnesota: Geological Society of America Field Guide 24, Trip number 7, p. 121-146; Miller, J.D. Jr. Houdak, G.J., Wittop, C, and McLughlin, P.I, eds.

Green, J.C., 2002, Volcanic and sedimentary rocks of the Keweenawan Supergroup in northeastern Minnesota, *in* Miller, J.D., Jr., Green, J.C., Severson, M.J., Chandler, V.W., Hauck, S.A., and Wahl, T.E., Geology and mineral potential of the Duluth Complex and related rocks of northeastern Minnesota: Minnesota Geological Survey Report of Investigations 58, p. 94-102.

Green, J. C., Davis, D.W., and Schmitz, M.D., 2001, Three new zircon dates for the Midcontinent Rift, North Shore, Minnesota: More data, more questions: Institute on Lake Superior Geology, 47th Annual Meeting, Madison, Wis., Proceedings, pt. 1, Programs and Abstracts, p. 29.

Green, J.C., Bornhorst, T.J., Chandler, V.W., Mudrey, M.G., Jr., Myers, P.E., Pesonen, L.J., and Wilband, J.T., 1987, Keweenawan dykes of the Lake Superior region: Evidence for evolution of the Middle Proterozoic Midcontinent Rift of North America, *in* Halls, H.C., and Fahrig, W.F., eds., Geological Association of Canada special paper 34, Mafic Dyke Swarms, Publication No. 0120 of the International Lithosphere Program, p. 289 – 302.

Green, J.C., and Fitz, T.J. III, 1993, Extensive felsic lavas and rheoignimbrites in the Keweenawan Midcontinent Rift plateau volcanics, Minnesota: petrographic and field recognition: Journal of Volcanology and Geothermal Research, v. 54, p. 177-196.

Hoaglund, S.A., Miller, J.D., Jr., Crowley, J.L., and Schmitz, M.D., U-Pb zircon geochron9llgy of the Duluth Complex and related hypabyssal intrusions: Investigating the emplacement history of a large multiphase intrusive complex related to the 1.1 Ga Midcontinent rift.

Jirsa, M.A., 1984, Interflow Sedimentary Rocks in the Keweenawan North Shore Volcanic Group, Northeastern Minnesota; Minnesota Geological Survey Report of Investigation 30, 20 p.

Jones, N.W., 1963, The relationship between the Duluth Gabbro and the dikes and sills in the vicinity of Hovland: Minneapolis, University of Minnesota, M.S. thesis, 90 p.

Miller, J.D., Jr., and Green, J.C., 2002, Geology of the Beaver Bay Complex and related hypabyssal intrusions, *in* Geology and mineral potential of the Duluth Complex and related rocks of northeastern Minnesota: Minnesota Geological Survey Report of Investigations 58, p. 144-163.

Ojakangas, RW., Dickas, A.B., and Green, J.C., eds., 1997, Middle Proterozoic to Cambrian rifting, central North America: Geological of Society Special Paper 312, 322 p.

Paces J.B., and Miller, J.D., Jr., 1993, Precise U-Pb ages of Duluth Complex and related mafic intrusions, northeastern Minnesota: Geochronological insights to physical, petrogenetic, paleomagnetic, and tectonomagmatic processes associated with the 1.1 Ga Midcontinent Rift System: Journal of Geophysical Research, V. 98, No. B8, p. 13,997-14,013.

Vervoort, J.D., Wirth, K., and Kennedy, B., 2007, The magmatic evolution of the Midcontinent rift: New geochronologic and geochemical evidence from felsic magmatism: Precambrian Research, vol. 157, no. 1-4, p. 235-268.

FIELD TRIP 9

Saturday, May 7, 2016

DULUTH HARBOR GEOLOGIC HISTORY BOAT CRUISE - PLEISTOCENE TO ANTHROPOCENE

Dr. Andy Breckenridge (University of Wisconsin-Superior; Natural Sciences Department)
Todd Kremmin (University of Minnesota-Duluth; Dept. of Earth & Environmental Sciences)
Eric Dott, P.G. and Irvin Mossberger, P.G. (Barr Engineering, Duluth, MN)

"there is nothing -- absolutely nothing -- half so much worth doing as simply messing about in boats"

-Wind in the Willows by Kenneth Grahame

Introduction

The St. Louis River flows into western Lake Superior to create one of the most remarkable coastal systems on the Great Lakes - the St. Louis estuary and harbor (Figure 1). The system is a ria, a coastal inlet formed by submergence of a former river valley. Post-glacial rebound drives the modern submergence of the St. Louis River valley, which probably began around 1000 years ago, but this is only the most recent of at least three periods of submergence, the first two of which were succeeded by lake level lowering and downcutting of the former lake plain. Morning stops highlight a few recent efforts to improve our understanding of the coastal morphology and geologic history of the western basin. These include Minnesota Point, the longest freshwater baymouth bar in the United States, and a tour of the RV *Blue Heron*, the only UNOLS research vessel on the Great Lakes. In the afternoon we will board the *Vista Queen*, a commercial tourist vessel, to draw attention to modern environmental challenges within the estuary. The harbor is the largest and busiest on the Great Lakes, and the long history of industry led to the St. Louis River being one of many federally designated "Great Lakes Areas of Concern," which are targeted for remediation and restoration due to severe environmental degradation. At the forefront of these restoration efforts are geoscientists. We hope that a cruise along the river will reveal that despite development, the St. Louis estuary is an urban wilderness waterway, with exceptional recreational opportunities and a natural beauty that rivals the Great Lake.

Background

The Pleistocene

The Superior Lobe of the Laurentide Ice Sheet filled the western Lake Superior basin during the last glacial maximum. Superior Lobe sediments are distinguished by a striking red color created by erosion of redbed sandstones and mafic igneous rock that underlie the lake. Ice retreat took thousands of years, and was punctuated by multiple readvances. Determining the extent of retreat prior to each readvance is challenging because readvances bury and often erode older landforms and sediments. Multiple Superior Lobe till sheets have been mapped. Younger tills are enriched in silt and clay upsection, suggesting that successive readvances overrode clay-rich glaciolacustrine sediments from pro-glacial lakes that formed after the ice front retreated to positions within the Lake Superior drainage basin.

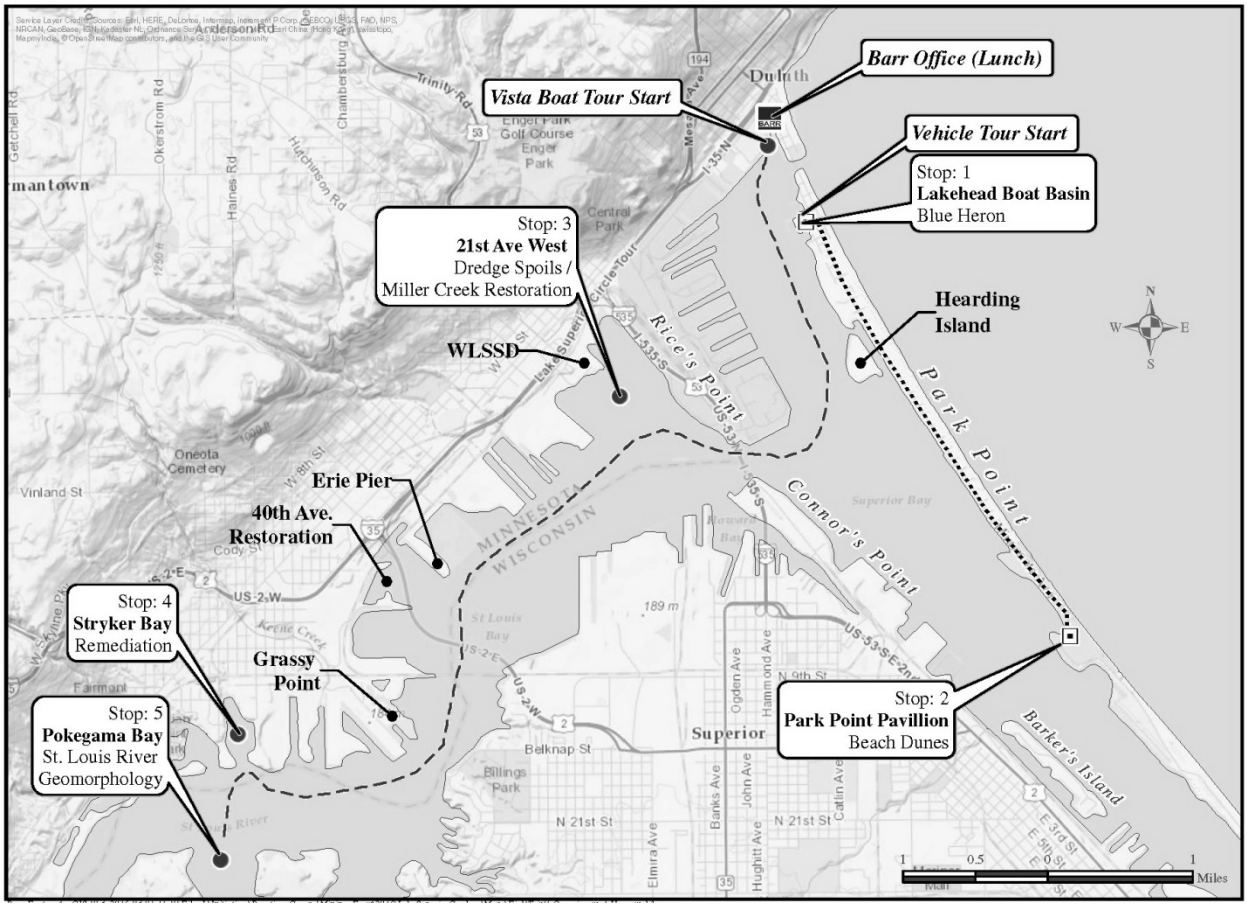


Figure 1. Field Trip 9 Overview: St. Louis River, Park Point, and Field Trip Stops.

In the western Lake Superior basin, most of the glaciogenic sediment has been mapped as the Barnum Formation (Hobbs, 2003; Knaeble and Hobbs, 2009; Johnson et al., 2016). Within the Barnum Formation are three texturally distinct tills (i.e. members). The youngest tills are the Moose Lake and Knife River members. Between these two tills are deltaic and lacustrine sediments mapped as the Wrenshall Member, which were deposited in glacial Lake Wrenshall (Figure 2A; Wright et al., 1970; Johnson et al., 2016). Glacial Lake Wrenshall (also referred to as an early phase of glacial Lake Duluth) was a pro-glacial lake fronted by Superior Lobe ice within the Lake Superior basin (Breckenridge, 2013). Overflow of glacial Lake Wrenshall routed initially through the Moose Lake (or Portage) outlet into the Kettle River, but ice margin retreat opened the slightly lower Brule outlet into the St. Croix River (Figures 2A, 3). At this time, lake levels within the St. Louis estuary were at around 325 m (~1070 ft) above sea level, probably at the Epi-Duluth level (Figure 4). The ancestral St. Louis River entered the lake just downstream of the area which is now Jay Cooke State Park and deposited deltaic sediment that has not been mapped in detail. Because the ancestral St. Louis River drained meltwater and glacial lakes associated with the Rainy Lobe to the north (Figure 2A), the discharge must have been far greater than for the modern river. Finer-grained lacustrine sediments were deposited distal to the river mouth, including glacial varves (Wright et al., 1970; Knaeble and Hobbs, 2009; Hobbs and Breckenridge, 2010). Clay associated with these lacustrine sediments was quarried for bricks, near the town of Wrenshall during the late 19th and early 20th centuries (Grout, 1919).

The timing of glacial Lake Wrenshall is poorly constrained. Basal radiocarbon dates from kettle lakes on the Nickerson moraine, (which precedes Lake Wrenshall), suggest the lake is at least as old as 12,800 cal

yr BP (~10.8 ^{14}C ka), but these are minimum ages and likely lag ice retreat (Florin and Wright, 1969). Spruce logs have been dated to as old as 11,700 cal yr BP (~10.1 ^{14}C ka) on the former Lake

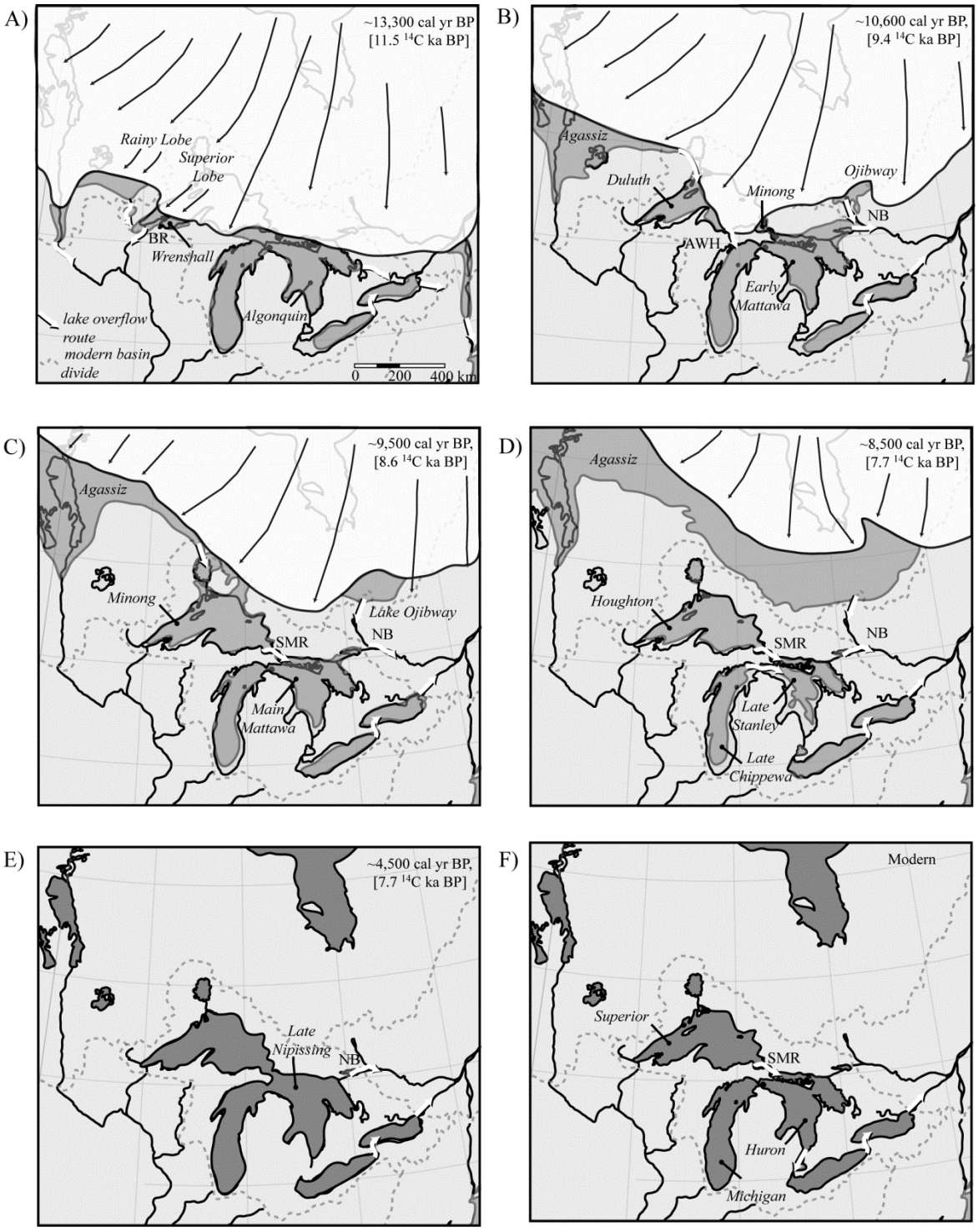


Figure 2. Selected paleogeographic reconstructions of the Great Lakes region through time (adapted from Breckenridge et al., 2010). Outlets for glacial lakes are provided by white arrows. Lake Superior outlets varied through time, and include the Brule (BR), Au train-Whitefish (AWH), St. Mary's River (SMR), and North Bay (NB).

Wrenshall lake plain in Wisconsin and Michigan, which necessitates lake levels lowered below the Brule outlet by this time (Black, 1976). This requires that the Superior Lobe retreated far enough to the northeast to open lower elevation routes into the Lake Michigan basin. This would have resulted in the first period of downcutting of the former lake plain by the St. Louis River within the reach that is now the St. Louis estuary. Note that a disconformity from this period of low lake levels has not been found within the western basin, but the area lacks detailed stratigraphic research.

The radiocarbon dated logs on the former Lake Wrenshall plain were buried by red clayey till, therefore the Superior Lobe re-advanced, blocked routes into the Lake Michigan basin, and raised lake levels back to the Brule outlet. This advance, known as the Marquette Advance in the eastern Lake Superior basin, created glacial Lake Duluth. The name Lake Duluth originates from Leverett (1928) after a series of prominent gravel beaches in the city of Duluth described by early geologists (Taylor, 1894). The Duluth level follows in a general way Skyline Parkway, but development and construction within the city of Duluth have obscured evidence of the strandline. Notable locations along Skyline Parkway that are at the lake Duluth level include a prominent terrace along the Spirit Mountain ski slope, the 1st United Methodist Coppertop church, and Heller Hall on the University of Minnesota Duluth campus where the Department of Geological Sciences is housed (Hobbs and Breckenridge, 2013). At the Lake Duluth level, overflow routed through the Brule outlet into the St. Croix River for a second time. Eventually ice retreat once again opened eastern outlets to the Lake Michigan basin causing lake levels to fall. Unlike the prior phase of lower levels, which is only inferred by wood on the former lake plain, the geomorphologic record of these lowered levels is preserved by a series of strandlines that are clearly visible on high resolution lidar DEMs (Figure 4; Breckenridge, 2013). Every one of these lower lake levels are named, typically after a town in which a strandline associated with the lake level is found (e.g. Highbridge, Washburn, and Beaver Bay) (Farrand, 1960; Farrand and Drexler, 1985). These strandlines are particularly useful for understanding the nature of glacial isostatic adjustment (GIA) because they can be traced around the basin. Glacial isostatic adjustment (or post-glacial rebound) is the rise of the lithosphere following deglaciation. Rebound rates are highest where the ice was thickest. In the Lake Superior basin, geomorphologic features provide a record of former lake levels (waterplanes) that rise in elevation to the northeast, where ice was thickest (Figure 3). Older waterplanes have undergone a longer period of GIA, and therefore rise more steeply.

The end of glacial Lake Duluth occurred when ice retreat allowed a union with glacial Lake Minong, a lake that initially was limited in extent to Whitefish Bay in southeastern Lake Superior and fronted to the northwest by ice from the Marquette advance (Figure 2B). The merger between glacial lakes Duluth and Minong created a lake that retains the name glacial Lake Minong (Farrand, 1960) (Figure 2C). Glacial Lake Minong drained over a drift-covered bedrock sill, called the Nodaway barrier, into the St. Mary's River (SMR). Progressive downcutting of the drift-covered sill at the St. Mary's River caused falling lake levels in Lake Minong, which include the Minong through post-Minong levels (Figure 2C; Breckenridge, 2013).

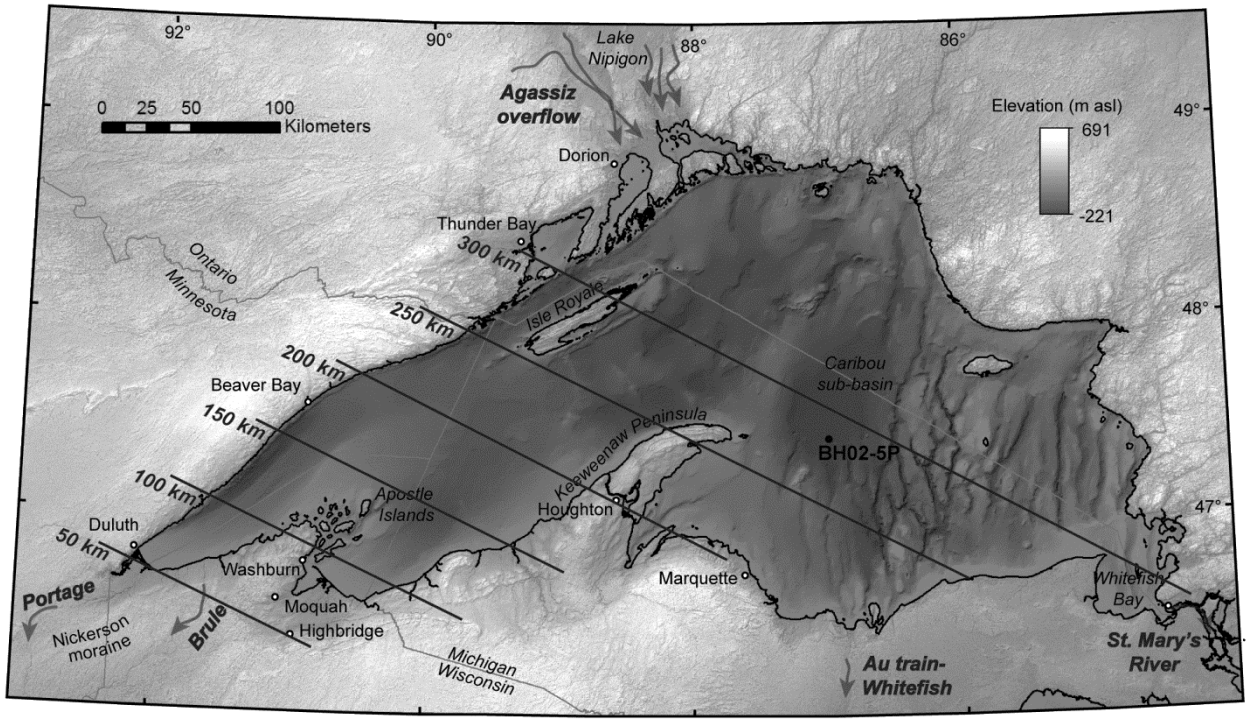


Figure 3. Map of Lake Superior with inlets and outlets (arrows), and contours for glacial isostatic adjustment used in Figure 4.

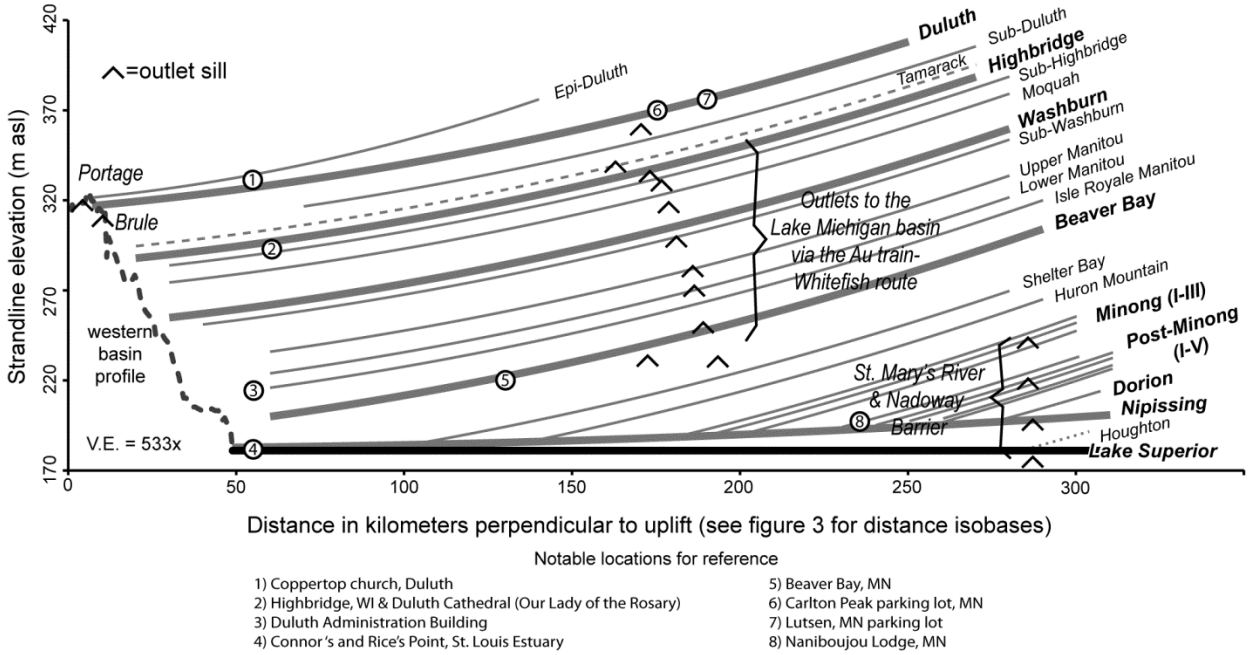


Figure 4. Former waterplanes of Lake Superior (adapted from Breckenridge, 2013).

The Holocene

Not until ~2500 years after the onset of the Holocene ~9100 cal yr BP (8100 ^{14}C yr BP), did glacial meltwater cease to discharge into the glacial Lake Minong (Breckenridge et al., 2004; Hyodo and Longstaffe, 2011). The earliest post-glacial (i.e. post-Minong) lake level is called the Houghton, which was established when the Nadoway barrier was cut down to bedrock at the St. Mary's River (SMR) (Figure 2D). Glacial isostatic adjustment (GIA) depressed the bedrock sill relative to the western basin, which resulted in the lowest lake levels ever in the Twin Ports region, probably 60-m below the modern level. In the Michigan and Huron basins, in situ stumps have been found that establish the immediate, post-glacial lake levels, and they appear to be ~20-m lower that the outlets for each lake (Lewis et al., 2008). This suggests a drier climate created closed-basins. No data has been found from the Superior basin to determine whether or not Lake Superior was a closed-basin lake at this time. By 8300 cal yrs BP, with the onset of a wetter climate, lake levels appear to have risen enough to overflow from Lake Huron into the North Bay outlet, which discharged to the Ottawa River (Figure 2D).

During the early to mid-Holocene, differential GIA caused the outlet for Lake Huron (North Bay) to rise above the elevation of Lake Superior's St. Mary's River (SMR) outlet. Rising levels in Lake Huron drowned the SMR and created a shared waterplane between the Superior, Michigan, and Huron basins known as Lake Nipissing (Figure 2E; Larsen, 1985; Baedke and Thompson, 2000). Lake Nipissing levels peaked in the Huron and Michigan basins at around 4500 cal yr BP (Thompson et al., 2011). At this time, rising lake levels likely breached the basin drainage divide between the Huron and Erie basins, or perhaps the Michigan basin and Mississippi River via the Chicago River (Thompson et al., 2011; Johnston et al., 2012). This resulted in a major shift in the drainage pathway for the upper Great Lakes, from a route into the Ottawa River via North Bay (Figure 2E), to a southern outlet (Figure 2F). Subsequent lake levels dropped due to a combination of sill incision of the new outlet and perhaps climate change (Thompson et al., 2011).

The Lake Nipissing level is commonly referred to as the Nipissing highstand, and strandlines formed at this level are readily apparent across much of the upper Great Lakes. At Sault Ste Marie (SSM), the Nipissing strandline is at 198 meters asl, 16-m above the modern level (Cowan, 1985), but the Nipissing elevation decreases to the west, converging towards modern lake levels due to GIA (Figure 4). Prior studies have suggested that Connor's and Rice's Point were a former baymouth bar formed by lake level rise to the Nipissing level (Loy, 1963; Barlaz, 1983). Longshore drift of sand eroded primarily from the southern shore, combined with sediment sourced from the Nemadji and St. Louis Rivers, likely built a spit across the head of the lake, but there have been no sediment or geomorphic studies to test this hypothesis.

Former lake levels since the Nipissing highstand have been established for Lake Superior by coring and dating foreshore sand deposits from multiple strandplains in the eastern Lake Superior basin (Figure 5; Johnston et al., 2012). The work is an impressive undertaking, and is currently the most detailed paleohydrograph anywhere on the Great Lakes. The data indicate a lake-level drop of almost 4-m shortly after the peak Nipissing, followed by steady lake level lowering until around 1000 cal yr BP; thereafter lake levels have been stable near the Lake Superior outlet. The steady drop in lake levels from 4000 to 1000 cal yr BP was probably the result of GIA; an outlet on the southern side of a basin would have caused lake levels to fall everywhere north of the outlet. Stabilization of lake levels at 1000 cal yr BP is attributed to the separation of Lake Superior from Lake Huron (Johnston et al., 2012). Lake levels have been constant at SSM since this time, but this paleohydrograph must be corrected for GIA to understand former lake levels within the estuary and Twin Ports region. GIA is causing SSM to rise relative to the St. Louis River estuary. For example, gauge data suggest that lake levels in the estuary have risen around 25-cm over the last 100 years due to differential GIA (Mainville and Craymer, 2005).

For this field guide, an empirically derived model of GIA by Lewis et al (2005) has been adapted to correct the Sault Ste Marie paleohydrograph using the isobases of Breckenridge (2013) (Figure 6). The model applies an exponential decay function to estimate the rate of uplift necessary to result in warped strandlines in the Great Lakes of known age (Figure 6B). The modeled GIA correction is poorly constrained and could be in error, but the underlying processes that affected lake levels in the Twin Ports are generally understood. The resultant hydrograph (Figure 6C) suggests rapid drawdown from the Nipissing highstand around 4000 cal yr BP was too fast to be countered by relatively slow rates of GIA, resulting in a rapid lake level drop. Steadily falling lake levels at Sault Ste Marie from 4000 to 1000 cal yr BP were likely countered by GIA in the Twin Ports, which may have resulted in relatively stable lake levels. When lake levels stabilized at Sault Ste Marie at 1000 cal yr BP, lake levels would have risen in the Twin Ports.

This abrupt change to rising lake levels is most likely responsible for drowning the St. Louis River to create the estuary. In addition, the rising lake levels probably initiated formation of Minnesota and Wisconsin Points. Ground penetrating radar surveys of Minnesota and Wisconsin Points suggest that the baymouth bar system is prograding lakeward (Morrison et al., 2015), presumably in response to lake level rise and increased sediment supply. One possibility is that the baymouth bar system is accreting vertically and lakeward on a former beach ridge that is just one of many that comprise a drowned strandplain now buried in the St. Louis Harbor. Evidence for this strandplain exists on the incredibly detailed bathymetric survey of the harbor and estuary completed by William Hearding in 1861 (Figure 7). Testing this model will necessitate detailed sediment and stratigraphic analysis of the harbor and baymouth bar sediments, combined with robust age dating.

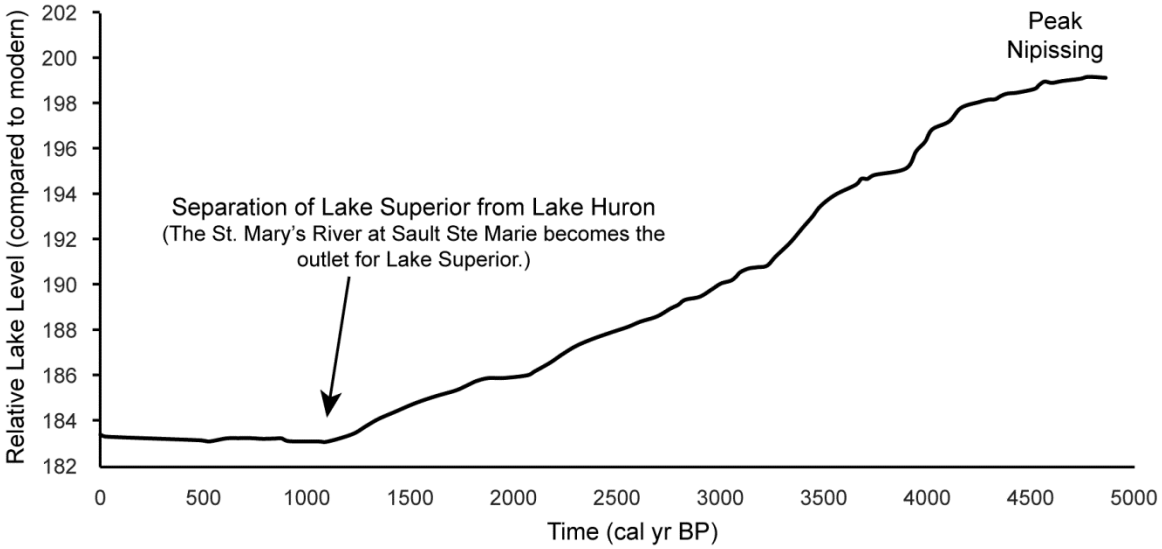


Figure 5. Lake levels at Sault Ste Marie since the Nipissing highstand, adapted from Johnston et al. (2012).

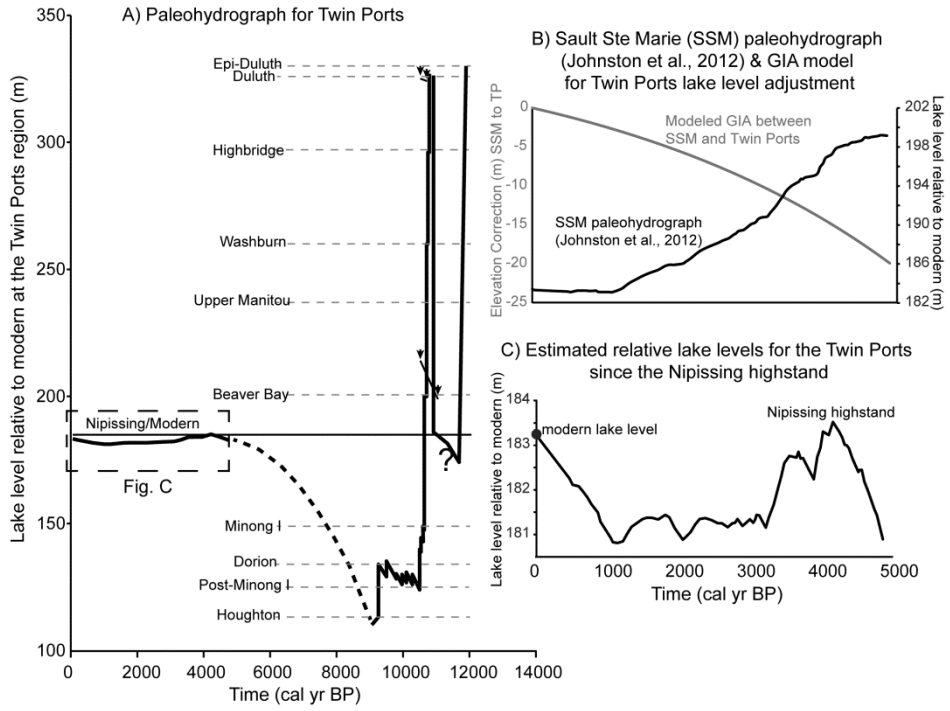


Figure 6. Relative lake level curves for the Twin Ports (unpublished). A) Lake levels since 12,000 cal yr BP include a lowstand that exposes the glacial Lake Wrenshall plain, which is reflooded, presumably due to ice re-advance around 11,500 cal yr BP. Subsequent ice retreat lowers lake level in abrupt drop as new outlets open. The lowest level is the Houghton, which is also the end of glacial Lake Minong. Lake levels rise to the Nipissing due to GIA of the North Bay and St. Mary's River outlets. B) Lake levels since the Nipissing highstand have been constrained Johnston et al., 2012 (see also Figure 5). Differential GIA caused levels to rise relative to Sault Ste Marie (SSM). C) Modeled GIA has been subtracted from the SSM hydrograph to estimate relative lake levels in the Twin Ports.

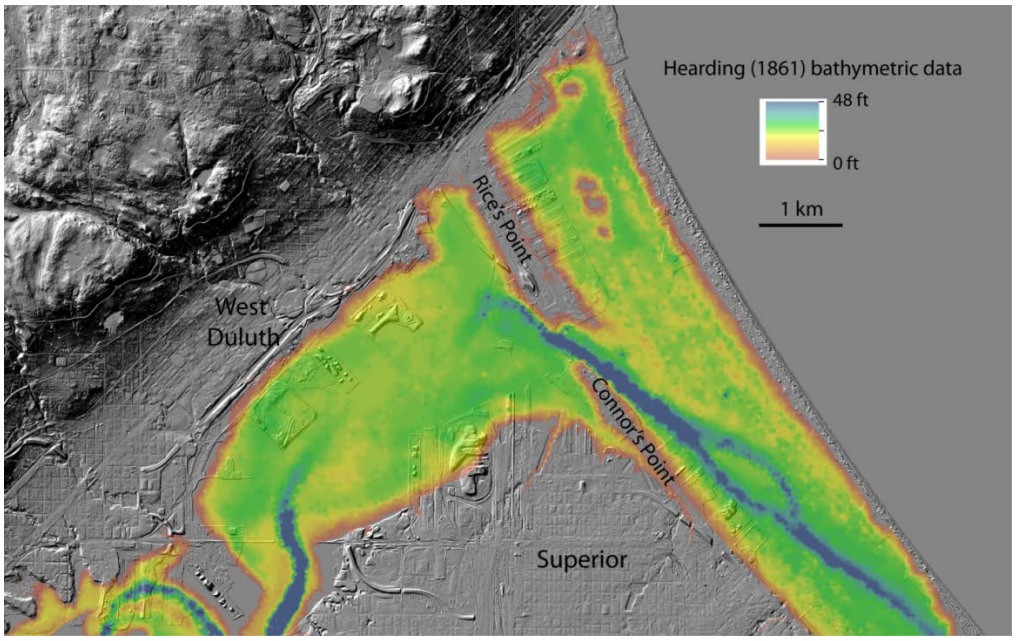


Figure 7. Bathymetric data from Hearding (1861) converted to raster data and overlayed with modern LIDAR DEM. Water depths in the harbor were generally between 6 and 9 feet, except for the deep river channel.

The Anthropocene

Various Native American peoples inhabited the western Lake Superior area throughout the Holocene. After the glaciers receded, Paleo-Indian cultures were the first to inhabit the land, succeeded by Eastern Archaic peoples, until about 1,000 B.C (Dierckins, 2006). The Eastern Archaic peoples gave way to the Woodland cultures, until roughly 1600 A.D. Next were Dakota tribes, who were soon pushed west by the Ojibwe, near the same time as the arrival of the first explorers and gun/fur traders, including Daniel Greysolon, Sieur du Lhut. The 1842 and 1854 Treaties of La Pointe ceded rights of ownership near Lake Superior in areas of Wisconsin and Minnesota respectively, to European settlers in the region, ushering in development of the Industrial Age.

The first iteration of modern locks at Sault Ste. Marie was completed in May 1855. In the Duluth/Superior Harbor, breakwaters were built, a shipbuilding industry began, and commercial fishing was established. Jay Cooke brought the Lake Superior & Mississippi Railroad to Duluth from St. Paul in the 1860's, spurring logging throughout the region, with lumber mills appearing from Rice's Point (Figure 1) to West Duluth (Dierckins, 2006). Grain elevators and railroad docks soon followed, connecting the waterfront to the railway. Other railroads began working their way to Duluth.

In 1870 Duluth incorporated as a city. At this time the Superior Entry was the only waterway connecting Lake Superior to the Duluth/Superior Harbor. Soon after, the Duluth Shipping Canal was built from 1870 to 1877. This new connection to the lake changed the currents and hydrodynamics of the harbor.

In the 1880's, with the development of the Mesabi, Cuyuna, and Vermillion Iron Ranges, iron ore shipping began, along with the subsequent construction of docks to handle the ore. In 1907 Duluth surpassed New York City in shipping tonnage (Dierckins, 2006). The United States Steel Corporation began construction of a steel plant at Spirit Lake around this time. Shipbuilding operations were founded in Superior and later Riverside around the time of the two World Wars. The uppermost reach of the St. Louis River estuary became constrained by the Fond du Lac Dam in Jay Cooke State Park, when its construction was completed in 1924. In 1959 the St. Lawrence Seaway was created, allowing large ocean vessels into the Port. To accommodate ever-larger ships, navigational dredging deepened the harbor in shipping channels, and the dredge spoils were used variously as fill for the port, to create man-made islands (e.g., Barker's Island, Figure 1), and the 90-acre Erie Pier dredge disposal facility. Recently, dredge spoils have begun to be beneficially reused to restore habitat at the 21st Ave. W. (Stop 3), 40th Ave. W., and Grassy Point sites (Figure 1).

The Western Lake Superior Sanitary District (WLSSD) treatment plant began operating in September 1978, consolidating 17 inadequately treated wastewater discharges. Water quality in the St. Louis River rapidly improved from essentially a sewer condition to becoming suitable again for fishing and recreation. The St. Louis River Great Lakes Area of Concern (AOC) was established in 1987 by the EPA. Work continues today to remove several beneficial use impairments from the AOC. For example, river sediment cleanup projects have been initiated at Stryker Bay (Stop 4) and the Former US Steel plant upstream at Spirit Lake. A revitalization plan for West Duluth neighborhoods was begun in 2012 to capitalize on the neighborhood's unique location along the St. Louis River corridor. Today, the harbor still handles many commodities ranging from coal, iron ore, grain, and limestone to cement, salt, wood pulp, wind turbine components and other heavy equipment.

Field Trip Stops

Vehicle Tour (meet at Stop 1 at 9:00am)

Stop 1: Blue Heron Research Vessel – Lakehead Boat Basin (Breckenridge)

Location: UTM Zone 15, 569377E 5180363N

The RV *Blue Heron* is part of the fleet of University National Oceanographic System (UNOLS) vessels and is operated by the Large Lakes Observatory at the University of Minnesota Duluth as a charter vessel for research scientists. The vessel was built in 1985 for fishing the Grand Banks, but was sold to the University of Minnesota and converted for research in 1998. Over the last 18 years many researchers have used a wide array of equipment aboard the *Blue Heron* to extend our knowledge about the geologic and modern history of Lake Superior. Notable equipment includes acoustic seismic profilers that operate on a range of frequencies for imaging both shallow and deep sediments, side-scan sonar for imaging the sea floor surface and composition, and a piston corer capable of recovering sediment cores up to 9 meters in length.

At this stop, we can tour the vessel and examine geophysical data collected aboard the Blue Heron from the harbor and greater lake. Examples include side scan sonar images of the harbor and the *Thomas Wilson*, a whaleback freighter that sank just outside the Duluth entrance in 1902. Selected sections from Lake Superior sediment cores BH02-5P, taken aboard the *Blue Heron*, will also be available for inspection. The core sections are on loan from the National Lacustrine Core Repository in Minneapolis where they are permanently archived in cold storage.

Core BH02-5P (Figure 8) is from the deep Caribou sub-basin of Lake Superior, east of the Keeweenaw peninsula (Figure 3). BH02-5P has been correlated with photographs from S62-8, a long gravity core that penetrated to bedrock. By combining these records, 1406 varves (annual couplets) have been measured that overlie a red till and the Cambrian Jacobsville sandstone. The entire record dates to between 9.3 and 8.1 ^{14}C ka BP (11,500-9,100 cal yr BP). The most intriguing aspect of this record is a series of ~36 anomalously thick varves that correlate with those from the northern Lake Superior sub-basins. These varves are at the very top of the glaciolacustrine record, when the ice margin was most distal, and must have resulted from anomalously high sediment and water fluxes into the Superior basin (Breckenridge et al., 2004; Breckenridge, 2007). In the Isle Royale trough, these individual varves can be up to 14-cm thick. Presumably this 36-year event of anomalously high sediment flux was caused by abnormally high discharge by the ice sheet, or by the influx of anomalously great overflow from glacial Lake Agassiz which spilled into the basin (Figure 2C). These great floods of water may have caused short term rises in lake levels in the Michigan, Huron, and Superior basins; presumably the flux of water was too great to be accommodated by outlet channels. Evidence for rapid, short term increases in water level at around this time, perhaps 12-m or more, is found in small lakes that appear to be flooded by sediments from Lake Superior, including Fenton Lake (Breckenridge et al., 2010) and Beaver Lake (Fisher and Whitman, 1999).



Figure 8. Glacial varves (annual couplets) from BH02-5P (see Fig.3 for core location). Winter (W) and summer (S) sediment laminae are noted.

Stop 2: – Formation of Minnesota/Wisconsin Point and the St. Louis River Estuary
(Kremmin/Breckenridge)

Location: UTM Zone 15, 572438.5E 5175762.3N. PLS: T.49N., R.14W., S.13, NE1/4.



Figure 9. View of Lake Superior, Duluth Harbor, Superior Bay, Minnesota Point, and Wisconsin Point from Enger Tower, Duluth, Minnesota (October 3rd, 2015). Photographer – Todd Kremmin.

Introduction –
Situated at the southwestern tip of Lake Superior, Minnesota Point and Wisconsin Point form a baymouth bar stretching northwest-southeast between Duluth, Minnesota and Superior, Wisconsin establishing the outer breakwater for the largest and farthest inland freshwater seaport in North America (Figure 9 and 10) (Duluth Seaway Port Authority, 2015). In combination, the baymouth bar of Minnesota and Wisconsin Points is approximately 16 kilometers in length and considered one of the longest freshwater bars in the world (Loy, 1962 & 1963; Bernard and Davidson, 1969). The material necessary for the formation of this sandy baymouth bar is attributed largely to littoral drift of sediments from the south shore of Lake Superior in Wisconsin, as well as secondary sources of sediment derived from outflows of the St. Louis and Nemadji Rivers. Research pertaining to the geomorphic development of the system has remained relatively surficial in nature: examining present day geomorphic structures, surveying bathymetry and topography, collecting surface sediment samples, extrapolating offset boreholes, and comparing analogous marine system bar developments (Merrill, 1939; Loy, 1962 & 1963; Kemp et al., 1978; Thomas and Dell, 1978; Sydor et al., 1979; Barlaz, 1983; Rasid and Hufferd, 1989; Rasid, et al., 1992; Albrecht, 2005; Hobbs, 2009). Moreover, research regarding the development of this baymouth bar in the context of post glacial isostatic rebound of the Lake Superior basin along with lake level variation has not been investigated.



Figure 10. Map view of Lake Superior, Duluth Harbor, Superior Bay, Allouez Bay, Minnesota Point, Park Point, Wisconsin Point, City of Duluth, City of Superior, St. Louis River, and Nemadji River (Google Earth, 2016).

The objective of this thesis research is to enhance previous observations of geomorphic development and continue further investigation into the subsurface of the baymouth bar system using Ground-Penetrating Radar (GPR). 40 kilometers of GPR data using both 250MHz and 100MHz antennae were obtained on Minnesota Point near the Park Point Recreational Area (Figure 11) for this project. To supplement and ground truth the GPR data, 8 vibracores (11.24 meters total) were drilled within the expanse of the acquired geophysical data (Figure 11). All sediment cores underwent Loss On Ignition (LOI) analysis and select portions of the cores were radiocarbon dated to provide chronology to the subsurface system and ultimately extrapolate findings across the entire baymouth bar.

Background –

Ground-Penetrating Radar

GPR is a geophysical method (similar to seismic reflection) which enables indirect insight into the subsurface using radar energy. This geophysical method allows researchers to view large expanses of the subsurface without altering the landscape, uncovering the architectural radar stratigraphy of shallow well sorted fluvial, aeolian, or coastal sediments (Stoker et al., 1997; Jol and Bristow, 2003). Radar signals are "pinged" into the ground and reflected back to a receiver, recording travel times (a proxy for depth) and the variable signatures of properties and materials encountered. Within the region of Minnesota Point and

specifically the Park Point Recreation Area, water saturation and organic content of the subsurface play an important role in the variations of reflections received. A variety of antennas can be used in GPR surveys, higher frequency antennas provide high resolution records, but limit subsurface penetration depths, lower frequency antennas provide deeper penetration depths, but limit resolution. When collected in tight grid spacing (≤1m), a spatially large (3D) volume of GPR data can be observed in planar dimensional slices with depth, permitting views on how systems have geomorphically changed over time at larger scales than traditional core observations.



Figure 11. Map view of Park Point Recreation Area on Minnesota Point. GPR grids – (Grid_Orig, Grid_01, Grid_02, Grid_03) and lines are shown along with core locations - (1A, 1B, 1C, 2A, 2B, 4A, 5A, 6A). (Google Earth, 2016).

Historical Context and Anthropogenic Influences

The baymouth bar made up of Minnesota and Wisconsin Points' remained in a natural state up until the 1860's (Figure 12) (Hearding, 1863; Demeter, 1993; Zenith City, 2016). During this period Duluth had recently paved a railroad under the direction of Jay Cooke. This railroad provided a shaky commercial industry, which began to rival the neighboring city of Superior, Wisconsin. The City of Superior had been commercially well off prior to the increase in population within Duluth simply due to the natural opening

of the baymouth bar. This natural opening, known as the Superior entry, allowed ships to enter from Lake Superior and easily harbor at the shores near the City of Superior. Around 1869 Duluth leaders discussed the idea of developing their own entry, but instead the Superior entry was securely modified with concrete

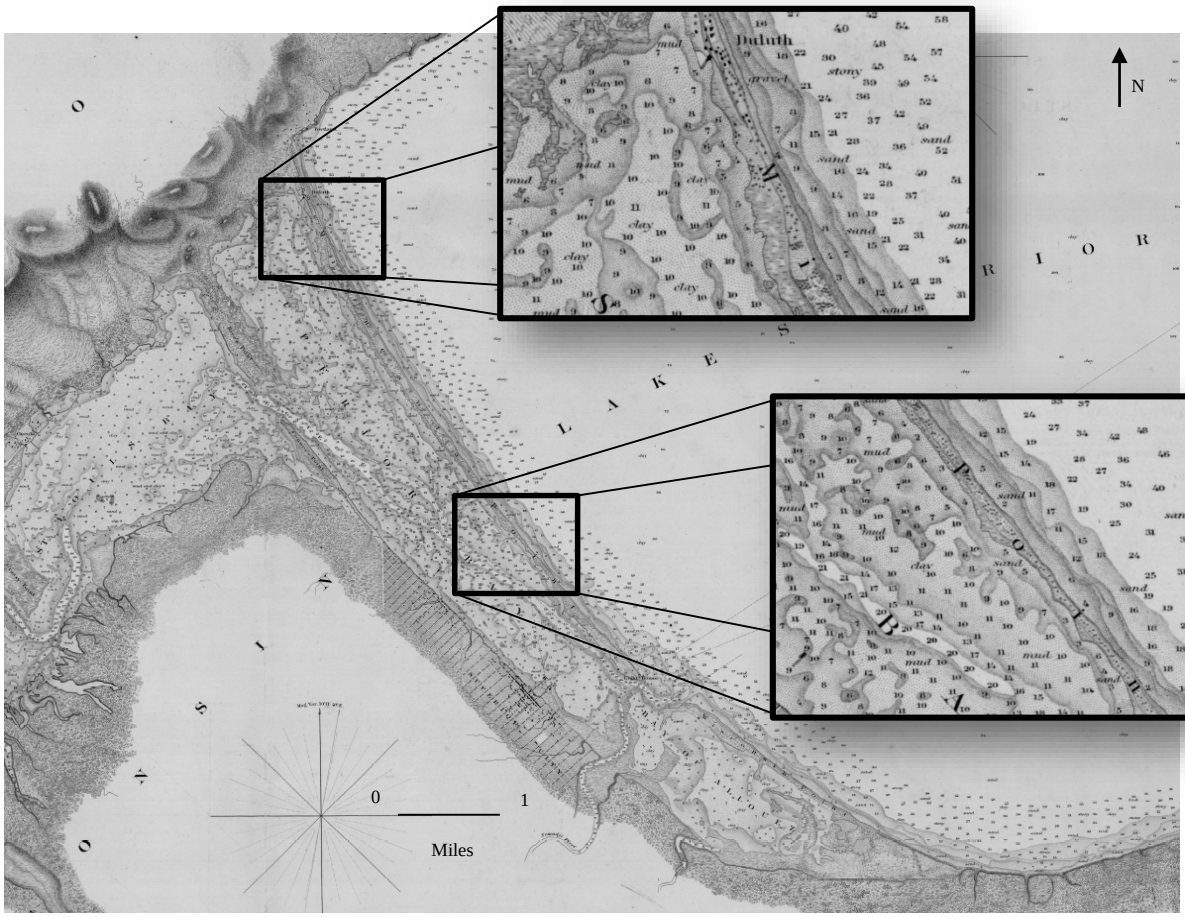


Figure 12. Historical Survey of the Northern and North Western Lakes made in obedience to acts of Congress and under the direction of The Bureau of Topographical Engineers of the War Department. Insets highlight the Duluth Canal prior to excavation (upper inset), along with the Park Point Recreation Area prior to dredge dumping (lower inset). (Hearding, 1863).

breakwaters in 1869 by the U.S. Army Corps of Engineers (Demeter, 1993). Outraged, Minnesota leaders lobbied for their own ship canal, and, in 1870, began dredging. Businessmen of Superior filed a federal suit against these actions, fearing a new canal would diminish the City of Superior's commercial industry. Shortly before the courier could arrive with the U.S. Supreme Courts orders to desist from excavating the canal, legend has it that all available citizens of Duluth had picked up their shovels and hand dug the remainder of the canal. This legend may be exaggerated, as other accounts claim the dredging operations handled most of the excavation. Regardless, a new unnatural entry had been built and marked the beginnings of the anthropogenic influences of the baymouth bar system (Zenith City, 2016). Following the establishment of the "Twin Ports," dredging operations have been ongoing and extensive to keep channels open for shipping vessels.

In the mid 1930's Duluth Parks Superintendent Rodney Paine submitted a proposal to the federal government for $338,000 to develop a new recreation center on Minnesota Point (Figure 13). Unfortunately, this proposal was submitted in the midst of a financial crisis during the depression era,

ending the idea before it even gained attention. President Franklin D. Roosevelt's Works Progress Administration (WPA) program revived the Park Point Recreation Area project, and in 1936 workers brought in approximately 150,000 yards^3 of fill to create new 'land' just south of 43rd street (Paine, 1936). A comparison of natural and man-made land is available to view in Figure 14. This historical context has relevance to this thesis project because a considerable amount of GPR data was collected on this new land made up of dredge material. These dredge spoils consist mainly of silty-sand and pebbles and can be readily differentiated between the natural underlying materials in both GPR and core observations.

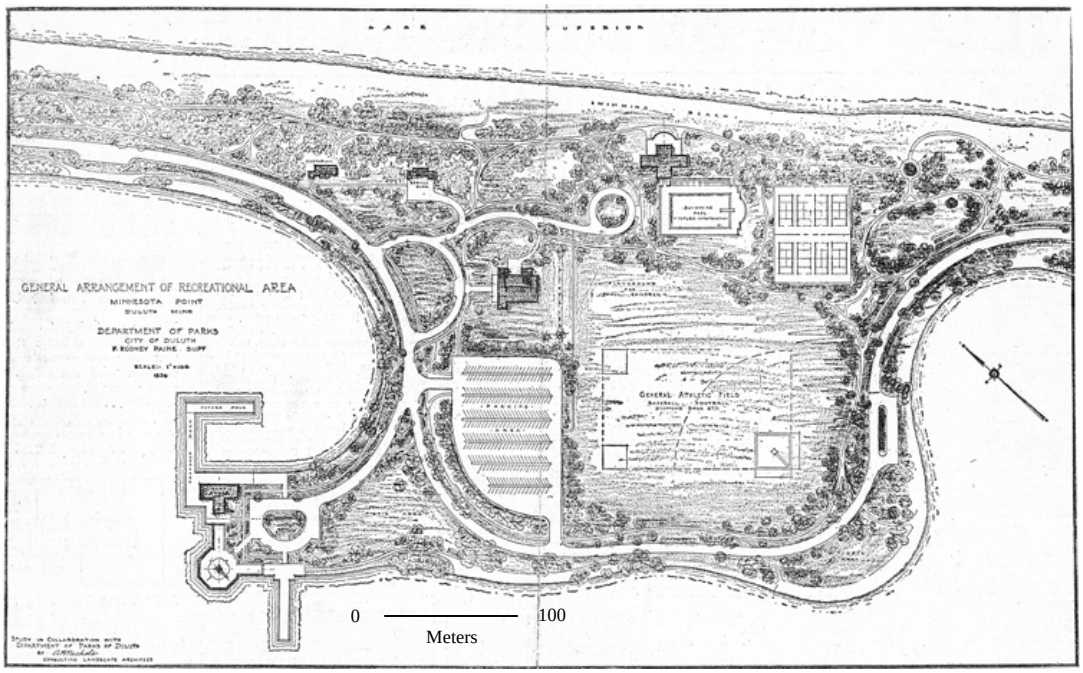


Figure 13. Preliminary drawings of proposed Park Point Recreation Area Project (Zenith City Online, 2016).

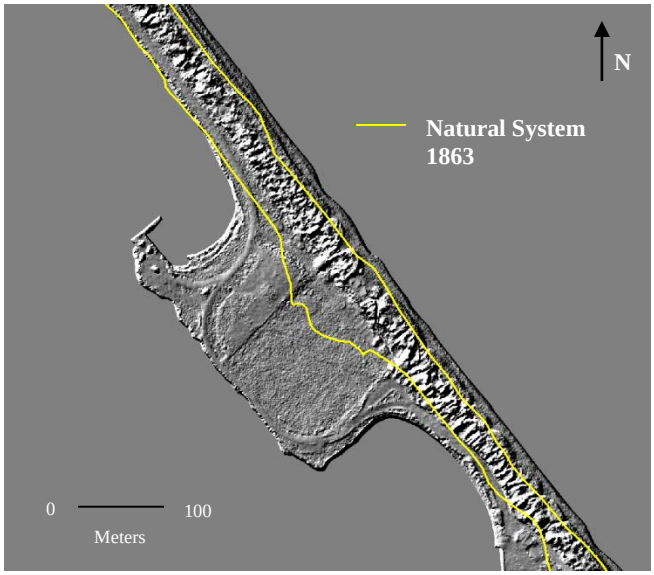


Figure 14. LiDAR map showing existing Park Point Recreation area and Minnesota Point system (grayscale). Natural Minnesota Point system (yellow) (Hearding, 1863; DNR LiDAR Data, 2016).

Results -

The most prominent grid - (Grid_02) (Figure 15) is 85m x 85m, with 1.0m spacing between lines, 0.05m step size, 0.25m antennae separation, and was collected in a half day using the 250 MHz Noggin Smartcart™ from Sensors & Software, Inc. Select planar slices were chosen showing amplitude variation of the evolving geomorphic system in 0.1m intervals (Figures 16 and 17). The lower right corner of each grid slice is North. Cross sections of GPR data are presented in Figures 18 and 19.



Figure 15. Map view of Park Point Recreation Area on Minnesota Point. GPR Grid_02 is shown with cross section lines A-A' and B-B' - please reference Figures 18 and 19 to view cross sections (Google Earth, 2016).

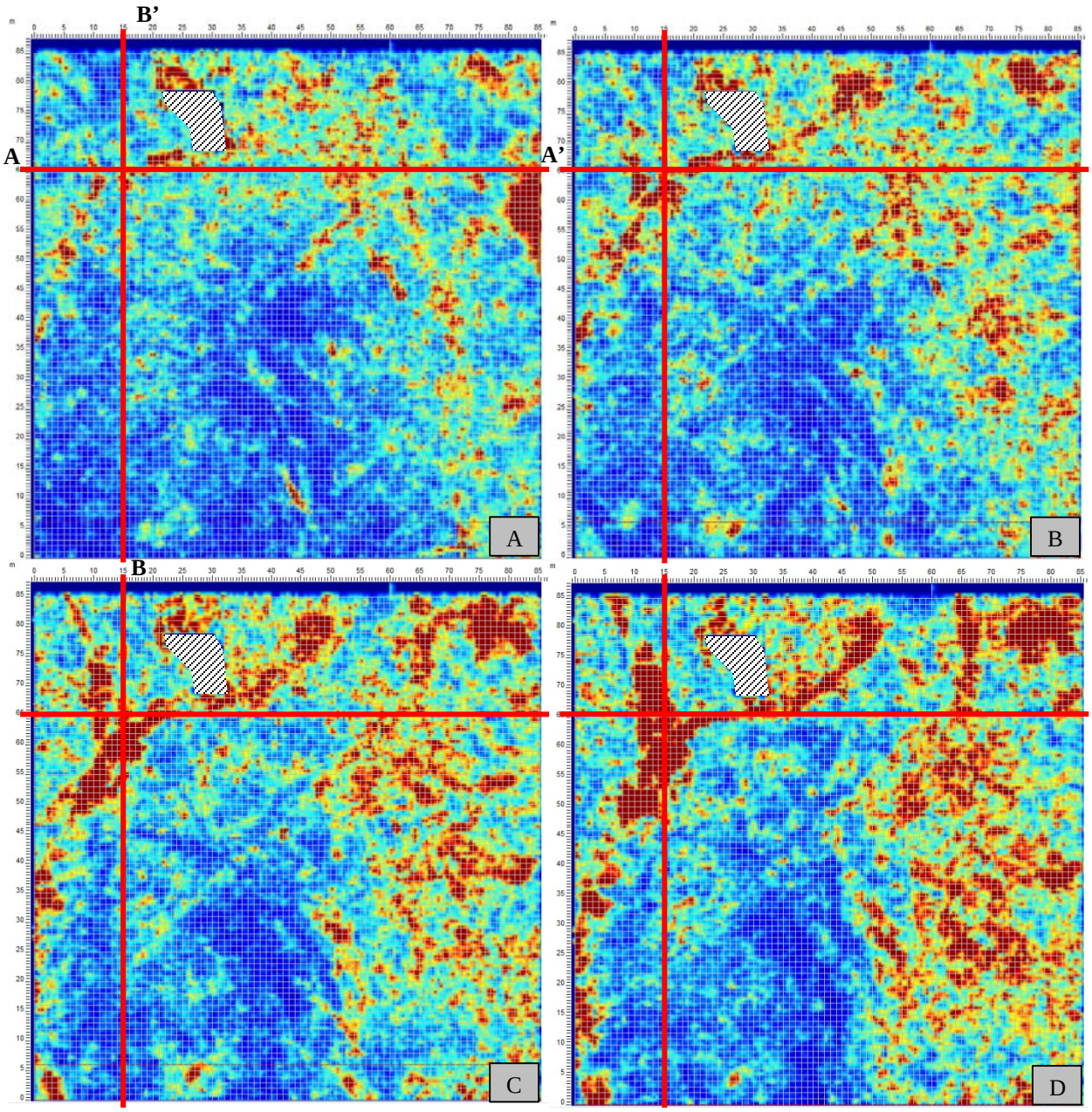


Figure 16. Grid_02 planar depth slices showing amplitude variation (red-high amplitude, blue-low amplitude). Variations in amplitude are believed to be derived from water and organic content variability in the subsurface (i.e. red = changing water/organic content with depth, blue = no change in water/organic content with depth). The lower right corner of each grid slice is North. Crosshatched region contains no data. Depths slices are indicated as the following intervals: A) 0.7-0.8m, B) 0.8-0.9m, C) 0.9-1.0m, D) 1.0-1.1m. A-A' and B-B' cross sections – refer to Figure 18 and 19. (*Please refer to original color version for precise amplitude variation analysis in upcoming master's thesis – Todd Kremmin UMD '16*).

High amplitude coherent variations of radar energy are visible (red) with depth beginning from 0.7m-1.5m. These coherent packages seem to migrate North-Northwest over time and extend from Superior Bay towards Lake Superior/Duluth (Figures 16 and 17). Medium to lower amplitude variations of radar energy (yellow-blue) do not have as coherent of patterns in these depth ranges. Figure 16 (C) and (D) and Figure 17 (A) and (B) show blotchy medium-low amplitude variation in the right half of the depth slices.

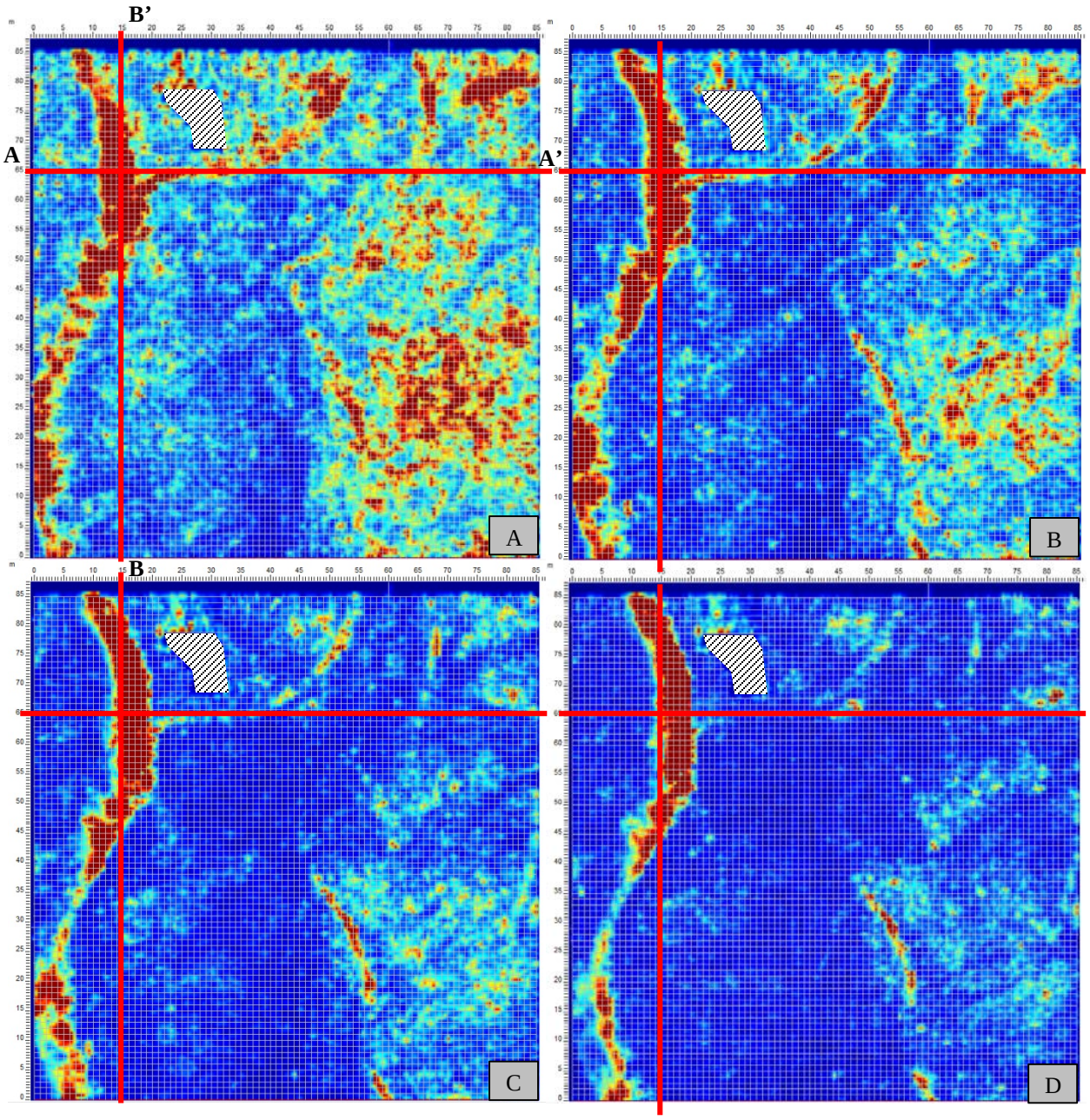


Figure 17. Grid_02 planar depth slices showing amplitude variation (red-high amplitude, blue-low amplitude). Variations in amplitude are believed to be derived from water and organic content variability in the subsurface (i.e. red = changing water/organic content with depth, blue = no change in water/organic content with depth). The lower right corner of each grid slice is North. Crosshatched region contains no data. Depths slices are indicated as the following intervals: A) 1.1-1.2m, B) 1.2-1.3m, C) 1.3-1.4m, D) 1.4-1.5m. A-A' and B-B' cross sections – refer to Figure 18 and 19. (*Please refer to original color version for precise amplitude variation analysis in upcoming masters thesis – Todd Kremmin UMD '16*).

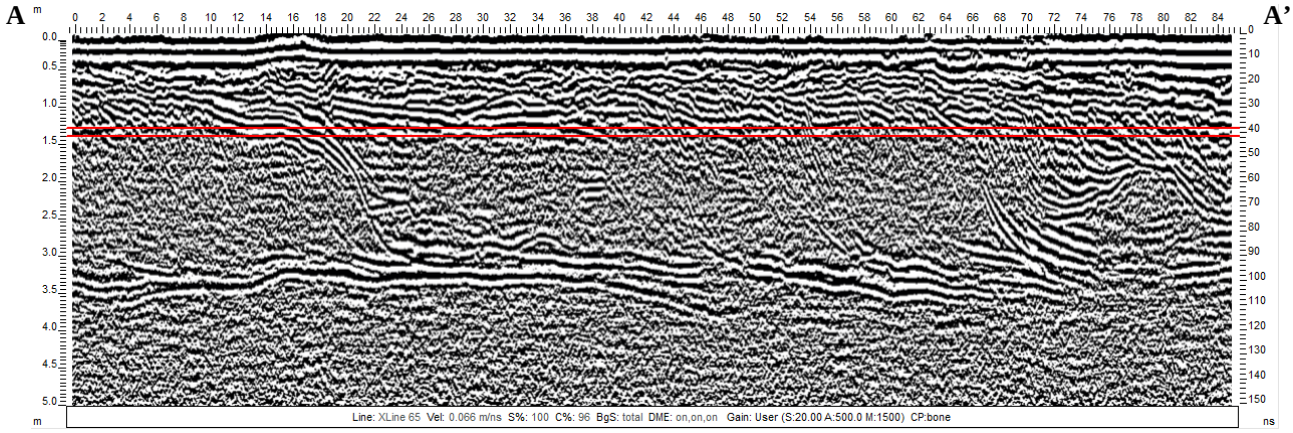


Figure 18. Cross Section GPR line A-A' (Grid_02 Line X65). Depth in meters on left, time in nanoseconds on right, and position lines in meters at top. Red window shows planar depth slice from 1.3-1.4m. 0.0-0.7m is believed to be dredge material. 0.7-3.0m is believed to be dune clinoforms. 3.0-5.0m is thought to be glacio-lacustrine material.

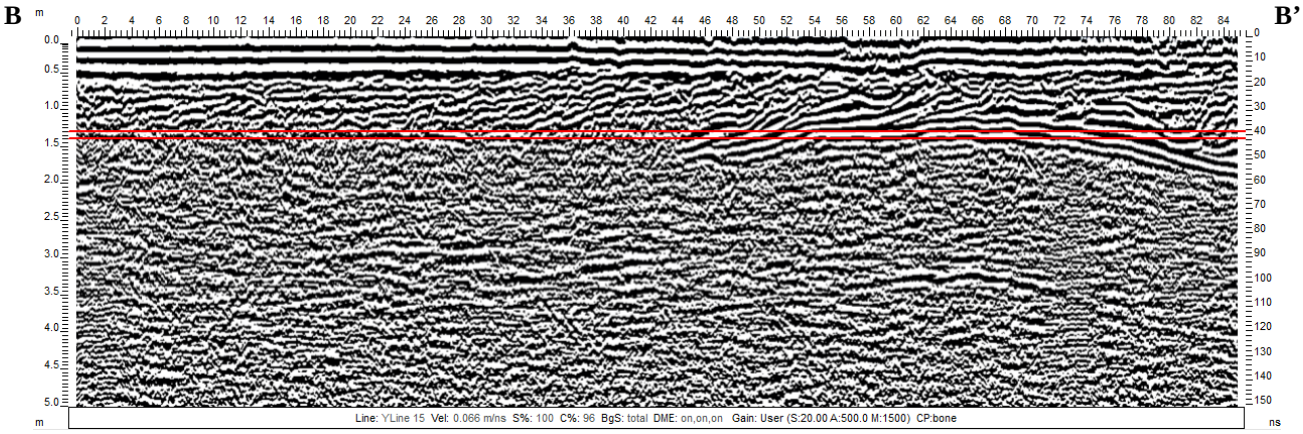


Figure 19. Cross Section GPR line B-B' (Grid_02 Line Y15). Depth in meters on left, time in nanoseconds on right, and position lines in meters at top. Red window shows planar depth slice from 1.3-1.4m. 0.0-0.7m is believed to be dredge material. 0.7-3.0m is believed to be dune clinoforms. 3.0-5.0m is thought to be glacio-lacustrine material

Conclusions -

Subsurface (0.7-3.0m) natural baymouth bar system development in a back bar setting indicates progradational/aggradational migration towards Lake Superior/Duluth. Above this interval (0.7-3.0m), incoherent radar amplitude reflectors differentiate the natural system with dredge material dumped here around 1936 (0.0-0.7m) (Paine, 1936). Core observations and radiocarbon ages support this hypothesis*. GPR cross section lines A-A' show clinoformal migration towards Lake Superior/Duluth at depths (0.7-3.0m). On occasion, GPR cross sections happen to cut clinoformal structures along-strike or obliquely (A-A' position lines 20-35m), (B-B' position lines 54-70m), negating the true stratigraphic architecture and dip of the reflectors. Loss of signal with depth indicates radar energy is attenuated (which happens when radar energy interacts with fine-grained materials). It is believed the baymouth bar system has developed over glacial/lacustrine material. The western Lake Superior Basin has seen increases in lake levels throughout the last ~2000 years due to differential isostatic rebound and changing outlets (Farrand and Drexler, 1985; Mainville and Craymer, 2005). This baymouth bar has responded to the increasing lake

level in a progradational and aggradational fashion. Smaller climatic driven lake level variations are observed in detail from core observations.

Although this baymouth bar is a young, non-marine system, reconstructing its geomorphic evolution in response to lake level change may become a useful analogue for similar, larger systems involved with base level change. In addition, stratigraphic findings of how such a system's architecture is configured may yield insightful clues towards vintage conventional exploration reservoirs. Finally, a stronger understanding of how such a system geomorphically evolved in the context of the Lake Superior region post glaciation may aid in reshaping knowledge of how other geomorphic features and processes have developed throughout the region, perhaps providing tangible framework for future engineering and environmental management undertakings.

*Sediment cores, radiocarbon ages, and additional GPR data will be available to view at Stop 2 during the field trip.

Lunch at Barr Engineering 5th floor lunchroom (see handout map)

Location: UTM Zone 15, 568970E 5181519N

Vista Queen Tour (boarding at 1:00pm, departing 1:30pm)

Stop 3: 21st Ave. West/Miller Creek restoration (Dott/Mossberger)

Location: UTM Zone 15, 567314E 5178430N

The St. Louis estuary is the largest estuary on Lake Superior, and is an important source of biological productivity, and wetland and aquatic habitat types for a wide variety of fish and wildlife communities.

The 21st Avenue West Habitat Complex (Figure 20) is one of several habitat restoration projects that are incorporating beneficial reuse of navigational dredge material (Host, et al., 2013). The site is located near the WLSSD treatment plant, which discharges an average of 43 million gallons per day of treated wastewater. The intent of the restoration is to improve habitat by implementing remedial activities to address sediment contamination while complementing the desired ecological vision of stakeholder teams.

The US Army Corps of Engineers started a pilot project for placement of material in the 21st Ave. W. Complex in 2013. Barr Engineering performed turbidity monitoring to help evaluate how suspended sediment generated during material placement would be transported, and provided preliminary cut and fill estimates for material quantities needed to implement the habitat plan. The MPCA received an approved Work in Public Waters permit in spring 2015 from the MNDNR for the design shown in Figure 20, so the final stages of the 21st Ave. W. Project may begin. It is anticipated that the base material and features will be constructed by 2017.

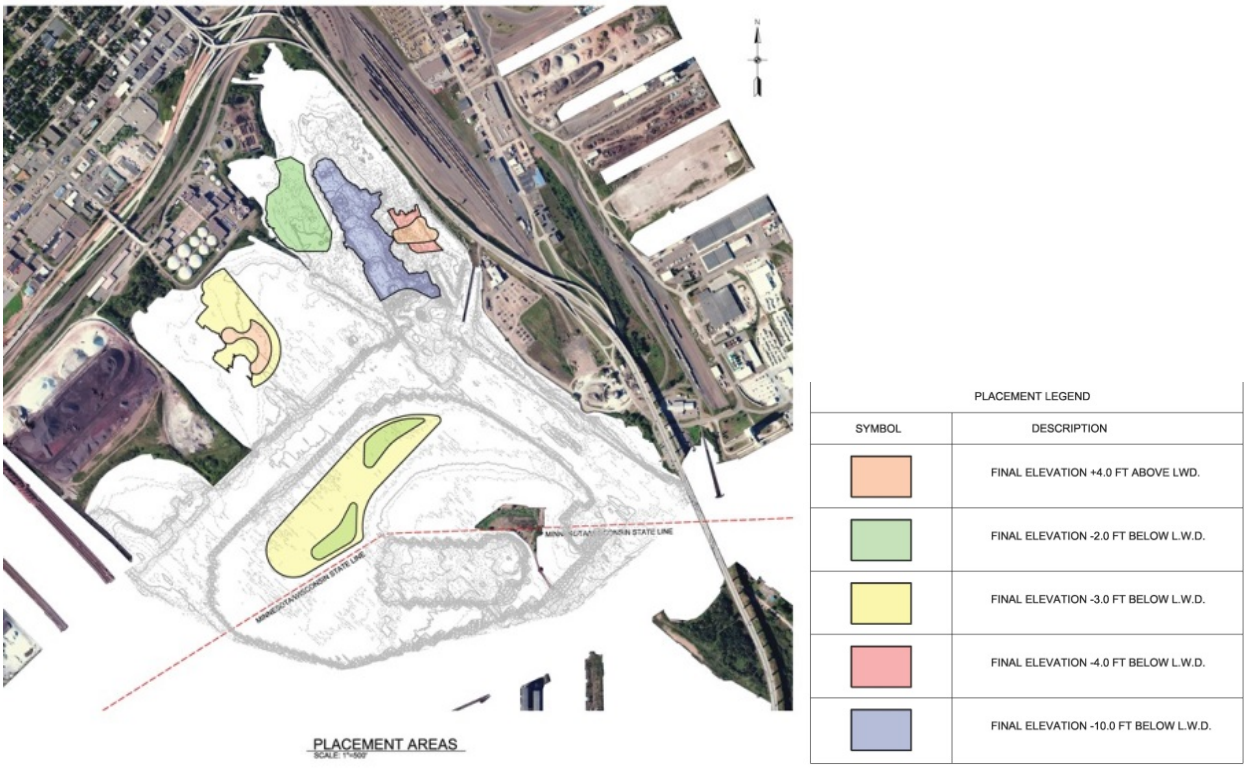


Figure 20. 21st Ave. W. Placement Plans – Islands (modified from USACE 2016).

Stop 4: SLIDRT, aka Stryker Bay (Dott/Mossberger)

Location: UTM Zone 15, 563072E 5174671N

The 255-acre St. Louis River/Interlake/Duluth Tar (SLRIDT) Superfund site is the largest sediment remediation project in Minnesota's history. Seven decades of industrial use had left polycyclic aromatic hydrocarbons (PAHs) and other contaminants in the St. Louis River estuary. Barr's work at the site included development of one of the nation's first "hybrid" sediment remedies, which combined dredging and capping at the site; surcharge capping to maintain wetland habitat; use of an activated carbon mat to prevent re-contamination – the first commercial application of this technology; and integration of remediation, mitigation and restoration. Costing $90 million less than an all-dredging approach, the project restored 106 acres of aquatic and riparian habitat for fish, wildlife, and the Duluth community.

Part of the investigation phase involved researching the history of the development of Stryker Bay and associated docks and slips. Figure 21 (SERVICE, 2002) shows a schematic of development of the site throughout the 98 years from 1903-2001. Fill (stippled areas in Figure 21) was brought into the proto-Stryker Bay in various phases, extending the land southward to accommodate industrial uses. Interestingly, the dock walls became confining barriers to shallow groundwater flow from the uplands to the river, causing artesian conditions to exist on the docks. An industrial water supply well was drilled near the southern tip on Dock 7, which was an artesian flowing well.

After the site was investigated with numerous soil borings and sediment cores, the remedial project began with capping of impacted material in Slip 7 (Figure 22). In subsequent years, construction of a dike across Slip 6 created a Confined Aquatic Disposal facility (CAD). Impacted material was dredged from Stryker Bay and the shipping channel, hydraulically pumped to the CAD, and evenly spread throughout

the CAD using a spreader barge. Part of Stryker Bay was separated from the rest with a sheet pile wall and was covered with an activated carbon mat and a surcharge to compress impacted material and cap it in place. The impacted material in the CAD was covered with an activated carbon mat, clean cap sand, and "environmental media" – material dredged and hydraulically pumped from a restoration project at Tallas Island approximately 2 miles upstream. The dike across the CAD was later removed, reconnecting it with the estuary.

The site is currently in a long-term monitoring and maintenance phase to confirm that the constructed caps are properly containing the contaminants of concern and that aquatic plant and benthic communities are recovering consistently with other areas of the St. Louis River estuary.

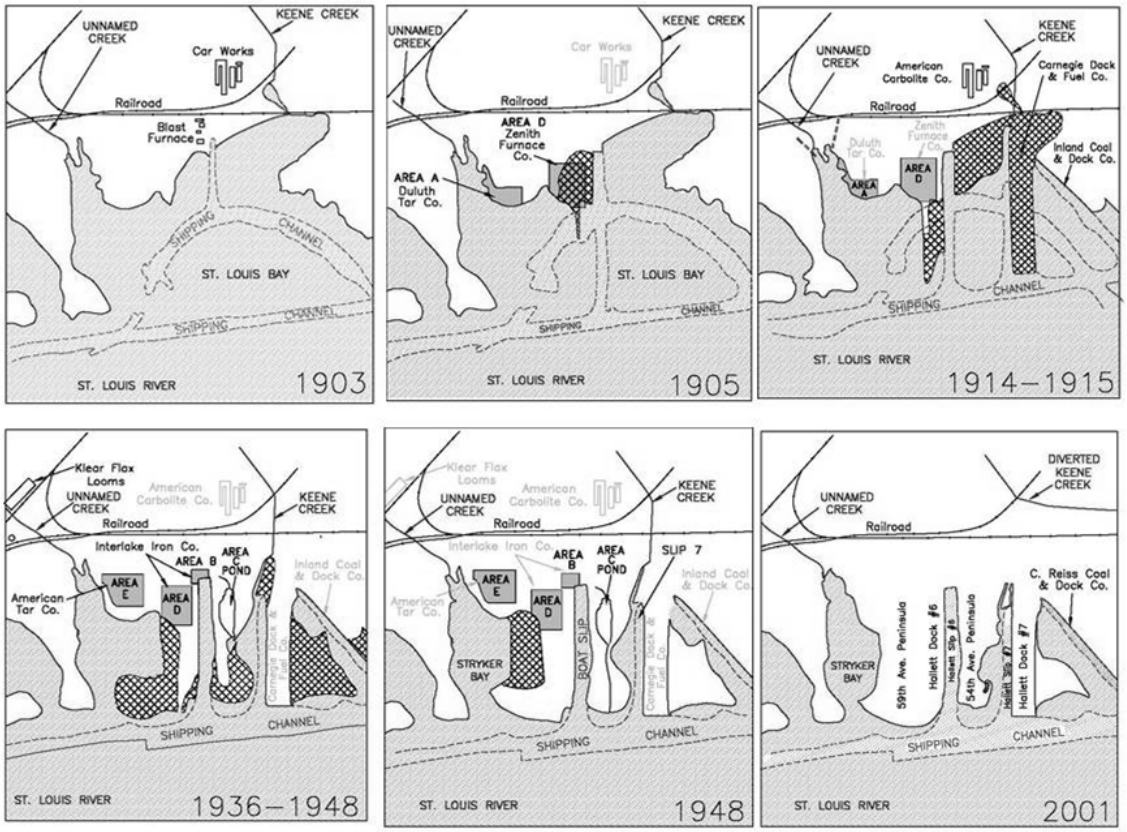


Figure 21. Industrial development of the SLRIDT site since 1903 (Modified from SERVICE, 2002).



Figure 22. SLRIDT Caps and Covers Map (Modified from Hard Hat Services, 2013).

Stop 5: St. Louis River and Glacial Lake Duluth Geomorphology: Pokegama Bay, Strandlines (Breckenridge/Mossberger)

Location: UTM Zone 15, 562881E 5173280N

The Pokegama River is a tributary of the St. Louis River, originating near Jay Cooke State Park on the Minnesota/Wisconsin border (Figure 23). It flows through the Superior Municipal Forest, where it empties into Pokegama Bay and the St. Louis River. The Pokegama-Carnegie wetlands are identified by the WDNR Bureau of Endangered Resources as a Lake Superior Basin Priority Site due to high quality wetland and occurrence of rare plant populations. The river is an important spawning area for walleye, northern pike, and other fish species. The Pokegama and its tributaries are deeply incised into red clay of the former lake bed, often forming steep stream banks with exposed clay. The exposed clay is susceptible to slumping and accelerated erosion (Mossberger, 2010).

Slumping of stream banks, such as those in the Pokegama River, increases erosion and downstream sedimentation by supplying freshly exposed sediment to the stream. Slumping and erosion can also threaten the stability of nearby structures. If a slump intersects a confined aquifer, water under high hydraulic head in the confined aquifer can then seep to the surface, contribute baseflow, and increase the sediment load to the streams.

Sedimentation from the St. Louis River deposits about half of the sediment yielded to the Duluth-Superior harbor (NRCS, 1996), and causes various economic and environmental problems. For example, a large plume of suspended sediment from the Pokegama River is often visible in the St. Louis River after rainstorms (Figure 24).



Figure 23. LiDar image of Clough Island and Dwight's Point at Pokegama Bay (DNR LiDAR Data, (2016).



Figure 24. Aerial image of Clough Island and Dwight's Point at Pokegama Bay (Google Earth, 2016).

One economic impact of excessive turbidity is the cost of dredging. Dredging is necessary to maintain adequate draft for ships that use the 17 miles of harbor shipping channels. Insufficient draft requires ships to reduce their cargo load, leading to increased transportation costs. The United States Army Corps of Engineers (USACE) has estimated that approximately 33,000 tons of sediment each year is dredged from the Duluth-Superior harbor (NRCS, 1998). The St. Louis River's contribution to the dredged sediment is approximately 14,000 tons, or 1,000 dump-truck loads, of sediment to the harbor annually, resulting in a burden to taxpayers for dredging and disposal of the river's sedimentation. The USACE's current dredge disposal facility for the harbor, Erie Pier needed to be expanded and reengineered because it was expected to run out of capacity in 2017 due to the accumulation of excess fine-grained material.

In addition to economic impacts, sediments can cause environmental problems. Suspended sediments are considered non-point pollution when they occur in high enough concentrations in designated surface waters. Industrial pollutants such as mercury, dioxins, and PCBs can attach to sediment particles, trapping toxins or oxygen-demanding materials in the harbor (Bridges, 2008). Dredging agitates and re-suspends settled pollutants, elevating toxin levels in the water and biota (MPCA, 1992).

The harbor became one of the 43 Areas of Concern (AOC) under the Great Lakes Water Quality Agreement (WQA) in 1972. In 1987, Remedial Action Plans (RAPs) were developed to improve the health of the Nemadji and St. Louis Rivers. The harbor was designated as impaired for five uses, including fish consumption advisories, degradation of benthos, restrictions on dredging, degradation of aesthetics, and loss of fish and wildlife habitat (NRCS, 1998).

In Pokegama Bay, there is a seasonal anoxic zone. The NOAA Sentinel Site Program is designed to create a national network of long-term research sites that measure the effects of climate change on our estuaries. The Lake Superior National Estuarine Research Reserve (LSNERR) has set up a Sentinel Site in Pokegama Bay. The goal will be to measure changes in climate and the associated effects on water quality, erosion, decomposition, marsh morphology, vegetation, and wildlife. A weather station, a water quality station, and 12 surface elevation tables (SETs) used to measure sediment accretion and subsidence were installed in 2011-2014.

Acknowledgements

Thanks to the following people and sources of information that helped shape this guidebook:

Mehgan Blair and Pete Kero, Barr Engineering.

Dan Breneman, Minnesota Pollution Control Agency.

http://zenithcity.com/

http://wlssd.com/about-us/history/

http://www.lre.usace.army.mil/Missions/Recreation/SooLocksVisitorCenter/SooLocksHistory.aspx

http://www.duluthport.com/port-history.php

REFERENCES

Albrecht, D.R. (2005). Geochemical Fingerprinting and the Role of the Nemadji River in Sediment Transport within Western Lake Superior. [Master's Thesis]: University of Minnesota Duluth, Duluth, Minnesota.

Barlaz, D.B. (1983). Sedimentation in the Duluth-Superior Harbor, Lake Superior. [M.S. Thesis]: University of Minnesota Duluth, Duluth, Minnesota.

Bernard, J.M., and Davidson, D.W. (1969). A Floristic Resurvey of a Landfill Area 32 Years after Deposition: The Oatka Beach Addition, Minnesota Point, Minnesota. American Midland Naturalist, 82(2), 559-563.

Black, R.F., 1976. Quaternary geology of Wisconsin and contiguous Upper Michigan. In: Mahaney, W.C. (Ed.), Quaternary Stratigraphy of North America. Dowden, Hutchinson, and Ross, Stroudesburg, Pennsylvania, pp. 93–117.

Breckenridge, A., 2007. Lake Superior varve stratigraphy and implications for eastern Lake Agassiz outflow from 10,700 to 9,040 cal BP (9.5-8.1 14C ka). Palaeogeography, Palaeoclimatology, Palaeoecology 246, 45-61.

Breckenridge, A. 2013, An analysis of the late glacial lake levels within the western Lake Superior basin based on digital elevation models: Quaternary Research v. 80, p. 383-395.

Breckenridge, A.J., Johnson, T.C., Beske-Diehl, S., Mothersill, J.S., 2004. The timing of regional late glacial events and post-glacial sedimentation rates from Lake Superior. Quaternary Science Reviews 23, 2355-2367.

Breckenridge, A., Lowell, T.V., Fisher, T.G., Yu, S., 2010. A late Minong transgression in the Lake Superior basin as documented by sediments from Fenton Lake, Ontario. Journal of Paleolimnology 47, 313–326.

Bridges, T.S., et al., 2008. The Four Rs of Environmental Dredging: Resuspension, Release, Residual, and Risk. U.S. Army Corps of Engineers Dredging Operations and Environmental Research Program, ERDC/EL TR-08-4.

Cowan, W.R., 1985. Deglacial Great Lakes shorelines at Sault Ste Marie, Ontario. In: Karrow, P.K., Calkin, P.E. (Eds.), Quaternary Evolution of the Great Lakes. Geological Association of Canada Special Paper 30, 33-37.

Demeter, S.C. (1993). U.S. Army Corps of Engineers Historic American Engineering Record No. MN-10: Duluth Ship Canal. Commonwealth Cultural Resources Group, Inc.

Dierckins, Tony. Zenith: A Postcard Perspective of Historic Duluth. Zenith City Press (X-Communication), Duluth, Minnesota: 2006.

DNR LiDAR Data, (2016). Retrieved from: http://arcgis.dnr.state.mn.us/maps/mntopo/

Duluth Seaway Port Authority, (2015). Retrieved from: http://www.duluthport.com/port.php

Farrand, W.R., 1960. Former Shorelines in Western and Northern Lake Superior Basin. PhD dissertation, University of Michigan, Ann Arbor, MI, 266 pp.

Farrand, W.R., & Drexler, C.W. (1985). Late Wisconsinan and Holocene History of the Lake Superior Basin. In: Karrow, P.K., and Calkin, P.E. (Eds.) Quaternary Evolution of the Great Lakes: Geological Association of Canada Special Paper, 30, 17-32.

Fisher, T.G., Whitman, R.L., 1999. Deglacial and Lake Level Fluctuation History Recorded in Cores, Beaver Lake, Upper Peninsula, Michigan. Journal of Great Lakes Research 25, 263-274.

Florin, M., and Wright, H.E., Jr., 1969, Diatom evidence for the persistence of stagnant glacial ice in Minnesota: GSA Bulletin, v. 80, p. 695-704.

Grout, F., 1919. Clays and Shales of Minnesota, United States Geological Survey, Bulletin 678, Washington, Government Printing Office.

Hard Hat Services, 2013. Long Term Monitoring & Maintenance Plan. St. Louis River/Interlake/Duluth Tar Site, Sediment Operable Unit Remediation. Prepared March 14, 20013 for XIK Corp.

Hearding, W.H. (1863). Survey of the Northern and North Western Lakes: West End of Fond Du Lac of Lake Superior Map. The Bureau of Topographical Engineers of the War Department.

Hobbs, H.C., 2003, Surficial geology of the Knife River quadrangle, St. Louis and Lake Counties, Minnesota; Minnesota Geological Survey Miscellaneous Map M-137, scale 1:24,000.

Hobbs, H.C. (2009). Surficial Geology of the Duluth Quadrangle, St. Louis County, Minnesota. Minnesota Geological Survey.

Hobbs, H.C., Breckenridge, A., 2011. Ice advances and retreats, inlets and outlets, sediments and strandlines of the western Lake Superior basin. In: Miller, J.D., Hudak, G.J., C. Wittkop, C., McLaughlin, P.I. (Eds.), Archean to Anthropocene: Field Guides to the Geology of the Mid-Continent of North America, GSA Field Guide 24, 299-315.

Hyodo, A., Longstaffe, F.J., 2011. The chronostratigraphy of Holocene sediments from four Lake Superior sub-basins. Canadian Journal of Earth Sciences 48, 1581–1599 .

Host, James, Buttermore, et al., An Ecological Design for the 21st Avenue West Remediation-to-Restoration Project. Natural Resources Research Institute, University of Minnesota Duluth Large Lakes Observatory, U.S. Fish and Wildlife Service. USFWS Cooperative Agreement F11AC00517June 2013 NRRI/TR-2013/24.

Johnson, M. D., Adams, R. S., Gowan, A. S., Harris, K. L.; Hobbs, H. C., Jennings, C. E., Knaeble, A.R.; Lusardi, B. A.; Meyer, G. N.. (2016). RI-68 Quaternary Lithostratigraphic Units of Minnesota. Minnesota Geological Survey. Retrieved from the University of Minnesota Digital Conservancy, http://hdl.handle.net/11299/177675.

Johnston, J.W., Argyilan, E.P., Thompson, T.A., Baedke, S.J., Lepper, K., Forman, S.L., Wilcox, D.A., 2012. A Sault-outlet-referenced mid- to late-Holocene paleohydrograph for Lake Superior constructed from strandplains of beach ridges. Canadian Journal of Earth Sciences 49, 1364-1371.

Jol, H.M., & Bristow, C.S. (2003). GPR in Sediments: Advice on Data Collection, Basic Processing and Interpretation, a Good Practice Guide. Geological Society London, Special Publications, 211, 9-27.

Kemp et al., (1978). Sedimentation rates and a sediment budget for Lake Superior. Journal of Great Lakes Research, 4, 276-287.

Knaeble, A.R., and Hobbs, H.C., 2009, surficial geology, Plate 3, and Quaternary stratigraphy, Plate 4 of Boerboom, T.J., project manager, geologic atlas of Carlton County, Minnesota: Minnesota Geological Survey County Atlas Series C-19, Part A, 6 plates, scale 1:100,000.

Larsen, C.E., 1985. Lake Level, uplift, and outlet incision, the Nipissing and Algoma Great Lakes. In: Karrow, P.K., Calkin, P.E. (Eds), Quaternary Evolution of the Great Lakes: Geological Association of Canada Special Paper 30, pp. 63-77.

Leverett, F. 1928. Moraines and shorelines of the Lake Superior basin. USGS paper 154-A, p. 1-72.

Lewis, CFM, et al., 2008. Dry climate disconnected the Laurentian Great Lakes, EOS 89(52), 541-542.

Loy, W.G. (1962). The Coastal Geomorphology of Western Lake Superior. [Master's Thesis]: University of Chicago, Chicago, Illinois.

Loy, W.G. (1963). Formation of the Duluth-Superior Harbor. The Minnesota Academy of Science Proceedings, 31, 28-35.

Loy, W.G. (1963). The Evolution of Bay-Head Bars in Western Lake Superior. Journal of Great Lakes Research, 10, 150-157.

Mainville, A., & Craymer, M.R. (2005). Present-Day Tilting of the Great Lakes Region Based on Water Level Gauges. Geological Society of America Bulletin, 117(7), 1070.

Minnesota Pollution Control Agency and Wisconsin Department of Natural Resources, 1992. St. Louis River System Remedial Action Plan, Stage One.

Merrill, J.A. (1939). The Wonderland of Lake Superior. Minneapolis, Minnesota: Burgess Publishing Company.

Morrison, S. M., Jol, H. M, Alger, R. Using radar stratigraphic analysis to identify erosion and deposition in the Duluth bay barrier, Lake Superior, NC-GSA poster presentation, Madison, WI.

Mossberger, I. G. (2010). Potential For Slumps, Sediment Volcanoes, And Excess Turbidity In The Nemadji River Basin (Masters Thesis, University of Minnesota-Duluth).

Natural Resources Conservation Service, 1996. Memorandum.

Natural Resources Conservation Service and U.S. Forest Service, 1998. Executive summary report: Erosion and sedimentation in the Nemadji River Basin: Nemadji River Basin Project, 16 p.

Paine, R.F (1936). City of Duluth Park Department – Annual Report 1936. Duluth Public Library, Duluth, Minnesota. Call 352.7. No. D88a. Vol.1936.

Rasid, H., & Hufferd, J. (1989). Hazards of Living on the Edge of Water: The Case of Minnesota Point, Duluth, Minnesota. Human Ecology, 17, 85-100.

Rasid et al., (1992). Coping with Great Lakes Flood and Erosion Hazards; Long Point, Lake Erie, vs. Minnesota Point, Lake Superior. Journal of Great Lakes Research, 18(1), 29-42.

SERVICE Engineering Group, 2002. Geology-Hydrogeology (of the) St. Louis River/Interlake/Duluth Tar Site, Duluth, MN. Appendix GH of the Data Gap Report.

Stoker, M.S., Pheasant, J.B., and Josenhans, H., 1997, Seismic Methods and Interpretations, in Davies, T.A., et al., eds., 1997, Glaciated Continental Margins: An Atlas of Acoustic Images; London, Chapman & Hall, 315 p.

Sydor et al., (1979). Red Clay Turbidity and its Transport in Lake Superior. Environmental Protection Agency Document. Grant No. R005175-01.

Taylor, F. B., 1894. A reconnaissance of the abandoned shore lines of the south coast of Lake Superior. American Geologist, 365-383.

Thomas, R.L. & Dell, C.I. (1978). Sediments of Lake Superior. Journal of Great Lakes Research, 4(3-4), 264-275.

Thompson, T.A., Lepper, K., Endres, A.L., Johnston, J.W., Baedke, S.J., Argyilan, E.P., Booth, R.K., Wilcox, D.A. 2011. Mid Holocene lake level and shoreline behavior during the Nipissing phase of the upper Great Lakes at Alpena, Michigan, USA. Journal of Great Lakes Research 37, 567–576.

U. S. Army Corps of Engineers, 2016. 21st Ave. West Restoration Placement Plan – Islands. Sheet GI001. Unpublished.

Wright, H.E., Jr., Mattson, L.A., Thomas, J.A., 1970. Geology of the Cloquet quadrangle, Carlton County, Minnesota: Minnesota Geological Survey Geologic Map Series GM-3.

Zenith City Historical Archive, (2016). Retrieved from: http://zenithcity.com/zenith-city-history-archiv